TECHNISCHE UNIVERSITÄT MÜNCHEN

TUM School of Life Sciences

Lehrstuhl für Technische Mikrobiologie

Molecular mechanisms of water kefir lactobacilli to persist in and shape their environment

Julia Doris Bechtner

Vollständiger Abdruck der von der TUM School of Life Sciences der Technischen Universität München zur Erlangung des akademischen Grades eines

Doktors der Naturwissenschaften (Dr. rer. nat.)

genehmigten Dissertation.

Vorsitzender: Prof. Dr. Wilfried Schwab

Prüfende der Dissertation:

1. Prof. Dr. Rudi F. Vogel
2. Prof. Dr. Wolfgang Liebl
3. Prof. Dr. Anja M. Wagemans

Die Dissertation wurde am 13.04.2021 bei der Technischen Universität München eingereicht und durch die TUM School of Life Sciences am 03.07.2021 angenommen.

Vorwort

Die vorliegende Arbeit entstand im Rahmen des durch das Bundministerium für Wirtschaft und Energie über die AiF-Forschungsvereinigung Wissenschaftsförderung der Deutschen Brauwirtschaft e.V. geförderten Projekts „Innovative Getränkezutaten“ (AiF 19180N).

Mein besonderer Dank gilt meinem Doktorvater Prof. Dr. Rudi F. Vogel, dessen große Freude an der Mikrobiologie mich während meiner Promotion und auch weiterhin motiviert. Danke für Deinen Einsatz und dafür, dass Deine Tür für uns immer offensteht.

Außerdem möchte ich mich bei Dr. Frank Jakob bedanken für seine fachliche Expertise, die Unterstützung und die langen Diskussionen über jedes Detail, das es zu beachten gab.

Zusätzlich gilt mein Dank Prof. Dr. Daniel Wefers und Dr. Christina Ludwig für die strukturchemischen und massenspektrometrischen Analysen, die vielen Diskussionen und die gute Zusammenarbeit. Darüber hinaus möchte ich mich bei Dr. Maximilian Miller und Dr. Michael Kiening für ihren wertvollen Input in bioinformatischen Fragestellungen bedanken.

Danke außerdem an Angela und alle Technikerinnen, besonders Meggie, für die tatkräftige Unterstützung und dafür, dass ihr den Laden am Laufen haltet.

Mein Dank gilt außerdem meinen Doktorandenkollegen, allen voran Viktor, Caro, Lara und Alex für die tolle Zeit und Unterstützung und natürlich für das super Arbeitsklima, ohne das die Arbeit nur halb so viel Spaß machen würde. Danke außerdem an meine Studentinnen, Henriette, Swetlana, Juliana und Sabine für die gute Zusammenarbeit.

Natürlich gilt mein Dank Jonas für das Korrekturlesen, die Unterstützung und die schöne Zeit im und außerhalb des Labors. Danke an meine Eltern, dass ihr mir alles ermöglicht und immer an mich glaubt.

Abbreviations

ABC	ATP-binding cassette
AF4	Asymmetric flow field flow fractionation
ANI	Average nucleotide identity
CPS	Capsular polysaccharide
dH_2O	Deionized water
DMSO	Dimethyl Sulfoxide
DP	Degree of polymerization
DTT	Dithiothreitol
dsr3510ΔC-term	C-terminally truncated variant of dsr3510
ED	Entner-Doudoroff pathway
EMP	Embden-Meyerhof-Parnas pathway
EPS	Exopolysaccharide
GH	Glycosyl hydrolase family
GO	Gene ontology
GOS	Gluco-oligosaccharide
HPAEC-PAD	High-performance anion exchange chromatography coupled to pulsed amperometric detection
HPLC	High-performance liquid chromatography
iBAQ	Intensity-based absolute quantification
iEP	Isoelectic point
IMO	Isomaltooligosaccharide
KEGG	Kyoto Encyclopedia of Genes and Genomes
LAB	Lactic acid bacteria
LFQ	Label-free quantification
MALS	Multi-angle laser light scattering
MFS	Major facilitator superfamily
mMRS	Modified MRS medium
MS	Mass spectrometry
M_w	Molecular weight
NCBI	National Center for Biotechnology Information
OD	Optical density

ORF	Open reading frame
ORP	Redox-potential
PAS	Periodic acid Schiff´s staining
PKP	Phosphoketolase pathway
PPP	Pentose phosphate pathway
PTS	Phosphotransferase system
RAPD	Randomly amplified polymorphic DNA
RAST	Rapid annotation using subsystem technology
rms	Root mean square
R_w	Averaged rms radii
SDS-PAGE	Sodium dodecyl sulfate polyacrylamid gel electrophoresis
WGS	Whole genome sequence

Index

1 Introduction

1.1 Microbial biofilms

Free-living microorganism commonly exist in multi-species consortia that either live in a planktonic state or accumulate at interfaces to form biofilms (Wingender *et al.*, 1999). The dry mass of these biofilms is, however, commonly only composed of 2-15 % microbial cells, while the residual 85-98 % are built-up from extracellular matrix compounds and water (Sutherland, 2001). The microorganisms inhabiting these biofilms mostly produce these matrix compounds themselves to ensure surface adhesion and/or coherence of the cells (Flemming *et al.*, 2010). The extracellular matrix compounds are commonly referred to as "extracellular polymeric substances", as diverse types of biopolymers, such as proteins, nucleic acids and polysaccharides contribute to the formation of the matrix (Karatan *et al.*, 2009; Sutherland, 2001; Wingender *et al.*, 1999). Although it is unclear, whether this applies to all the microorganism within a biofilm, the extracellular matrix provides several advantages for the inhabiting microbiota (Xavier *et al.*, 2007). Thereby, cells can adhere to and colonize biotic or abiotic surfaces and form aggregates that ensure close proximity of the cells and thus cell-cell communication and a reduced dissipation of nutrients. Moreover, the extracellular matrix leads to the retention of microbial enzymes and water, preventing the cells from desiccation (Flemming *et al.*, 2010). Furthermore, biofilm formation provides the microorganism with protection from exogenous harmful impacts, such as host immune-defence, predatory microorganisms, antimicrobial agents and reactive oxygen species (Santos *et al.*, 2018; Yan *et al.*, 2016). Extracellular matrices were furthermore shown to accumulate organic and inorganic compounds that may serve as nutrients or support ion-exchange (Donlan, 2002). Moreover, especially polysaccharides are formed within microbial biofilms to store excess energy that may be needed in times of nutrient depletion (Flemming *et al.*, 2010; Madigan *et al.*, 2009). Extensive research has been done to understand the formation of biofilms, as biofilms are frequently involved in pathogenesis of certain microorganisms. An estimated 80 % of all recurrent and chronic human infectious diseases is caused by bacterial biofilms that are not efficiently treatable due to their resistance to antimicrobials (Sharma *et al.*, 2019). A well-studied example is represented by *Pseudomonas aeruginosa* that causes severe pneumonia especially in immunocompromised patients and is resistant to a multitude of antibiotics (Maurice *et al.*, 2018). An infection with this pathogen is thus difficult, or even impossible to treat. The infection is often acquired within the hospital, as *Pseudomonas aeruginosa* is an efficient biofilm producer enabling the cells to adhere and reside in almost any niche within the

hospital, including water supply pipelines and implanted biomaterials (Maurice *et al.*, 2018; Mulcahy *et al.*, 2014; Peleg *et al.*, 2010). Another less severe, but quite costly disease is caused by oral streptococci (e.g. *Streptococcus mutans* and *S. sobrinus*) that largely contribute to biofilm-formation on the teeth, called dental plaques, using extracellular enzymes that synthesize large polysaccharides (Forssten *et al.*, 2010; Lembo *et al.*, 2007). Among other compounds within dental plaque biofilms, these polysaccharides enable streptococci, but also other microorganisms to adhere to the teeth enamel, while providing protection against antimicrobial compounds of the saliva. Subsequently, acid formation of the microorganisms inhabiting this biofilm leads to enamel and thus to dental decay (Forssten *et al.*, 2010).

Moreover, biofilms do not only play an adverse role in medical topics, but also in industrial processes. Especially in the manufacturing of foods, biofilms of spoiling microorganisms frequently lead to huge economical losses (Galié *et al.*, 2018). In this context, examples of nearly any niche within the food industry can be found, including spoilage of beer, wine, sugar cane and meat. However, spoilage is not always caused by the biofilm itself, but rather by the bacteria producing un-desired off-flavours or even causing disease (Bartowsky *et al.*, 2008; Bittner *et al.*, 2016; Fraunhofer *et al.*, 2018; Galié *et al.*, 2018; Hector *et al.*, 2015; Kubota *et al.*, 2009; Kwon *et al.*, 2017; Riedl *et al.*, 2019; Wickramasinghe *et al.*, 2019). Nonetheless, industry would not be industry if they would have overlooked the biotechnological potential of biofilm-forming microorganisms. Herein, especially microorganisms with the ability to produce polysaccharides increasingly gained biotechnological interest (Freitas *et al.*, 2011).

1.2 Microbial polysaccharides

Microbial polysaccharides are commonly produced by bacteria, microalgae, yeasts and fungi and represent a heterogenous group of microbial metabolites that are composed of carbohydrate subunits bound together by glycosidic linkages (De Vuyst *et al.*, 1999; Paniagua-Michel *et al.*, 2014; Parolis *et al.*, 1998; Ruiz-Herrera, 1991; Selbmann *et al.*, 2003; Welman *et al.*, 2003).

They are classified into three major groups according to their biological role (Schmid *et al.*, 2015). The first group is represented by intracellular polysaccharides like glycogen that are limited in use and are often referred to as storage polysaccharides (Nwodo *et al.*, 2012). The second group is termed capsular polysaccharides (CPS) that are intracellularly synthesized, secreted, and subsequently remain tightly attached to the cells (Rehm, 2010). They protect the cells from environmental influences such as desiccation but are more commonly described in the context of pathogenicity, as CPS help the bacteria to defend themselves against or avoid the

host immune system (Rehm, 2010; Willis *et al.*, 2013). The third and most heterogenous group is summarized by the term exopolysaccharides (EPS) that can be either secreted or synthesized extracellularly. However, this distinction is not used clearly since CPS are equally localized extracellular, CPS and EPS are often summarized as EPS, while EPS-producing strains are easily identifiable by their slimy or ropy appearance on agar-plates containing the substrate for EPS formation (Rehm, 2010).

With regards to their monomeric composition, EPS are classified into two major groups, namely homopolysaccharides (HoPS) exhibiting only a single type of monosaccharide and heteropolysaccharides (HePS) consisting of multiple types of monosaccharides (De Vuyst *et al.*, 1999; Monsan *et al.*, 2001; Schmid *et al.*, 2015). The latter ones are produced intracellularly upon the use of nucleotide activated sugar donors and are subsequently secreted by different pathways that mainly predetermine, where the assembled polysaccharide will reside outside the cell, i.e. attached to the cell or released. In general, formation of HePS (e.g. xanthan) is rather complex requiring several catalytic steps that are mediated by different enzymes (De Vuyst *et al.*, 1999; Schmid, 2018). The genetic information for these enzymes is encoded within operons that can reach a size of 30 open reading frames (ORFs), as it was shown for the K40 type polysaccharide of *Klebsiella* sp. (Pan *et al.*, 2015).

HoPS formation is either achieved by synthase-dependent pathways or by single enzymes that are attached to the cell surface or released into the surrounding milieu. The synthase-dependent pathways occur intracellularly using sugar nucleotide donors and thus resemble HePS´s biosynthesis (Schmid *et al.*, 2015). Most information on this type of bacterial HoPS formation focusses on the synthesis of β-glucans that are found among different lactic acid bacteria (LAB) species, e.g. *Pediococcus* spp. and *Oenococcus* spp., but also in gram-negative bacteria such as *Agrobacterium* sp. and *Komagataeibacter xylinus* (Bockwoldt *et al.*, 2020; Ibarburu *et al.*, 2007; Stasinopoulos *et al.*, 1999; Werning *et al.*, 2006; Wong *et al.*, 1990). Interestingly, *Lactobacillus johnsonii* was proposed to produce the α-glucan dextran from intracellular activated sugar moieties, however, a detailed characterization of this particular pathway is still pending (Dertli et al., 2013; Mayer et al., 2020). Additionally, HoPS can be synthesized by single extracellular sucrase-type enzymes that use the energy conserved within the glycosidic bond of their substrate sucrose. Although, the first evidence for bacterial jellification of sugar cane were already shown by Pasteur back in 1861 (Pasteur, 1861), discovery of novel sucrase-type enzymes with new product-specificities is still ongoing (Gangoiti *et al.*, 2018; W. Xu *et al.*, 2019).

These enzymes are further divided into fructansucrases (glycosyl hydrolase (GH) 68 family) and glucansucrases (GH70 family), depending on the monosaccharide moiety that is transferred from sucrose to a growing polysaccharide (van Hijum *et al.*, 2006). To date, glucansucrases are known to be exclusively expressed by LAB, while fructansucrases are found in a vast variety of gram-positive and gram-negative bacteria. Furthermore, two types of fructansucrases are distinguished so far: inulosucrase (E.C. 2.4.1.9) that synthesizes fructans with β-1,2-glycosidic linkages, and levansucrase (E.C. 2.4.1.10) that synthesizes β-2,6-glycosidic linkages. (van Hijum *et al.*, 2006; Velázquez-Hernández *et al.*, 2009). The different types of glucansucrases will be described in the following sections.

1.2.1 Glucansucrases

1.2.1.1 Distribution and structure

Glucansucrases, also known as glycosyltransferases or glycoside hydrolases, are enzymes that are classified into family GH70 according to the CAZy classification system (http://www.cazy.org). Therefore, glucansucrases are structurally and functionally related to the GH families 13, the α-amylase family, and GH77, only containing 4-α-glucanotransferase (E.C. 2.4.1.25). All three glycosyl hydrolase families are summarized within the GH-H clan (Cantarel *et al.*, 2009; MacGregor *et al.*, 2001; Stam *et al.*, 2006). So far, glucansucrases have been described exclusively for LAB of the genera *Streptococcus*, *Weissella*, *Leuconostoc*, *Oenococcus* and several species of the *Lactobacillaceae* family, e.g. *Lentilactobacillus*, *Limosilactobacillus* and *Liquorilactobacillus*, that has undergone a recent taxonomic re-ordering (Leemhuis *et al.*, 2013b; Meng *et al.*, 2016; Zheng *et al.*, 2020). Glucansucrases are distinguished by the predominant type of glycosidic linkage that is present within the main-chain or backbone of the synthesized polysaccharide. They are thus differentiated into mutansucrases (α-1,3-glucan, E.C. 2.4.1.125), reuteransucrases (α-1,4-glucan, E.C. 2.4.1.-), dextransucrases (α-1,6-glucan, E.C. 2.4.1.5) and alternansucrases (glucan with alternating α-1,3 and α-1,6 linkages, E.C. 2.4.1.140) (Leemhuis *et al.*, 2013b; Monchois *et al.*, 1999; Monsan *et al.*, 2001; Mooser, 1992; Sidebotham, 1974; Zheng *et al.*, 2020). While all these enzymes use sucrose as substrate, enzymes of the GH70 subfamily 4,6-α-glucanotransferases (E.C. 2.4.1.-) degrade the α-1,4 glycosidic linkages of maltooligosaccharides to synthesize a glucan with α-1,6 glycosidic linkages (Kralj *et al.*, 2011; Leemhuis *et al.*, 2013a). Moreover, a novel type of GH70 enzyme was discovered recently that synthesizes alternating α-1,3/α-1,4 glycosidic linkages using amylose as substrate and was thus termed 4,3-α-glucanotransferase (E.C. 2.4.1.-)(Gangoiti *et al.*, 2017).

Glucansucrases are large enzymes with variable molecular weights that commonly range between 120 – 200 kDa, however, some glucansucrases have been shown to be even larger (Bozonnet *et al.*, 2002; Leemhuis *et al.*, 2013b). When looking at the primary structure of glucansucrase enzymes, a large variety of domain architectures can be found even within the sub-groups that are described above (Leemhuis *et al.*, 2013b; Meng *et al.*, 2016). As depicted exemplarily in Figure 1A, all glucansucrases exhibit one GH70 catalytic domain, however, some glucansucrases feature a second one (Bozonnet *et al.*, 2002). Within the catalytic core, four sequence motifs are conserved among all GH70 enzymes that are involved in the binding of the substrate (Devulapalle *et al.*, 1997; Kralj *et al.*, 2004). Additionally, all glucansucrases possess at least one N- and/or C-terminal glucan-binding domain that includes several glucan-binding repeat motifs (Janeček *et al.*, 2000). Most glucansucrases exhibit an N-terminal variable region and a signal-peptide to ensure efficient secretion into the extracellular environment (van Hijum *et al.*, 2006). However, not all glucansucrases feature this signal-peptide. Some glucansucrases were additionally shown to have a cell-wall anchor (van Hijum *et al.*, 2006).

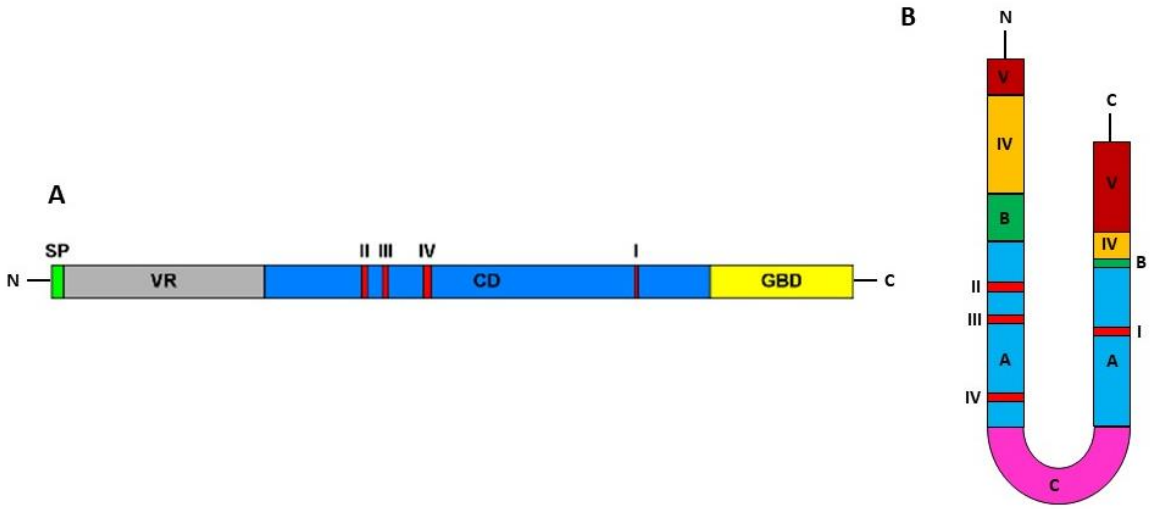

Figure 1 Schematic depiction of domain architecture of glucansucrase enzymes. (**A**) Domain architecture according to function, SP = signal peptide, VR = variable region, CD = GH70 catalytic domain, GBD = glucan-binding domain, I-IV = substrate-binding motifs; (**B**) Domain architecture according to three-dimensional "U-shape" structure. The figure was constructed in Microsoft office powerpoint according to similar figures within the literature (Leemhuis *et al.*, 2013b; Meng *et al.*, 2016).

As the first crystal structure of a glucansucrase enzyme became available, it was possible to arrange the domains of the primary into a tertiary structure, which appeared to be "U-shaped", as domains A, B, IV and V are constituted from two discontinuous N- and C-terminal regions, respectively (Figure 1B) (Vujičić-Žagar *et al.*, 2010). The crystallographic investigation of the

3D structure of these enzymes furthermore helped to elucidate the evolutionary relationship between GH70 and GH13 enzymes, as both enzyme families exhibit domains A, B and C, but domains IV and V are unique for GH70 enzymes (Vujičić-Žagar *et al.*, 2010). Domains A, B and C represent the catalytic domain of the enzyme, while domain A contains the substrate-binding sites, and was shown to have an α-amylase like (β/α)-barrel structure that is circularly permutated in contrast to GH13 and GH77 enzymes. (MacGregor *et al.*, 1996; Vujičić-Žagar *et al.*, 2010). Domain B appeared to be necessary for the shaping of the groove in proximity to the catalytic site and provides a binding site for Ca^{2+} that was shown to be essential for glucansucrase activity (Kralj *et al.*, 2004; Vujičić-Žagar *et al.*, 2010). The role of domain C is not known so far. Simultaneously, the role of domain IV is yet unknown, as the domain appeared to have no structural similarity to any other known protein. However, domain IV was proposed to overtake a "hinge"-function that provides flexibility between domain B and V (Ito *et al.*, 2011). Domain V is not constituted from any stretches belonging to the catalytic domain as shown in Figure 1A, but from one or two discontinuous segments depending on the presence of an N- and/or C-terminal domain that vary greatly in size (Meng *et al.*, 2016). These segments often contain conserved domains that are referred to as glucan-binding domains, but the exact function has not been clarified. Although it could be shown that these domains do not exhibit any direct catalytic activity, it was proposed that they may play a role in the binding of a growing polysaccharide chain that may thus be held in close proximity to the catalytic site (Abo *et al.*, 1991; Funane *et al.*, 1998; Kingston *et al.*, 2002; Vincent Monchois *et al.*, 1998; Monchois *et al.*, 1999; Remaud-Simeon *et al.*, 2000; Vujičić-Žagar *et al.*, 2010). Moreover, it was observed that the truncation of N-terminal glucan-binding domains leads to a shifted ratio between sucrose hydrolysis and transglycosylation (Kralj *et al.*, 2004). It was furthermore speculated that glucan-binding domains may be involved in cell surface attachment, as some enzymes exhibit peptide sequence motifs similar to that in choline-binding motifs of streptococcal autolysin LytA (Fernández-Tornero *et al.*, 2001; Olvera *et al.*, 2007).

The direct evidence for the binding of glucans by the glucan-binding pockets of domain V was eventually provided by Brison *et al*. (2016) who resolved the structure of a GH70 enzyme in complex with isomaltosyl and isomaltotriosyl residues. They could show that the gluco-oligosaccharides (GOS) are held within domain V by a network of hydrogen bonds and van der Waals interactions.

1.2.1.2 Reactions catalyzed by glucansucrases

The glucansucrase reaction follows an α-retaining double displacement reaction mechanism that is highly similar to that of family GH13 enzymes (Albenne *et al.*, 2004; Devulapalle *et al.*, 1997; MacGregor *et al.*, 2001; Monchois *et al.*, 1997). It is mainly catalyzed by three amino acid residues located within the conserved sequence motifs II – IV: a nucleophile that is represented by an aspartate residue in motif II, a general acid/base, represented by a glutamate residue within motif III, and a transition state stabilizer that is again an aspartate residue, but within motif IV (Ito *et al.*, 2011; Vujičić-Žagar *et al.*, 2010). First, the nucleophilic aspartate attacks the α,β-glycosidic linkage of sucrose to form a covalent β-glucosyl-enzyme intermediate, which is subsequently stabilized by the transition-state stabilizing aspartate (Barends *et al.*, 2007; Mooser *et al.*, 1991; Mooser *et al.*, 1989). Then, the catalytic glutamate residue protonates the fructosyl moiety, releasing the fructose from the enzyme, while deprotonating the acceptor substrate. Finally, the glucosyl moiety is transferred to the non-reducing end of this acceptor substrate (MacGregor *et al.*, 2001). The active site of the enzyme appears to be blocked by additional conserved amino acid residues, shaping it like a pocket (Vujičić-Žagar *et al.*, 2010). This leaves the active site of GH70 enzymes narrower and thus allows for the transfer of only one glucosyl-moiety per reaction cycle, while the active site of GH13 family enzymes is larger and allows for the binding of GOS as substrates (Leemhuis *et al.*, 2013b; Vujičić-Žagar *et al.*, 2010).

In contrast to the residues within the substrate binding site, the amino acid residues within the acceptor binding site are less conserved among different glucansucrases, which most likely leads to different orientations of the acceptor molecules within the binding site and thus determines the linkage type within the resulting polysaccharide (Hellmuth *et al.*, 2008; Kralj *et al.*, 2005; Leemhuis *et al.*, 2012; van Leeuwen *et al.*, 2009). In addition to the main linkage type of the polysaccharide´s backbone, glucansucrases commonly insert certain amounts of linkages and branches of another type, which enormously increases the variability of the products. Thereby, glucans with different portions of branches and linkages in positions *O*2, *O*3, *O*4 and *O*6 are produced, which most likely involves a second binding mode of the acceptor binding site (Leemhuis *et al.*, 2013b; Meng *et al.*, 2014; Vujičić-Žagar *et al.*, 2010). A special type of GH70 enzyme is represented by the dextransucrase that is expressed by several *Leuconostoc* (*Lc.*) *mesenteroides* and *citreum* strains, as this enzyme features two catalytic domains instead of only one. The C-terminal catalytic domain gained special interest, since it was unable of catalyzing the polymerization reaction, but inserted α-1,2 branches into a present dextran acceptor molecule (Amari *et al.*, 2015; Bozonnet *et al.*, 2002; Brison *et al.*, 2012).

In general, glucansucrase reactions are quite versatile (Figure 2) (Monsan *et al.*, 2010). While sucrose is the only known glucosyl-donor substrate, GH70 enzymes glycosylate a vast variety of acceptor substrates. Instead of using water as acceptor, which leads to the hydrolysis of sucrose, the glucosyl moiety may be transferred onto glucose or gluco-oligo- and polysaccharides, which leads to a further elongation of the polymer (Moulis *et al.*, 2006). In addition, the glucosyl moiety may be transferred onto fructose, leading to the formation of sucrose or sucrose isomers like leucrose or palatinose (Moulis *et al.*, 2006; Seo *et al.*, 2007).

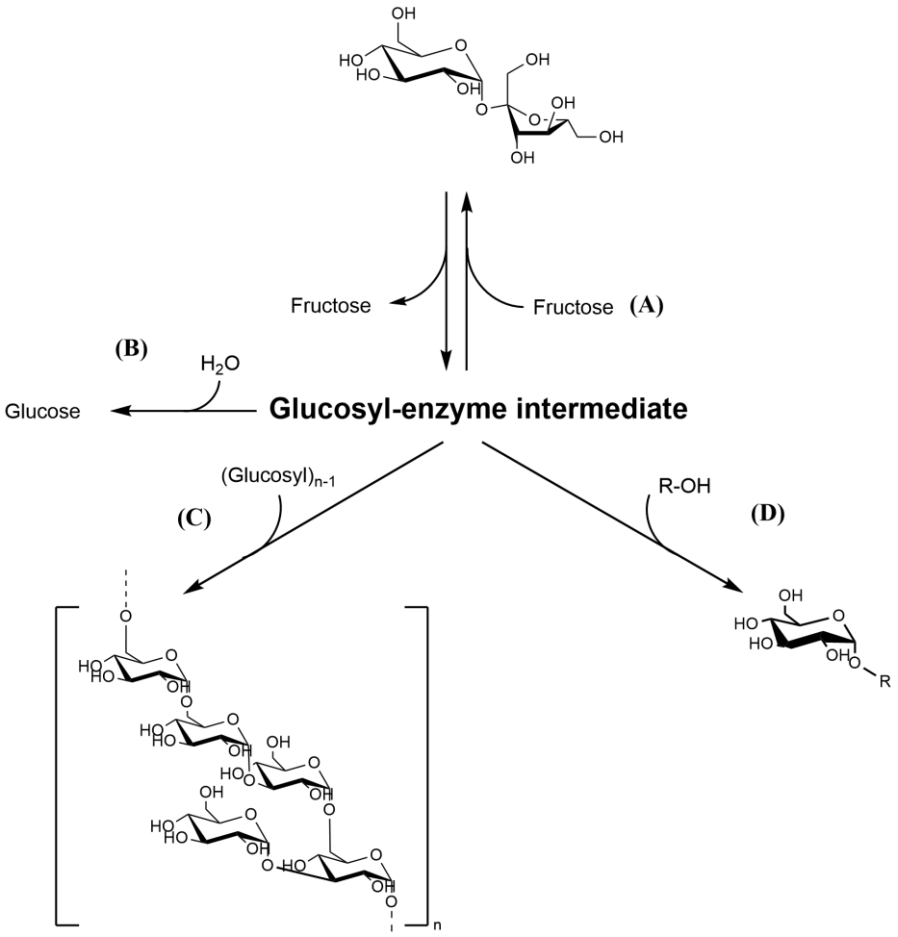

Figure 2 Reactions catalyzed by glucansucrases. (**A**) Glycosylation of fructose, yielding sucrose (or sucrose-isomers); (**B**) Hydrolysis of sucrose; (**C**) Elongation of an oligo- or polysaccharide – in this case a dextran with α-1,3-linkages and branches; (**D**) Acceptor reaction leading to the glycosylation of various substrates with hydroxyl groups. The figure was constructed in ChemDraw (v. 19.1, PerkinElmer, Waltham, USA) following a similar graphic in Monsan *et al.* (2010).

Moreover, other substrates with hydroxyl-groups are effectively glycosylated by glucansucrases, as shown for sucrose, maltose, raffinose, gentibiose, alditols, hydroquinone and L-ascorbic acid among others (Côté, 2009; Côté *et al.*, 2009; Demuth *et al.*, 2002; Kim *et al.*, 2010; Moulis *et al.*, 2006; Rabelo *et al.*, 2006; Seo *et al.*, 2009). The substrates accepted for glycosylation were, however, shown to be specific for a certain glucansucrase, which is why

the synthesis of particular products needs for the application of a suitable enzyme (Côté *et al.*, 2005). The product palette synthesized by glucansucrases is additionally enlarged, as they commonly produce polydisperse mixtures of polysaccharides with various degrees of polymerization (DPs) (Falconer *et al.*, 2011; Moulis *et al.*, 2006). In contrast to the linkage type, which is determined by the type of glucansucrase, the DP and branching can be influenced by the reaction conditions, such as enzyme and substrate concentration, pH, temperature and salt (Falconer *et al.*, 2011; Kim *et al.*, 2003; Prechtl *et al.*, 2018b). Polymerization occurs in a semi-processive mode, which means that the glucansucrase reaction proceeds in a non-processive mode to synthesize smaller oligosaccharides. Once, a critical chain length is reached the reaction switches to a processive mechanism, further elongating pre-synthesized oligosaccharides (Moulis *et al.*, 2006). The processive mode is mediated by domain V, which holds the growing polysaccharide chain at the enzyme and ensures efficient transglycosylation (Claverie *et al.*, 2020).

1.2.2 Biology of α-glucan formation

Glucansucrase encoding genes are either located on chromosomes or plasmids or possibly both, as some LAB were shown to encode several glucansucrases (Nácher-Vázquez *et al.*, 2017; Passerini *et al.*, 2015). Especially strains of the genus *Leuconostoc* are prone to encode more than one glycosyltransferase (Amari *et al.*, 2015). The analysis of these strains additionally showed that glucansucrases may be transferred by horizontal gene transfer (Amari *et al.*, 2015; Passerini *et al.*, 2015). The most famous example for such a development is represented by *Streptococcus mutans*, which is postulated to have acquired its cariogenic potential by the horizontal transfer of glucansucrases from bacteria within fermented foods (Argimón *et al.*, 2013; Hoshino *et al.*, 2012).

The expression of the glucansucrase genes, as well as the beneficial effects for the respective microorganism were shown to be quite versatile. While some glucan-producers, especially those of the genera *Streptococcus* and *Weissella*, as well as of the *Lactobacillaceae* family were shown to express their respective glucansucrases constitutively, glucansucrase expression is often inducible in *Leuconostoc* strains (Bounaix *et al.*, 2010b; Kim *et al.*, 1994; Prechtl *et al.*, 2018a; Quirasco *et al.*, 1999; Schwab *et al.*, 2007). Although induction of glucansucrase expression was mostly achieved by the presence of sucrose, also other factors like temperature or the exposure to oxygen have been reported to influence the expression (Besrour-Aouam *et al.*, 2019; Yan *et al.*, 2016). Interestingly, expression of a dextransucrase gene was reported to be concomitant with the replication of the plasmid encoding this enzyme in *Latilactobacillus*

(*L.*) *sakei* (formerly *Lactobacillus sakei* (Zheng *et al.*, 2020))(Nácher-Vázquez et al., 2017). Taken together, not only the existence, but also the surrounding conditions influence glucan production in LAB. *Vice versa*, little is known about the role of polysaccharide formation in the shaping of the environment of the synthesizing LAB and their co-inhabitants, providing protection against environmental influences or contributing to adherence/coherence to surfaces or other microorganisms, as it is generally known for biofilms (section 1.1)(Flemming *et al.*, 2010). Furthermore, in the context of a biotechnological exploitation of these enzymes, there are knowledge gaps in the biology behind glucan formation in a certain microorganism, which hinder the design of a desired product.

1.3 Properties and biotechnological relevance of α-glucans

In general, polysaccharides alter the behaviour of aqueous solutions. Therefore, they are biotechnologically exploited to viscosify, emulsify, chelate, stabilize, retain water or to form films, membranes or gels (Lapasin *et al.*, 1995). Many polysaccharides of plant or algae origins, such as cellulose, starch, arabic gum and carageen have a long history of industrial application (Imeson, 2010; Lapasin *et al.*, 1995). However, production and isolation of some of these polysaccharides are expensive, time consuming, and often yield impure and low amounts of product (Imeson, 2010). Certain polysaccharides are suspected of having adverse effects on health, reducing their potential application fields (Younes *et al.*, 2018). Moreover, polysaccharides like arabic gum have to be imported from politically instable countries, resulting in unreliable supply chains (Imeson, 2010). Furthermore, some polysaccharides, e.g. starch, are insoluble in water at low temperatures and have to be modified artificially to maintain their beneficial effects (Taggart *et al.*, 2009; Viswanathan, 1999). By contrast, microbial production of polysaccharides can be performed locally under controllable environmental conditions (Zannini *et al.*, 2016). Although some examples have demonstrated the economically reasonable production of bacterial polysaccharides, a further reduction of costs needs to be achieved in order to gain higher industrial interest in these materials (Velásquez-Riaño *et al.*, 2017; Zannini *et al.*, 2016; Zhao *et al.*, 2018). Nonetheless, microbial polysaccharides may have their highest potential in industrial niches that demand a high degree of purity or specific characteristics of polysaccharides, such as in pharmaceuticals, cosmetics, foods or medicine (Freitas *et al.*, 2011). As described above, bacterial polysaccharide production is quite versatile and some synthesis pathways may exhibit advantages over others – dependent on the application of the polysaccharide. The synthesis of HePS and some HoPS

occurs intracellularly and utilizes nucleotide-activated sugars and is thus linked to the growth and central carbon metabolism of the producer strain (De Vuyst *et al.*, 1999). Moreover, isolation of these polysaccharides is challenging and general yields of fermentative production are low (De Vuyst *et al.*, 1999; Grobben *et al.*, 1996; Zhu *et al.*, 2016). Nonetheless, the purified glycosyltransferase enzymes involved in the biosynthesis pathway of the respective polysaccharides may be applied. The advantage of these enzymes over GH70 family enzymes is represented by efficient and highly specific transglycosylation activities that lead to narrow product spectra and thus to the synthesis of tailored polysaccharides or glycosylation products (Mestrom *et al.*, 2019). By contrast, glucansucrases produce a polydisperse mixture of polysaccharides with various DPs, as well as other oligosaccharide side-products (Claverie *et al.*, 2020; Moulis *et al.*, 2006; Seo *et al.*, 2007). However, production of polysaccharides by glucansucrases is comparatively cheap, as they utilize the low-cost substrate sucrose to produce large amounts of products that can be efficiently purified from culture media (Leemhuis *et al.*, 2013b; Ruas-Madiedo *et al.*, 2005).

The physico-chemical properties such as viscosity, turbidity, stickiness or solubility of α-glucans are determined by the type and amounts of linkages and branches, as well as the length of these branches and the overall size of the polymers (Leemhuis *et al.*, 2013b). Due to the existence of a huge variety of different glucansucrases, the field of possible applications is equally large (Gangoiti *et al.*, 2018). In cosmetics, alternans are patented to be applied as texturizing agent in order to substitute oil (Frohberg *et al.*, 2009). Dextrans are widely applied in medicine for the use as blood-plasma expander and anticoagulant, in pharmaceutics as drug carriers and in biotechnology as matrix for chromatographic columns among others (Howard *et al.*, 1959; Naessens *et al.*, 2005; Siakotos *et al.*, 1965; Varshosaz, 2012; Walton, 1952). Furthermore, dextran of *Lc. mesenteroides* NRRL B-1498 has been reported to exhibit anti-corrosive activity on steel (Finkenstadt *et al.*, 2011). Despite the century-long exploitation of EPS-producing LAB in traditional food fermentations, α-glucans only received minor attention in the food industry so far (Zannini *et al.*, 2016). However, the interest in α-glucans increased in recent decades as they may act as natural, food-safe and functional additives that may reduce or even replace the external addition of conventional hydrocolloids (Giraffa, 2004; Leemhuis *et al.*, 2013b; Leroy *et al.*, 2004; Torino *et al.*, 2015). In this sense, dextran produced by *Weissella cibaria* and *Limosilactobacillus* (*L.*) *reuteri* (formerly *Lactobacillus reuteri* (Zheng *et al.*, 2020)) strains has been reported to enhance the moisture content of cheddar and therefore improves the texture of cheese (Lynch *et al.*, 2014). Compared to their non-glucan-forming counterparts, dextran-producing *Latilactobacillus* (*L.*) *curvatus* and *sakei* (formerly

Lactobacillus curvatus (Zheng *et al.*, 2020)) strains were furthermore shown to improve the spreadability of fat-reduced raw fermented sausages that would otherwise exhibit a reduced spreadability due to their low fat content (Hilbig *et al.*, 2020; Prechtl *et al.*, 2018a; Prechtl *et al.*, 2018b). Moreover, the α-glucan producing potential of several strains of the genera *Weissella* and *Leuconostoc*, as well as of the *Lactobacillaceae* family (e.g. *L. curvatus*, *L. reuteri*) appeared to improve the water-binding capacity of (gluten-free) sourdough breads, which may reduce crumb-hardness and enhance shelf-life, texture of the breads, as well as machinability of the dough (Bounaix *et al.*, 2010a; Galle *et al.*, 2010; Galle *et al.*, 2012; Rühmkorf *et al.*, 2012; Wolter *et al.*, 2014a; Wolter *et al.*, 2014b). Beyond the physico-chemical properties described above, α-glucans are known to be non-degradable by mammalian digestive enzymes. Therefore, they may be considered as low-calory dietary fibers, as they do not release large amounts of glucose during digestion and were shown to induce satiety in humans (Gangoiti *et al.*, 2018). Furthermore, the production of GOS is a growing market, as GOS may serve as prebiotics that enhance gut-health by promoting the growth of beneficial bacteria (Gibson *et al.*, 1995; Kim *et al.*, 2021; Lee *et al.*, 2019; Sarbini *et al.*, 2014). Since GH70 enzymes are efficient in transglycosylation of other carbohydrate and non-carbohydrate acceptors, which commonly occurs at the expense of polymeric glucan, a vast variety of different oligosaccharides with putative beneficial health effects may be synthesized (Monsan *et al.*, 2010). Therefore, oligosaccharides obtained from acceptor reactions of gentibiose with alternansucrase were shown to be selectively fermented by some beneficial gut microbes. However, the authors of one of the studies raised some concerns about the health-promoting effects, as the applied gentibiose-derived oligosaccharides simultaneously led to an increase in the number of *Clostridia* (Rycroft et al., 2001; Sanz et al., 2006). Furthermore, acceptor-reaction products of maltose obtained with alternansucrase or dextransucrase were shown to exhibit prebiotic effects on artificial gut-microbiota consortia (Mäkeläinen *et al.*, 2009; Robyt *et al.*, 1978; Sanz *et al.*, 2005). Similar effects have been investigated and observed also for other glycosylation products of glucansucrases (Bivolarski *et al.*, 2018; Côté *et al.*, 2009).

In order to improve the techno-functional properties of foods, the food industry especially focused on the *in situ* formation of oligo- and polysaccharides to additionally profit from other beneficial compounds produced by the applied microorganisms, as specified below (Torino *et al.*, 2015). Furthermore, recent trends in consumer´s lifestyles towards a healthy and more "natural" diet reduced the acceptance of external additives. The *in situ* formation of α-glucans is thus a promising yet faintly exploited possibility to improve the techno-functional properties of processed foods with "clean label" status (Asioli *et al.*, 2017; Sloan, 2018; Torino *et al.*,

2015). As a consequence, the demand for these natural ingredients is high, while knowledge on well-characterized glucansucrases and their producing strains, as well as sophisticated processes yielding tailored oligo- and polysaccharides is lacking behind (Hugenholtz, 2008; Torino *et al.*, 2015).

Moreover, there is a particular need for new polysaccharide-producing strains that are adapted to ferment plant-derived substrates, as the demand for plant-based alternatives to conventional animal products is evermore increasing (Craig, 2010; Fehér *et al.*, 2020; Hughes, 1995; Rotz *et al.*, 2010).

In general, LAB have a long history in food fermentations. Herein, they are exploited to preserve foods by lowering the pH upon acid formation and by producing antimicrobial compounds (De Vuyst *et al.*, 2007; Leroy *et al.*, 2004). Furthermore, they produce compounds of nutritional and sensorial value, such as bioactive peptides, vitamins, low-calory sweeteners and flavour compounds (Ardö, 2006; Hugenholtz, 2008; Hugenschmidt *et al.*, 2010; LeBlanc *et al.*, 2011; Martinez-Villaluenga *et al.*, 2017; Masuda *et al.*, 2012; Ortiz *et al.*, 2013). Some LAB are even considered as probiotics conferring health benefits (Azaïs-Braesco *et al.*, 2010). LAB that have been isolated from traditional fermented foods are generally recognised as save (GRAS) and are thus ready to be applied in novel food fermentations (Leroy *et al.*, 2004). Therefore, searching for α-glucan-producing LAB within traditionally fermented foods is reasonable, while they are easily distinguishable by their mucoid phenotype on solid media containing sucrose (Sutherland, 1972). Consequently, such LAB strains have been successfully isolated from diverse sources, such as sourdough, fermented vegetables (e.g. kimchi, sauerkraut), raw sausage-fermentations, wine and water kefir (Bounaix *et al.*, 2010a; Bounaix *et al.*, 2010b; Choi *et al.*, 2012; Dimopoulou *et al.*, 2014; Gulitz *et al.*, 2011; Kim *et al.*, 2008; Rühmkorf *et al.*, 2013; Wang *et al.*, 2019; Yang *et al.*, 2015).

1.4 Water kefir as a reservoir for α-glucan producing lactic acid bacteria

Water kefir is traditional plant-based fermentation leading to a sour, fruity, carbonated and slightly alcoholic beverage that is prepared from water, high amounts of sucrose, dried or fresh fruits (e.g. figs or raisins) and lemon slices (Gulitz *et al.*, 2011; Pidoux, 1989; Verce *et al.*, 2019). As shown in Figure 3, water kefir is divided into two “phases”: the upper liquid and turbid phase that comprises the actual drinkable beverage and the bottom phase that is made up from slightly translucent, water-insoluble grains. The beverage itself is believed to exhibit anti-inflammatory, antibacterial, anti-hyperglycemic, anti-allergic and further beneficial health

effects, while the inhabiting microorganisms are considered with a “history of safe use” for consumption or even probiotic (Angelescu *et al.*, 2019; Engel *et al.*, 2011; Fiorda *et al.*, 2017; Golowczyc *et al.*, 2007; Koh *et al.*, 2018; Leite *et al.*, 2015; Moreira *et al.*, 2008; Rodrigues *et al.*, 2016).

Each fermentation cycle is started by back-slopping of the kefir grains that are also named “ginger beer plant”, “Japanese beer seeds”, “Tibi” or “Tibicos” and are commonly passed on between private households (Kebler, 1921; Lutz, 1899; Marsh *et al.*, 2013; Ward, 1892). The grains constitute a biofilm that predominantly consist of polysaccharides, which harbour a specialized and stable, presumably symbiotic multi-species consortium that generally comprises LAB, acetic acid bacteria and yeasts (Gulitz *et al.*, 2011; Laureys *et al.*, 2014; Pidoux, 1989). Moreover, *Zymomonas* species were detected by culture-independent methods, while *Bifidobacteria* were described as stable part of the water kefir microbiota very recently (Eckel *et al.*, 2020a; Eckel *et al.*, 2020b; Gulitz *et al.*, 2013; Laureys *et al.*, 2016; Marsh *et al.*, 2013).

Figure 3 Home-made fermented beverage water kefir.

Although, water kefir has been a matter of research for a long time already, it was neither possible to reconstitute granule formation nor to entirely elucidate the complex processes that

are involved in the formation of this beverage so far (Eckel *et al.*, 2020a; Laureys *et al.*, 2018; Verce *et al.*, 2019).

The microorganisms need to cope low amino acid concentrations, high osmotic pressure due to high sucrose concentrations, low pH, as well as increasing amounts of alcohol during fermentation and thus need to be perfectly adapted to survive in the challenging water kefir environment. Furthermore, the inhabiting microorganisms have to compete for the scarce resources (Gulitz *et al.*, 2011; Laureys *et al.*, 2014). Therefore, maintaining synergistic relationships with other species within the consortium may represent a decisive strategy to sustain in this environment. As such, Stadie *et al.* (2013) could show that *Liquorilactobacillus* (*L.*) *hordei* and *L. nagelii* (formerly *Lactobacillus hordei* and *L. nagelii* (Zheng *et al.*, 2020)) profit from amino acids and vitamin B_6 released by the yeast *Zygotorulaspora florentina*, while the yeast *vice versa* appreciates the acidic environment generated by LAB. Most water kefir related studies focused on the microbial diversity of the beverage, however, few also described the metabolites that are generated upon fermentation and thus contribute to aroma formation. Besides lactic and acetic acid, ethanol and carbon dioxide formation, also glycerol and mannitol production were observed during water kefir fermentation (Laureys *et al.*, 2014; Verce *et al.*, 2019). Furthermore, the consortium produced volatile compounds, including ethyl acetate, isoamyl acetate, ethyl octanoate, 2-methyl-1-propanol, ethyl decanoate, ethyl hexanoate and isoamyl alcohol (Laureys *et al.*, 2014; Laureys *et al.*, 2017).

In order to sustain in the water kefir environment, the inhabiting microbiota must be well prepared for an efficient degradation of sucrose, as water kefir is otherwise poor in nutrients (Gulitz *et al.*, 2011; Verce *et al.*, 2019). This may not be achieved only by up-take and intracellular sucrose metabolism, but also by extracellular invertases, splitting sucrose into glucose and fructose, and glucan- or fructansucrases, leading to the formation of polysaccharides upon glucose or fructose release. While invertases were reported to be encoded by water kefir yeasts, the presence of EPS-producing LAB and acetic acid bacteria was described in several studies (Fels *et al.*, 2018; Gulitz *et al.*, 2011; Jakob *et al.*, 2012; Verce *et al.*, 2019; Xu *et al.*, 2018). Especially the acetic acid bacterium *Gluconobacter albidus* TMW 2.1191 has been extensively characterized for its fructan-producing capabilities, as well as the exploitation of such in gluten-free sourdoughs (Jakob *et al.*, 2020; Jakob *et al.*, 2012; Ua-Arak *et al.*, 2016, 2017a, 2017b). Regarding glucan formation in water kefir, the only available study on the identification and characterization of a glucansucrase was performed for a strain of the species *Lentilactobacillus* (*L.*) *hilgardii* (formerly *Lactobacillus hilgardii* (Zheng *et al.*, 2020)), which produces a water-insoluble dextran that is mainly found within the kefir granules

(Waldherr *et al.*, 2010). Therefore, several studies proposed that the kefir granules are mainly produced by this species (Fels *et al.*, 2018; Pidoux, 1989; Waldherr *et al.*, 2010). In this sense, knowledge on the presence, distribution and characteristics of glucansucrases among water kefir-derived LAB, as well as their individual roles in the shaping of this habitat may largely contribute to a better understanding of the complex processes involved in water kefir formation. Additionally, water kefir represents a yet unexplored reservoir of LAB with potentially new types of glucansucrases that may be applied in novel food and beverage fermentations.

2 Motivation and aims of this work

Water kefir is a traditional fermented beverage inhabited by various LAB that are specialized to subsist in and shape this environment. The adaptative strategies of the inhabiting LAB towards the fermentation of these plant-derived substrates are unknown so far, hindering an understanding of the establishment and cooperation of the microbiota of water kefir and finally of the formation of the beverage itself. Furthermore, the glucan-synthesizing capabilities of some of these LAB are important for the formation of this habitat and beverage, while certain strains may hence be exploited biotechnologically in novel (plant-based) food fermentations and also for the production of tailored α-glucans. However, the role of certain glucansucrases in the shaping of the two-phase habitat of water kefir to harbour a specialized biofilm consortium remains unknown. Also, a detailed understanding is missing of the enzymes to (i) produce tailored polysaccharides of the desired techno-functional characteristics, (ii) exploiting glucan-producing strains as starter cultures in novel applications and (iii) understand mechanisms of the establishment of the water kefir consortium. This includes a knowledge gap on the conditions influencing glucansucrase formation within the respective microorganisms, as well as an understanding of reactions that may occur in addition or competing to the glucansucrase reaction. This work is therefore divided into two parts based on the following working hypotheses and experimental approaches:

Water kefir contains a variety of α-glucan-producing LAB and formation of these polysaccharides is attributable to the expression of a glucansucrase encoded by the respective LAB strain.

- LAB isolated from water kefir should be investigated for their potential to form α-glucans by culture-dependent methods and subsequent investigation of the produced EPS.
- Potential glucansucrase genes should be identified within candidate strains using bioinformatic and molecular biological methods.
- The characteristics of glucan-formation by these enzymes should be elucidated using either the native or heterologously expressed enzymes.

LAB from water kefir are specifically adapted to this environment.

- The genetic adaptation of candidate strains from part A should be deduced by comparative genomics and physiological characterization.
- Reactions that take place in addition or in competition to the glucansucrase reaction should be investigated using bioinformatic analysis of the carbohydrate metabolism, as well as analysis of the proteomic states under glucan-forming conditions.

3 Materials and Methods

3.1 General microbiological techniques

3.1.1 Strains and culture conditions

Bacterial cultures were stored at – 80 °C in the respective cultivation medium containing 34 % (v/v) glycerol.

LAB isolated from water kefir or obtained from strain collections were cultivated statically in liquid modified MRS medium (mMRS) (10 g/L soy peptone, 5 g/L yeast extract, 10 g/L meat extract, 2 g/L dipotassium phosphate, 5 g/L sodium acetate, 2 g/L ammonium citrate, 0.2 g/L magnesium sulfate, 0.05 g/L manganese sulfate, 1 g/L Tween80, 25 g/L glucose, pH 6.2)(De Man *et al.*, 1960) at 30 °C. Depending on the experiment, glucose was replaced by sucrose, fructose or a mixture of glucose and fructose (12.5 g/L each).

Strains of *Escherichia* (*E.*) *coli* and *Micrococcus* (*M.*) *luteus* were cultivated in lysogeny broth (LB-Lennox, 10 g/L tryptone, 5 g/L yeast extract, 5 g/L sodium chloride, pH 7.2).

For solid media, 15 g/L agar were added. After pH adjustment, the solutions were sterilized by autoclaving for 20 min at 121 °C. Sugars were autoclaved separately and added to the cooled media.

Precultures of LAB were prepared in 15 mL of liquid mMRS medium in closed vessels (Sarstedt AG & Co., Germany) by direct inoculation from cryopreserved cultures and incubation for 48 h at 30 °C. Cultures of *E. coli* and *M. luteus* were prepared by inoculating cell material either grown on solid media or directly from cryopreserved culture and subsequent incubation at 37 °C and 200 rpm. Strains used or isolated in this study are listed in Table 1.

Table 1 Bacterial strains used in this study

Species	TMW-Strain	Source of isolation
L. hilgardii	1.1819	Water kefir A[1]
L. hilgardii	1.828	Water kefir[2]
L. hilgardii	1.2196	Water kefir A[1]
L. hilgardii	1.45^T (= DSM 20176^T)	Wine
L. hordei	1.1817	Water kefir A[1]
L. hordei	1.1821	Water kefir A[1]
L. hordei	1.1822	Water kefir F[1]
L. hordei	1.1907	Water kefir W[1]
L. hordei	1.2353^T (= DSM 19519^T)	Malted barley
L. hordei	1.2375	Water kefir[3]
L. hordei	1.2376	Water kefir[3]
L. hordei	1.2377	Water kefir[3]
L. nagelii	1.1823	Water kefir A[1]

L. nagelii	1.1824	Water kefir F[1]
L. nagelii	1.1825	Water kefir W[1]
L. nagelii	1.1826	Water kefir F[1]
L. nagelii	1.1827	Water kefir F[1]
L. nagelii	1.2352^T (= DSM 13675^T)	Partially fermented wine
L. satsumensis	1.1829	Water kefir F[1]
Lc. mesenteroides	2.1073	Water kefir A[1]
Lc. mesenteroides	2.1075	Water kefir F[1]
Lc. mesenteroides	2.1076	Water kefir F[1]
Lc. mesenteroides	2.1195	Water kefir W[1]
Lc. citreum	2.1194	Water kefir W[1]
E. coli K12 DH5α	2.582	
E. coli ROSETTA	2.1106	
M. luteus	2.96	

[1] Dissertations Anna Gulitz and Jasmin Stadie (Gulitz, 2013; Stadie, 2013)
[2] Isolated from household water kefir of Florian Waldherr (2010)
[3] Isolated in this study

3.1.2 Isolation of lactic acid bacteria from water kefir

A water kefir culture was obtained from wellness-drink.de and was subsequently propagated two times. Therefore, kefir grains were inoculated into tibi medium that was prepared from 100 g/L sucrose, one dried fig per liter cut into pieces (unsulfurated, Seeberger, Germany) and a 0.5 cm wedge-shaped lemon segment (bio quality, obtained from a local supermarket) per liter in tab water. The mixture was stirred at room temperature for 3 h and subsequently filtered (270 mm pleated filter, REF 591027, Machery-Nagel, Düren, Germany) to remove any solid parts. Afterwards, the medium was sterilized by autoclaving for 20 min at 121 °C. The inoculated kefir culture was allowed to grow for 2 days at room temperature. To isolate LAB, water kefir granula were washed with sterile saline (0.9 % (w/v) sodium chloride). Subsequently, 10 g of granula were mixed with 90 mL of saline and homogenized. A serial dilution of this homogenizate was then plated on mMRS agar containing 30 mg/L nystatin to avoid the growth of yeasts.

3.1.3 Strain verification using MALDI-TOF MS

Identification and verification of microbial strains was performed on species level using matrix assisted laser desorption ionization – time of flight mass spectrometry (MALDI-TOF MS). Therefore, single colonies of microorganisms grown on agar plates for 48 h at 30 °C were directly applied to a stainless steel target (Bruker Daltonics, Germany) using sterile toothpicks. Subsequently, 1 µl of formic acid (70 % (v/v), Sigma-Aldrich GmbH, Germany) was applied to each spot, followed by 1 µl of an α-cyano-4-hydroxycinnamic acid matrix solution (Bruker

Daltonics, Germany). Mass spectrometry was carried out with a Microflex LT MALDI-TOF MS (Bruker Daltonics, Germany) equipped with a nitrogen laser (λ = 337 nm). Mass spectra were obtained in a linear positive ion detection mode under the control of Biotyper Automation Control 3.0 (Bruker Daltonics, Germany) (Usbeck *et al.*, 2013).

3.1.4 Determination of viable cell counts

For the determination of viable cell counts (cfu/mL) in bacterial cultures, 100 µl of appropriate dilutions in Ringer´s solution (Merck KGaA, Darmstadt, Germany) were spread on mMRS agar plates using sterile glass beads (2.7 mm, Carl Roth GmbH, Karlsruhe, Germany) and incubated at 30 °C for 48 h.

3.1.5 Determination of growth characteristics

Cells were pre-cultured as stated in section 3.1.1. Subsequently, pre-cultures were used to inoculate liquid mMRS media containing either glucose, fructose, sucrose or a mixture of glucose and fructose to a final OD_{590nm} of 0.1. Growth experiments were carried out in a volume of 250 µl in 96-well plates (Sarstedt AG & Co., Nümbrecht, Germany) overlaid with 50 µl paraffin oil to prevent cultures from desiccation. In the absence of paraffin oil, the outer wells of the 96-well plates were filled with sterile dest. H_2O. Automated monitoring of cell growth was performed by OD_{590nm} measurement every 30 min for 30 h at 30 °C on a SPECTROstar Nano Platereader (BMG Labtech, Ortenburg, Germany). Prior to each measurement, plates were shaken at 400 rpm for 30 s. The grofit package for RStudio (v. 3.3.3) was used to determine maximum growth rates (μ_{max}) and time spans of lag-phases (λ), as it was described by Kahm et. al. (Kahm *et al.*, 2010). The same mMRS media were used to monitor continuous acidification during microbial growth for 30 h in the iCinac system (AMS, Frépillon, France). Therefore, 30 mL of growth medium was inoculated to a final OD_{590nm} of 0.1, respectively, and subsequently incubated at 30 °C in a water bath.

To determine the respective cell density at mid-exponential growth phase for further experiments, cell growth was monitored manually in a higher culture volume of 50 mL in closed reaction vessels (50 mL, Sarstedt AG & Co., Nümbrecht, Germany) using mMRS medium with glucose. Therefore, 1 L of medium was inoculated to an OD_{590nm} of 0.1 and subsequently split into 20 reaction vessels that were incubated at 30 °C for at least 40 h. Every 2-3 h one of these cultures was taken for subsequent cell density measurement. After the sedimented cultures were mixed by inverting, 1 mL of culture was transferred to a cuvette (1 mL polystyrol, Sarstedt AG & Co., Nümbrecht, Germany) and cell density was measured at a wavelength of 590 nm in a

spectrophotometer (Novaspec Plus, GE Healthcare Company, Chicago, IL, USA). The cultures were diluted appropriately in mMRS medium, if that was necessary to remain within the range of $OD_{590nm} \leq 1.0$. All experiments were performed as biological triplicates.

The ability of the tested microorganisms to ferment certain carbohydrates was investigated using API®50 CHL test stripes (bioMérieux, Marcy-l´Étoile, France) according to the manufacturer´s instructions. Therefore, bacterial cultures were grown in 15 mL of mMRS medium for 24 h at 30 °C. The cells were harvested by centrifugation at 3000 xg for 5 min at 4 °C. After discarding the medium, the cell pellets were washed twice in sterile Ringer´s solution (Merck KGaA, Darmstadt, Germany) and were finally resuspended in mMRS medium containing no glucose, but 0.17 g/L of bromcresol purple at a pH of 6.7. The test stripes were incubated at 30 °C for 7 days and were checked daily for positive results that were indicated by a colour change from purple to yellow.

3.2 Molecular biological techniques

3.2.1 Isolation of genomic DNA

To obtain genomic DNA for subsequent analyses, microbial cultures were grown for 24 h at 30 °C in 15 mL liquid mMRS medium supplemented with glucose. Subsequently, 4 mL of these cultures were pelletized by centrifugation (4000 xg, 5 min, 4 °C) and washed once with a Tris-EDTA buffer (10 mM Tris-HCl, 10 mM EDTA, pH 8.0). The DNA was isolated using the E.Z.N.A™ Bacterial DNA Kit (Omega Bio-Tek Inc., Norcross, GA, USA) according to the manufacturer´s instructions, but with a prolonged incubation time of 2 h for cell lysis.

To obtain high molecular weight DNA for subsequent PacBio sequencing, the method of Wright et al. was applied (Wright *et al.*, 2017). Therefore, cells were grown as stated above and 10 mL of each culture were pelletized by centrifugation at 7500 xg for 10 min at 4 °C. The supernatant was discarded and the cell pellet was resuspended in 467 µL Tris-EDTA buffer (50 mM Tris, 10 mM EDTA, pH 8.0) containing 100 µg/mL RNAse A (ThermoFisher Scientific, Waltham, MA, USA). The suspension was transferred to a 1.5 mL microcentrifuge tube (Sarstedt AG & Co., Nümbrecht, Germany) and added with 8 µL lysozyme (24,000 kU/mL, SERVA Electrophoresis GmbH, Heidelberg, Germany) and 5 µL achromopeptidase (50 kU/mL, Sigma-Aldrich, St. Louis, MO, USA). After gentle mixing, the suspension was incubated for 60 min at 37 °C in a water bath. Afterwards, 30 µL of sodium dodecyl sulfate (SDS, 10 % (w/v), SERVA Electrophoresis GmbH, Heidelberg, Germany) and 3 µL proteinase K (20 mg/mL, ThermoFisher Scientific, Waltham, MA, USA) were added, followed by gentle

inverting of the mixture and subsequent incubation for 60 min at 50 °C. To separate the DNA from other cellular components, 525 µL of UltraPure™ Phenol:Chloroform:Isoamylalcohol (25:25:1 (v/v), ThermoFisher Scientific, Waltham, MA, USA) were added. Subsequently, the solution was mixed for 10 min by gentle inversion prior to centrifugation at 12,000 xg for 15 min. Without disturbing the bilayer, the upper aqueous phase was transferred to a fresh 1.5 mL microcentrifuge tube and the DNA was subsequently precipitated with ice-cold ethanol (99 % (v/v), Carl Roth GmbH, Karlsruhe, Germany). After centrifugation at 12,000 xg for 20 min at 4 °C, the supernatant was discarded and the DNA was washed once with ice-cold ethanol and centrifugation. The supernatant was decanted and the pelletized DNA was dried at room temperature. Finally, the DNA was resuspended overnight at 4 °C in 50 µL Tris buffer (10 mM Tris, pH 8.0). The quality of the high molecular weight DNA was checked by agarose gel electrophoresis (see 3.2.4).
Quantitation and purity control of DNA samples was performed on a NanoDrop® ND-1000 spectrophotometer (PeQlab Biotechnologie GmbH, Erlangen, Germany).
All DNA samples were kept at – 20 °C until further use.

3.2.2 Isolation of plasmid DNA

Cells were grown as stated in section 3.2.1 and 4 mL of bacterial culture were used for subsequent plasmid DNA isolation. Therefore, either the Monarch® Plasmid DNA Miniprep Kit (New England BioLabs Inc., Ipswich, MA, USA) or the QIAprep Spin Miniprep Kit (Qiagen, Hilden Germany) was used according to the manufacturer´s instructions. Plasmid samples were kept at – 20 °C until further use.

3.2.3 PCR amplification

Polymerase chain reaction (Saiki *et al.*, 1988) was performed for randomly amplified polymorphic DNA (RAPD-PCR)(Williams *et al.*, 1990) or for specific amplification of target sequences using the *Taq* DNA CORE Kit 10 (MP Biomedicals, Irvine, CA, USA). For specific amplifications, 2.5 µL *Taq* 10× buffer with magnesium chloride, 0.5 µL dNTPs (10 mM each), 1 µL forward primer (50 mM), 1 µL reverse primer (50 mM), 0.25 µL *Taq*-polymerase (5 u/µL) and 18.75 µL PCR-H_2O were mixed with 1 µL of template DNA. For RAPD-PCR, 5 µL *Taq* 10× buffer without magnesium chloride, 10 µL magnesium chloride (25 mM), 2 µL dNTPs (10 mM each), 0.5 µL M13V-primer, 0.3 µL *Taq*-polymerase (5 u/µL) and 32.2 µL deionized H_2O (dH_2O) were mixed with 1 µL of template DNA. Primers used in this study are listed in Table 2.

Table 2 Primers used for RAPD-PCR and specific detection of glucansucrase genes.

Primer	Sequence (5´→ 3´)	Annealing temperature	Product length	Application
M13V	GTTTTCCCAGTCACGAC	See below	-	RAPD-PCR
DSc_2906-forward	CAMAWGTTATYTWTCAAGGC	52.5 °C	315 bp	Detection of various glucansucrases
DSc_2906-reverse	ACCCAATCALCAATTGCYT			
Hordei-Dsr-forward	TTCAAGCAGCWACTAACGGM	64 °C	691 bp	Detection of *L. hordei* type glucansucrase
Hordei-Dsr-reverse	GCWCCWGCTGGCACCCAGAC			
Nagelii-Dsr-forward	CGCAGTATCGGACAAGTGGT	63 °C	825 bp	Detection of *L. nagelii* type glucansucrase
Nagelii-Dsr-reverse	CAGTCTCCATCGCTCCTGTC			
Hilgardii-Dsr-forward	ACGRACTCAAGGGATGGSWG	62 °C	271 bp	Detection of *L. hilgardii* type glucansucrase
Hilgardii-Dsr-reverse	AACCCAGGCGGCYAAGTAKC			

For amplification using specific primers, denaturation of the DNA templates was performed at 95 °C for 1 min, followed by primer annealing for 45 s and elongation for 1 min at 72 °C. After 28 cycles, products were finally elongated for 10 min at 72 °C. For RAPD-PCR, denaturation was carried out at 95 °C for 3 min, followed by annealing at 40 °C for 5 min and elongation at 72 °C for 5 min for three cycles. Then, denaturation was performed at 94 °C for 1 min, followed by annealing at 60 °C for 2 min and elongation at 72 °C for 3 min. After 32 cycles, final elongation was done at 72 °C for 5 min.

3.2.4 Agarose gel electrophoresis

PCR products (see section 3.2.3), as well as purified DNA (see sections 3.2.1 and 3.2.2) samples were applied for analytical agarose gel electrophoresis (Sambrook *et al.*, 1989). Therefore, samples were mixed with 6x loading dye (ThermoFisher, Rockford, IL, USA) and subsequently applied on an agarose (1 % (w/v)) gel in 1× TAE buffer (40 mM Tris, 20 mM acetic acid, 1 mM EDTA, pH 8.2). Electrophoresis was carried out for 90 min at 100 V in a PeQLab electrophoresis chamber (PeQLab Biotechnologie GmbH, Erlangen, Germany), driven by an electric power supply (Power Pack P25, Biometra GmbH, Göttingen, Germany). For analysis

of purified high molecular weight DNA, only 0.5 % (w/v) of agarose was applied. A 1kb oder 100 bp DNA ladder (ThermoFisher Scientific, Waltham, MA, USA) was applied as reference. RAPD patterns were obtained by agarose (1.4 % (w/v)) gel electrophoresis in 0.5× TBE buffer (45 mM Tris-HCl, 45 mM boric acid, 1 mM EDTA, pH 8.0) and electrophoresis was carried out at 150 V for 2.5 h. As reference, the λ-DNA/EcoRI + HindIII ladder (ThermoFisher Scientific, Waltham, MA, USA) was applied.

After electrophoresis, DNA was stained in a saturated dimidium bromide solution (Carl Roth GmbH, Karlsruhe, Germany) for 10 min, followed by washing in dH_2O for 10 min. Finally, DNA visualization was performed with an UVT-28M transilluminator (Herolab, Wiesloch, Germany).

3.3 Proteinchemical methods

3.3.1 Protein quantification

Protein amounts were quantified according to the method of Bradford (Bradford, 1976). Each sample was diluted appropriately in dH_2O and analyzed as technical triplicates using the Coomassie (Bradford) Protein Assay Kit (ThermoFisher Scientific, Waltham, MA, USA) according to the manufacturer´s instructions on the standard microplate or micro-microplate procedure. The measurements were carried out at 595 nm in a FLUOstar Omega Microplate reader (BMG Labtech, Ortenburg, Germany). Finally, protein amounts were quantified according to standard dilution series of bovine serum albumin (BSA) included within the assay kit.

3.3.2 SDS-PAGE and sample preparation

Proteins were separated by vertical sodium dodecyl sulfate polyacrylamide gel electrophoresis (SDS-PAGE) (Laemmli, 1970), carried out in a Mini-PROTEAN Tetra Cell Electrophoresis System (Bio-Rad laboratories, Hercules, USA). The recipe for a separation gel (10 % (w/v)) and a stacking gel (4 % (w/v)) that were used in this study is shown in Table 3.

Table 3 Recipies for the preparation of two SDS gels with a resolving and a stacking gel.

Compound	Separation gel	Stacking gel
Acrylamid/Bis 37.5:1 (30 % (w/v))	3.33 mL	0.53 mL
dH_2O	4.01 mL	2.40 mL
Tris buffer (1.5 M Tris-HCl, pH 8.8)	2.5 mL	-
Tris buffer (0.5 M Tris-HCl, pH 6.8)	-	1.00 mL
SDS (10 % (w/v))	100 µL	40 µL
Tetramethylethylendiamine (TEMED)	5 µL	4 µL
Ammonium persulfate (APS, 10 % (w/v))	50 µL	20 µL

After mixing of the separation gel compounds, the solution was immediately poured between a spacer plate (1 mm) and a cover plate (Bio-Rad laboratories, Hercules, USA) and covered with 100 µL isopropanol to obtain a straight surface. Once polymerization was finished, the isopropanol was discarded and the separation gel was overlaid with the stacking gel. Ten sample slots were generated by insertion of a comb (1 mm, Bio-Rad laboratories, Hercules, USA) to the non-polymerized stacking gel. SDS-PAGE was carried out in 1x Tris-glycine running buffer (3 g/L Tris base, 14.4 g/L glycine, 1 g/L SDS). Separation was initially started at 100 V for 10 min and continued at 150 V for 60 min, driven by a Power Pack 3000 unit (Bio-Rad laboratories, Hercules, USA). If not stated otherwise, samples were mixed with 2× Laemmli sample buffer (Sigma-Aldrich, St. Louis, USA) and denatured at 90 °C for 10 min. Subsequently, 15 – 20 µL of each prepared sample were applied onto the SDS-gel. 4 µL of the PageRuler Plus Prestained Protein Ladder (ThermoFisher Scientific, Waltham, MA, USA), that provides a protein ladder from 10 – 250 kDa, served as a marker for molecular weight estimation of analyzed proteins.

3.3.3 Staining procedures

3.3.3.1 Silver and Coomassie staining

After SDS-PAGE, proteins were visualized by either silver staining or Coomassie staining. Silver staining was performed according to the method of Blum *et al.* (Blum *et al.*, 1987). Therefore, proteins were fixed for a minimum of 4 h in fixation solution (40:10 % (v/v) ethanol : acetic acid in dH_2O) and subsequently washed two times for 20 min in washing solution

(30 % (v/v) ethanol), followed by a washing step in dH_2O for 20 min. The gels were then incubated for a maximum of 60 s in thiosulphate solution (0.2 g/L sodium thiosulphate) for sensitization. After washing the gels in dH_2O three times for 20 s in dH_2O, proteins were labelled for 20 min with silver solution (2 g/L silver nitrate). Following washing of the gels three times for 20 s in dH_2O, the gels were transferred to a freshly prepared developer solution (30 g/L sodium carbonate, 0.005 g/L sodium thiosulfate, 0.37 % formaldehyde) and incubated until protein bands occurred (~ 3 – 5 min). After shaking in dH_2O for three times a´ 20 s, gels were finally transferred to a stopping solution (5 g/L glycine).
As an alternative for silver staining, Coomassie staining was applied. Therefore, proteins were stained using the Roti® Blue colloidal CBBG-250 staining solution (Carl Roth GmbH, Karlsruhe, Germany) according to the manufacturer´s instructions.
If not stated otherwise, all steps were carried out on a shaker at room temperature.

3.3.3.2 Activity staining of glucansucrases

To specifically detect glucansucrases among other proteins after SDS-PAGE, an activity staining was applied. Thereby, the glucansucrases produced glucan within the gels, which was then visualized by periodic acid Schiff´s staining (Miller *et al.*, 1986; Zacharius *et al.*, 1969). In a first step after electrophoresis, SDS gels were washed three times for 10 min in renaturing buffer (20 mM sodium acetate, 0.3 mM $CaCl_2$, 0.1 % Tween 80, pH 5.4) at 4 °C. Subsequently, gels were incubated in the same buffer containing 5 % (w/v) sucrose, at 30 °C overnight. Afterwards, the gels were washed for 30 min in washing solution (50 % (v/v) methanol, 10 % (v/v) acetic acid in dH_2O) followed by washing in dH_2O for 30 min. The formed glucans were then oxidized by incubation in freshly prepared periodic acid solution (1 % (w/v) periodic acid, 3 % (v/v) acetic acid) for 45 min followed by another washing step in dH_2O for 1 h. Finally, staining of the polysaccharides was performed by incubation in Schiff´s reagent (Sigma-Aldrich, St. Louis, USA) until discrete magenta bands appeared (~ 2 – 8 min). Subsequently, the gels were washed in dH_2O for 5 min. If not stated otherwise, all steps were carried out at room temperature.

3.3.3.3 Glycoprotein staining

The detection of glycoproteins after SDS-PAGE was performed applying periodic acid Schiff´s staining according to the method of Zacharius *et al.* (Zacharius *et al.*, 1969) as already described in section 3.3.3.2, using the Pierce™ Glycoprotein Staining Kit (ThermoFisher, Scientific, Waltham, MA, USA) according to the manufacturer´s instructions. However, gels were stained

directly after electrophoresis and no glucan was formed within SDS-gels prior to staining. As the method is quite insensitive (detection limit = 1 mg/mL of glycoprotein), proteins were concentrated prior to analysis. Therefore, 45 mL of protein samples (obtained from supernatants of buffered cell suspensions, section 3.4.2.1) were precipitated with 100 % (w/v) ammonium sulfate and left overnight at 4 °C. After centrifugation for 15 min at 10,000 xg and 4 °C, the supernatants were decanted and proteins were redissolved in 0.5 mL dH_2O.

3.3.4 Zymogram analysis of lytic enzymes

In order to detect cell wall degrading enzymes in culture supernatants, zymogram analysis was performed according to the method of Lepeuple *et al.* (Lepeuple *et al.*, 1998). Therefore, SDS-gels were prepared as stated in section 3.3.2, but the 1.5 M Tris buffer used for the preparation of the separation gels was replaced by the same Tris buffer containing heat-inactivated bacterial substrate (cells of *L. hordei* TMW 1.1822, *L. nagelii* TMW 1.1827 or *M. luteus* TMW 2.96). Bacterial substrates of *L. hordei* TMW 1.1822 and *L. nagelii* TMW 1.1827 were prepared by inoculation of 50 mL liquid mMRS medium to an OD_{590nm} of 0.1 using freshly prepared pre-cultures. Cells were then grown to mid-exponential growth phase and harvested by centrifugation for 5 min at 3000 xg and 4 °C. The resulting cell pellet was washed once with 5 mL of Tris buffer (20 mM Tris, 100 mM NaCl, pH 7.4, 4 °C) and finally resuspended in 4 mL of the buffer used for the preparation of SDS-gels. Prior to use, the bacterial substrates were heat-inactivated by incubation at 95 °C for 10 min. Cells of *M. luteus* TMW 2.96 were directly inoculated from cryopreserved culture into LB-Lennox medium and grown overnight at 37 °C and 200 rpm. Harvesting of the cells was performed as described for *L. hordei* and *L. nagelii*.
Prior to loading on the gel, samples were mixed with 2x native PAGE sample buffer (60 g/L Tris base, 40 g/L SDS, 20 % (v/v) glycerol (87 %), traces of bromophenol blue) and incubated at 50 °C for 10 min. Following electrophoresis, gels were washed twice in dH_2O at room temperature on a shaker for 30 min. Subsequently, gels were shaken in renaturing buffer (20 mM Tris, 50 mM NaCl, 20 mM $MgCl_2$, 0.5 % Triton X-100, pH 7.4) for 30 min at room temperature. Afterwards, gels were incubated overnight at 30 °C in fresh renaturing buffer. To improve the visibility of lytic zones, gels were finally incubated in staining solution (1 g/L methylene blue, 0.1 g/L KOH) for 2 h at room temperature. Lytic zones appeared as clear bands against blue background.

3.4 Production and purification of EPS

3.4.1 Fermentative production of EPS

Fermentative production of EPS was performed in collaboration with Dr. Viktor Eckel at Technical Microbiology (TUM). Precultures of several LAB from water kefir were grown as stated in section 3.1.1 to inoculate 15 mL of mMRS supplemented with 20 g/L of sucrose to a final OD_{590nm} 0.1. These cultures were grown for 24 h and subsequently centrifuged for cell removal at 10000 xg and 4 °C for 15 min (*L. hilgardii* strains were centrifuged for 1 h). The supernatants were transferred to a fresh 50 mL reaction vessel and EPS was precipitated by 2 volumes of ice-cold ethanol (99 % (v/v)). Precipitation was carried out at overnight at 4 °C. Subsequently, the samples were centrifuged at 10000 xg and 4 °C for 20 min and supernatants were discarded. The pellets were resuspended in dH_2O and subjected for dialysis against dH_2O at 4 °C for 2 days with at least five exchanges of dH_2O using MEMBRA-CELL dialysis tubes (SERVA Electrophoresis GmbH, Heidelberg, Germany) with a molecular weight cut-off of 3.5 kDa. The purified glucan samples were subsequently lyophylized for 48 h. Finally, the monomer compositions of these EPS were determined (section 3.5.1).

3.4.2 Production and purification of glucans using native glucansucrases

3.4.2.1 Recovery of native glucansucrase containing supernatants from buffered cell suspensions

Crude enzyme extracts were obtained from buffered cell suspensions in order to identify glucansucrases in supernatants and their release conditions, as well as to analyze glucan formation of the native enzymes. Therefore, pre-cultures prepared as stated in section 3.1.1 were used to inoculate 45 mL mMRS medium supplemented with glucose to a final OD_{590nm} of 0.1 prior to incubation for 24 h at 30 °C. Subsequently, the cells were harvested by centrifugation at 5000 xg for 10 min at 4 °C. The resulting cell pellets were resuspended in 15 mL citrate-phosphate buffer (0.05 M citrate, 0.1 M disodium phosphate, pH 6.5) supplemented with either 0.05 M sucrose or no sucrose, respectively, which concentrated the cells three times. After incubation at 30 °C for 3 h, a 1 mL sample was taken for subsequent cell lysis by the addition of 10 mg/mL lysozyme (SERVA Electrophoresis GmbH, Heidelberg, Germany) and incubation at 37 °C for 2 h. The buffered cell suspensions were centrifuged at 5000 xg for 10 min at 4 °C to remove the cells, the pH was determined using a pH electrode (Mettler Toledo, Columbus, OH, USA) and the supernatants were subsequently filtered sterile (0.2 µm nylon filters, Phenomenex Inc., Torrance, CA, USA). Samples of cell-free supernatants

were taken for protein quantification (section 3.3.1), SDS-PAGE (section 3.3.2) and sugar quantification (section 3.5.1.2 and 3.5.2).

The culture volumes and starting pH values were subsequently varied. To identify glycosylated proteins in buffer supernatants, three volumes of the buffer supernatants (= 45 mL) prepared without sucrose were precipitated with 100 % (w/v) ammonium sulfate and left overnight at 4 °C. After centrifugation for 15 min at 10,000 xg and 4 °C, the supernatants were discarded and the precipitated proteins were resuspended in 0.5 mL dH_2O. These samples were applied for SDS-PAGE (section 3.3.2) and subsequent glycoprotein staining (section 3.3.3.3).

For analysis of cell-free glucan production after incubation of cells at varying pH (section 3.4.2.3), 270 mL of culture were set up in mMRS supplemented with glucose. After incubation, the cultures were split into six 50 mL closed reaction vessels (Sarstedt AG & Co., Nümbrecht, Germany)(= 45 mL each) and resuspended in citrate phosphate buffer (0.05 M citrate, 0.1 M disodium phosphate) with a pH of either 4.5, 5.5 or 6.5, that were either supplemented with 0.05 M sucrose or no sucrose.

To monitor glucan formation over time, cells were grown in 135 mL of mMRS with glucose and were subsequently resuspended in 45 mL of citrate-phosphate buffer (0.05 M citrate, 0.1 M disodium phosphate, pH 6.5), supplemented with sucrose or no sucrose.

Were appropriate, experiments were performed as biological triplicates.

3.4.2.2 Determination of Michaelis constants, optimum pH and temperature of native enzymes

In order to determine the optimum pH and temperature of the native glucansucrases of *L. hordei* TMW 1.1822 and *L. nagelii* TMW 1.1827, 80 µL of citrate phosphate buffer (0.05 M citrate, 0.1 M disodium phosphate) were mixed with 10 µL of 2 M sucrose solution and 10 µL of enzyme extract obtained in sucrose-supplemented buffers as stated in section 3.4.2.1. The reactions were then incubated for 60 min and subsequently stopped by the addition of 100 µL of 0.25 M sodium hydroxide solution. The optimum pH was determined in a range between 3.0 and 7.8 (at 30 °C), while optimum temperatures were determined in a range between 10 to 70 °C (at pH 5.0). Michaelis constants (K_M) and maximum reaction rates (v_{max}) were determined at pH 5 and 30 °C applying different sucrose concentrations ranging from 1.56 – 500 mM.

Dose-response curves of the *L. nagelii* glucansucrase were performed by diluting the enzyme extract 2-fold, 4-fold and 10-fold with citrate-phosphate buffer (pH 5.0). The undiluted, as well as the diluted enzyme extracts were mixed with 50 µL of citrate phosphate buffer (pH 5.0)

supplemented with 1.56 – 400 mM sucrose. After incubation at 30 °C for 10 min, the reactions were stopped by the addition of 5 µL of a 2.5 M sodium hydroxide solution.
All samples were applied for glucose and fructose quantification and subsequent determination of volumetric activities (see section 3.5.1.2). Following, K_M and v_{max} were calculated using the "Enzyme kinetics" plugin tool within the OriginPro software (v. 9.7, OriginLab Corporation, Northampton, MA, USA) under default settings for Michaelis-Menten kinetics. All experiments were carried out as biological triplicates.

3.4.2.3 Cell-free glucan production, purification and quantification

Sterile filtered, crude enzyme extracts obtained from buffered cell suspensions (section 3.4.2.1) were used to produce glucans under constant reaction conditions. Therefore, one volume of enzyme extract was mixed with an equal volume of a citrate-phosphate buffer (0.05 M citrate, 0.1 M disodium phosphate, 0.4 M sucrose), which adjusted the reaction to pH 5.0. To investigate the influence of different enzyme concentrations, the enzyme extracts were additionally diluted 2-fold, 4-fold or 10-fold with citrate-phosphate buffer (0.05 M citrate, 0.1 M disodium phosphate, pH 5.0) prior to starting the reaction as stated above. All reactions were carried out at 30 °C for at least 24 h.
To monitor glucan formation over time, the reaction mixture was split into four separate reaction vessels to obtain glucan samples after 10 min, 60 min, 180 min and 24 h of incubation, respectively.
Of each reaction mixture, a 1 mL sample was taken for subsequent sugar quantification (section 3.5.1.2), which was immediately mixed with an equal volume of 0.25 M sodium hydroxide solution to stop the reaction. The remaining solutions were dialyzed against dH_2O at 4 °C for 2 days with at least five exchanges of dH_2O using MEMBRA-CELL dialysis tubes (SERVA Electrophoresis GmbH, Heidelberg, Germany) with a molecular weight cut-off of 3.5 kDa. The purified glucan samples were subsequently lyophylized for 48 h and quantified by weighing on an analytical balance (BP210S, Sartorius AG, Göttingen, Germany). Polysaccharide samples were stored at 4 °C until further use. All experiments were carried out as three biological replicates.

3.4.3 Production of glucans using heterologously expressed glucansucrases

3.4.3.1 Cloning and expression of glucansucrases in *E. coli*

The identified glucansucrase gene of *L. nagelii* TMW 1.1827 (BSQ50_03510) and a truncated variant of the same glucansucrase (dsr3510ΔC-term), shortened by the deletion of its C-terminal

glucan-binding domain, were cloned into pBAD/*Myc*-HisA expression vectors (Invitrogen, Carlsbad, CA, USA) that code for a C-terminal 6× histidine tag for subsequent purification of the expressed proteins. Genomic DNA of *L. nagelii* TMW 1.1827 was isolated using the E.Z.N.A. Bacterial DNA Kit (section 3.2.1). Plasmid DNA, containing the pBad/*Myc*-HisA vector, was isolated from an overnight culture of *E. coli* K12 DH5α TMW 2.582 grown in LB-Lennox broth (section 3.1.1) supplemented with 100 µg/mL ampicillin. Therefore, the QIAprep Spin Miniprep Kit (Qiagen, Hilden Germany) (section 3.2.2) was applied.

Primers used for the amplification of both glucansucrase variants are listed in Table 4. All cloning primers featured a restriction enzyme cleavage site, respectively, enabling in-frame cloning into the multiple cloning site of the pBAD/*Myc*-HisA vector. The inserts of both glucansucrase variants were first amplified by PCR using the Phusion High Fidelity DNA Polymerase Kit (New England BioLabs Inc., Ipswich, MA, USA) according to manufacturer´s instructions, applying a temperature gradient of 65 ± 5 °C for primer annealing. After gel electrophoresis (section 3.2.4), PCR products were purified using the E.Z.N.A. Cycle Pure Kit (Omega Bio-tek Inc., Norcross, GA, USA) according to the manufacturer´s instructions. Subsequently, both inserts, as well as the vector were cut using the FastDigest™ restriction enzymes *Xho*1 and *Bsp119*I (ThermoFisher Scientific, Waltham, MA, USA). Therefore, 3 µL FastDigest™ 10× buffer, 2 µL *Bsp119*I, 1 µL *Xho*1, DNA template (~ 1 µg) were added up to 30 µL with nuclease free water and incubated at 37 °C for 30 min. The vector DNA was additionally treated with shrimp alkaline phosphatase (1 u/µL, New England BioLabs Inc., Ipswich, MA, USA), by adding 0.2 µL of the enzyme directly to the restriction digest reaction. After purification of the digested DNA samples, the inserts were ligated into the pBAD/*myc*-HisA vector using the T4 DNA Ligase Kit (ThermoFisher Scientific, Waltham, MA) according to manufacturer´s instructions, applying 50 ng vector DNA and 50 ng insert DNA, respectively. Subsequently, 100 µL of *E. coli* Rosetta, that were prepared chemically competent by the rubidium chloride method (Kushner, 1978), were mixed with 10 µL of construct DNA (0.01 µg/µL), respectively. Transformation was performed by incubation on ice for 20 min, followed by heat shocking for 90 s at 42 °C. After incubation on ice for another 2 min, 4 volumes of LB-Lennox broth supplemented with 100 µg/mL ampicillin (amp100) and 68 µg/mL chloramphenicol (cmp68) were added. 100 µL of each transformation mixture were plated on LB-Lennox (amp100, cmp68) agar plates and incubated overnight at 37 °C. To control for correct insertion of the glucansucrase fragments, as well as for nucleotide substitutions, plasmid DNA of both variants was isolated and sent to Eurofins Genomics (Ebersberg, Germany) for SupremeRun Sanger sequencing using the primers listed in Table 4.

Clones of both glucansucrases were assigned the strain numbers TMW 2.2239 (complete variant) and TMW 2.2240 (dsr3510ΔC-term variant).

Table 4 Primers used for cloning of glucansucrase variants and sequencing of constructs.

Primer	Sequence (5´→3´)	Application
Nag-forward	GC**CTCGAG**AGATTCAACACCACAAAATG[1]	Primer for cloning of both variants
Nag-complete-reverse	GC**TTCGAA**GCAAGTTTTCTACCGGTTTTAG[2]	Primer for cloning of complete glucansucrase
Nag-truncated-reverse	GC**TTCGAA**GCATTATCGTCACTACGTAAAAC[2]	Primer for cloning of dsr3510ΔC-term glucansucrase
Nag-1-Fwd	CGGATCCTACCTGACGCTTT	Sequencing of constructs
Nag-2-Fwd	GGTGAGTACGAAAAAGTTGGCG	Sequencing of constructs
Nag-3-Fwd	AACTGGTTGCGTCAGATTATGC	Sequencing of constructs
Nag-4-Fwd	CAAAAGGCAATTCAAGCAGCCA	Sequencing of constructs
Nag-5-Fwd	GCTAACCCGGATGTAACTGGA	Sequencing of complete glucansucrase construct
Nag-6-Fwd	CTTGGTCGCGGTAGCGATTA	Sequencing of complete glucansucrase construct
Nag-7-Fwd	TGGCTGGCAGTATATTAGCG	Sequencing of complete glucansucrase construct
Nag-8-Fwd	ATTGCTGATTGGGTGCCGGA	Sequencing of truncated glucansucrase construct
Nag-9-Fwd	CTGATGACAATGCTCCGATTGC	Sequencing of truncated glucansucrase construct

[1] **Bold and underlined bases = *Xho*I restriction site**
[2] **Bold bases = *Bsp119*I restriction site**

To obtain both glucansucrase variants for further experiments, cell material of ¼ of an LB-Lennox agar plate was transferred to 100 mL LB-Lennox medium (amp100, cmp68) in a 250 mL Erlenmayer flask, respectively. Cells were grown to an OD_{590nm} of ~ 0.5 – 0.6 at 37 °C on a rotary shaker at 200 rpm. To induce glucansucrase expression, L-arabinose was added to a concentration of 0.2 % (w/v) and cultures were subsequently incubated overnight at 16 °C and 150 rpm. Afterwards, cells were harvested by centrifugation for 10 min at 5000 xg and 4 °C. For protein purification (section 3.4.3.2), cells were resuspended in 5 mL of binding buffer (50 mM sodium dihydrogen phosphate, 300 mM sodium chloride, 10 mM imidazole, pH 8.0). For activity analysis (section 3.4.3.3), cells were resuspended in 5 mL of either citrate-phosphate buffer (0.05 M citrate, 0.1 M disodium phosphate, pH 5.0) or sodium acetate buffer (0.05 M, pH 5.0). Subsequently, cell lysis was performed by sonification on ice (settings: cycle

5, 90 %) for 4 × 20 s with a 1 min break between every cycle. After lysis, cell debris was removed by centrifugation for 15 min at 10,000 xg and 4 °C. Protein amounts in supernatants were quantified as stated in section 3.3.1 and protein compositions were analyzed by SDS-PAGE (section 3.3.2). Protein samples were kept on ice until further use.

3.4.3.2 Purification of recombinant proteins

Polyhistidine-tagged recombinant glucansucrases were purified using HisPur™ Cobalt Resin (ThermoFisher Scientific, Waltham, MA, USA) according to the manufacturer´s instructions on the batch method with some changes. The resin was equilibrated with binding buffer (section 3.4.3.1) with a pH of 8.0 to reduce unspecific protein binding to the resin. Prior to the addition of 300 µL resin/ 5 mL cell lysate, cells were also resuspended in binding buffer. Furthermore, the resin was washed with a separate wash buffer (50 mM sodium dihydrogen phosphate, 500 mM sodium chloride, 10 mM imidazole, pH 7.0) for six times. Elution was performed four times instead of three times. Afterwards, protein samples were desalted using Amicon® Ultra 0.5 mL centrifugal filters (Sigma-Aldrich, St. Louis, MO, USA) with a molecular weight cut-off of 100 kDa according to the manufacturer´s instructions on desalting using dH_2O.

3.4.3.3 Activity assays

All experiments were conducted using the crude enzyme extracts with an overall protein concentration adjusted to 200 µg/mL if not stated otherwise. Firstly, optimum temperature and pH of the heterologously expressed glucansucrase variants were determined in citrate phosphate buffer as described for native enzymes in section 3.4.2.2. Additionally, the influence of cations was tested by the addition of either 1 mM $CaCl_2$, $CuCl_2$, $FeCl_2$, $MgCl_2$, $MnCl_2$, or NaCl. Therefore, the citrate-phosphate buffer was replaced by sodium acetate buffer (0.05 M, pH 5.0). All experiments were incubated for 60 min (complete variant) or 180 min (truncated variant).
K_M and v_{max} were determined in sodium acetate buffer (0.05 M, 1 mM $CaCl_2$, pH 5.0) at 30 °C using sucrose concentrations from 1.56 mM to 500 mM. The complete glucansucrase variant was applied at an overall protein concentration of 500 µg/mL and incubation for 10 min, while the truncated variant was applied at an overall protein concentration of 2500 µg/mL and incubation for 60 min. As negative control, all mixtures were additionally prepared without the addition of enzyme extract. Additionally, cell lysates of un-induced cultures were tested for activity on sucrose, glucose and fructose.

All reactions were performed as triplicates and stopped by the addition of 5 µL of a 2.5 M sodium hydroxide solution. Subsequently, glucose and fructose concentrations were quantified as stated in section 3.5.1.2.

3.4.3.4 Glucan formation

Both glucansucrase variants were recovered in sodium acetate buffer (0.05 M, 1 mM $CaCl_2$, pH 5.0) as stated in section 3.4.3.1 and adjusted to an overall protein concentration of 1000 µg/mL (= 1X) in the same buffer. The enzyme solutions were subsequently diluted 2-fold, 4-fold and 10-fold. Subsequently, 4 mL of each dilution were mixed with 4 mL of sodium acetate buffer supplemented with 0.4 M sucrose. Reactions were incubated for 24 h at 30 °C. A 200 µL sample of each reaction was stopped by the addition of 10 µL of a 2.5 M sodium hydroxide solution and kept for subsequent sucrose, glucose and fructose quantification (section 3.5.1.2). Glucan samples were treated with trichloroacetic acid (10 % (w/v)) for 10 min on ice and subsequent centrifugation for 20 min at 15,000 xg and 4 °C for protein precipitation. Purification and quantification of glucan samples was performed by dialysis, lyophilization and subsequent weighing as described in section 3.4.2.3.

3.5 Analytical methods

3.5.1 Analysis of glucan formation

3.5.1.1 Determination of monomer composition of EPS produced by LAB

Monomer compositions of EPS produced by LAB were conducted in collaboration with Dr. Viktor Eckel at Technical Microbiolgy (TUM). To determine the monomeric composition of the produced EPS and thus investigate the presence of a glucan or fructan, 10 mg of lyophilized EPS were dissolved in 930 µL dH_2O and 70 µL of perchloric acid (70 % (v/v)) were subsequently added. The EPSs were hydrolyzed at 100 °C for 4 h und subsequently centrifuged at 10000 xg for 10 min. The cooled supernatants were filtered (0.2 µm nylon filters, Phenomenex, Aschaffenburg, Germany) and applied for HPLC analysis (section 3.5.2).

3.5.1.2 Quantification of sugars using the Glucose/Fructose/Sucrose assay kit

A sucrose/ $_D$-Fructose/ $_D$-Glucose Assay Kit (Megazyme, Wicklow, Ireland) was used for quantification of sucrose consumption, as well as glucose and fructose release during enzymatic glucan formation, if not stated otherwise. The assay kit exploits the enzymatic turnover of sugar substrates upon simultaneous reduction of $NADP^+$, which subsequently changes its absorbance

maximum. In a first step, free glucose and fructose are both phosphorylated by hexokinase (E.C. 2.7.1.1) upon ATP consumption. Glucose-6-phosphate is then converted by glucose-6-phosphate dehydrogenase (E.C. 1.1.1.49) under $NADP^+$ reduction, leading to an absorbance increase at 340 nm. The conversion of fructose-6-phosphate to glucose-6-phosphate by phosphoglucose isomerase (E.C. 5.3.1.9) leads subsequently to a second increase in absorbance. To determine sucrose concentrations, the sugar is first cleaved into glucose and fructose applying β-fructosidase.

Due to the high sensitivity of this assay, samples were diluted appropriately in dH_2O prior to analysis. 10 µL of each diluted sample were then transferred to a microtest plate (96-wells, Sarstedt, Nümbrecht, Germany), mixed with 200 µL of dH_2O, 10 µL solution I (buffer, pH 7.6) and 10 µL solution II ($NADP^+$ and ATP) of the assay kit, respectively, and subsequently incubated for 3 min prior to absorbance measurement A1. Then, 10 µL of solution III (Hexokinase and Glucose-6-phosphate dehydrogenase) were added, the plate was shaken for 10 s and incubated for 10 min until absorbance A2 was measured. Finally, 10 µL of solution IV (phosphoglucose isomerase solution) were added, the plate was shaken again and incubated for 10 min prior to absorbance measurement A3. Sucrose quantification was carried out in an additional assay, where 10 µL of each diluted sample were mixed with 20 µL of solution VI (β-fructosidase) and incubated for 5 min prior to the described procedure. Subsequently, only 180 µL of dH_2O were added to the samples. All samples were measured as technical duplicates, incubations were carried out at room temperature and absorbance measurements were performed at 340 nm on a FLUOstar Omega Microplate reader (BMG Labtech, Ortenburg, Germany). dH_2O was used as blank sample.

Glucose concentrations were calculated by subtracting blank corrected A2 minus A1 (= $\Delta A_{Glucose}$), while fructose concentrations were calculated by subtracting blank corrected A3 minus A2 (= $\Delta A_{Fructose}$). Sucrose concentrations were calculated by subtracting $\Delta A_{Glucose}$ of the glucose measurement from $\Delta A_{Glucose}$ of the sucrose measurement. To calculate the respective sugar concentration in g/L, the following formula was applied.

$$c = \frac{V \times M_w}{\varepsilon \times d \times v} \times \Delta A$$

V = final volume [µL]; M_w = molecular weight of substance measured [g/mol]; ε = extinction coefficient of NADPH at 340 nm = 6300 L × mol^{-1} × cm; d = light path [cm]; v = sample volume [µL]

To calculate glucansucrase activities, the resulting sugar concentrations were divided by the respective incubation times at which the samples were collected. For overall activities, released fructose concentrations were used, while hydrolase activities were calculated over the amount of released glucose. Transferase activities were calculated by subtracting the fructose concentrations minus the respective glucose concentrations. Subsequently, transferase activities were used to calculate the theoretically formed amount of glucan, which is thus denoted as "predicted amount".

3.5.1.3 Analysis of oligosaccharides by HPAEC-PAD

Measurements were performed in cooperation by Prof. Dr. Daniel Wefers at the Department of food chemistry, affiliated to the Martin-Luther-University in Halle-Wittenberg.

Mono-, di- and oligosaccharides obtained from glucansucrase reactions were analyzed by high performance anion exchange chromatography coupled to pulsed amperometric detection (HPAEC-PAD) on an ICS-6000 system (ThermoFisher Scientific Dionex, Sunnyvale, CA, USA) equipped with a CarboPac PA200 column (250 × 2 mm i.d., 5.5 µm particle size, ThermoFisher Scientific Dionex). Therefore, a column temperature of 30 °C and a detector compartment temperature of 25 °C were applied. For separation, a gradient of (A) ddH_2O, (B) 0.01 M sodium hydroxide, (C) 0.1 M sodium hydroxide and (D) 0.1 M sodium hydroxide + 0.5 M sodium acetate was applied at a flow rate of 0.4 mL/min. Prior to each run, the column was flushed with 100 % solution D for 10 min and subsequently with 100 % solution C for 15 min, followed by equilibration with 100 % solution B for 20 min. After injection of the sample, a gradient was used as follows: isocratic 100 % solution B (0 – 15 min), linear from 100 % solution B to 100 % solution C (15 – 30 min), isocratic 100 % C (30 – 45 min), linear from 100 % solution C to 80 % solution C + 20 % solution D (60 – 65 min), isocratic 80 % solution C + 20 % solution D (65 – 70 min), linear from 80 % solution C + 20 % solution D to 100 % solution D (70 – 75 min) and finally isocratic 100 % solution D. Mono-, di- and oligosaccharides were identified using external standards, while glucose, fructose and leucrose were quantified by external standard curves of these sugars.

3.5.1.4 Analysis of macromolecular glucan structures by AF4-MALS-UV

Enzymatically produced glucans were separated by asymmetric flow field flow fractionation (AF4) (Wyatt technology, Dernbach Germany) according to theoretical principles described by Rübsam et al. (2012) and Nilsson et al. (2013). Molecular weights (M_w) and root mean square (rms) radii were subsequently determined by multi-angle laser light scattering (MALS) (Dawn

Heleos II, Wyatt Technology, Dernbach, Germany). Additionally, the AF4 system was coupled to an UV detector (Dionex, Sunnyvale, CA, USA) for quantitative detection at a wavelength of 400 nm. Lyophilized glucans were redissolved in dH_2O at a concentration of 0.1 mg/mL. Driven by a Dionex high-performance liquid chromatography (HPLC) autosampler and pump system (Dionex Ultimate 3000, ThermoFisher Scientific, MA, USA), 100 µL of a sample were automatically injected to the AF4 channel with a 10 kDa regenerated cellulose membrane (Superon GmbH, Dernbach, Germany). An aqueous solution containing 50 mM $NaNO_3$ served as an eluent. Samples were injected at an injection flow of 0.2 mL/min and concentrated at a focus flow of 1.5 mL/min. The detector flow was kept at 1 mL/min, while separation of glucan molecules was performed by a linear gradient of the cross flow from 3 to 0.1 mL/min within 10 min. Subsequently, the cross flow was kept at 0.1 mL/min for 15 min and finally set to 0 mL/min to elute any remaining particles. The analysis of the signals obtained from AF4-MALS-UV measurements was performed in ASTRA 6.1 software (Wyatt technology, Dernbach, Germany). Rms radii were calculated from MALS signals in *particle mode* applying the Berry model (best fit), which is suitable for large molecules ($M_w > 1 \times 10^6$ Da). Molar masses were absolutely calculated applying a refractive index increment (*dn*/*dc*) value of 0.1423 mL/g for glucans (Yuryev *et al.*, 2007) and specific UV extinction coefficients that were determined for each glucan sample as it was performed for levans by Ua-Arak *et al.* (2017b). Therefore, UV extinction coefficients (ε_{400nm}; [mL × mg^{-1} × cm^{-1}]) were determined as the slopes of calibration curves that were obtained from the UV extinction values of respective concentration series (0.1 – 5 mg/mL) of glucans in dH_2O according to the Beer-Lambert law.

3.5.1.5 Chemical structural analysis of glucans

Methylation analysis and *endo*-dextranase assays were performed in cooperation by Prof. Dr. Daniel Wefers at the Department of Food Chemistry and Phytochemistry, affiliated to the Institute of Applied Bioscience of the Karlsruher Institute of Technology (KIT) and later at the department of food chemistry at Martin-Luther-University in Halle-Wittenberg.

3.5.1.5.1 Methylation analysis

Methylation analysis was performed in order to determine glycosidic linkage types of the produced glucans, as well as their relative abundancies (Fels *et al.*, 2018; Wefers *et al.*, 2015). Therefore, samples were re-dissolved in dimethyl sulfoxide (DMSO) and permethylated using freshly ground sodium hydroxide and methyl iodide. The methylated polysaccharides were then extracted into dichloromethane and the organic layer was washed with 0.1 M sodium thiosulfate

and twice with water. After evaporation and drying, the methylated glucans were hydrolyzed using 2 M trifluoroacetic acid (TFA) and incubation for 90 min at 121 °C. TFA was subsequently removed by evaporation and the partially methylated glucans were reduced with sodium borodeuteride in aqueous 2 M ammonia solution. The reaction was stopped using glacial acetic acid, followed by acetylation using 1-methylimidazole and acetic anhydride. The partially methylated alditol acetates (PMAAs) were finally extracted using dichloromethane. Residual water was removed by freezing overnight. PMAAs were analyzed by GC-MS (GC-2010 Plus and GC-MS-QP2010 Ultra, Shimadzu, Kyoto, Japan) equipped with a DB-5MS column (30 m × 0.25 mm i.d., 0.25 µm film thickness, Agilent Technologies, Santa Clara, CA, USA) under the following conditions: Initial column temperature 140 °C, held for 2 min; ramped at 1 °C/min to 180 °C, held for 5 min; ramped at 10 °C/min to 300 °C, held for 5 min. Helium was used as carrier gas at a rate of 40 cm/s. The transfer line was kept at 275 °C and electron impact mass spectra were recorded at 70 eV. A split ratio of 30:1 was used for split injection and the injection temperature was 250 °C. Relative abundancies of PMAAs were quantified on a GC-FID system (GC-2010 Plus, Shimadzu, Kyoto, Japan), applying the same conditions as described above, but with a reduced split ratio of 10:1. The FID temperature was 240 °C and nitrogen served as makeup gas. Measurements were carried out in duplicate and molar response factors were used to calculate the portions of the PMAAs (Sweet *et al.*, 1975).

3.5.1.5.2 Endo-dextranase assay of glucans

Information on the glucan fine structures was obtained by enzymatic fingerprinting as described by Katini *et al.* and Xu *et al*. (Xu *et al.*, 2018). Therefore, 1 mg/mL of glucan was hydrolyzed by *endo*-dextranase (E.C. 3.2.1.11, from *Chaetomium* sp., Megazyme, Bray, Ireland, 5 U/mg polysaccharide) for 24 h at 40 °C. After heat-inactivation of the enzyme at 100 °C for 5 min, hydrolysates were diluted and analyzed by HPAEC-PAD on an ICS-5000 system (ThermoFisher Scientific, Waltham, MA, USA) equipped with a CarboPac PA-200 column (250 mm × 3 mm i.d., 5.5 µm particle size, ThermoFisher Scientific, Waltham, MA, USA). The flow rate was kept at 0.4 mL/min and a gradient of eluent A (ddH_2O), eluent B (0.1 M sodium hydroxide) and eluent C (0.1 M sedum hydroxide, 0.5 M sodium acetate) was applied at 25 °C. Prior to every measurement, the column was flushed with 100 % eluent C for 10 min and equilibrated with 90 % eluent A and 10 % eluent B for 20 min. After injection of the hydrolysate sample, a ratio of 90 % eluent A and 10 % eluent B was kept isocratic for 10 min. Then, a linear gradient from 90 % eluent A and 10 % eluent B to 100 % eluent B over 10 min

was applied. Finally, another linear gradient from 100 % eluent B to 100 % eluent C was performed over 70 min.

3.5.2 Quantification of sugars and organic acids by HPLC

Sugars, sugar alcohols and organic acids were measured in culture supernatants using a HPLC system (Dionex Ultimate 3000, ThermoFisher Scientific, Waltham, MA, USA) coupled to a refractive index (RI) detector (Refractomax ERC, Munich, Germany). For organic acid quantification, 1 mL of each sample was added with 50 µL perchloric acid (70 % (v/v)), mixed thoroughly and incubated overnight at 4 °C. Then, samples were centrifuged for 30 min at 13,000 xg and 4 °C. All samples were filtered (0.2 µm nylon filters, Phenomenex, Aschaffenburg, Germany) to remove any aggregates that would disturb HPLC measurements. Following, 20 µL of each sample were automatically injected to the HPLC system. Organic acids were measured with a Rezex ROA H^+ column (Phenomenex, Aschaffenburg, Germany) at a flow rate of 0.7 mL/min at 85 °C, with 2.5 mM H_2SO_4 prepared in filtered dH_2O as eluent. Sugars and sugar alcohols were measured on a Rezex RPM Pb^{2+} column (Phenomenex, Aschaffenburg, Germany) at a flow rate of 0.6 mL/min at 85 °C using filtered dH_2O as eluent. Identification and quantification of sugars and organic acids was performed according to external standards using the Chromeleon software (v. 6.8; ThermoFisher Scientific, Waltham, MA, USA).

3.5.3 Protein identification

Selected protein bands were cut from silver stained SDS-gels and sent to Zentrallabor für Proteinanalytic (ZfP) of Ludwig-Maximilians Universität München for mass-based peptide sequencing. The obtained “mascot generic format (.mgf)” formatted files were processed to peptide sequences using PepNovo (Frank *et al.*, 2005). The peptide sequences were then blasted against the *in silico* proteomes of the respective microorganisms. Furthermore, the “.mgf” files were analyzed by Mascot (v. 2.3.02) (Perkins *et al.*, 1999) using the following settings: MS tolerance: 10 ppm, MS/MS tolerance: 0.5 Da, peptide false discovery rate (FDR): 0.1, protein FDR: 0.01, minimum peptide length: 5, fixed modification: carbamidomethyl (C) and variable modification: oxidation (M).

3.6 Bioinformatical methods

3.6.1 Statistics and data visualization

Data visualization was predominantly performed using the OriginPro software (v. 9.7, OriginLab Corporation, Northampten, MA, USA). Data that were not visualized appropriately by this software were plotted in R-Studio (v. 1.4.1103, RStudio, Boston, MA, USA) running under R software (v. 4.0.3, https://www.r-project.org). Where appropriate, statistical analysis was performed in OriginPro, R-Studio or Perseus software (v. 1.6.14.0)(Tyanova *et al.*, 2016). Correlation analyses were conducted by Spearman´s rank correlation and significant ($p < 0.05$) correlation coefficients (ρ) were interpreted according to Mukaka (2012).

The following R packages were used for data analysis and visualization.

Table 5 R-packages used in this study.

R-package	Function	Purpose	Reference
psych	corr.test	Calculation of Spearman´s rank correlation	(Revelle, 2020)
pheatmap	pheatmap	Visualization of correlation matrices	(Kolde, 2018)
ComplexUpset	upset	Creating upset plots	(Krassowski, 2021)
topGO		Enrichment analysis of gene ontologies of proteomic data sets	(Alexa A. *et al.*, 2020)
grofit	grofit	Fitting growth curves in R	(Kahm *et al.*, 2010)

3.6.2 Genomics

3.6.2.1 Genome sequencing, assembly and annotation

After DNA isolation (section 3.2.1.), genome sequencing was performed applying a PCR-free library preparation on a MiSeq sequencing platform (Illumina, Inc. San Diego, CA, USA). Subsequently, processing and assembly were carried out using SPAdes v. 3.9.0 (Bankevich *et al.*, 2012) following the method of Huptas *et al.* (2016). Illumina MiSeq sequencing was performed in collaboration with the Next-Generation-Sequencing Core Facility of the Institute for Food and Health (TUM, Freising, Germany), while selection of organisms and whole genome sequence (WGS) analyses were carried out in collaboration with Dr. Viktor Eckel (2020) and Dr. Di Xu (2019).

For PacBio Single Molecule Real-Time (SMRT) sequencing and subsequent WGS assembly, DNA was sent to Eurofins Genomics (Ebersberg, Germany). Genomic sequences obtained and used in this study are listed in Table 6.

Table 6 Genome sequences obtained and used in this study.

Species	Strain	Accession number	Sequencing technology
L. hilgardii	TMW 1.828	NSMC00000000	Illumina MiSeq[1]
L. hilgardii	TMW 1.2196	PPFW00000000	Illumina MiSeq[1]
L. hilgardii	TMW 1.45^{T} = DSM 20176	ACGP00000000	Illumina MiSeq[2]
L. hordei	TMW 1.1822	CP018176.1 – CP018179.1	PacBio SMRT[1]
L. hordei	TMW 1.1907	PDDD00000000	Illumina MiSeq[1]
L. hordei	TMW 1.2353^{T}	CP049301 – CP049303	PacBio SMRT[1]
L. nagelii	TMW 1.1823	PDDB00000000	Illumina MiSeq[1]
L. nagelii	TMW 1.1827	CP018180.1 – CP018183.1	PacBio SMRT[1]
L. nagelii	TMW 1.2352^{T}	CP049304 – CP049305	PacBio SMRT[1]
L. satsumensis	TMW 1.1829	PDDC00000000	Illumina MiSeq[1]
Lc. citreum	TMW 2.1194	PDDF00000000	Illumina MiSeq[1]
Lc. mesenteroides	TMW 2.1073	PDDE00000000	Illumina MiSeq[1]
Lc. mesenteroides	TMW 2.1195	PKPE00000000	Illumina MiSeq[1]
Apilactobacillus kunkeei	DSM 12361	JXDB00000000	Illumina MiSeq[2]
Holzapfelia floricola	DSM 23037	AYZL01000000	Illumina MiSeq[2]
Dellaglioa algidus	DSM 15638	AZDI00000000	Illumina MiSeq[2]

[1] Obtained in this study
[2] Obtained from NCBI Genbank

The assembled WGSs were subsequently submitted to the National Center for Biotechnology Information (NCBI) Genbank, where they were further annotated by the NCBI Prokaryotic Genome Annotation Pipeline (https://www.ncbi.nlm.nih.gov/genome/annotation_prok). Additionally, WGSs were submitted to the Rapid Annotation using Subsystem Technology (RAST) server (https://rast.nmpdr.org), which provides a SEED-based prokaryotic annotation service (Aziz *et al.*, 2008; Overbeek *et al.*, 2014). Files containing raw contig sequences, as well as ORFs and translated ORFs (= putative functional proteome) were generated from NCBI Genbank files applying in-house bash-tools. Moreover, ORFs of the WGSs were assigned to TIGRFAMs that provide insights into molecular functions and biological processes in which the putative protein may be involved (Selengut *et al.*, 2007). This annotation furthermore provided enzyme commission (E.C.) numbers and gene ontology (GO) identifiers for metabolic reconstruction. The subcellular localization of proteins was predicted using the PSORTb tool (v. 3.0.2, http://www.psort.org/psortp)(Gardy *et al.*, 2005; Yu *et al.*, 2010).

If available, WGSs of highly similar strains were used as template to re-order contigs of draft genome sequences obtained from Illumina Miseq sequencing to generate predictively complete sequences of chromosomes and plasmids of the respective microorganisms. This was achieved using Mauve (v. 2.4.0)(Darling *et al.*, 2004) and CLC Main Workbench (v. 8.1, Qiagen, Hilden, Germany). In all genomes, the chromosome start was set to the gene coding for DNA polymerase III (dnaN).

The PlasmidFinder web tool (v. 2.01, https://cge.cbs.dtu.dk/services/PlasmidFinder-2.0/) was used to identify plasmids within WGSs that were obtained from Illumina MiSeq sequencing (Carattoli *et al.*, 2014).

The PHASTER web tool (Arndt *et al.*, 2016) was used to identify genomic regions corresponding to prophage DNA.

3.6.2.2 Whole genome comparison

Average nucleotide identity (ANI) values of WGS were calculated by pairwise genome comparison applying the ANIb algorithm (Goris *et al.*, 2007) that is available on the JspeciesWS web service (Richter *et al.*, 2015).

OrthoFinder software (Emms *et al.*, 2019) was used to identify shared and accessory gene contents among groups of LAB by the inference of orthogroups. Herein, each orthogroup represents a group of orthologous genes that have to be present at least twice in the pangenome of the tested genomes, which additionally allows for the identification of duplications within one genome. Thereby, orthogroups are defined with respect to the phylogenetic relationship in the context of a species tree of the tested genomes. In order to achieve accurate rooting of this species tree, the WGSs of three outgroup species were added to the analysis (*Apilactobacillus kunkeei* DSM 12361, *Holzapfelia floricola* DSM 23037 and *Dellaglioa algidus* DSM 15638) due to their phylogenetic placements postulated by the literature (Zheng *et al.*, 2020).

3.6.2.3 Synteny analysis

Collinear genomic regions were identified on intra- and interspecies level applying i-ADHoRe 3.0 software (Proost *et al.*, 2012). Therefore, general feature format (= .gff) files were exported from WGSs processed by CLC Main Workbench (see section 3.6.2.1) to obtain i-ADHoRE input files containing gene order and orientation information. Orthogroups obtained from OrthoFinder analysis (see section 3.6.2.2) were used as BLAST table. I-ADHoRe was run under the following settings: alignment method = greedy, graph-based algorithm 2 (Fostier *et al.*, 2011), gap size = 30, cluster gap = 35, q-value = 0.75, probability cut-off = 0.01, anchor points

= 3, level-2-only = TRUE and multiple hypothesis correction = false discovery rate (FDR). The obtained segments files were subsequently used for synteny visualization using the circos software package (v. 0.69-9)(Krzywinski *et al.*, 2009).

3.6.2.4 Metabolic reconstruction and functional analysis

WGSs were functionally analyzed using the obtained SEED categories and subsystems (Aziz *et al.*, 2008; Overbeek *et al.*, 2014), as well as the TIGRFAMs. Where appropriate, this analysis was complemented with GO (Ashburner *et al.*, 2000). To generate an overview of metabolic capabilities, enzyme commission (E.C.) numbers, obtained by RAST annotation, were imported into the Kyoto Encyclopedia of Genes and Genomes (KEGG) pathway map pipeline (https://www.genome.jp/kegg/pathway.html). Final predictively functional metabolic pathways were generated manually based on literature without the use of automatic pipelines. Also, KEGG and the BioCyc Database Collection (https://biocyc.org/) were used as reference. All enzymes involved in each metabolic reaction were manually reviewed when their presence of the respective ORFs was predicted from NCBI and RAST annotations. Therefore, the corresponding ORF was imported into the NCBI conserved domain search (https://www.ncbi.nlm.nih.gov/Structure/cdd/wrpsb.cgi) and Smart BLAST (https://blast.ncbi.nlm.nih.gov/smartblast/?LINK_LOC=BlastHomeLink) to confirm the presence of the predictively functional protein. If a certain protein was predictively absent within the annotated ORFs, a list of ORFs from closely related microbial species corresponding to this enzyme was created and blasted against the contigs or ORFs of the WGSs lacking this enzyme using smart or protein BLAST algorithms (Altschul *et al.*, 1990; Camacho *et al.*, 2009). Reference sequences were obtained from NCBI or UniProt (https://www.uniprot.org/). If applicable, proteins were subjected for signal peptide prediction analysis using SignalP v. 4.1 (Petersen *et al.*, 2011).

3.6.3 Sequence alignments, dendrograms and primer design

Alignments of gene or amino acid sequences were created using the ClustalW algorithm (Thompson *et al.*, 2003) that is implemented in MEGA7 (Kumar *et al.*, 2016). Alignments were visualized in dendrograms created with MEGA7 applying the maximum-likelihood method based on the JTT matrix-based model (Felsenstein, 1981; Jones *et al.*, 1992). Primer design was conducted using the Primer-BLAST online tool provided by NCBI (https://www.ncbi.nlm.nih.gov/tools/primer-blast). To detect the presence of a gene in several

strains or species, the consensus sequence of the alignment of the corresponding genes was used for primer design.

For clustering of band patterns obtained by RAPD-PCR, the BioNumerics software (v. 7.6, Applied Maths, Belgium) was applied.

Moreover, Easifig software (v. 2.2.5)(Sullivan *et al.*, 2011) was applied for sequence alignments of genomic regions exhibiting several different features and subsequent analysis of gene cluster organization. This software tool provided a built-in tblastx version that was used with an E-value cut-off of 0.01.

3.6.4 Protein structure modelling

The SWISS-MODEL webtool (https://swissmodel.expasy.org/) was used for homology modelling of 3D structures of glucansucrases. Therefore, amino acid sequences of these enzymes were used to search for highly similar proteins with a known 3D structure. These analyses enabled for the identification of amino acids involved in substrate and ligand binding within the primary sequences of the tested enzymes.

3.7 Proteomics

Parts of the proteomic study were performed in cooperation by Dr. Christina Ludwig affiliated to the Bavarian Center for Biomolecular Mass Spectrometry (BayBioMS, Freising, Germany).

3.7.1 Experimental setup

The experimental procedure was done according to Prechtl *et al.* (2018a) with some changes. The differential expression and release of proteins as a result of sucrose-treatment was investigated by a proteomic experiment, involving *L. hordei* TMW 1.1822 and *L. nagelii* TMW 1.1827. 50 mL of mMRS medium (25 g/L glucose) were inoculated to a final OD_{590nm} of 0.1, respectively, using freshly prepared pre-cultures (section 3.1.1). The cultures were grown to mid-exponential growth phase (*L. hordei* TMW 1.1822 OD_{590nm} ~ 2.0, *L. nagelii* TMW 1.1827 OD_{590nm} ~ 3.6) at 30 °C. 30 mL of each culture were then distributed to two fresh 15 mL reaction vessels and cells were subsequently pelletized by centrifugation for 5 min at 3000 xg and 4 °C. After washing the cell pellet with fresh medium, cells were resuspended in 15 mL of medium supplemented with either glucose or sucrose (25 g/L each). After incubation for 2 h at 30 °C, a 100 µL sample was taken from each culture for the determination of viable cell counts (section 3.1.4). Subsequently, cultures were centrifuged for 5 min at 3000 xg and 4 °C to

separate the supernatants (denoted as “exoproteomic samples”) from the cells. The exoproteomic samples were immediately frozen at -20 °C until further use. The cells were washed twice using 10 mL Ringer´s solution (4 °C), immediately frozen in liquid nitrogen and stored at -80 °C for subsequent proteomic analysis.

3.7.2 Sample preparation

3.7.2.1 Cellular proteomes

Cellular proteomes were prepared as described in Xu *et al.* (2019a) and Prechtl *et al.* (2018a). In a first step, frozen cell pellets were resuspended in 900 µL lysis buffer (8 M urea, 5 mM EDTA, 100 mM NH_4HCO_3, 1 mM dithiotheitol (DTT) in water, pH 8.0) supplemented with 10x solution SIGMA*FAST*™ protease inhibitor cocktail (Sigma-Aldlich, St. Louis, MO, USA) according to the manufacturer´s instructions. Cell lysis was then performed mechanically using 400 mg glass beads (G8772, 424-600 µm, Sigma-Aldrich, St. Louis, MO, USA) at 4 °C for 10 min. Total protein concentrations were then measured as described in section 3.3.1. 100 µg of protein extract of each sample was subsequently used for in-solution digestion. First, proteins were reduced with 10 mM dithiothreitol for 30 min at 30 °C and 300 rpm and carbamidomethylated with 55 mM chloroacetamine (CAA) for 30 min at room temperature in the dark. After 6x dilution of the protein samples with freshly prepared 0.05 M NH_4HCO_3 solution, 1 µg of trypsin (trypsin to protein ratio 1:100) was added to each sample, followed by incubation for 4 h at 30 °C and 300 rpm. After the addition of the same amount of trypsin, samples were incubated overnight at 30 °C and 300 rpm. Protein digestion was stopped by the addition of 1 % (v/v) formic acid. Desalting of digested protein samples was performed using C18 solid phase extraction with Sap-Pak columns (WAT054960, Waters, Milford, MA, USA) according to the manufacturer´s instructions. The purified peptide samples were then dried in a SpeedVac and re-dissolved in an aqueous solution containing 2 % (v/v) acetonitrile and 0.1 % (v/v) formic acid at a final concentration of 1 µg/µL.

3.7.2.2 Exoproteomes

Exoproteomic samples were prepared as described by Heinze *et al.* (Heinze *et al.*, 2018). Therefore, 30 µL of each culture supernatant and un-inoculated medium samples as a negative control were mixed with lithium dodecyl sulfate (LDS) sample buffer (ThermoFisher Scientific, Waltham, MA, USA). Subsequently, samples were reduced with 25 mM DTT, incubated at 10 min at 95 °C and carbamidomethylated with 55 mM chloroacetamine. To concentrate the proteins prior to digestion, samples were applied on a 4 – 12 % NuPAGE gel (ThermoFisher

Scientific, Waltham, MA, USA) and run for about 1 cm. In-gel digestion was then performed according to standard procedures as described by Shevchenko *et al.* (Shevchenko *et al.*, 2006). The collected supernatants (= 130 µL) were finally dried in a SpeedVac and re-dissolved in an aqueous solution containing 2 % (v/v) acetonitrile and 0.1 % (v/v) formic acid at a final concentration of 1 µg/µL.

3.7.3 Peptide separation and mass spectrometry

All nano-flow liquid chromatography-mass spectrometry/mass spectrometry (LC-MS/MS) measurements were carried out on a Fusion Lumos Tribrid mass spectrometer coupled to an Ultimate 3000 RSLCnano system (both from ThermoFisher Scientific, Waltham, MA, USA). For peptide analysis of each sample, 0.1 µg of cellular peptides or 0.5 µg of exoproteomic peptides were applied to a trap column (ReproSil-purC18-AQ, 5 µm, 20 mm × 75 µm, self-packed, Dr. Maisch GmbH, Ammerbuch-Entringen, Germany), respectively, at a flow rate of 5 µL/min in 100 % solvent A (0.1 % (v/v) formic acid in HPLC-grade H_2O for 10 min. Then, peptides were transferred to an analytical column (ReproSil Gold C18-AQ, 3 µm, 450 mm × 75 µm, self-packed, Dr. Maisch GmbH, Ammerbuch-Entringen, Germany) and separated by a 50 min gradient from 4 % to 32 % of solvent B (0.1 % (v/v) formic acid in acetonitrile and 5 % (v/v) DMSO) at a flow rate of 300 nL/min. Both nanoLC solvents contained 5 % (v/v) HPLC grade H_2O.

The mass spectrometer was operated in data-dependent acquisition and positive ionization mode. MS1 spectra (360 – 1300 m/z) were recorded at a resolution of 60,000 by an automatic gain control target value of 4×10^5 and maximum injection time of 50 ms. After peptides were fragmented by higher energy collision induced dissociation, MS2 spectra (200 – 2000 m/z) of up to 20 precursor peptides were recorded at a resolution of 15,000 using an automatic gain control target value of 5×10^4 and maximum injection time of 22 ms. While precursor isolation window width was set to 1.3 m/z, the normalized collision energy was 30 %. Dynamic exclusion was enabled with 20 s exclusion time (mass tolerance +/- 10 ppm). All peptide precursors that were singly charged, unassigned or with a charge state higher than 6+ were excluded for fragmentation.

3.7.4 Protein identification and quantification

The MaxQuant software package (v. 1.6.3.4) (Cox *et al.*, 2008) with its built-in search engine Andromeda (Cox *et al.*, 2011) was used to identify and quantify peptides and proteins. Therefore, MS2 spectra were searched against the predicted *in silico* proteomes of *L. hordei*

TMW 1.1822 and *L. nagelii* TMW 1.1827 that were obtained from genome analysis of both microorganism (section 3.6.2.1), supplemented with common contaminants (built-in option in MaxQuant). Trypsin/P was specified as the proteolytic enzyme, precursor tolerance was set to 4.5 ppm and fragment ion tolerance to 20 ppm. The results were adjusted to a false discovery rate (FDR) of 1 % on peptide spectrum match level and protein level, applying a target-decoy approach using reversed protein sequences. Furthermore, the minimal peptide length was defined as 7 amino acids, while the "match-between-run" function was disabled. Carbamidomethylated cysteine was set as fixed modification and oxidation of methionine and N-terminal protein acetylation were set as variable modifications. Relative protein abundancies were compared between samples using label-free quantification (LFQ). Moreover, intensity-based absolute quantification (iBAQ) was applied, providing an estimation of the absolute protein abundance and thereby a proportional quantification unit for the abundance of different proteins within one sample. The output of MaxQuant analyses were further processed and statistically analyzed in Perseus software (v. 1.6.14.0)(Tyanova *et al.*, 2016). Only proteins identified in four out of five biological replicates in at least one group (glucose or sucrose) were considered for further analysis. Missing values were imputed from a normal distribution (width: 0.2; down shift: 1.8). The obtained $\log_2$-transformed LFQ intensities were used for Student´s T-test analysis (permutation-based FDR = 0.01, S0 = 0.1). Absolute protein abundancies at each condition were estimated using the averaged $\log_{10}$-transformed iBAQ intensities that were ranked in descending order for each group.

In order to prioritize extracellular proteins that were released into the surrounding medium due to some form of active biological process rather than cell death or lysis, MS intensities of lysates and exoproteomes were compared. Therefore, the $\log_{10}$-transformed iBAQ intensities were first normalized by z-scoring in Perseus software using the average and standard deviation over all iBAQ intensities within each sample (matrix access: column). The obtained z-scores were statistically analyzed by Student´s T-test analysis as described above. Proteins with a significantly higher abundance within exoproteomes and a difference between z-score (exoproteome) minus z-score (cellular proteome) higher or equal than 2.0 were considered as being actively released with high confidence.

3.7.5 Proteomic data deposition

All LC-MS/MS data files and MaxQuant output files were deposited in the ProteomeXchange Consortium (http://proteomecentral.proteomexchange.org) *via* the PRIDE partner repository

with the dataset identifier PXD020664 for *L. hordei* TMW 1.1822. A public version of the *L. nagelii* TMW 1.1827 proteomic raw data is pending.

3.7.6 Gene ontology enrichment analysis

GO enrichment analysis was performed in order to fill the gaps left by SEED-based functional analysis. GO enrichment analysis was carried out on the basis of the statistically analysed proteomic datasets obtained from LFQ intensity analysis (section 3.7.4). Therefore, the topGO package (v. 2.40.0) for RStudio (v. 4.0.2)(Alexa A. *et al.*, 2020) was used. The genes were filtered according to their significance as obtained ruing statistical analysis in Perseus and their up- or down-regulation in sucrose and glucose-treated cells. Significantly enriched GO terms were indicated by a Fisher´s exact p-value < 0.05 (classicFisher).

4 Results

4.1 Strain selection

4.1.1 Identification and selection of glucan-producing LAB from water kefir

In order to identify glucan-producing LAB, 18 strains of our in-house culture collection that were isolated from water kefir and investigated in previous studies (Gulitz *et al.*, 2013; Gulitz *et al.*, 2011; Waldherr *et al.*, 2010), as well as three newly isolated strains of *L. hordei* from water kefir were plated on mMRS agar plates supplemented with sucrose. Moreover, the type strains of *L. hordei, L. nagelii* and *L. hilgardii*, respectively, that were isolated from different sources were additionally applied for this experiment. After 48 h of incubation at 30 °C, the plates were screened for EPS formation based on a slimy or ropy phenotype and EPS production was scored as described by Stadie (2013). To explicitly identify glucan-producing strains for further experiments, monomeric compositions of the produced EPS were determined. Apart from both type strains and *L. nagelii* TMW 1.1825, all isolates were capable of EPS-production from sucrose, as shown in Table 7. Thereby, only *Lc. mesenteroides* TMW 2.1075 and TMW 2.1076 produced a fructan-type of EPS, as determined by monomer identification.

Table 7 HoPS-production capabilities of LAB isolated from water kefir and their identified monomeric composition. 0 = no visible EPS production; + = slight EPS production; ++ = strong EPS production; +++ = very strong EPS production.

Species	TMW strain	EPS production	Identified monomers
L. hilgardii	1.1819	0	Glucose
L. hilgardii	1.828	+++	Glucose
L. hilgardii	1.2196	+++	Glucose
L. hilgardii	1.45^{T}	0	
L. hordei	1.1817	+	Glucose
L. hordei	1.1821	+	Glucose
L. hordei	1.1822	++	Glucose
L. hordei	1.1907	++	Glucose
L. hordei	1.2353^{T}	0	
L. hordei	1.2375	++	Glucose
L. hordei	1.2376	+	Glucose
L. hordei	1.2377	++	Glucose
L. nagelii	1.1823	++	Glucose
L. nagelii	1.1824	++	Glucose
L. nagelii	1.1825	0	
L. nagelii	1.1826	+	Glucose
L. nagelii	1.1827	++	Glucose
L. nagelii	1.2352^{T}	0	
L. satsumensis	1.1829	++	Glucose
Lc. mesenteroides	2.1073	+++	Glucose

Lc. mesenteroides	2.1075	++	Fructose
Lc. mesenteroides	2.1076	++	Fructose
Lc. mesenteroides	2.1195	+	Glucose
Lc. citreum	2.1194	+++	Glucose

In order to select for distinctly different strains for subsequent whole genome sequencing, RAPD-PCR was applied. The obtained band patterns were clustered as shown in Figure 4.

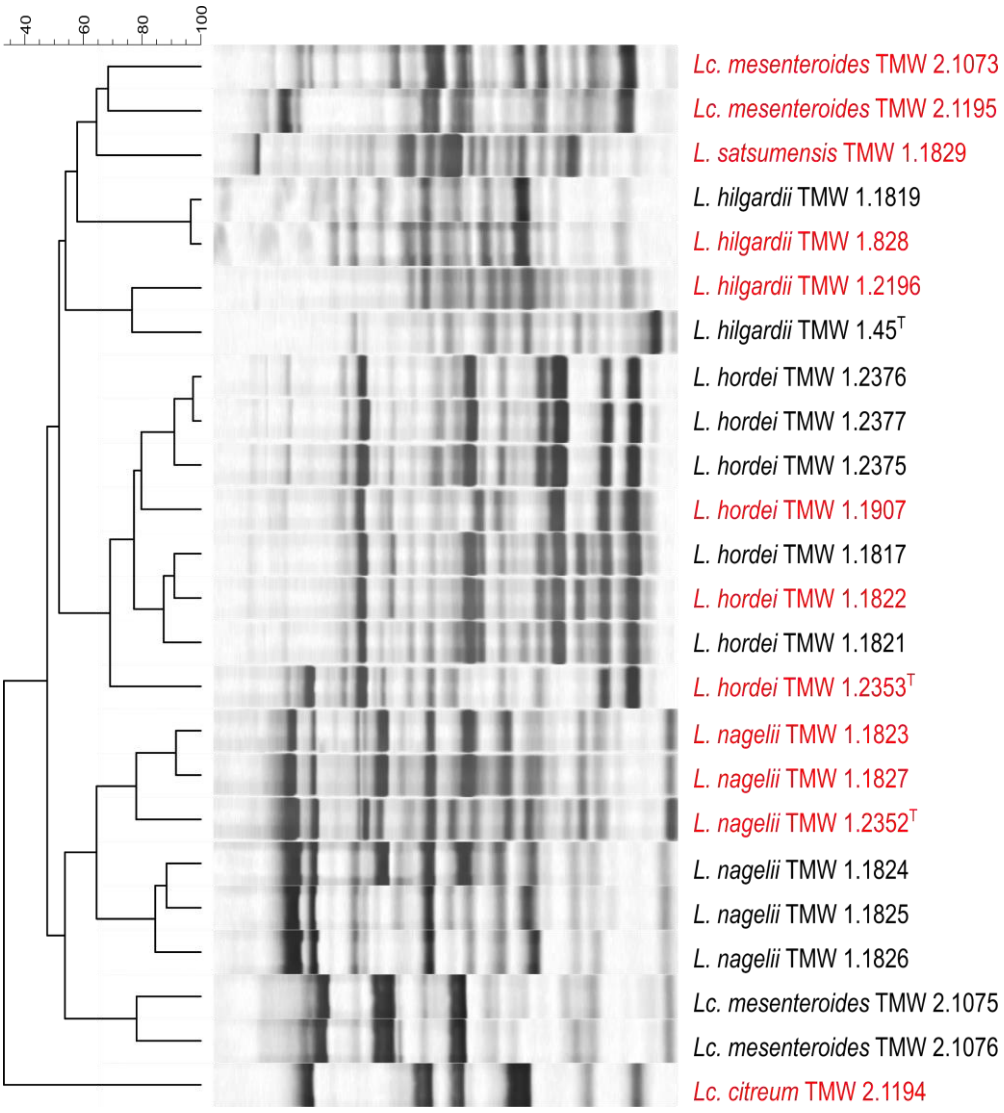

Figure 4 RAPD patterns of strains used in this study. The dendrogram was calculated by the unweighted pair group method with arithmetic mean (UPGMA) with Dice´s similarity coefficient and 1 % tolerance. Scale bar refers to the similarity coefficients. Strains that were selected for genome sequencing are marked in red.

Based on RAPD-patterns and the glucan-forming capabilities, 12 different strains were subsequently chosen for DNA sequencing and functional annotation. Genbank accession numbers are listed in Table 6.

4.1.2 Identification of glucansucrase genes in LAB from water kefir by genome analysis

BLAST analysis was performed to search for glucansucrase genes within the obtained WGS using the nucleotide sequences of known glucansucrases. Subsequently, the translated ORFs of predicted glucansucrases were applied for BLAST analysis against the NCBI database. As listed in Table 8, the type strains *L. hordei, L. nagelii* and *L. hilgardii* exhibited no glucansucrase genes, while *L. satsumensis* TMW 1.1829 and all strains of the genus *Leuconostoc* featured two or more glucansucrase genes. While being highly similar for glucansucrases within the same species, the theoretical molecular weight differed largely among all obtained glucansucrases. As different molecular weights may come from different domain architectures, all sequences were applied for conserved domain search. Thereby, all glucansucrases exhibited only one GH70 catalytic domain, while dsr2135 of *Lc. citreum* TMW 2.1194 featured two catalytic domains. Furthermore, the glucansucrases differed largely in their amount and position of glucan-binding domains that include several glucan-binding repeats. Detailed domain architectures of glucansucrases are shown in Figure 5.

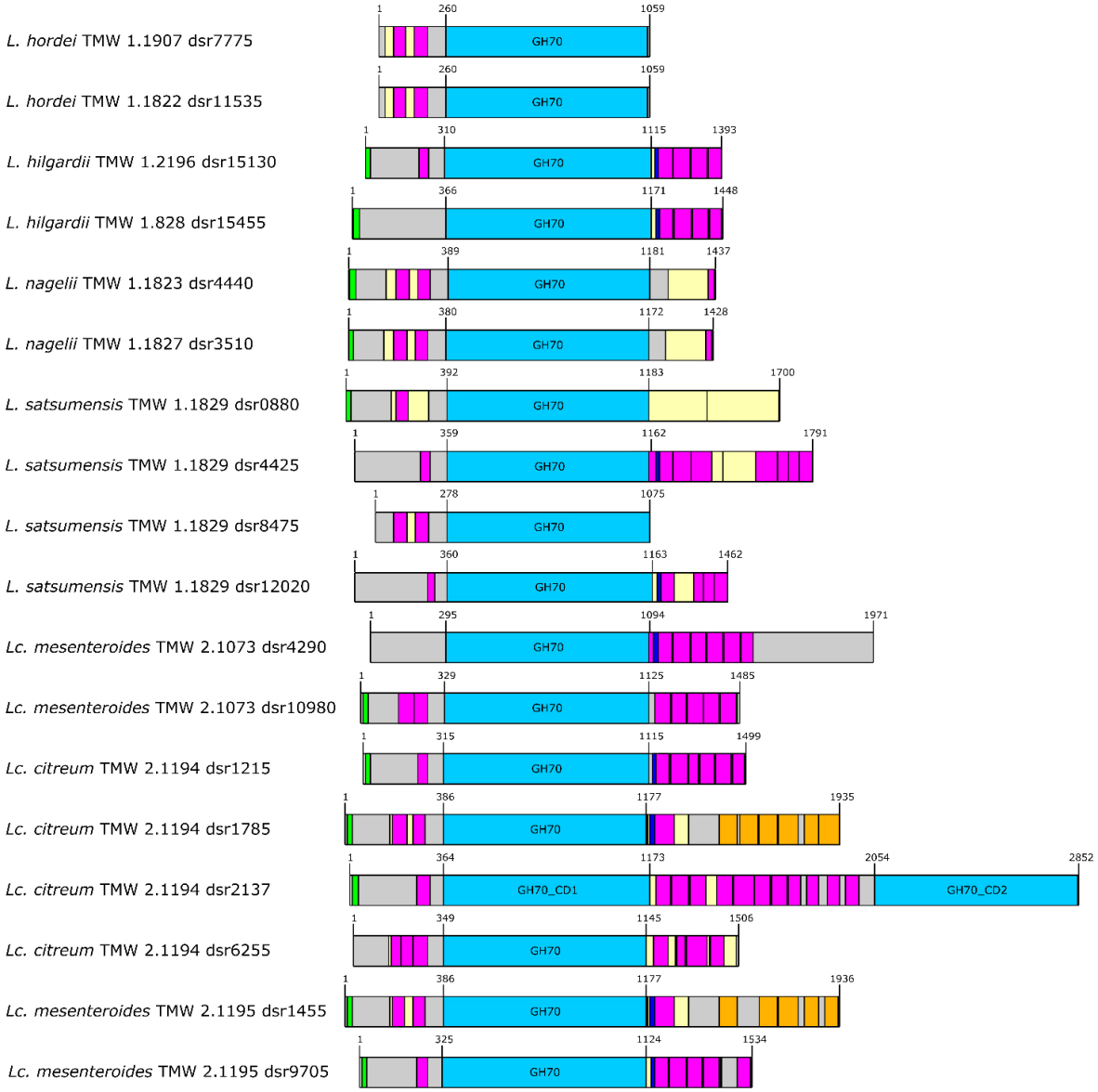

Figure 5 Domain architecture of glucansucrase amino acid sequences obtained from WGS of LAB isolated from water kefir. Blue = GH70 catalytic domain; yellow = glucan-binding domain; pink = glucan-binding repeats; dark blue = choline-binding/ cell wall binding motif; green = signal peptide; orange = SH3 domain, gray = variable.

Furthermore, none of the obtained glucansucrases featured an LPxTG motif, which would enable covalent binding to the cell wall. The N-terminal signal peptide that appeared to be present in some glucansucrase sequences was of the KxYKxGKxW-type. Theoretical isoelectric points (iEPs) ranged between 4.36 and 5.25, while only glucansucrases within the genus *Leuconostoc* exhibited iEPs above 5.00.

Table 8 Overview of glucansucrase genes found in sequenced LAB.

Species	Strain	Quantity	Locus tag	Theoretical M_w [kDa]	Theoretical iEP	Quantity GH70	Quantity GBD	Signal peptide
L. hilgardii	TMW 1.2196	1	C2L99_15130	158.77	4.50	1	1	X
L. hilgardii	TMW 1.828	1	CLI91_15355	152.9	4.51	1	1	X
L. hilgardii	TMW 1.45^T	0						
L. hordei	TMW 1.1822	1	BSQ49_11535	118.11	4.66	1	1	-
L. hordei	TMW 1.1907	1	CRI84_07775	118.12	4.66	1	1	-
L. hordei	TMW 1.2353^T	0						
L. nagelii	TMW 1.1823	1	CRI83_04440	159.83	4.66	1	2	X
L. nagelii	TMW 1.1827	1	BSQ50_03510	158.61	4.63	1	2	X
L. nagelii	TMW 1.2352^T	0						
L. satsumensis	TMW 1.1829	4	CRI87_00880	188.36	4.99	1	3	X
			CRI87_04425	196.06	4.71	1	3	-
			CRI87_08475	118.50	4.87	1	3	-
			CRI87_12020	158.80	4.61	1	1	-
Lc. citreum	TMW 2.1194	4	CRI81_01215	167.44	5.25	1	1	X
			CRI81_01785	215.90	5.21	1	2	X
			CRI81_02135	314.90	4.72	2	2	X
			CRI81_06255	167.99	4.86	1	4	-
Lc. mesenteroides	TMW 2.1073	2	CRI85_04290	213.74	5.31	1	1	-
			CRI85_10980	163.25	4.36	1	2	X
Lc. mesenteroides	TMW 2.1195	2	COV80_04155	215.98	5.20	1	3	X
			COV80_09705	168.20	4.36	1	1	X

The glucansucrases found during this study were compared with known enzymes using amino acid sequence alignments. Due to the differences in domain architecture, reasonable alignments were only achieved by sequence comparison of the respective GH70 catalytic domains. The alignment was subsequently visualized in a phylogenetic tree, as shown in Figure 6. Thereby, it could be shown that especially glucansucrases obtained from WGS of *Leuconostoc* species were highly similar to already known glucansucrases of other strains of this genus. However, dsr10980 of *Lc. mesenteroides* TMW 2.1073 appeared to cluster isolated from other glucansucrases. Equally, glucansucrases from *L. hordei* and *L. nagelii,* as well as two glucansucrases of *L. satsumensis* TMW 1.1829 formed a new subgroup among known glucansucrases, while being highly similar to each other. Furthermore, a BLAST search of the complete *L. hordei* glucansucrases against the NCBI database revealed that the best scored hit of an enzyme that was effectively analysed for its glucan-producing abilities was *L. sakei* Kg15 dextransucrase (Uniprot ID: Q5SBM3) with a coverage of 95 % and an amino acid sequence identity of 51 %. The best scored hit for the complete *L. nagelii* glucansucrases was the *Lc. mesenteroides* L0309 dextransucrase (Uniprot ID: Q6TXV4) with a coverage of 99 % and an amino acid sequence identity of 45 %. These BLAST analyses were conducted in January 2018 confirming the glucansucrases of *L. hordei* and *L. nagelii* to be new types of glucansucrases.
Thus, *L. hordei* and *L. nagelii* were selected for further analyses. As *L. hilgardii* strains also exhibited only one gene coding for a glucansucrase that was already described in previous studies (Waldherr *et al.*, 2010), this species was consulted for comparative analyses, as well as improvement of sample size. Amino acid sequences of *L. hordei* and *L. nagelii* glucansucrases are deposited in Appendix 1 and Appendix 2.

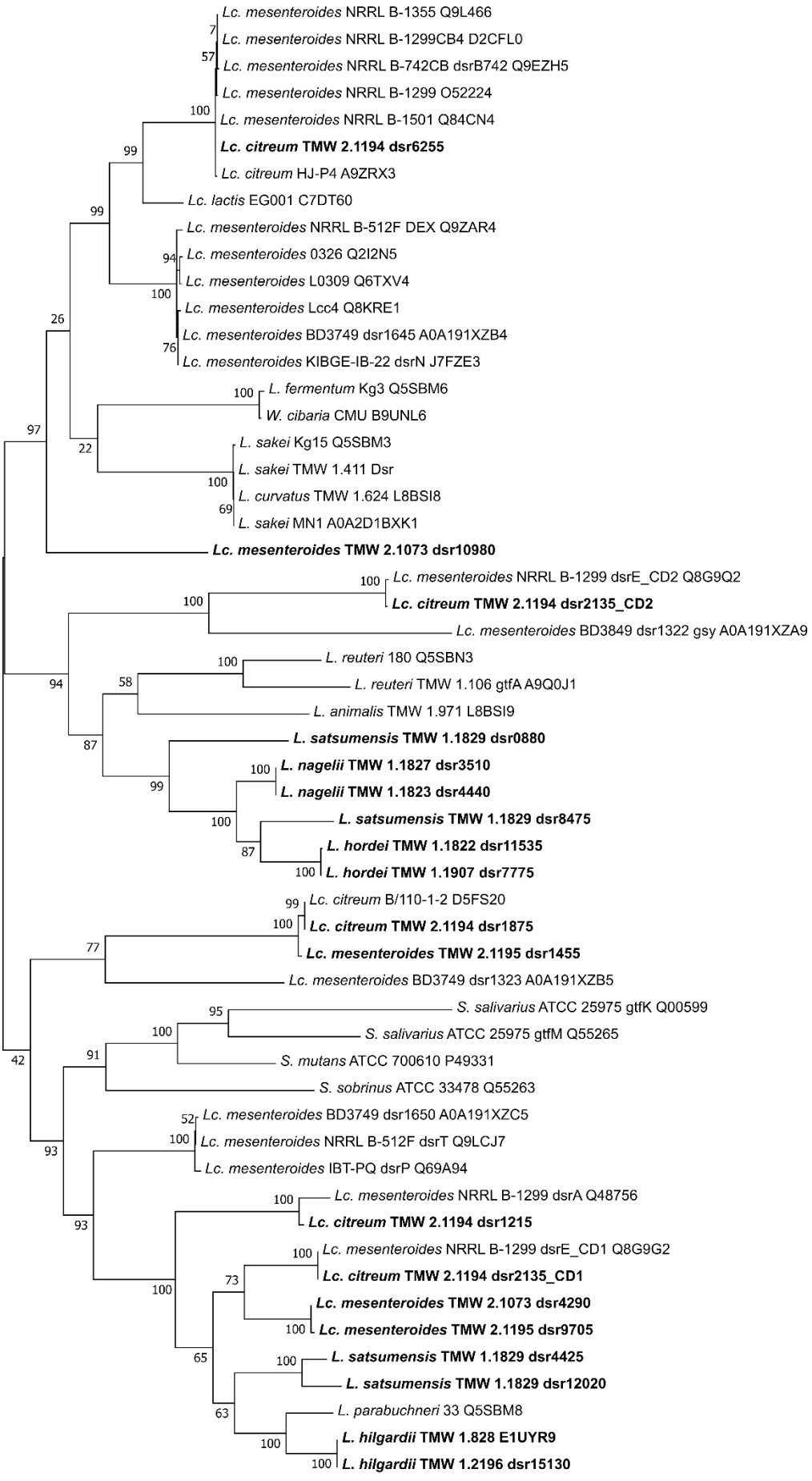
Lc. mesenteroides NRRL B-1355 Q9L466
Lc. mesenteroides NRRL B-1299CB4 D2CFL0
Lc. mesenteroides NRRL B-742CB dsrB742 Q9EZH5
Lc. mesenteroides NRRL B-1299 O52224
Lc. mesenteroides NRRL B-1501 Q84CN4
Lc. citreum TMW 2.1194 dsr6255
Lc. citreum HJ-P4 A9ZRX3
Lc. lactis EG001 C7DT60
Lc. mesenteroides NRRL B-512F DEX Q9ZAR4
Lc. mesenteroides 0326 Q2I2N5
Lc. mesenteroides L0309 Q6TXV4
Lc. mesenteroides Lcc4 Q8KRE1
Lc. mesenteroides BD3749 dsr1645 A0A191XZB4
Lc. mesenteroides KIBGE-IB-22 dsrN J7FZE3
L. fermentum Kg3 Q5SBM6
W. cibaria CMU B9UNL6
L. sakei Kg15 Q5SBM3
L. sakei TMW 1.411 Dsr
L. curvatus TMW 1.624 L8BSI8
L. sakei MN1 A0A2D1BXK1
Lc. mesenteroides TMW 2.1073 dsr10980
Lc. mesenteroides NRRL B-1299 dsrE_CD2 Q8G9Q2
Lc. citreum TMW 2.1194 dsr2135_CD2
Lc. mesenteroides BD3849 dsr1322 gsy A0A191XZA9
L. reuteri 180 Q5SBN3
L. reuteri TMW 1.106 gtfA A9Q0J1
L. animalis TMW 1.971 L8BSI9
L. satsumensis TMW 1.1829 dsr0880
L. nagelii TMW 1.1827 dsr3510
L. nagelii TMW 1.1823 dsr4440
L. satsumensis TMW 1.1829 dsr8475
L. hordei TMW 1.1822 dsr11535
L. hordei TMW 1.1907 dsr7775
Lc. citreum B/110-1-2 D5FS20
Lc. citreum TMW 2.1194 dsr1875
Lc. mesenteroides TMW 2.1195 dsr1455
Lc. mesenteroides BD3749 dsr1323 A0A191XZB5
S. salivarius ATCC 25975 gtfK Q00599
S. salivarius ATCC 25975 gtfM Q55265
S. mutans ATCC 700610 P49331
S. sobrinus ATCC 33478 Q55263
Lc. mesenteroides BD3749 dsr1650 A0A191XZC5
Lc. mesenteroides NRRL B-512F dsrT Q9LCJ7
Lc. mesenteroides IBT-PQ dsrP Q69A94
Lc. mesenteroides NRRL B-1299 dsrA Q48756
Lc. citreum TMW 2.1194 dsr1215
Lc. mesenteroides NRRL B-1299 dsrE_CD1 Q8G9G2
Lc. citreum TMW 2.1194 dsr2135_CD1
Lc. mesenteroides TMW 2.1073 dsr4290
Lc. mesenteroides TMW 2.1195 dsr9705
L. satsumensis TMW 1.1829 dsr4425
L. satsumensis TMW 1.1829 dsr12020
L. parabuchneri 33 Q5SBM8
L. hilgardii TMW 1.828 E1UYR9
L. hilgardii TMW 1.2196 dsr15130
0,10

Figure 6 Phylogenetic tree calculated on the basis of aligned amino acid sequences of the GH70 catalytic domains of glucansucrases from LAB. The tree was built using the Maximum Likelihood method based on the JTT matrix-based model. Bootstrap test (1000 replicates) percentages are shown on the branch nodes. Branch length are measured in the number of substituted amino acids per site. Each protein is labelled with its Uniprot ID, if available. New glucansucrase sequences obtained during this study are indicated in bolt letters. dsrE of *Lc. mesenteroides* NRRL B-1299 and dsr2135 of *Lc. citreum* TMW 2.1194 both exhibit two GH70 domains that are therefore named catalytic domain (CD) 1 and 2.

4.2 Characterization of the ability of selected strains to ferment certain substrates

All *L. hordei* and *L. nagelii*, as well as *L. hilgardii* strains were investigated with regards to their ability to ferment certain substrates using API®50CHL test stripes. The results were subsequently correlated (Spearman´s rank) with the isolation source water kefir. In order to improve sample size for this analysis, fermentation profiles of additional *L. hilgardii* strains were taken into account that were obtained from the Master´s thesis of Sabine Winkler, who was co-supervised during this work. Thus, four different strains from water kefir (*L. hilgardii* TMW 1.2251, TMW 1.2290, TMW 1.2296 and TMW 1.2297), two strains from unknown source (*L. hilgardii* TMW 1.423 and TMW 1.434) and one strain from Yuca starch (*L. hilgardii* TMW 1.586) were additionally analysed. Only significant correlation coefficients ($p < 0.05$) were considered for discussion and correlation coefficients (ρ) were subsequently interpreted according to Mukaka (2012). The API-test results are shown in Figure 7. Spearman´s rank analysis designated only two fermented substrates as significantly correlated with the isolation source water kefir: L-arabinose ($p = 0.016$) and D-mannitol ($p = 0.002$). According to the obtained correlation coefficients (L-arabinose = 0.52, D-mannitol = 0.65), the ability to ferment these carbohydrates appeared to be moderately correlated with the isolation source water kefir. A complete list of all correlation coefficients is attached to the appendix (see Appendix 3).

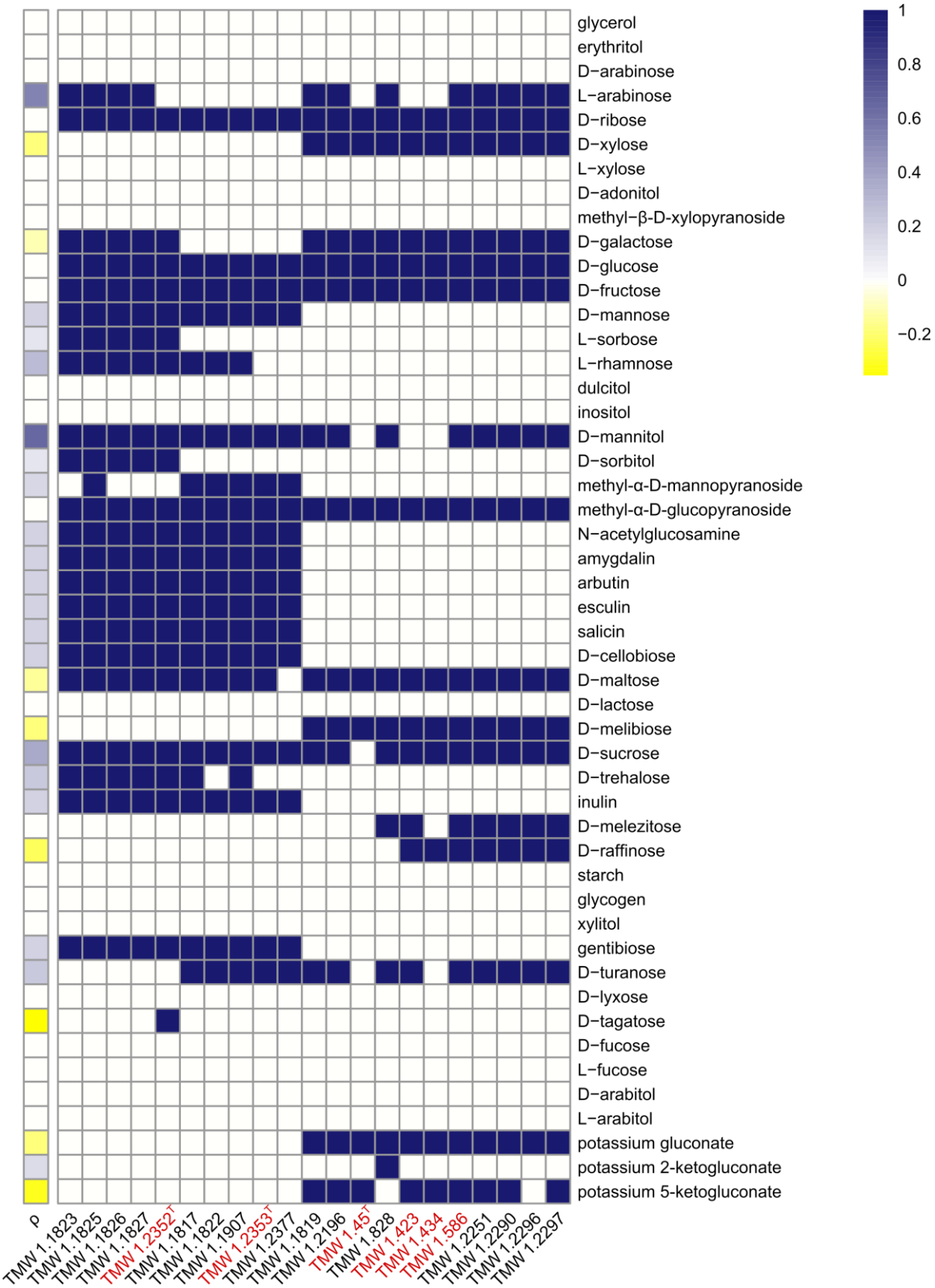

Figure 7 Heatmap of fermentation profiles of *L. nagelii, L. hordei* and *L. hilgardii* strains using API®50CHL test stripes and correlation coefficients (ρ, Spearman´s rank) of these profiles with the isolation source water kefir. Strains not isolated from water kefir are indicated in red letters. Dark blue (main heatmap) = positive API-test, white (main heatmap) = negative API-test. The scale on the right side shows the continuous colormap for correlation coefficients from positive correlation (= blue) over no correlation (= white) to negative correlation (= yellow).

4.3 Characterization and comparison of the native *L. hordei* TMW 1.1822 and *L. nagelii* TMW 1.1827 glucansucrases

4.3.1 Recovery and identification of the native glucansucrases in buffered cell suspensions

Due to the lack of a known type of cell wall anchor, the native glucansucrases of *L. hordei* TMW 1.1822 and *L. nagelii* TMW 1.1827 were recovered using cell suspensions in citrate-phosphate buffer at a starting pH of 6.5 either supplemented with sucrose or no sucrose to study the substrate-dependent release of these enzymes by subsequent SDS-PAGE. To distinguish the glucansucrases from other proteins present within the supernatants, an activity staining was additionally performed that is based on the in-gel formation of glucan from sucrose, which is subsequently stained by periodic acid Schiff´s staining (PAS). Supernatants of *L. hilgardii* TMW 1.828 were applied as a positive control, as this glucansucrase has shown good results within this assay in previous studies (Waldherr *et al.*, 2010). As shown in Figure 8, both glucansucrase protein bands of *L. nagelii* and the one of *L. hilgardii* appeared in a range from 130 to 250 kDa, while the one of *L. hordei* appeared in a range between 100 to 130 kDa. These results were consistent with the predicted molecular weights of the respective glucansucrases (Table 8). The differential staining of glucansucrases was subsequently used to identify the corresponding bands on a silver-stained gel. As depicted in Figure 8B, several other proteins were hence released into the buffer supernatant by all species. However, the total protein content of all supernatants was lower for *L. hordei* (~ 90 µg/mL) than for *L. nagelii* (~ 100 µg/mL), which was also visible from a Coomassie-stained SDS-gel (Figure 9B). Herein, the glucansucrase protein band of *L. hordei* appeared empirically less prominent than the glucansucrase bands of *L. nagelii.* Although protein contents of *L. nagelii* supernatants were invariably higher than the ones of *L. hordei* when incubations in buffer were carried out with a starting pH of 6.5, both protein contents varied between different experiments (*L. hordei* ~ 40 – 90 µg/mL, *L. nagelii* ~ 100 – 216 µg/mL).

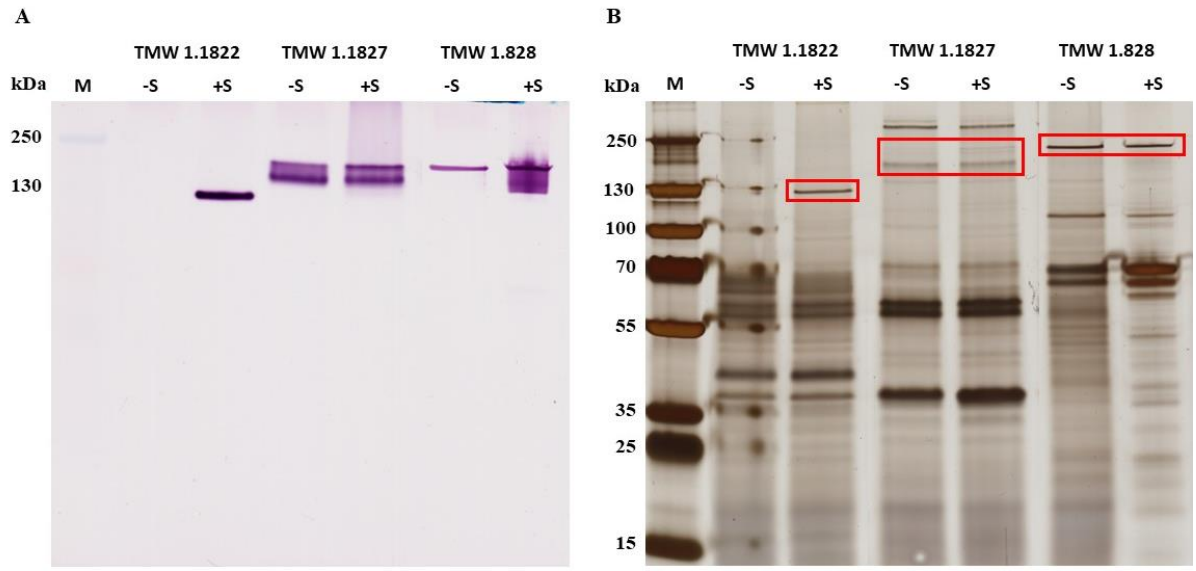

Figure 8 SDS-gels of supernatants obtained in the presence (+S) or absence (-S) of sucrose. Gels were either stained by PAS (A) or silver staining (B).

Moreover, glucansucrases of all strains were present in supernatants when cells were incubated in the presence of sucrose. In the absence of sucrose, however, only *L. nagelii* TMW 1.1827 and *L. hilgardii* TMW 1.828 appeared to release their respective glucansucrases. To investigate, if this was an effect of expression or release of the glucansucrase in *L. hordei*, cells obtained in the absence of sucrose were subjected for cell lysis and subsequent SDS-PAGE. As depicted in Figure 9A, the glucansucrase of *L. hordei* TMW 1.1822 was detectable in lysates of cells that were incubated in buffers without sucrose, indicating that not the expression, but the release of this enzyme is induced by the presence of sucrose.

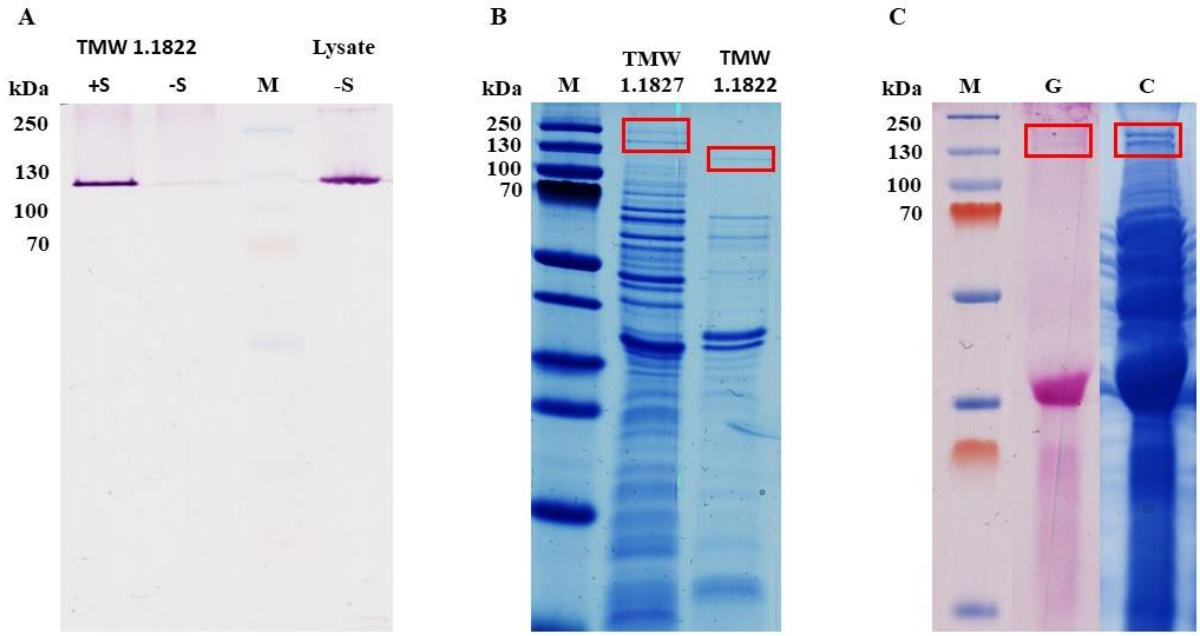

Figure 9 SDS-gels of supernatants and cell lysates of *L. hordei* TMW 1.1822 stained with PAS (A), supernatants of *L. hordei* TMW 1.1822 and *L. nagelii* TMW 1.1827 obtained in the presence of sucrose, stained with Coomassie staining (B) and concentrated supernatants of *L. nagelii* TMW 1.1827 obtained in the absence of sucrose stained with glycoprotein staining (G) and Coomassie staining (C) (C).

Furthermore, the *L. nagelii* glucansucrase displayed several protein bands on SDS-gels of all analyses. In order to investigate, if this may come from protein glycosylation, in particular different protein glycosylation patterns, proteins of supernatants obtained in the absence of sucrose were concentrated and applied for SDS-PAGE. Subsequently, glycoproteins were stained by PAS staining, revealing both protein bands of the *L. nagelii* glucansucrase to be glycosylated (Figure 9C).

4.3.2 Characterization of the native extracellular glucansucrases of *L. hordei* TMW 1.1822 and *L. nagelii* TMW 1.1827

Native glucansucrases of both *L. hordei* and *L. nagelii* were recovered in buffered cell suspensions supplemented with sucrose at a starting pH of 6.5. Subsequently, supernatants were used to determine optimum reaction pH and temperature by measuring overall fructose release at the end of each reaction. As shown in Figure 10, the reaction optimum was about pH 5.0 for both glucansucrases, while volumetric activities decreased rapidly at pH lower than 4.0. Although volumetric activity of the *L. nagelii* glucansucrase stayed constantly high until pH 6.0, it rapidly decreased at higher pH, while volumetric activities of the *L. hordei* glucansucrase decreased less drastic with increasing pH.

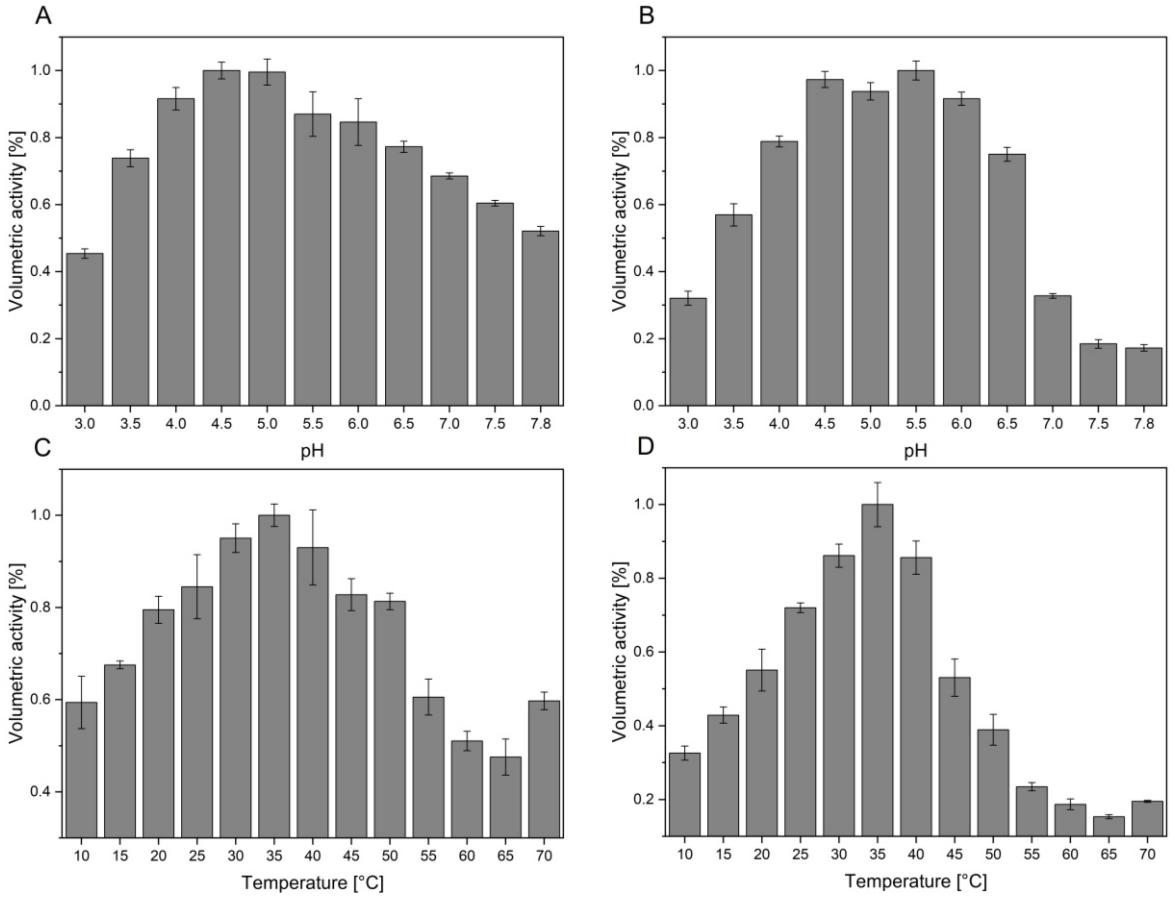

Figure 10 Relative volumetric activities of native glucansucrases of *L. hordei* TMW 1.1822 (A+C) and *L. nagelii* TMW 1.1827 (B+D) at different pH (A+B) and temperatures (C+D). Experiments at different pH were conducted at 30 °C, while experiments at different temperatures were conducted at pH 5.0.

The temperature optimum of both glucansucrases appeared to be at 35 °C. Below and above this temperature, the volumetric activity of both glucansucrases decreased, which again appeared to be more drastic for the *L. nagelii* glucansucrase. Interestingly, both glucansucrases showed an increase in volumetric activity at 70 °C. Despite having temperature optima at 35 °C, subsequent experiments were carried out at 30 °C, which was used as incubation temperature for the growth of both microorganisms. Both glucansucrases appeared to follow Michaelis-Menten kinetics (see Appendix 4). Concomitantly, the Michaelis constant K_M of the *L. hordei* glucansucrase was 17.93 mM and was thus higher than the K_M of the *L. nagelii* glucansucrase, comprising 12.46 mM. By contrast, the maximum reaction rate v_{max} of the *L. nagelii* glucansucrase (= 0.25 mmol/min*L^{-1}) was about 6.25 times higher than v_{max} of the *L. hordei* glucansucrase (=0.04 mmol/min*L^{-1}).

4.3.3 Investigation and comparison of glucan formation applying the native extracellular glucansucrases of *L. hordei* TMW 1.1822 and *L. nagelii* TMW 1.1827

Cell-free supernatants of *L. hordei* and *L. nagelii* obtained in buffered cell suspension supplemented with sucrose were used to produce glucans for 24 h at equal reaction conditions of pH 5.0, 30 °C and 0.2 M sucrose.

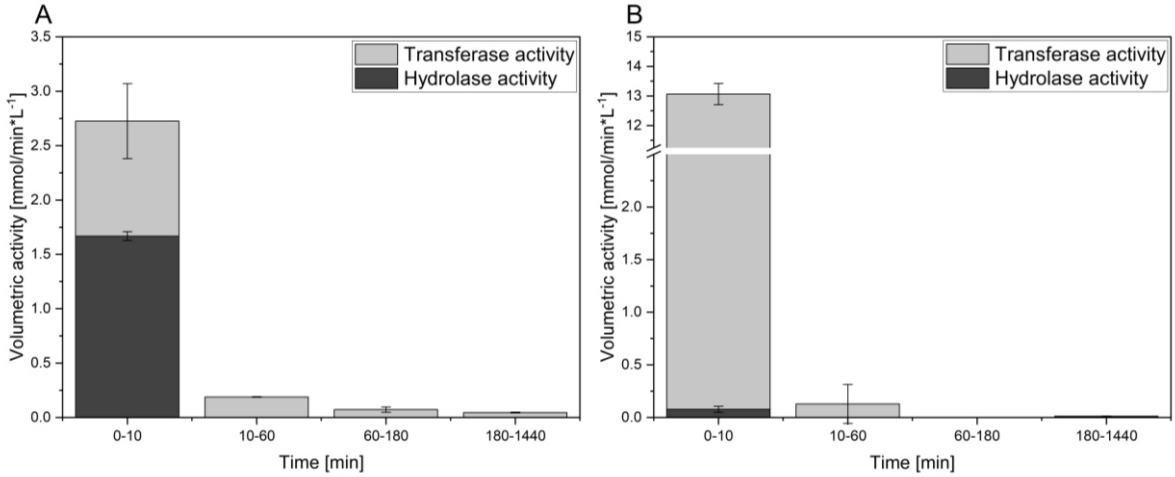

Figure 11 Volumetric activities of the glucansucrases of *L. hordei* TMW 1.1822 (A) and *L. nagelii* TMW 1.1827 (B). Transferase activities (light gray columns) and hydrolase activities (dark gray columns) were calculated from released fructose and glucose concentrations determined by HPLC analysis.

As shown in Figure 11, the transferase rate of the *L. hordei* glucansucrase was about ~ 39 % (85 % within 24 h) within the first 10 min of incubation, while the *L. nagelii* glucansucrase exhibited a much higher transferase rate of ~ 99 % (95 % within 24 h) within this time. Interestingly, the glucansucrase of *L. nagelii* consumed the total sucrose within the first 10 min of reaction. By contrast, the *L. hordei* glucansucrase converted only ~ 83 % of the total substrate within 24 h.

The glucans that were produced after 24 h were subsequently investigated by methylation analysis. As shown in Figure 12, 1,6-glycosidic linkages appeared to be predominant in both glucans, identifying these polysaccharides as dextrans. Additionally, small portions of the dextran backbones or side chains were 1,3-linked. Furthermore, about 2 % of the dextran backbone units of *L. hordei* and about 3 % of the *L. nagelii* dextran backbone units were branched at position *O*3.

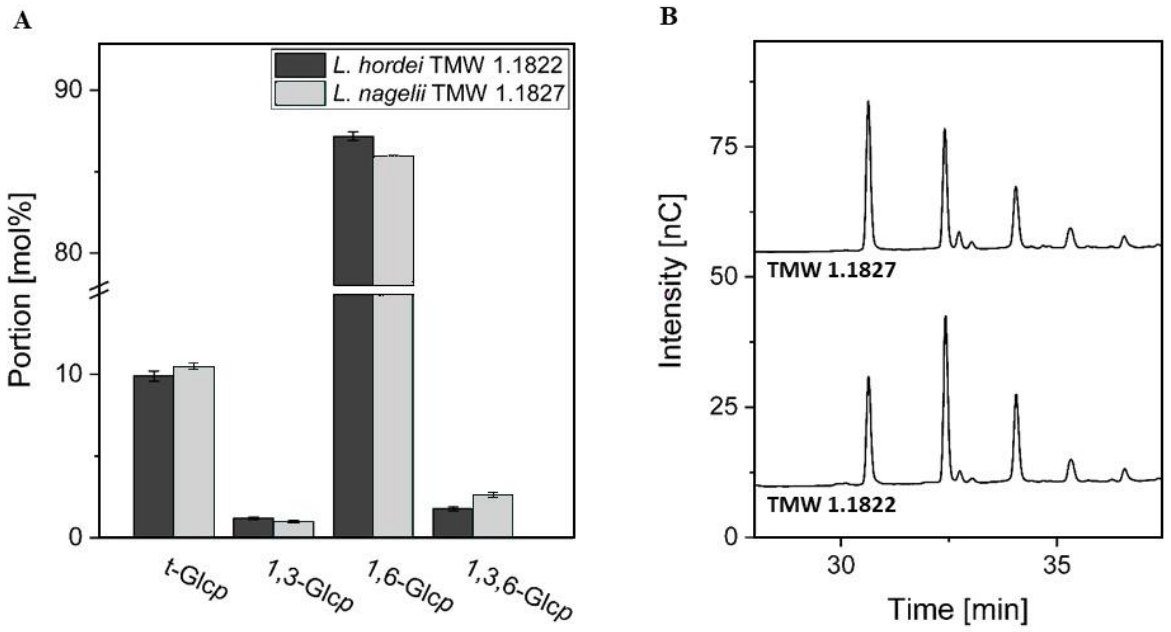

Figure 12 Glycosidic linkages (mol%) as determined by methylation analysis (A) and HPAEC-PAD chromatograms of the *endo*-dextranase hydrolysates of dextrans produced at 30 °C and pH 5.0 for 24 h. t = terminal, Glc = glucose, *p* =pyranose.

To gain further insights into the structural architecture of the formed dextrans, polysaccharide samples were digested using *endo*-dextranase, which specifically cleaves the α-1,6-linked dextran backbone liberating isomaltose and branched oligosaccharides. Subsequently, the hydrolysate products were analysed by HPAEC-PAD measurements. As depicted in Figure 12B, both dextrans comprised the same structural elements, but the peak eluting after ~ 31 min showed a higher abundance for the *L. nagelii* dextran. While this peak is characteristic for monomeric, *O*3-bound side chains, the two later eluting peaks come from oligosaccharides with di- and trimeric *O*3-linked side chains, respectively (Münkel *et al.*, 2019). The results from *endo*-dextranase digestion thus indicate differences in the side-chain length of the dextrans produced by *L. nagelii* TMW 1.1827 and *L. hordei* TMW 1.1822, while featuring identical molecular components. Additionally, AF4-MALS-UV measurements were conducted to study the macromolecular structure of the dextrans produced under constant conditions using cell-free supernatants.

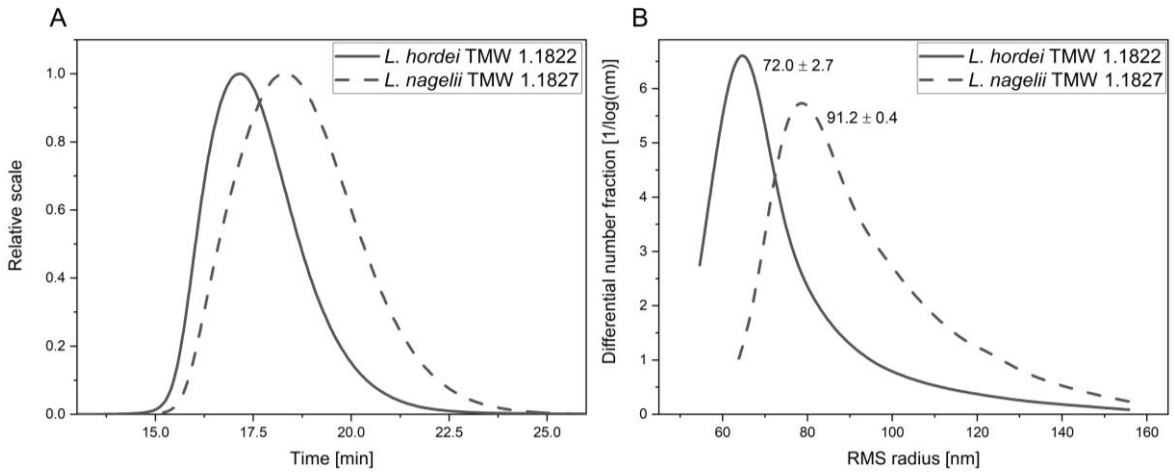

Figure 13 Light scattering signals at 90° (A) and differential rms radius distributions (B) obtained by AF4-MALS-UV measurements of dextrans produced by the native extracellular dextranuscrases of *L. hordei* TMW 1.1822 and *L. nagelii* TMW 1.1827. Average rms radii (R_w, B) are given as mean ± standard deviation.

As shown in Figure 13A, the *L. nagelii* dextran eluted at ~ 19 min and thus later than the *L. hordei* dextran eluting at ~ 17.5 min. The rms radius distributions (Figure 13B) furthermore indicated that the average rms radii of the *L. hordei* dextrans were smaller than in *L. nagelii* dextrans, coinciding with the shifted retention times according to the principles of AF4 separation (Ua-Arak *et al.*, 2017a).

4.3.4 Investigation and comparison of dextran formation applying different concentrations of dextransucrase-containing supernatants of *L. hordei* TMW 1.1822 and *L. nagelii* TMW 1.1827

In order to investigate if differences in volumetric activity, as well as dextran macromolecular structure originated in different amounts of native extracellular dextransucrase in supernatants of *L. hordei* TMW 1.1822 and *L. nagelii* TMW 1.1827, enzyme extracts that were diluted 2-fold, 4-fold and 10-fold were used to form dextrans for 24 h at pH 5.0 and 30 °C. Along with a gradual decrease in overall and transglycosylation activity, the amount of isolated and predicted amount (for calculation see section 3.5.1.2) of dextran obtained from the *L. hordei* dextransucrase gradually decreased with increasing dilution of the enzyme extract (Figure 14). Moreover, the difference between isolated and predicted dextran converged with increasing dilution. By contrast, the amount of isolated dextran stayed constant until a 4-fold dilution of the enzyme extract of *L. nagelii*, while decreasing slightly, yet significantly at a 10-fold dilution. This appeared to be more drastic for the predicted amount of dextran. Simultaneously, overall and transglycosylation activities stayed constant until decreasing at a 10-fold dilution.

Furthermore, even the undiluted enzyme extract of *L. hordei* was not capable of producing the same amount of isolable and predicted amount of dextran as a 10-fold dilution of the *L. nagelii* enzyme extract.

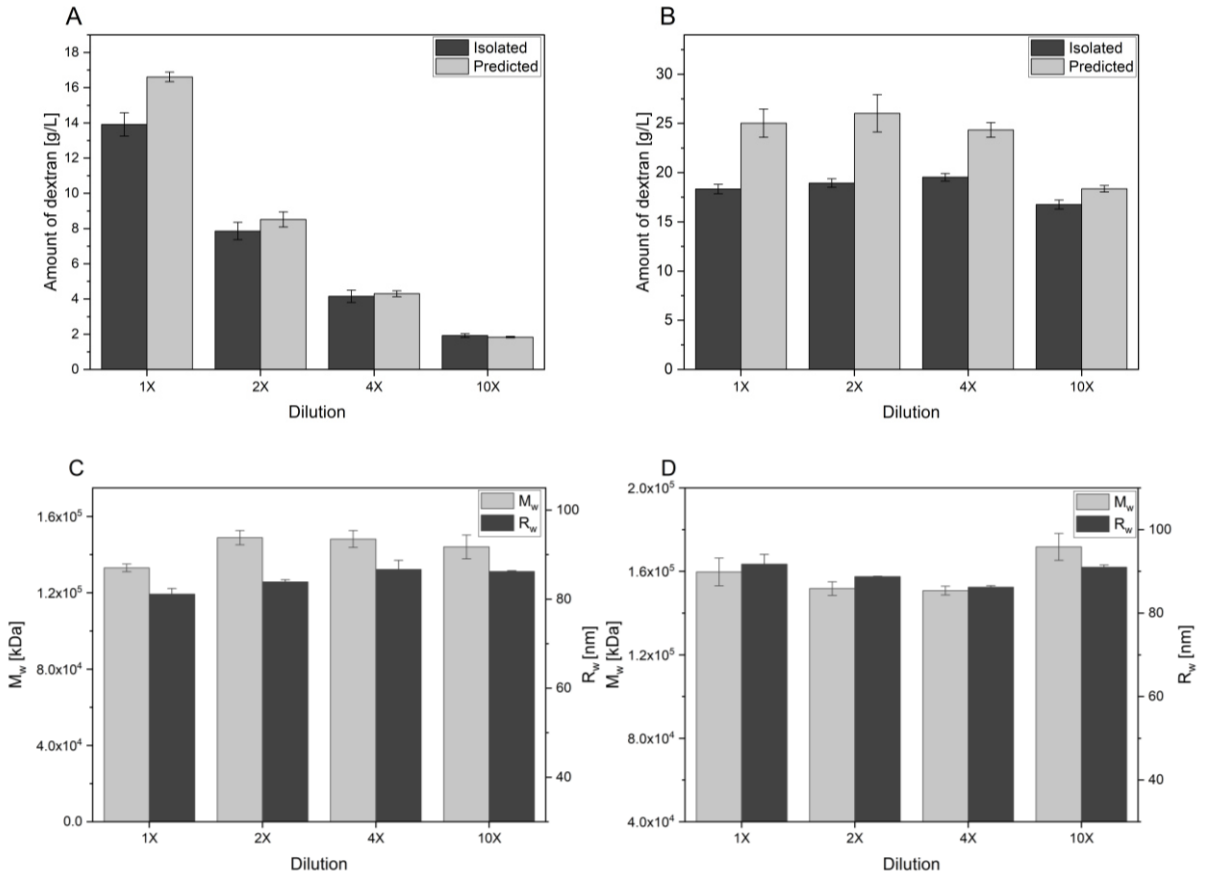

Figure 14 Isolated and predicted amounts of dextran (A+B) and average molecular weight (M_w) and average rms radii (R_w)(C+D) obtained by distinct amounts of enzyme extract of *L. hordei* TMW 1.1822 (A+C) and *L. nagelii* TMW 1.1827 (B+D). Predicted amounts of dextran and M_w are depicted in light gray, isolated amounts of dextran and R_w are displayed in dark gray.

The average M_w of all dextrans produced by *L. nagelii* enzyme extracts appeared to be higher than for all dilutions of the enzyme extract of *L. hordei*. However, only the dextrans of the undiluted enzyme extract of *L. hordei,* as well as of the 10-fold diluted enzyme extract of *L. nagelii* showed significantly different average M_w compared to the enzyme extracts obtained from the respective other microorganism. The average R_w of dextrans obtained from enzyme extracts of *L. hordei* ranged between 81.1 - 86.7 nm, while dextrans of *L. nagelii* exhibited higher R_w ranging between 86.2 - 91.7 nm. Between dextrans obtained from both microorganisms, significant differences in average R_w could be shown for the undiluted, as well as 2-fold diluted enzyme extracts of *L. hordei* compared to all dilutions of enzyme extracts of *L. nagelii*. Furthermore, the 10-fold diluted enzyme extract of *L. nagelii* produced a dextran of

significantly higher average R_w than all enzyme dilutions of *L. hordei* did. All p-values obtained from statistical analysis are summarized in Appendix 5.

4.3.5 Heterologous expression and characterization of the *L. nagelii* dextransucrase compared to a truncated variant

In order to investigate if differences in dextran formation between the *L. hordei* and *L. nagelii* dextransucrases originate in the additional C-terminal glucan-binding domain of the *L. nagelii* dextransucrase, the *L. nagelii* dextransucrase dsr3510, as well as a truncated variant (dsr3510ΔC-term) of this enzyme (see Appendix 2) were expressed heterologously in *E. coli*.

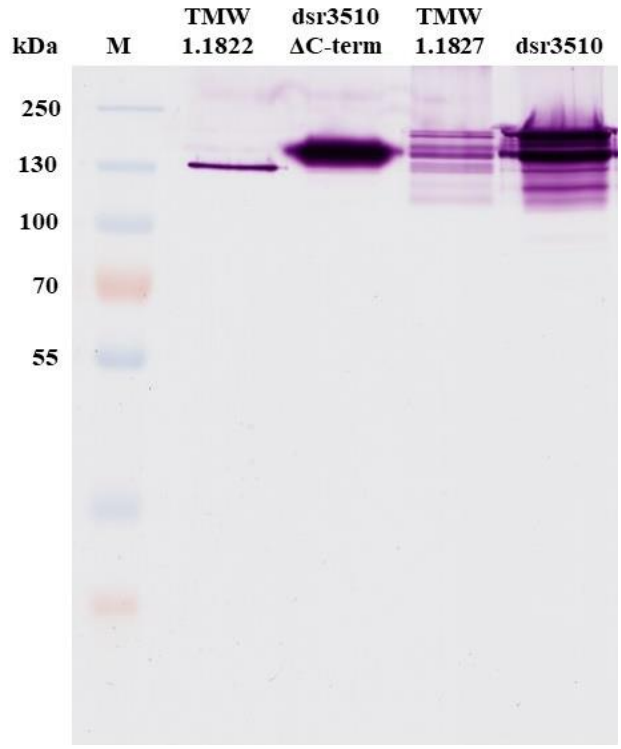

Figure 15 PAS-stained SDS-gel of the complete dsr3510 and the truncated variant dsr3510ΔC-term compared to the native dextransucrases of *L. hordei* TMW 1.1822 and *L. nagelii* TMW 1.1827.

As displayed in Figure 15, the complete variant of the *L. nagelii* dextransucrase formed a similar protein band pattern than the native enzyme. By contrast, the truncated variant dsr3510ΔC-term formed only one protein band at the same molecular weight of the lower predominant band of the native *L. nagelii* dextransucrase. However, Co^{2+}-affinity purification of the heterologously expressed dextransucrase variants led to a complete loss of enzyme activity. As the crude

protein extract of un-induced *E. coli* cultures exhibited no activity on sucrose, glucose and fructose at the applied conditions, following experiments were conducted with these extracts.

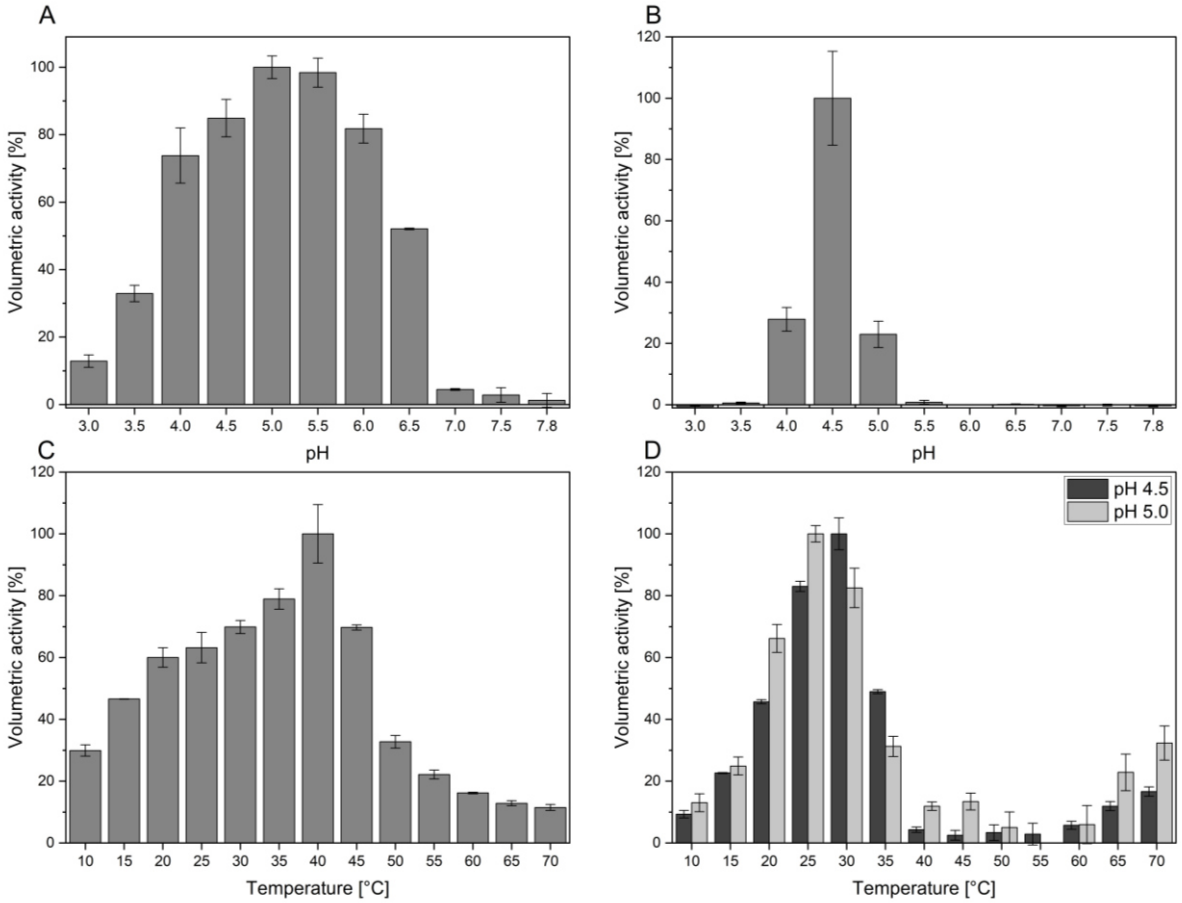

Figure 16 Relative volumetric activities of complete dsr3510 (A+B) and dsr3510ΔC-term (B+D) at different pH (A+B) and temperature (C+D). Measurements at different pH were conducted at 30 °C, while measurements at different temperatures were conducted at pH 5.0 and pH 4.5 in case of the truncated variant.

As shown in Figure 16, the pH optimum of the complete dsr3510 variant was at 5.0 – 5.5, while overall activity decreased rapidly below pH 4.0 and above pH 6.0. By contrast, the truncated variant exhibited a clear pH optimum of pH 4.5, while no activity was detectable below pH 4.0 and above pH 5.0. Furthermore, the temperature optimum of the complete dextransucrase variant was at 40 °C, while activity decreased rapidly at temperatures above 45 °C. This decrease was, however, less drastic with decreasing temperatures. At pH 5.0, the truncated variant exhibited the highest activity at 25 °C, while having a temperature optimum of 30 °C at pH 4.5. Additionally, the truncated variant exhibited an increase in activity above 60 °C independently from the pH.

Since a Ca^{2+} binding motif was found in the native dextransucrase of *L. nagelii* TMW 1.1827 (positions E511, D517, N561 and D1044) using homology modelling (using known crystal

structures of dextransucrase (best fit) of *Lc. mesenteroides* NRRL B-1299 DSR-M, PDB Accession No. 5ngy.2 and of *L. reuteri* 121 GTFA, PDB Accession No. 4amc.1.A), the influence of different cations on enzyme activity of the heterologously expressed dextransucrase variants was tested. As depicted in Figure 17, the activity of both enzyme variants was higher when Ca^{2+} was present, while a decrease in activity was observed in the presence of Cu^{2+} and Mn^{2+}. The activity of the truncated variant was additionally reduced in the presence of Mg^{2+}.

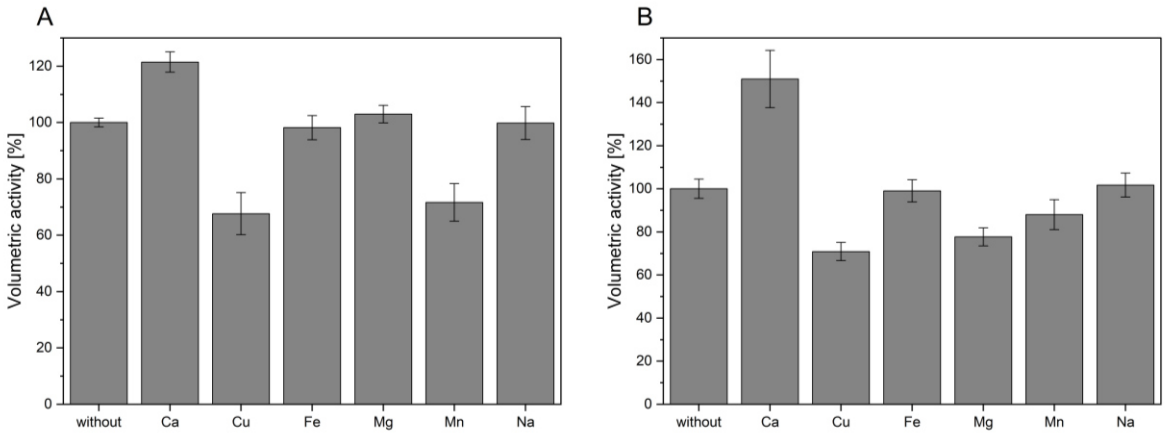

Figure 17 Influence of cations on volumetric activity of complete dsr3510 (A) and truncated dsr3510 (B).

Enzyme kinetics were thus recorded at 30 °C and pH 5.0 applying 1 mM $CaCl_2$. At these conditions, the maximum reaction rate v_{max} of the complete dsr3510 variant corresponded to 1.19 mmol/min*L^{-1}, being ~ 14 times higher than v_{max} of the truncated variant corresponding to 0.089 mmol/min*L^{-1}. However, the Michaelis constant K_M for the complete dsr3510 corresponded to 10.97 ± 1.56 mM and for the truncated variant to 12.57 ± 0.73 mM. Subsequently, the heterologously expressed enzyme variants were used to produce dextrans in the presence of 1 mM $CaCl_2$ at 30 °C and pH 5.0 for 24 h.

Therefore, the crude protein extracts were applied undiluted (= 500 µg/mL overall protein concentration), as well as diluted 2-fold, 4-fold and 10-fold.

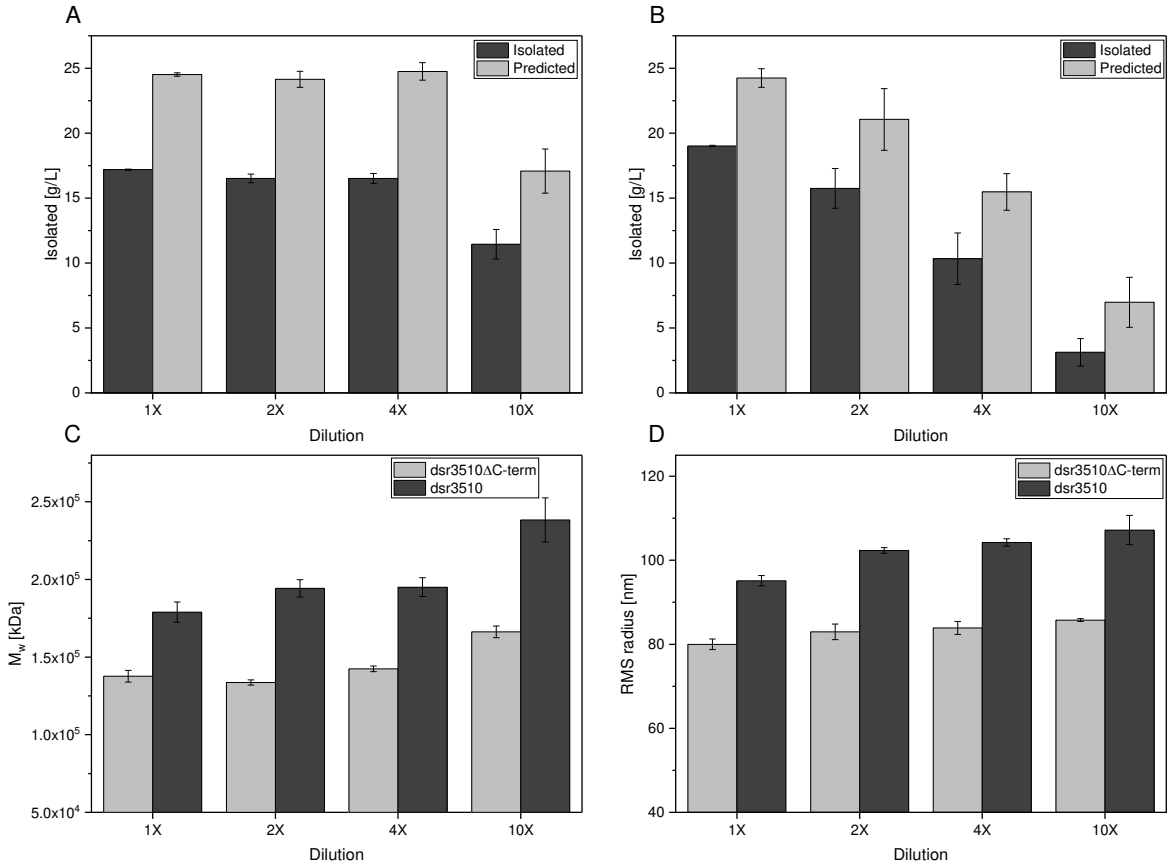

Figure 18 Isolated and predicted amounts of dextran produced by the heterologously expressed complete dsr3510 (A) and truncated dsr3510ΔC-term (B) dextransucrase variants and average M_w (C), as well as average rms radii (D) of these dextrans as determined by AF4-MALS-UV measurements.

As displayed in Figure 18A + B, amounts of isolable and predicted dextran stayed constant until a 4-fold dilution of the complete dextransucrase variant, while significantly decreasing at a 10-fold dilution. Simultaneously, overall and transglycosylation activity stayed constant until decreasing at a 10-fold dilution. By contrast the amounts of dextran gradually decreased with increasing dilution of the truncated dextransucrase variant, as it was also the case for the overall and transglycosylation activities of the enzyme. Moreover, the undiluted truncated variant produced higher amounts of isolable dextran than all reactions applying the complete enzyme variant. The predicted dextran amount was, however, similar for the undiluted truncated variant compared to the complete enzyme variant until a 4-fold dilution.

Furthermore, the macromolecular structures of these dextrans were determined by AF4-MALS-UV measurements. This revealed a significantly higher average M_w for dextrans obtained with the full-length enzyme variant than for dextrans obtained with the truncated enzyme (Figure 18C). Furthermore, the average M_w of dextrans produced by both dextransucrase variants increased with increasing dilution. Simultaneously, the average rms radii of dextrans obtained

from the complete dextransucrase were consistently higher than of dextrans obtained with the truncated variant (Figure 18D). Along with increasing dilution of both enzyme extracts, average rms radii increased. All p-values of the comparisons of the amount of isolated and precited dextran, as well as comparisons of rms radii and molecular weights are listed in Appendix 6. Additionally, the molecular fine structures of dextrans obtained with 4-fold and 10-fold diluted enzyme extracts were analysed by *endo*-dextranase fingerprinting (see Appendix 7). Thereby, it could be shown that the dextrans obtained with both enzyme variants featured the same molecular components as the native dextransucrases of *L. nagelii* TMW 1.1827 and *L. hordei* TMW 1.1822. Moreover, the portions of these components were highly similar within dextrans obtained by both heterologously expressed variants, as well as to the dextrans obtained by the native enzyme of *L. nagelii* TMW 1.1827.

4.4 Detailed characterization of native extracellular dextran formation in *L. nagelii* TMW 1.1827

4.4.1 Comparison of dextran formation using enzyme extracts obtained at different incubation conditions

Results described in section 4.1.2 showed that the *L. nagelii* TMW 1.1827 dextransucrase was present within the supernatants of buffered cell suspensions independent of the presence of sucrose. Therefore, the dextransucrase was recovered in the absence and presence of sucrose using buffered cell suspension of this strain to investigate the influence of sucrose treatment on the release of dextransucrase (activity) into the extracellular environment. This experiment was performed applying different initial pH (pH 4.50, pH 5.50 and pH 6.50) of the buffered cell suspensions, since preliminary experiments had shown an increase in cell numbers (medium = $1.64 \pm 0.28 \times 10^9$ cfu/mL, buffer without sucrose = $1.51 \pm 0.38 \times 10^9$ cfu/mL, buffer with sucrose = $3.56 \pm 0.62 \times 10^9$ cfu/mL; amounts were corrected with respect to the concentrating factor of the buffered cell suspensions), as well as acidification of the surrounding milieu in the presence of sucrose. After 3 h of incubation in buffers, the cells were removed and the pH, as well as the amounts of protein released into the buffers were determined.

Table 9 Final pH and amounts of released protein after incubation in buffers with different initial pH and in the presence or absence of sucrose. Protein concentrations and final pH are given as value ± standard deviation.

starting pH	+ sucrose		without sucrose	
	final pH	Amount of protein [µg/mL]	final pH	Amount of protein [µg/mL]
4.50	3.89 ± 0.01	107.9 ± 4.6	4.52 ± 0.02	73.2 ± 3.0
5.50	4.31 ± 0.02	122.7 ± 2.6	5.49 ± 0.01	138.1 ± 3.9
6.50	4.98 ± 0.13	216.5 ± 3.6	6.50 ± 0.00	221.0 ± 4.8

As shown in Table 9, all buffers supplemented with sucrose led to a decrease in pH, while it stayed constant in buffers containing no sucrose. Furthermore, sucrose had no effect on the total amount of protein released except for an initial pH of 4.50, where more protein was released in the presence of sucrose. However, the initial pH affected the released overall protein amount, which appeared to decrease with decreasing initial pH.

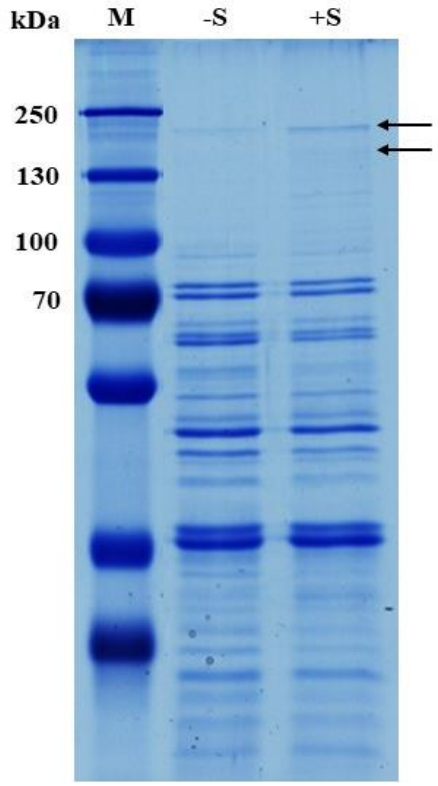

Figure 19 Coomassie-stained SDS-gel of supernatants obtained from buffered cell suspensions of L. nagelii TMW 1.1827 at pH 6.5 in the absence (-S) and presence (+S) of sucrose. Black arrows indicate the protein bands corresponding to the dextransucrase.

Exemplarily, Figure 19 shows the protein patterns of supernatants of *L. nagelii* that were obtained at an initial pH of 6.5 in the presence or absence of sucrose. Thereby, the protein bands of the dextransucrase appeared to be empirically less strong in the absence of sucrose, while

overall protein band patterns were highly similar for both conditions. This trend was comparable for initial pH of 5.5 and 4.5. Since the overall protein content decreased, it was, however, difficult to compare dextransucrase contents empirically on Coomassie-stained gels. Subsequently, the crude enzyme extracts of all six conditions were applied for dextran formation at pH 5.0 and 30 °C for 24 h, respectively.

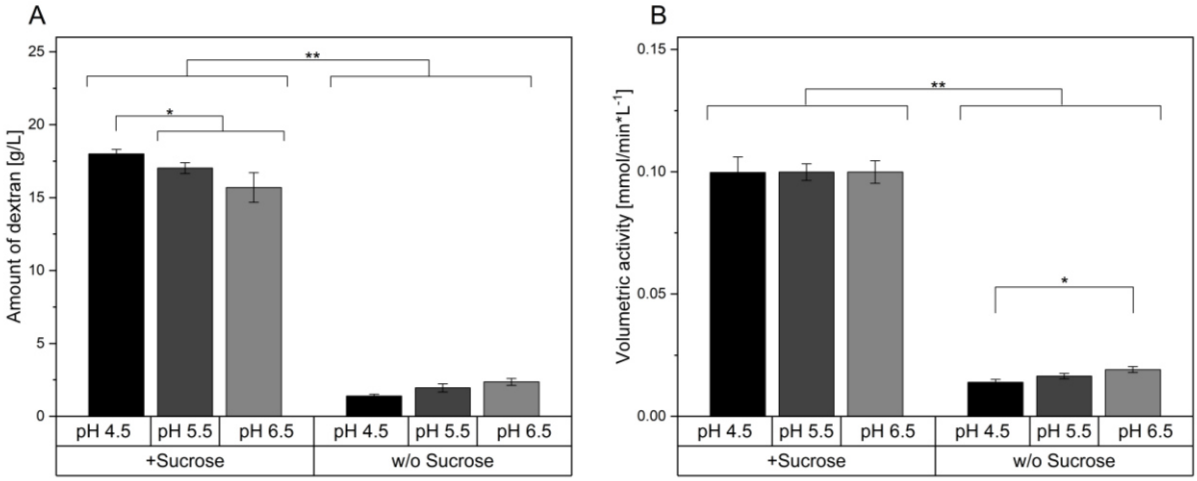

Figure 20 Amounts of isolated dextran (A) and average volumetric dextransucrase activities (B) of supernatants obtained in the absence or presence of sucrose at different initial pH. * = $p < 0.05$; ** = $p \leq 0.01$.

As displayed in Figure 20, significantly lower amounts of dextran were isolated, when dextransucrase containing supernatants were obtained in the absence of sucrose (factor 6- to 12-fold). Additionally, a significantly lower volumetric activity averaged over 24 h was detected in these supernatants (factor 5- to 7-fold). Furthermore, the volumetric activity, as well as the amount of isolated dextran of supernatants obtained in the absence of sucrose increased with increasing initial pH of the buffered cell suspension. This effect appeared to be inverse for supernatants obtained in the presence of sucrose, while being significantly lower at an initial pH of 5.5 and especially 6.5 than for an initial pH of 4.5. However, this was not observed for the averaged volumetric dextransucrase activities of these supernatants. The corresponding p-values of these comparisons are listed in Appendix 8.

4.4.2 Dose-response curves of native extracellular dextran production applying varying enzyme concentrations

Previous experiments on diluted enzyme extracts obtained from buffered cell suspensions of *L. nagelii* TMW 1.1827 implied that comparable amounts of dextran are formed by different

enzyme concentrations (see section 4.3.4). In this experiment it was, however, not possible to distinguish whether this was due to a prolonged incubation time or to inhibiting substances, e.g. metabolic products that exhibited the highest concentration within the undiluted enzyme extract and kept the enzyme from forming more dextran than in diluted enzyme extracts. Therefore, diluted enzyme extracts were applied to convert different amounts of substrate within 10 min of incubation, ranging from 1.56 – 400 mM of sucrose.

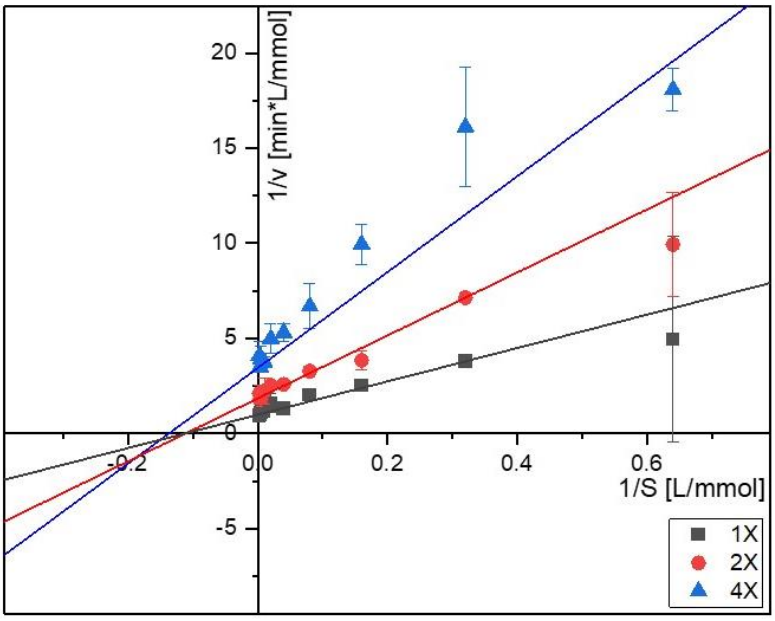

Figure 21 Double-reciprocal plot of dose-response curves obtained with different amounts of enzyme extracts.

While appropriate evaluations could be performed for enzyme extracts until a 4-fold dilution, the substrate conversion was below the detection limit of the sucrose/ D-Fructose/ D-Glucose assay kit when a 10-fold dilution of the enzyme extract was applied.

As visualized in

Figure 21, the Michaelis constants of the dextransucrase were not affected by enzyme dilution. However, the maximum reaction rates were reduced with increasing dilution. Exact values of K_M and v_{max} are given in Table 10, highlighting that v_{max} decreases linearly with increasing dilution.

Table 10 Kinetic parameters K_M and v_{max} obtained from dose-response curves of diluted enzyme extracts. Values are given ± standard deviaton and were obtained by automated graph fitting using the "Enzyme kinetics" plug-in tool of the OriginPro Software.

Dilution	1X	2X	4X
K_M [mM]	12.99 ± 3.74	10.39 ± 2.07	12.96 ± 2.57
v_{max} [mmol/min*L^{-1}]	1.03 ± 0.07	0.55 ± 0.02	0.29 ± 0.01

4.4.3 Analysis of time-dependent dextran formation of the native extracellular dextransucrase of *L. nagelii* TMW 1.1827

Previous experiments on the *L. nagelii* dextransucrase had shown that it consumed the whole amount of sucrose within the first 10 min of incubation (see section 4.3.3) when obtained at pH 6.5 in sucrose-supplemented buffer. However, the experimental setup of this experiment did not allow for investigating if formation of high molecular weight dextran is already finished at this point of time. Therefore, the experimental setup was varied with regards to the volume of the reaction mixture enabling isolation of dextran after 10, 60 and 180 min, as well as 24 h.

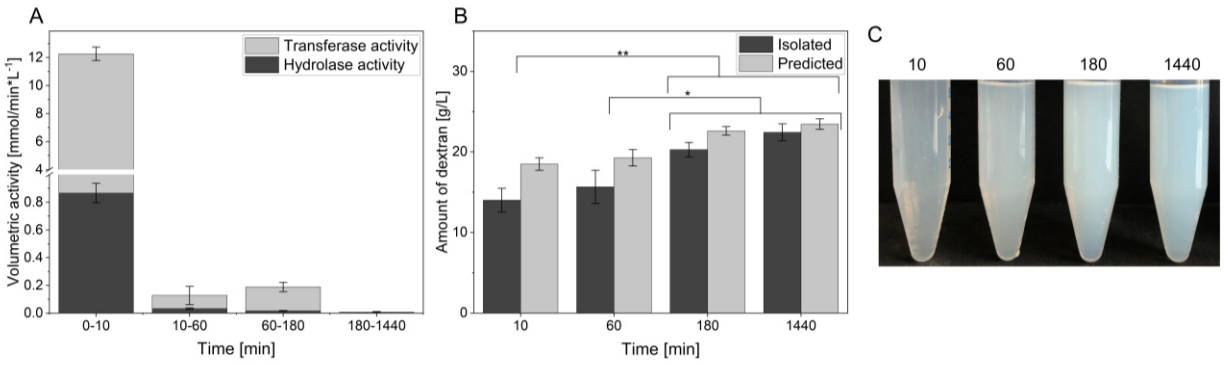

Figure 22 Volumetric activities (A) and amounts of isolated (black columns) and predicted (gray columns) dextran (B) as formed by the native extracellular dextransucrase of *L. nagelii* TMW 1.1827 at pH 5.0 and 30 °C. Figure C displays dextran formed in the cell-free buffer system at the end of each incubation period. * = $p < 0.05$; ** = $p \leq 0.01$.

As shown in Figure 22A, the volumetric activity of the native extracellular dextransucrase of *L. nagelii* was highest within the first 10 min of incubation, exhibiting a transferase rate of ~ 93 %. Within 24 h, a transferase rate of ~ 90 % was detected, while glucose was only released in quite low amounts (= 15.8 mM). Furthermore, no sucrose was detectable after 10 min of incubation, while neither fructose release nor dextran formation was finished at this point of time (Figure 22B). This was already visible from increasing turbidities (Figure 22C) within the reaction mixtures due to the cloud-forming properties of dextrans (Eckel *et al.*, 2019). Corresponding p-values of these comparisons are listed in Appendix 9.

In order to investigate substrate consumption and the resulting products more detailed, the samples obtained prior to dialysis after 10 min and 24 h of incubation were analysed by HPAEC-PAD (Figure 23). This confirmed the release of high amounts of fructose and comparably low amounts of glucose. Moreover, the sucrose isomers leucrose and palatinose, as well as several isomaltooligosaccharides (IMOs) and later eluting peaks (20 – 24 min retention time) were detected after 10 min and 24 h of incubation.

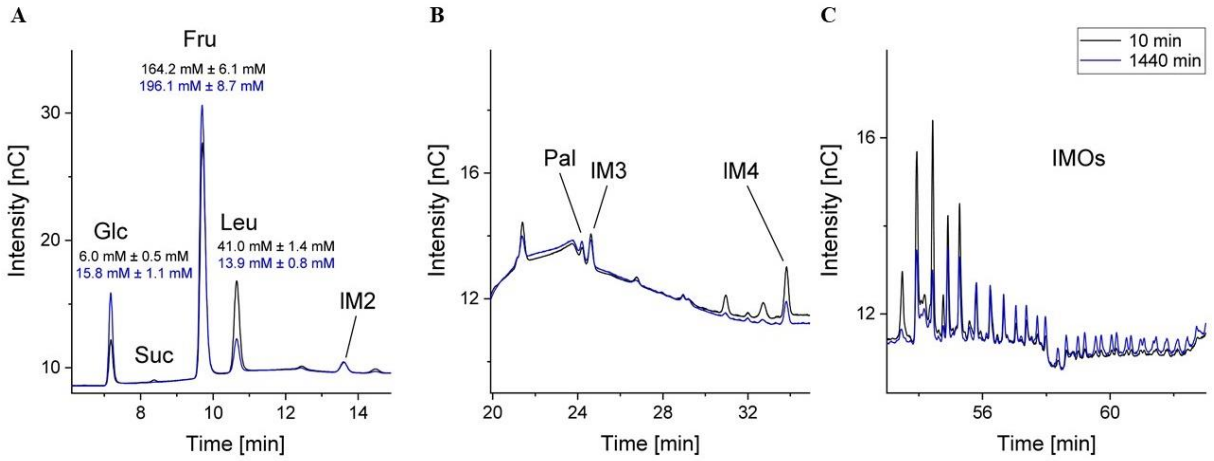

Figure 23 HPAEC-PAD chromatograms of samples obtained at 10 min and 24 h of incubation. Suc = sucrose; Glc = glucose; Fru = fructose; Leu = leucrose; Pal = palatinose; IM2 = isomaltose; IM3 = isomaltotriose; IM4 = isomaltotetraose; IMOs of DP > 4.

The leucrose concentration decreased by 27.1 mM over time, while concentrations of isomaltose and isomaltotriose did not change. Moreover, peak intensities of IMOs with a lower DP decreased, while peak intensities of a series of IMOs with a higher DP increased (Figure 23C) over 24 h of incubation.

4.4.4 Structural analysis of time-dependently formed dextrans

In order to obtain information on the molecular and macromolecular structures of dextrans that were formed within different incubation periods using the native extracellular dextransucrase of *L. nagelii* TMW 1.1827, AF4-MALS-UV measurements, *endo*-dextranase fingerprint and methylation analyses were applied.

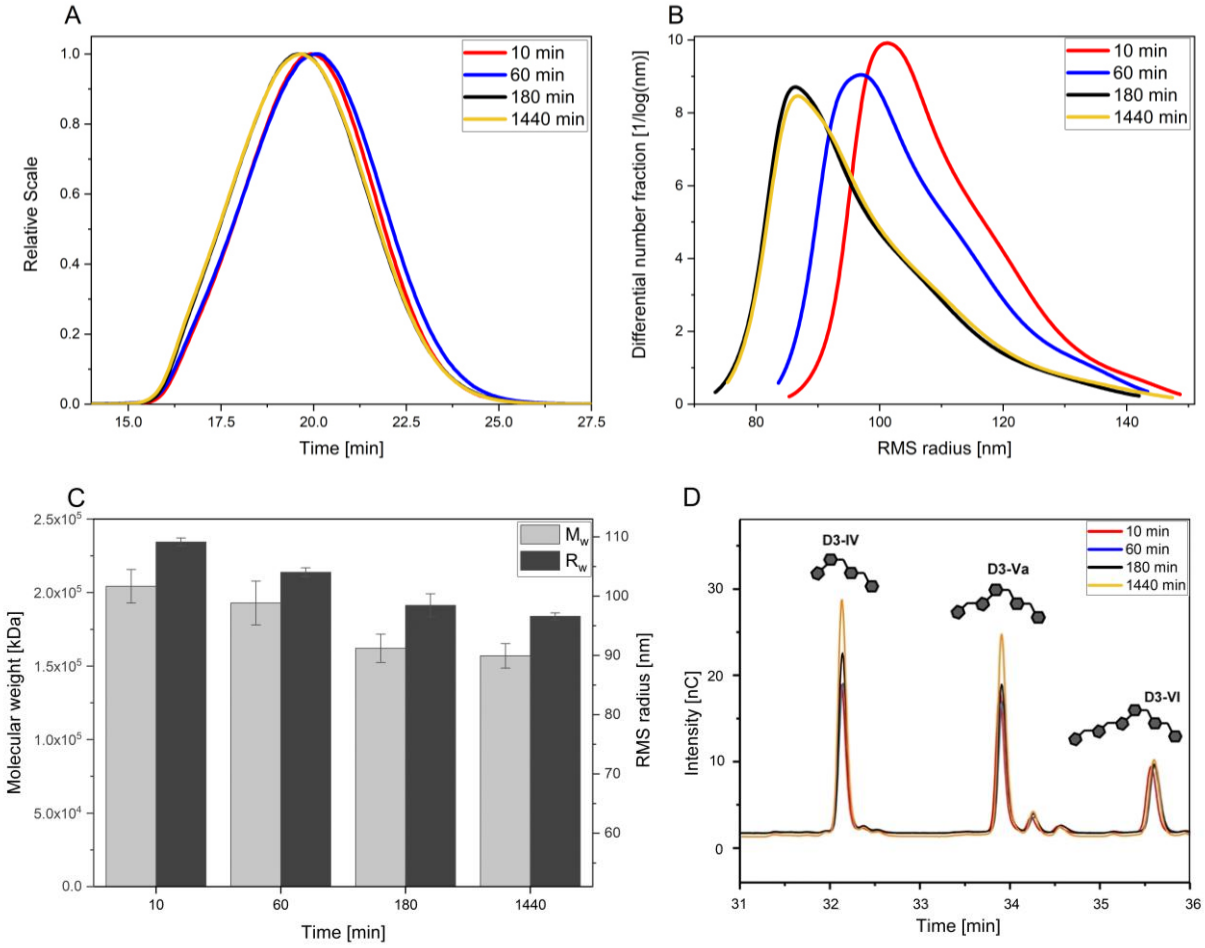

Figure 24 Chromatograms (A), differential rms radius distributions (B), average M_w and R_w (C) and *endo*-dextranase fingerprints (D) of time-dependently formed dextrans of the native extracellular dextransucrase of *L. nagelii* TMW 1.1827. *Endo*-dextranase fingerprints are shown as HPAEC-PAD chromatograms that were scaled to an equal intensity of the isomaltose peak (elution at ~ 13 min) and liberated branched oligosaccharides were identified according to external standard compounds (Münkel *et al.*, 2019).

As displayed in Figure 24A, chromatograms of these dextrans showed only minor differences among each other, while dextrans produced within 180 min and 24 h eluted faintly earlier than those obtained after 10 min and 60 min, respectively. Furthermore, differential radius distributions were broadened over time (Figure 24B). Dextrans produced for 180 min and 24 h exhibited fractions with distinctly smaller rms radii than dextrans obtained after 10 min and 60 min, while radius distributions overlapped widely at higher rms radii. However, fractions of high rms radius appeared to be present in relatively smaller amounts within the 180 min and 24 h dextrans. Accordingly, the average rms radii declined with increasing incubation time, which was also observed for the average molecular weights of these dextrans (Figure 24C). Furthermore, the most drastic decrease occurred between 60 min and 180 min of incubation, while appearing bigger for the rms radii of the dextran molecules. Corresponding p-values of these comparisons are listed in Appendix 9.

As expected, methylation analysis revealed the predominant presence of 1,6-linked glucose comprising between 85.8 and 87.8 % (Table 11). Besides terminal and 1,3-linked glucose units, 2.2 – 2.6 % of 1,3,6-linked glucose units were detected. Additionally, a slightly decreased ratio between 1,6-linked and 1,3,6-linked glucose units was observed for dextrans obtained after 180 min and 24 h compared to dextrans isolated at lower incubation times. Therefore, these dextrans were slightly more branched. This assumption was supported by enzymatically liberated oligosaccharides using *endo*-dextranase (Figure 24D), where higher peak intensities were observed for branched oligosaccharides exhibiting one or two glucose units within the side chain when incubation was prolonged.

Table 11 Glycosidic linkages (mol%) as determined by methylation analysis of time-dependently formed dextrans. Values are given ± standard deviation. t = terminal; Glc = glucose; *p* = pyranose.

Glycosidic linkage	10 min	60 min	180 min	24 h
t-Glc*p*	9.8 ± 0.9	9.2 ± 0.0	10.9 ± 2.3	10.4 ± 0.4
1,3-Glc*p*	0.8 ± 0.1	0.8 ± 0.0	0.8 ± 0.1	1.0 ± 0.1
1,6-Glc*p*	87.3 ± 0.9	87.8 ± 0.1	85.8 ± 2.0	86.1 ± 0.5
1,3,6-Glc*p*	2.2 ± 0.1	2.2 ± 0.1	2.4 ± 0.4	2.6 ± 0.1
Ratio 1,6-Glc*p*/1,3,6-Glc*p*	40.3 ± 1.1	40.2 ± 2.6	36.8 ± 5.2	33.6 ± 1.3

4.5 Genomic properties of selected LAB from water kefir

In the following, genomic properties of selected LAB from water kefir were extensively studied in order to predict metabolic capabilities under dextran forming conditions (= in the presence of sucrose), as well as in the presence of other sugars that were predominantly metabolized by water kefir LAB (see section 4.2). Additionally, theses analyses should identify genomic properties that are unique or correlated to LAB from water kefir. In order to improve sample size for a higher validity of results from genomic analyses, *L. hilgardii* strains were also taken into account. In a first step, basic information on draft genomes were obtained and ANI values were calculated by comparing each genome versus all other genomes. The available WGSs were a mixture of genomes sequenced by PacBio technology that gave complete chromosomal and plasmid sequences and genomes sequenced by Illumina MiSeq shotgun sequencing, giving contigs without this information. However, for later-on whole-genome synteny analysis, this information is inevitably necessary. Thus, draft genomes were searched for plasmid sequences using PlasmidFinder 2.0 (Carattoli *et al.*, 2014). As this analysis yielded only insufficient results, contigs of draft genomes were re-ordered along a template genome using Mauve

(Darling *et al.*, 2004) and CLC main workbench software that was ideally obtained from a closely related microorganism (e.g. *L. hordei* TMW 1.1907 was re-ordered along *L. hordei* TMW 1.1822 and *L. nagelii* TMW 1.1823 was re-ordered along *L. nagelii* TMW 1.1827). The resulting putatively complete chromosomes and plasmids were subsequently used for whole-genome synteny analysis. Due to the lack of such template sequences, draft genome sequences of *L. hilgardii* strains could not be re-ordered and were thus impractical for whole-genome synteny analysis. In order to identify genomic regions that may differ between genome sequences during synteny analysis due to the integration of prophage sequences, the online tool PHASTER (Arndt *et al.*, 2016) was used. The software tool i-ADHoRe 3.0 was used to predict collinear genomic regions (Proost *et al.*, 2012), which requires a BLAST table and information on the location and orientation of every gene within the analyzed genomes. The latter information came from files that either contained this information already (obtained from annotated PacBio-sequenced strains) or were generated after re-ordering of the annotated draft genomes as stated above. The BLAST table was produced using OrthoFinder software (Emms *et al.*, 2019) that generates a rooted phylogenetic tree in order to identify correct orthogroups of orthologous genes among the analyzed strains using translated coding sequences. Herein, an orthogroup is defined as a group of two or more protein sequences that most likely exhibit the same biological function within one or more organisms. However, as there are also strain-specific non-duplicated genes present within an organism, these gene contents were manually added to the analysis and were designated as orthogroups for simplicity. Beyond that, the OrthoFinder output was used to compare the analyzed strains regarding their putative functional properties obtained from RAST and TIGRFAMs annotation services (Overbeek *et al.*, 2014; Selengut *et al.*, 2007). Additionally, interesting target genes (e.g. genes involved in a certain metabolic route) were identified searching the NCBI annotations by this term or by BLASTing a list of genes against the genome.

4.5.1 Genomic properties of sequenced *L. hordei* and *L. nagelii* strains

As listed in Table 12, genomes of *L. nagelii* and *L. hordei* strains were of 2.38 – 2.59 Mbp in size and featured one or more plasmids. While the genome of *L. hilgardii* TMW 1.45^{T} differed only by about 0.13 Mbp, both water kefir isolates of this species were much larger in size. Due to the nature of shotgun sequencing, no plasmids could be derived from draft genome sequences of *L. hordei* TMW 1.1907, *L. nagelii* TMW 1.1823 and all *L. hilgardii* strains, respectively.

Table 12 Genomic features of *L. hilgardii*, *L. hordei* and *L. nagelii* analysed in this study.

Strain	Size [Mbp]	Contigs	Plasmids	GC content [%]	CDS	Coding density [%]
L. hilgardii TMW 1.2196	3.20	80	n.a.	39.86	3068	84.88
L. hilgardii TMW 1.828	3.20	87	n.a.	39.87	3084	84.88
L. hilgardii TMW 1.45^T	2.72	113	n.a.	38.17	2596	82.35
L. hordei TMW 1.1822	2.59	4	3	35.25	2461	86.08
L. hordei TMW 1.1907	2.38	15	n.a.	34.79	2251	86.80
L. hordei TMW 1.2353^T	2.44	3	2	34.97	2324	85.96
L. nagelii TMW 1.1823	2.49	29	n.a.	36.64	2374	87.87
L. nagelii TMW 1.1827	2.55	4	3	36.83	2391	86.98
L. nagelii TMW 1.2352^T	2.56	2	1	36.83	2470	87.04

While the PlasmidFinder 2.0 online service (Carattoli *et al.*, 2014) could not identify sequences originating from plasmids in *L. hordei* TMW 1.1907 and *L. hilgardii* strains, contig 15 and 16 of *L. nagelii* TMW 1.1823 were found to be located on a plasmid. However, whole genome comparison using Mauve software indicated that contigs 7, 10, 11, 14 and 15 of *L. hordei* TMW 1.1907 and contigs 15-17, 20, 22, 25, 27 and 28 of *L. nagelii* TMW 1.1823 exhibited no corresponding region within the chromosomes of the other strains of the respective species, indicating them to be potentially plasmid encoding. Additionally, the GC content of these sequences was distinctly different from the sequences that were assigned to the chromosome, respectively (see Appendix 10).

Moreover, whole genome analysis showed that none of the *L. hordei* strains shared plasmids with another strain of this species, while both water kefir borne strains of *L. nagelii* shared at

least two plasmids. Thus, plasmid 1 (CP018181) of strain TMW 1.1827 corresponded to contigs 15, 17 and 27 of strain TMW 1.1823, while plasmid 3 (CP018183) corresponded to contig 16 of strain TMW 1.1823. Interestingly, two plasmids of *L. hordei* TMW 1.1822 and *L. nagelii* TMW 1.1827 were found to be present in both strains, respectively. While plasmid 1 (CP018177) of *L. hordei* TMW 1.1822 corresponded to plasmid 1 of *L. nagelii* TMW 1.1827, plasmid 3 (CP018179) of *L. hordei* corresponded to plasmid 2 (CP018182) of *L. nagelii*. Additionally, *L. hordei* TMW 1.1907 and *L. nagelii* TMW 1.1823 appeared to share at least some contigs that may lay on plasmids or exhibit mobile genetic elements. Thereby, contig 10 of *L. hordei* was highly similar to contig 21 of *L. nagelii* and contig 7 of *L. hordei* was split onto contigs 15 and 17 in *L. nagelii*. Moreover, contig 11 of *L. hordei* appeared to be present as contig 25 in *L. nagelii*. These analyses enabled the assemblies of putatively complete chromosomes for the draft genome sequences of both, *L. hordei* TMW 1.1907 and *L. nagelii* TMW 1.1823 and two putatively complete plasmids of *L. nagelii* TMW 1.1823 using the WGSs of the other water kefir isolate of the respective species as a template.
Furthermore, WGSs were compared by ANIb analysis.

Table 13 ANI values [%] and aligned percentages (in brackets) [%] of analysed strains.

	TMW 1.2196	**TMW 1.45**	**TMW 1.828**	**TMW 1.1822**	**TMW 1.1907**	**TMW 1.2353**	**TMW 1.1823**	**TMW 1.1827**	**TMW 1.2353**
***L. hilgardii* TMW 1.2196**	*	96.29 (70.44)	99.99 (99.45)	66.68 (22.39)	67.87 (21.58)	66.19 (21.38)	67.83 (22.65)	66.79 (22.54)	66.21 (22.11)
***L. hilgardii* TMW 1.45**	97.01 (81.44)	*	97.01 (81.48)	66.07 (23.89)	65.72 (23.11)	65.91 (23.27)	66.34 (23.79)	66.27 (23.81)	66.17 (23.44)
***L. hilgardii* TMW 1.828**	99.98 (99.28)	96.33 (70.20)	*	66.64 (22.35)	68.06 (21.45)	66.22 (21.29)	68.15 (22.48)	66.97 (22.27)	66.41 (21.60)
***L. hordei* TMW 1.1822**	67.90 (27.03)	67.36 (25.07)	67.90 (27.04)	*	98.33 (84.30)	97.46 (75.68)	72.14 (47.34)	72.75 (48.58)	70.62 (44.94)
***L. hordei* TMW 1.1907**	66.31 (26.72)	65.97 (25.44)	66.30 (26.78)	98.85 (90.01)	*	98.12 (79.30)	70.28 (46.38)	70.27 (46.32)	69.95 (45.85)
***L. hordei* TMW 1.2353**	67.38 (27.81)	66.71 (26.95)	67.38 (27.79)	97.99 (81.65)	98.13 (80.21)	*	71.82 (47.35)	71.87 (47.58)	70.44 (45.94)
***L. nagelii* TMW 1.1823**	67.14 (26.93)	66.65 (25.53)	67.25 (27.01)	71.47 (48.26)	69.94 (45.28)	70.27 (44.29)	*	99.99 (98.76)	98.38 (86.84)
***L. nagelii* TMW 1.1827**	67.59 (27.60)	67.18 (25.73)	67.64 (27.72)	72.67 (49.61)	70.46 (44.77)	70.82 (44.40)	99.89 (97.40)	*	98.21 (86.49)
***L. nagelii* TMW 1.2353**	66.99 (26.60)	67.10 (25.21)	66.99 (26.54)	70.69 (45.02)	70.08 (44.11)	70.41 (43.37)	98.38 (85.61)	98.39 (86.06)	*

As shown in Table 13, ANI values were above 96 % within one species, while a higher ANI value was found for the comparison of the water kefir isolates within one species rather than

for the comparison between the typestrains and the respective water kefir isolates. Moreover, the water kefir isolates of *L. hordei* exhibited a lower ANI value than the water kefir isolates of the other two species.

4.5.2 Co-linear regions of *L. hordei* and *L. nagelii* strains

Based on the OrthoFinder output and the genetic location and orientation of the genes encoding the proteins that were used to generate the OrthoFinder output, co-linear stretches of the genomes were predicted. This analysis should give insights into long-term adaptation of the respective microorganism arising from a common ancestor. As listed in Table 14, the genetic organization of *L. nagelii* strains was generally quite similar among each other, as even the typestrain TMW 1.2352^T exhibited a minimum of 90.12 % co-linearity to *L. nagelii* TMW 1.1823 and TMW 1.1827, respectively. By contrast, genetic organization of the *L. hordei* strains was more diverse. While the sequence of strain TMW 1.1907 was ~ 97 % co-linear to the one of strain TMW 1.1822, the sequence of strain TMW 1.1822 was inversely only ~ 93 % co-linear to that of strain TMW 1.1907. This means that in strain TMW 1.1822 ~ 7 % of the annotated genes are not present in blocks co-linear to the genome of strain TMW 1.1907 exhibiting at least three consecutive genes. This was even more drastic for the comparison of the two water kefir strains with the typestrain of *L. hordei*. Comparing *L. hordei* and *L. nagelii* strains among each other, the level of co-linear sequences within *L. hordei* strains was comparable for all *L. nagelii* strains, while the lowest values were achieved for the water kefir isolates compared to the *L. nagelii* typestrain. By contrast, the highest amount of co-linearity of *L. hordei* TMW 1.2353^T was achieved for the comparison with the *L. nagelii* typestrain, indicating that the genome of this strain is more similarly arranged as compared to the water kefir isolates of *L. nagelii*. Comparing the genomes of the *L. nagelii* strains to the genomes of the *L. hordei* strains revealed that the highest level of co-linearity of all *L. nagelii* strains was achieved for the comparison with strain TMW 1.1822, while being lowest for the comparison with the *L. hordei* typestrain. As depicted in Figure 25, the genetic arrangements of the chromosomes were highly similar within one species, respectively, while they were more diverse between both species, as exemplarily shown for the comparison of *L. hordei* TMW 1.1822 with *L. nagelii* TMW 1.1827. All three plasmids of *L. hordei* TMW 1.1822 exhibited short co-linear regions with either the chromosome of the other two strains or plasmid 2 of strain TMW 1.2353^T. However, none of the plasmids of the *L. hordei* strains was shared completely by another strain, while plasmid 1 of strain TMW 1.2353^T exhibited no co-linear region at all compared to the other strains.

Table 14 Co-linear portions relative to the complete genomes [%] of comparisons between *L. hordei* TMW 1.1822, TMW 1.1907 and TMW 1.2353^T and *L. nagelii* TMW 1.1823, TMW 1.1827 and TMW 1.2352^T. The portions also include inverted segments.

	TMW 1.1822	**TMW 1.1907**	**TMW 1.2353**	**TMW 1.1823**	**TMW 1.1827**	**TMW 1.2352**
***L. hordei* TMW 1.1822**	100.00	92.86	87.99	74.62	76.60	74.16
***L. hordei* TMW 1.1907**	97.09	100.00	91.04	78.67	79.30	77.15
***L. hordei* TMW 1.2353**	89.93	88.36	100.00	74.31	74.31	77.80
***L. nagelii* TMW 1.1823**	74.54	72.58	68.77	100.00	99.15	95.09
***L. nagelii* TMW 1.1827**	75.88	72.79	68.21	98.90	100.00	94.40
***L. nagelii* TMW 1.2352**	73.19	71.38	68.02	90.12	90.12	100.00

This also applied for contigs 11, 14 and 15 of strain TMW 1.1907. About 12 % of contig 7 of this strain were co-linear to plasmid 1 of strain TMW 1.1822. The dextransucrase genes of both, strain TMW 1.1907 and TMW 1.1822, was located within a genomic stretch that was not co-linear to any other segment within the genome of the *L. hordei* typestrain. In *L. hordei* TMW 1.1822 two stretches and *L. hordei* TMW 1.1907 one larger stretch of non-collinearity with *L. hordei* TMW 1.2353^T were found that encoded for pro-phages according to the PHASTER online tool.

The chromosomal sequences of the *L. nagelii* strains were highly similar to each other, displaying two larger regions in strain TMW 1.2352^T that were not present in the other two strains. Both segments encoded for pro-phage sequences. As already mentioned above, plasmids 1 and 3 of *L. nagelii* TMW 1.1827 were shared with strain TMW 1.1823, while no plasmids were shared with the *L. nagelii* typestrain. Additionally, contig 24 of *L. nagelii* TMW 1.1823 was highly similar to a segment within the chromosome of both other strains, respectively. Contigs 20, 22, 25, 27, 28 and 29 of strain TMW 1.1823 displayed no homologous regions within the genomes of both other strains. The genetic locus of the dextransucrase gene was identical in both water kefir isolates, while the genomic region of this location was within a chromosomal stretch that was co-linear for all three *L. nagelii* strains.

Co-linearity analyses of strains of two different species resulted in a rather confusing picture, as the genetic arrangement differed largely between *L. hordei* and *L. nagelii* strains. However, *L. hordei* TMW 1.1822 shared plasmid 1 and 3 with *L. nagelii* TMW 1.1827, while plasmid 2 exhibited several segments co-linear to stretches within the chromosome and plasmids of strain TMW 1.1827. Inversely, this also applied for plasmid 3 of *L. nagelii* TMW 1.1827. The dextransucrase gene of *L. hordei* TMW 1.1822 was located in a large genomic region that was not co-linear to any segment of the genome of *L. nagelii* TMW 1.1827. By contrast, the *L. nagelii* dextransucrase was located in a small stretch of co-linearity to the *L. hordei* chromosome. All relative amounts of co-linearity are listed in Appendix 11.

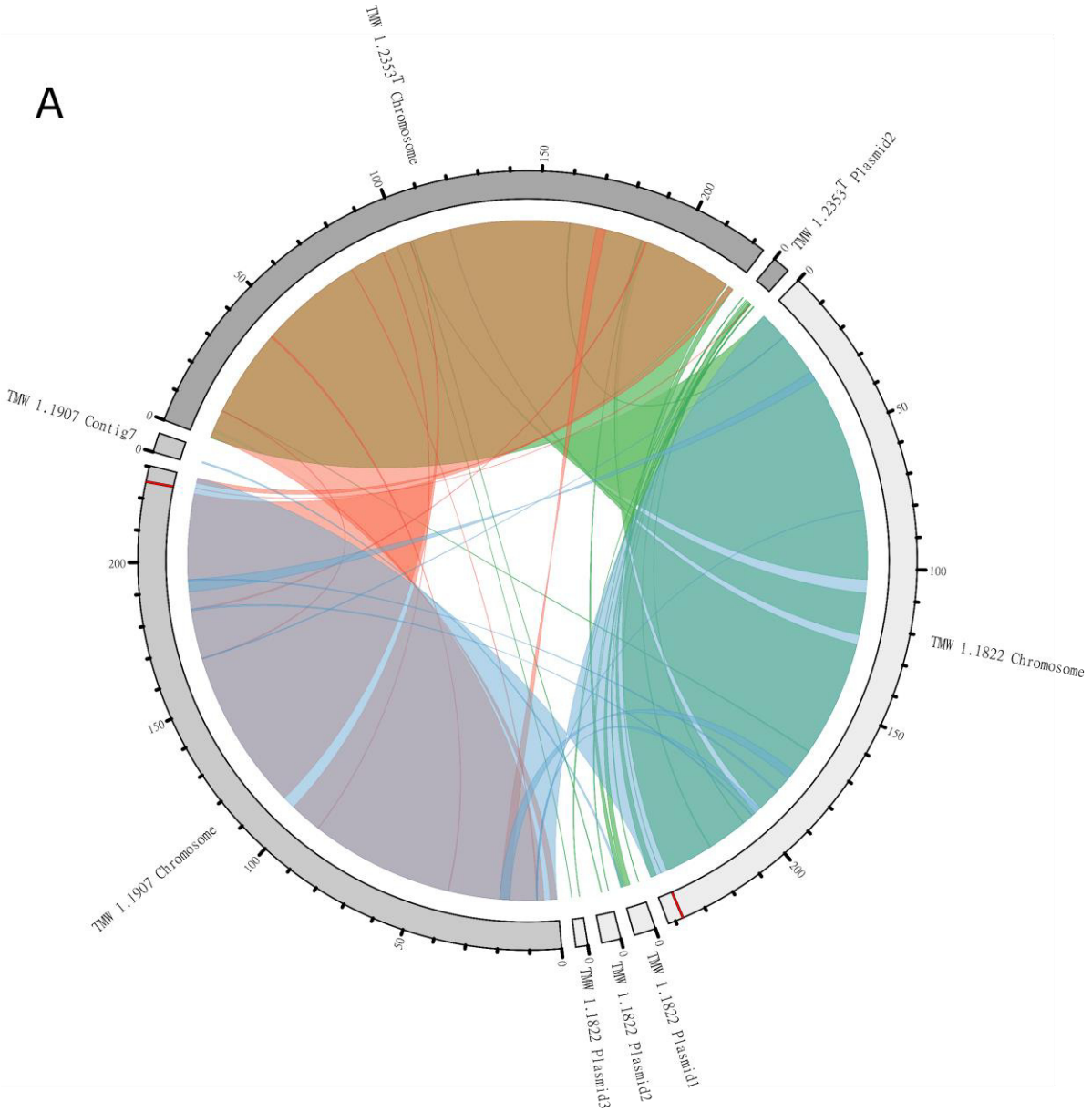

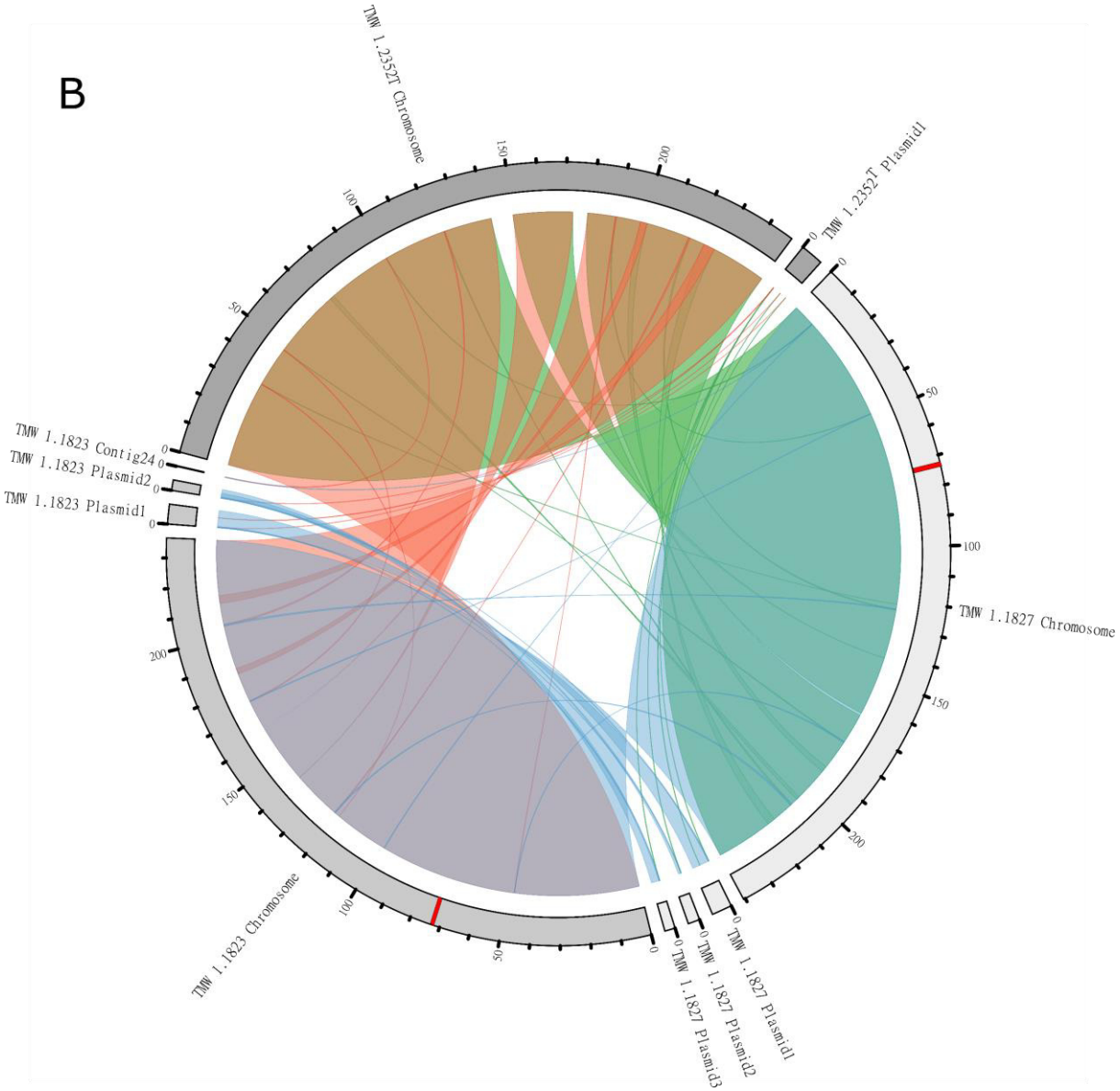
B
TMW 1.2352T Chromosome
TMW 1.2352T Plasmid1
TMW 1.1827 Chromosome
TMW 1.1827 Plasmid1
TMW 1.1827 Plasmid2
TMW 1.1827 Plasmid3
TMW 1.1823 Chromosome
TMW 1.1823 Contig24
TMW 1.1823 Plasmid2
TMW 1.1823 Plasmid1

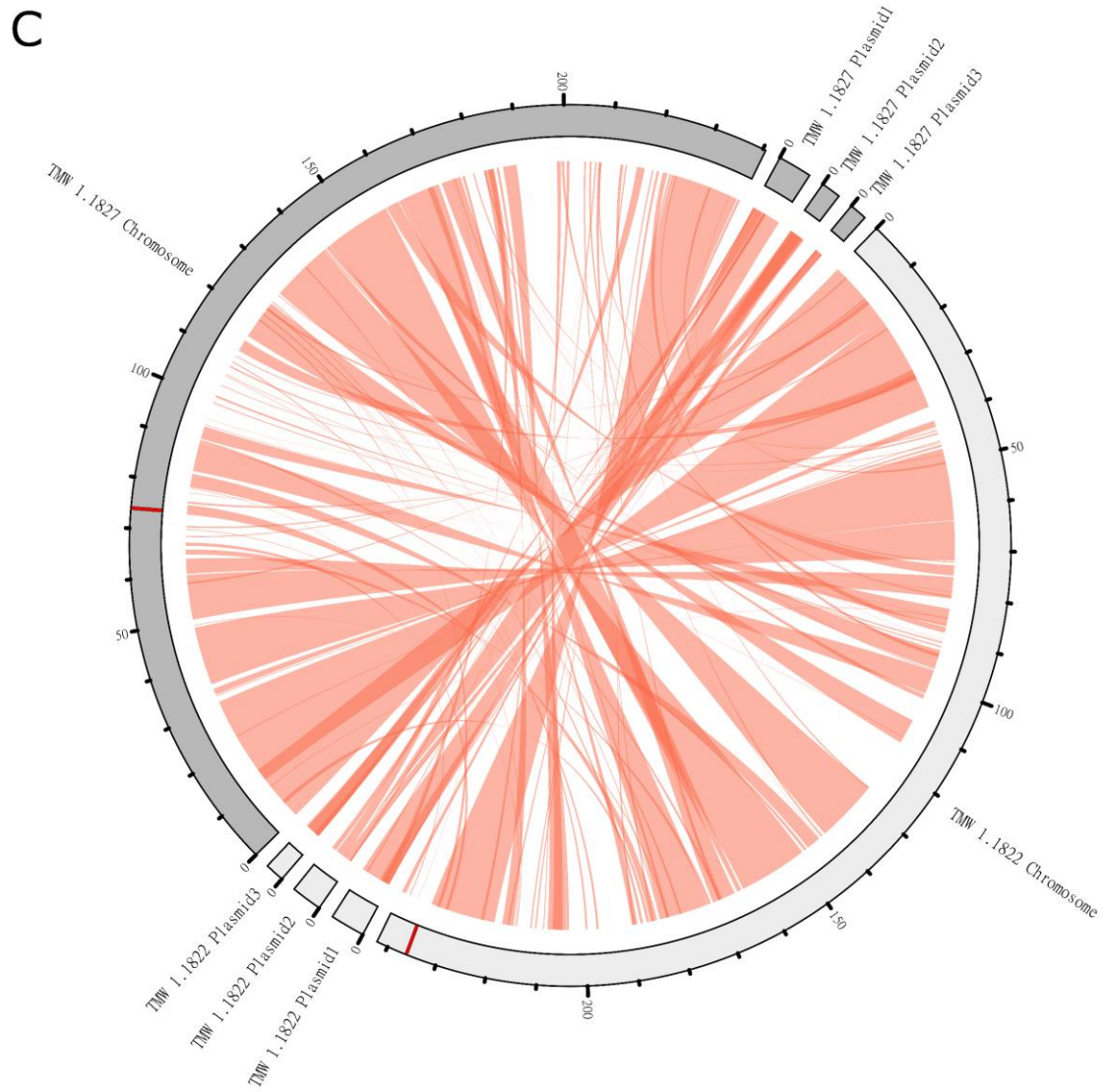

Figure 25 Circular plots of genome comparisons of *L. hordei* strains (A), *L. nagelii* strains (B) and exemplarily of *L. hordei* TMW 1.1822 compared to *L. nagelii* TMW 1.1827 (C). Chords link co-linear segments. Plasmids and contigs with no co-linear segments are not shown. The genetic locations of the dextransucrase genes are indicated in red colour. Ticks represent 10 kbp.

4.5.3 Shared gene contents

As described above, shared gene contents were identified on the basis of translated coding sequences using OrthoFinder software (Emms *et al.*, 2019). In total, 3895 orthogroups with at least two orthologs within the genomes of one or more strains were defined, of which 61 orthogroups were only present in one of the tested strains. Additionally, 775 coding sequences were present as strain-specific one-copy genes.

As visualized in Figure 26, *L. hilgardii* strains from water kefir exhibited the highest number of orthogroups per strain. The largest intersection appeared to be composed of all tested strains,

exhibiting 1092 orthogroups with an average of 9.91 orthologs per orthogroup. The largest orthogroup possessed 109 orthologs, that corresponded to transposases, however, as this orthogroup corresponded to a group of only two intersections, it is not shown in Figure 26.

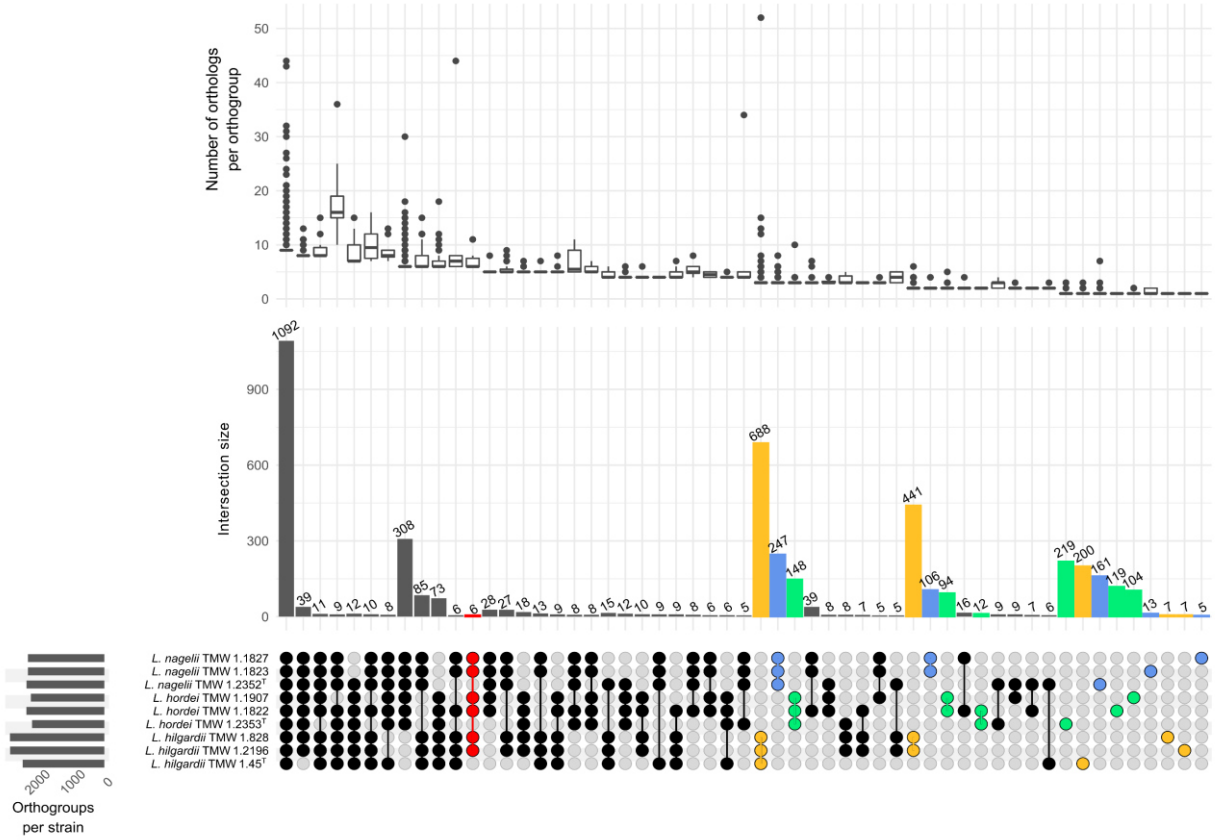

Figure 26 OrthoFinder analysis output. The left panel shows the number of orthogroups per strain, while the bottom panel shows an intersection matrix of strains exhibiting the same orthogroups. The panel in the middle indicates the amount of orthogroups that are present within each intersection and the top panel shows a boxplot for each intersection indicating the amount of orthologs per orthogroup. Red = orthogroups only found in water kefir isolates, yellow = only found in *L. hilgardii* strains, blue = only found in *L. nagelii* strains, green = only found in *L. hordei* strains. For reasons of clarity, only intersections with a minimum of five orthogroups are displayed.

The species *L. hilgardii* exhibited the highest number of species-specific orthogroups, followed by *L. nagelii* and *L. hordei*. Equally, the water kefir isolates of *L. hilgardii* possessed the highest number of orthogroups that were found for a certain species, while these intersection sizes appeared to be similar for *L. nagelii* and *L. hordei* strains. The highest amount of strain-specific orthogroups was found for the typestrain of *L. hordei,* followed by the typesrains of both, *L. hilgardii* and *L. nagelii.* Additionally, six orthogroups appeared to be only present in the water kefir isolates of all three species, but not in the typestrains that were isolated from different sources (see Figure 26 and Table 15). These results are presented more detailed in the next sections.

Table 15 Orthogroups only found in water kefir strains.

OG	TMW 1.2196	TMW 1.828	TMW 1.1822	TMW 1.1907	TMW 1.1823	TMW 1.1827	Annotation
414	C2L99_15130	CLI91_15455	BSQ49_11535	CRI84_07775	CRI83_04440	BSQ50_03510	Dextransucrase
1137	C2L99_14160, C2L99_14175	CLI91_14060, CLI91_14075	BSQ49_11765, BSQ49_12140	CRI84_10735	CRI83_11600, CRI83_11965	BSQ50_11580, BSQ50_11595	GntR Transcriptional regulator
1614	C2L99_14150, C2L99_14560	CLI91_14050, CLI91_14485	BSQ49_12135	CRI84_10740	CRI83_11960	BSQ50_11600	ABC transporter permease
1833	C2L99_14180	CLI91_14080	BSQ49_11780	CRI84_10730	CRI83_11595	BSQ50_11575	Fructoselysine-6-P deglycase
1835	C2L99_14135	CLI91_14035	BSQ49_12120	CRI84_10755	CRI83_11945	BSQ50_11615	Fructoselysin-6 kinase
2011	C2L99_14130	CLI91_14030	BSQ49_12115	CRI84_10760	CRI83_11940	BSQ50_11620	Fructoselysine-6-P deglycase

Moreover, OrthoFinder results were used to calculate the amounts of genes within the pan-, core- and species-specific accessory genomes.

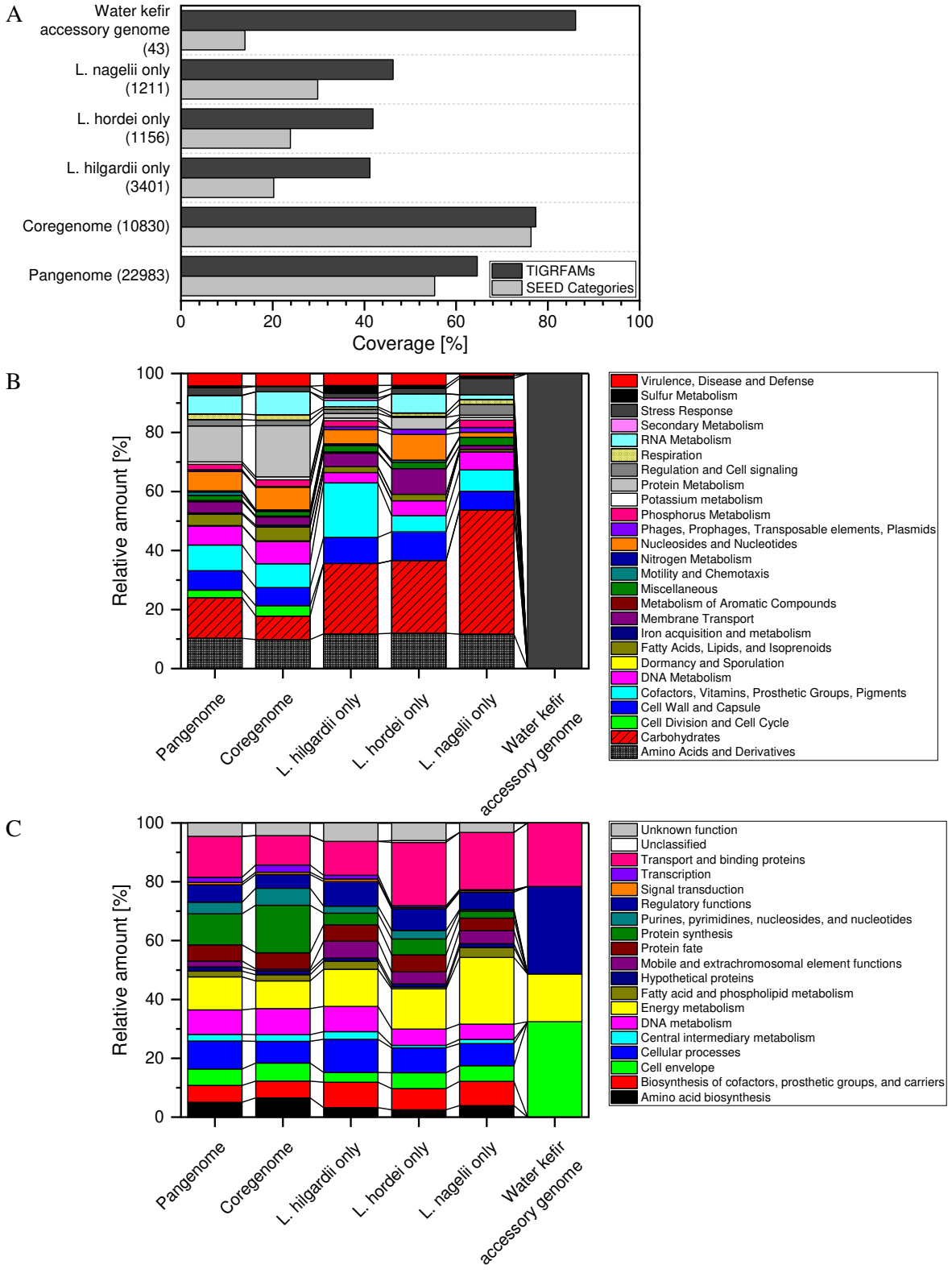

Figure 27 Functional annotations of pan-, core- and species-specific accessory genomes. Amounts of pan-, core- and species-specific accessory genomes and the coverage of the respective gene contents within SEED categories and TIGRFAMs (A), relative amounts of gene contents within each SEED category (B) and TIGRFAM (C).

As OrthoFinder analysis only runs on already translated coding sequences, it is important to note, that genes not coding for putatively functional proteins (e.g. tRNAs and rRNAs) were not included within these analyses. Furthermore, it should be mentioned that for reasons of clarity species-specific accessory genomes not only included such genes that were present in all three strains of a species, but also in only one or two strains of a species, respectively. As displayed in Figure 27, the pangenome of all nine strains comprised 22983 genes, of which about 47 % were part of the coregenome of these strains. The highest number of species-specific genes was found for the species *L. hilgardii,* while the accessory genomes of *L. hordei* and *L. nagelii* were comparable.

In general, TIGRFAM coverages were higher than SEED category coverages, which was especially prominent for the genes included within the water kefir accessory genome. Herein, the six orthogroups already mentioned above were distributed over 43 genes. Only one of these orthogroups was functionally sorted into a SEED category, namely “stress response”, which was assigned for the dextransucrase orthologs. By contrast, five orthogroups were assigned to TIGRFAMs, respectively, namely, “transport and binding proteins” (OG1614), “regulatory functions” (OG1137), “cell envelope” (OG1833, 2011) and “energy metabolism” (OG1835). Within the coregenome, most SEED categories appeared to exhibit a constant relative amount, when compared to the pangenome. Most prominently identifiable were a higher relative number of genes related to protein metabolism and a distinctly lower number of genes related to carbohydrate metabolism within the coregenome. This category was accordingly higher within the species-specific accessory genomes. This was also observable for TIGRFAMs annotations, where the relative amount of the category “protein synthesis” was higher within the coregenome compared to the pangenome, while the category “energy metabolism” was lower. This also applied for the category “transport and binding proteins”.

4.5.3.1 Orthogroups specific for the isolation source water kefir

As stated in section 4.5.3 and Table 15, only six orthogroups appeared to be exclusively present in the strains that were isolated from water kefir. The dextransucrase genes were not located within a conserved genomic region, however, the other genes were all found to be organized within one gene cluster as shown below.

4.5.3.1.1 Dextransucrase

The genetic loci of the dextransucrase genes appeared to be quite different among different species. The gene was found to be located on the chromosomes of both, *L. hordei* and *L. nagelii*

strains. However, no such information could be derived from WGSs of *L. hilgardii* strains, as the dextransucrase was the only gene on the obtained contig, respectively. The dextransucrase locus was identical in *L. hordei* TMW 1.1822 and TMW 1.1907. However, by comparing the corresponding genomic regions with the genome of the typestrain *L. hordei* TMW 1.2353^T, the dextransucrase gene appeared to be located in a large region (~ 41 kbp) that exhibited no collinear region within the typestrain´s genome (see section 4.5.2, for a detailed view of the genomic region see Appendix 12). Within this genomic stretch, other proteins involved in carbohydrate metabolism (Man-Family PTS, glucohydrolase, see section 4.5.4) were found in both water kefir strains. Moreover, in the close proximity of the dextransucrase gene, a gene encoding an NAD(P)-dependent dehydrogenase (quinone), was found.

By contrast, the genetic environment of the dextransucrase gene was more conserved among *L. nagelii* strains, as the locus differed only in very few genes (Figure 28). Instead of the dextransucrase gene, an ATP-dependent exonuclease and a nucleotide phosphorylase, the typestrain TMW 1.2352^T encoded for a type I restriction modification system and several IS3 family transposases at the same locus. Interestingly, this restriction modification system was absent within the WGSs of the water kefir isolates TMW 1.1823 and TMW 1.1827.

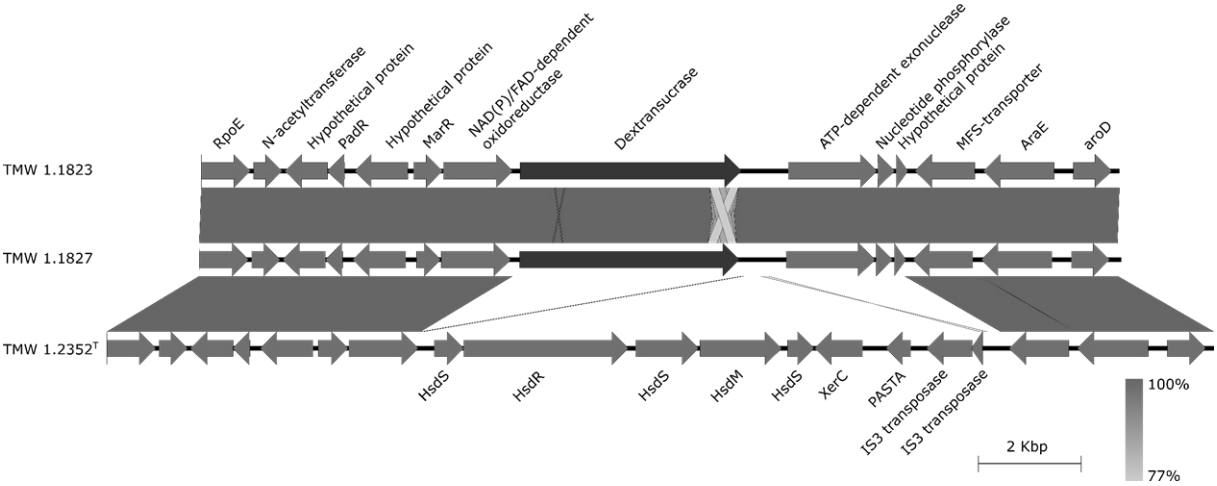

Figure 28 Comparison of the genetic loci coding for dextransucrase in *L. nagelii* strains. Shades of grey of connecting lines represents percent blast identity according to scale on the right. RpoE = RNA-polymerase σ70 factor, PadR + MarR = transcriptional regulators, AraE = MFS-transporter putatively involved in the uptakte of arabinose or xylose, aroD = type I 3-dehydroquinate dehydratase, HsdS/HsdR/HsdM = subunits of type I restriction-modification system family IC, XerC = site-specific integrase, PASTA = PASTA-domain containing protein.

The presence or absence of dextransucrase genes in other LABs of the species *L. hordei, L. nagelii* and *L. hilgardii* was furthermore investigated by PCR analysis using specific or degenerated primers. Additionally, plasmid DNA of *L. hilgardii* strains was tested in this assay.

All LABs from water kefir appeared to be positive for such genes, while strains isolated from different sources were tested negative for the dextransucrase gene. Additionally, a positive result was achieved for the plasmid DNA of *L. hilgardii* TMW 1.2196 and TMW 1.828. Interestingly, *L. nagelii* TMW 1.1825 that was not capable of EPS production on sucrose-containing agar plates (see section 4.1.1) also showed a positive PCR result, but with a shorter PCR-product. PCR-results are shown in Appendix 13 and were derived from the Bachelor´s thesis of Henriette Leicher, who was supervised during this work.

4.5.3.1.2 Fructoselysine gene cluster

The gene cluster that codes for proteins that may predictively be involved in the degradation of fructoselysine appeared to be located on plasmid 1 that was shared by *L. hordei* TMW 1.1822, *L. nagelii* TMW 1.1827 and most likely *L. nagelii* TMW 1.1823 (see section 4.5.1). In *L. hordei* TMW 1.1907, the gene cluster was located on contig 7 that may also be plasmid-derived. However, the genetic environment appeared to be different in this strain, as partially depicted in Figure 29. The organization of the gene clusters for fructoselysine-degradation were highly similar for all six strains isolated from water kefir. Within this genomic region, the fructoselysine-6-kinase (E.C. 2.7.1.218, FrlB) was encoded twice, while fructoselysine-6P deglycase (FrlD) was only encoded once. Moreover, a transcriptional regulator of the GntR-family was found in all strains, however, it appeared to be disrupted by transposable insertion elements in *L. hordei* TMW 1.1822 and *L. nagelii* TMW 1.1827. In both *L. hilgardii* strains, the transcriptional regulator was not disrupted, but encoded twice. All strains encoded an ABC-transporter within their respective gene clusters, that was predicted to transport amino acids according to NCBI annotation. The gene clusters were compared to homologous gene clusters that were described within the literature (Deppe *et al.*, 2011b; Wiame *et al.*, 2002; Yang *et al.*, 2008). *E. coli* K-12 substrain MG1655 encoded a fructoselysine-specific permease instead of the ABC-transporter and an additional fructoselysine-3-epimerase (E.C. 5.1.3.41, FrlC). By contrast, *Bacillus* (*B.*) *subtilis* subsp. *subtilis* strain 168 coded for an ABC-transporter somewhat similar to that of the water kefir LAB, but with an additional permease domain.

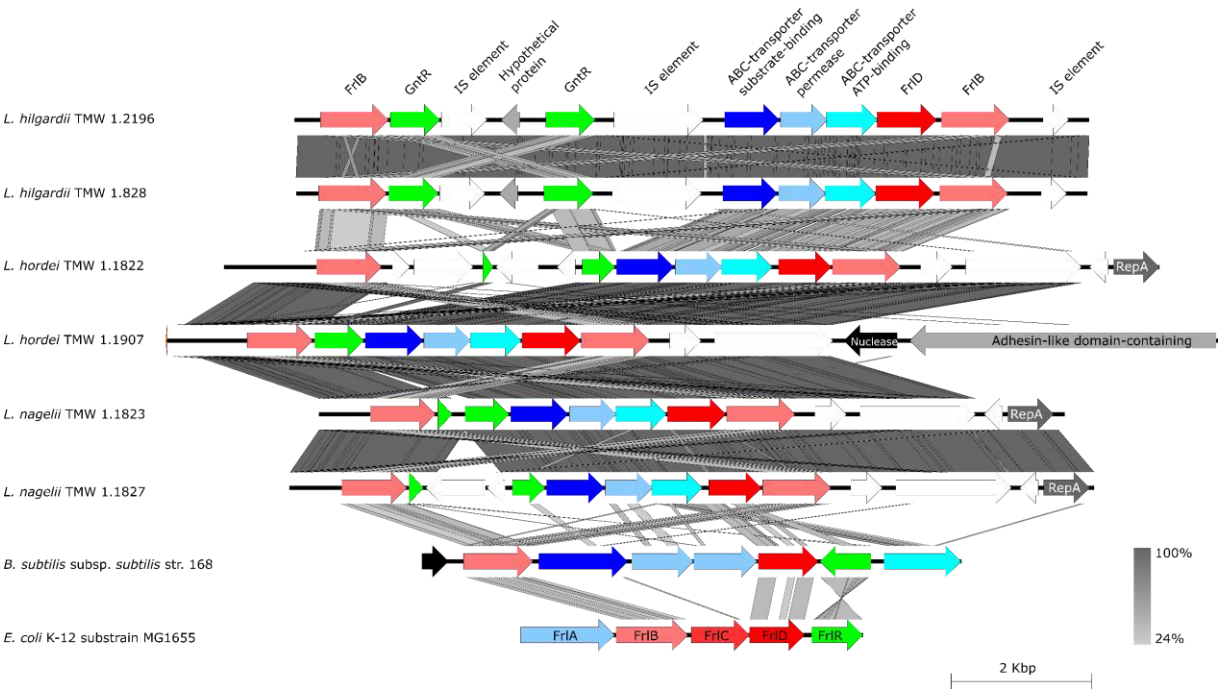

Figure 29 Fructoselysine gene cluster in water kefir isolates compared to *B. subtilis* subsp. *subtilis* strain 168 and *E. coli* K-12 substrain MG1655. Identical colours represent genes coding for functionally equal proteins. Colour of connecting lines represents percent blast identity according to scale on the right. FrlA= fructoselysine transporter, FrlB = fructoselysine-6-P deglycase, FrlC = fructoselysine-3-epimerase, FrlD = fructoselysine-6-kinase, FrlR/GntR = transcriptional regulators, RepA = plasmid replication initiation protein. Genomic regions according to locus-tags: *L. hilgardii* TMW 1.2196 C2L99_14180-C2L99_14125, *L. hilgardii* TMW 1.828 CLI91_14080-CLI91_14025, *L. hordei* TMW 1.1822 BSQ49_11780-BSQ49_12095, *L. hordei* TMW 1.1907 CRI84_10725-CRI84_10780, *L. nagelii* TMW 1.1823 CRI83_11595-CRI83_11600 and CRI83_11965-CRI83_11920, *L. nagelii* TMW 1.1827 BSQ50_11575-BSQ50_11640; *B. subtilis* subsp. *subtilis* strain 168 (Genbank Accession No. AL009126, BSU_32550 - BSU_32620); *E. coli* K-12 substrain MG1655 (Genbank Accession No. NC_000913, b3370 – b3375).

The analysis of this gene cluster uncovered the presence of another gene cluster in *L. hordei* TMW 1.1822 (BSQ49_12345 - BSQ49_12400) with a predictively similar role. This cluster was found to be located on plasmid 2 that was not shared with any of the other water kefir isolates investigated in this analysis. Moreover, OrthoFinder analysis could not identify any genes within this cluster being orthologous to genes within the other strains indicating this gene cluster to be strain-specific for *L. hordei* TMW 1.1822. As depicted in Figure 30, the gene cluster coded for a PTS of the Man-family, fructoselysine-6-P deglycase and fructoselysine-6-kinase. Similar gene clusters were described for *Enterococcus* (*E.*) *faecium* and *L. curvatus* (Terán *et al.*, 2018; Wiame *et al.*, 2005). However, none of the compared gene clusters exhibited a gene for fructoselysine-6-kinase. Instead, *E. faecium* DO encoded a glucosamine-fructose-6P transaminase (E.C. 2.6.1.16, GlmS), while the fructoselysine-6-P deglycase (FrlB) homologue was in fact shown to be a glucoselysine-6-P deglycase (Wiame *et al.*, 2005).

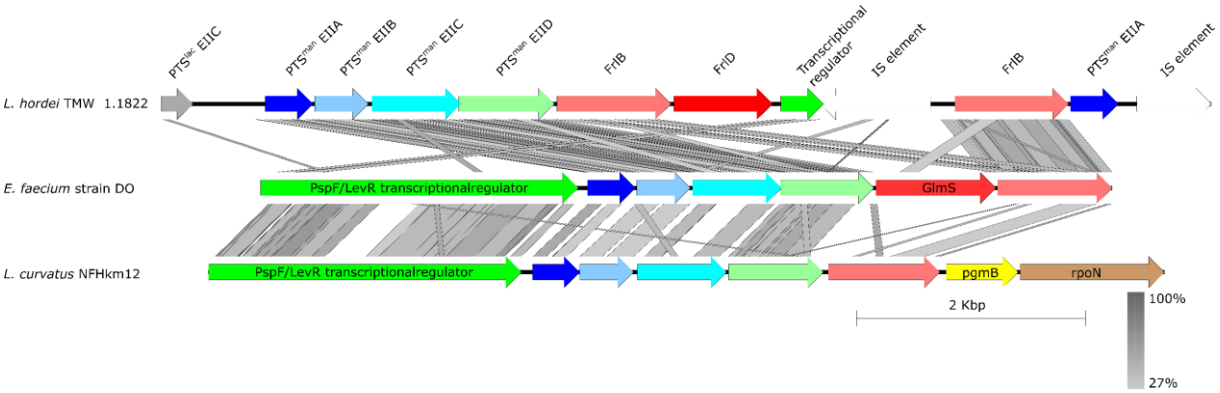

Figure 30 Fructoselysine gene cluster No. 2 of *L. hordei* TMW 1.1822 compared to similar clusters in *E. faecium* strain DO and *L. curvatus* NFHkm12. Identical colours represent genes coding for functionally equal proteins. Colour of connecting lines represents percent blast identity according to scale on the right. FrlB = fructoselysine-6-P deglycase, FrlD = fructoselysine-6-kinase, GlmS = glutamine-fructose-6P transaminase (isomerizing), pgmB = β-phosphoglucomutase, rpoN = RNA-polymerase σ54-factor. Genomic regions: *L. hordei* TMW 1.1822 BSQ49_12345 - BSQ49_12400; *E. faecium* strain DO (Genbank Accession No. AAAK03000010, EfaeDRAFT_2264 - EfaeDRAFT_2270); *L. curvatus* NFHkm12 (Genbank Accession No. AP018699, NFHkm12_09850 - NFHkm12_09920).

4.5.4 Carbohydrate metabolism

Since category-based comparisons predicted that adaptations to the water kefir environment may predominantly reside in the carbohydrate metabolism of *L. hilgardii, L. hordei* and *L. nagelii,* the putative functional proteomes of these species were analyzed for their initial and central carbohydrate metabolism, as well as their different capabilities of degrading pyruvate. Additionally, this should predict metabolic output, as well as reactions that may occur in addition or instead of the dextransucrase reaction.

4.5.4.1 Carbohydrate transporters

The WGSs were searched for phosphotransferase systems (PTS), major facilitator systems (MFS), ATP-binding cassette (ABC) transporters and permeases that were predicted to operate as carbohydrate importers.

In general, *L. hordei* and *L. nagelii* strains exhibited a higher number of PTS compared to *L. hilgardii* strains, while this species exhibited a higher number of MFS transporters compared to the other two species. As shown in Table 16, all strains possessed at least one PTS of the Man-family (PTS^{man}), enabling the import of fructose (→ fructose-6-P), sorbose (→ sorbose-1-P), N-acetylglucosamine (→ N-acetylglucosamine-6-P), mannose (→ mannose-6-P) or fructoselysine/ glucoselysine (→ fructoselysine-6-P/ glucoselysine-6-P), of which no closer specification was possible. Additionally, all strains were putatively capable of importing sucrose *via* PTS^{scr} (→ sucrose-6-P). Furthermore, *L. hordei* and *L. nagelii* strains exhibit Fru-family PTS (PTS^{fru}) for the import of fructose and mannitol (→ fructose-1-P, mannitol-1-P)

and several Glc-family PTS (PTS^{glc}) for the uptake of β-glucosides of unknown specificity. Furthermore, Lac-Family PTS (PTS^{lac}) for the uptake of lactose (→ lactose-6-P) or cellobiose (→ cellobiose-6-P) were found in all *L. hordei* and *L. nagelii* strains, however, *L. nagelii* strains exhibited the highest amount of PTS^{lac}. Moreover, all *L. nagelii* strains possessed at least two Gat-family PTS (PTS^{gat}) for the import of galacticol (→ galacticol-1-P) or galactose (→ galactose-6-P), while *L. hordei* TMW 1.1822 exhibited one PTS^{gat}. Furthermore, all *L. nagelii* strains exhibited a Gut-family PTS (PTS^{gut}) for the import of sorbitol (→ sorbitol-6-P). Additionally, several isolated PTS subunits of different types of PTS were found distributed over the genomes of all strains (= not organized in a gene cluster together with other relevant subunits). It is important to note that a PTS-family was only assigned when sequence analysis clearly suggested for a certain PTS-family. Corresponding locus-tags of all PTS genes are summarized in Appendix 14.

Table 16 Distribution of different types of PTS among analyzed strains.

Family	**TMW 1.2196**	**TMW 1.828**	**TMW 1.45^T**	**TMW 1.1822**	**TMW 1.1907**	**TMW 1.2353^T**	**TMW 1.1823**	**TMW 1.1827**	**TMW 1.2352^T**
HPr	1	1	1	1	1	1	1	1	1
EI	2	2	2	1	1	1	1	1	1
PTS^{man}	1	1	1	7	5	4	6	6	6
PTS^{fru}	-	-	-	3	3	3	3	3	5
PTS^{scr}	1	1	1	1	1	1	1	1	1
PTS^{gat}	-	-	-	2	-	-	2	2	2
PTS^{gut}	-	-	-	-	-	-	1	1	1
PTS^{lac}	-	-	-	1	1	1	4	4	4
PTS^{glc}	-	-	-	5	4	1	4	4	5
Isolated PTS subunits	4	4	4	10	9	10	9	9	10

Apart from the import *via* PTS, several different MFS permeases and other transporters appeared to be encoded by the genomes of all nine strains (Table 17). Thereby, all strains may be capable of importing glucose (and putatively rhamnose), melibiose, raffinose or lactose and sucrose. Apart from that, all strains are predictively capable of importing arabinose, xylose and/ or galactose *via* MFS transporters. Additionally, some strains possessed at least one MFS transporter for the import of hexuronate, galactonate, galactarate or glucarate, however, sequence analysis could not detect the exact specificity of these transporters. Moreover, only *L. hilgardii* strains exhibited an MFS transporter specific for fucose, while some of the tested strains possessed an additional MFS transporter involved in oligosaccharide import that may

also contribute to sucrose import. Corresponding locus-tags of all transporters listed in Table 17 are shown in Appendix 15.

Table 17 Transporters and MFS transporters involved in the putative functional metabolism of sugars and sugar alcohols as derived from WGS analysis.

Compound	TMW 1.2196	TMW 1.828	TMW 1.45^T	TMW 1.1822	TMW 1.1907	TMW 1.2353^T	TMW 1.1823	TMW 1.1827	TMW 1.2352^T
Fucose	2	2	2	-	-	-	-	-	1
Glucose/Rhamnose (possibly incomplete)	4	4	4	2	2	2	4	4	4
Arabinose/Xylose/Galactose	5	5	8	2	1	2	2	2	1
Hexuronate/Glucarate/Galactarate/Galactonate	1	1	1	-	1	1	1	1	1
Melibiose/Lactose/Raffinose	5	5	4	2	1	1	4	4	5
Sucrose	4	4	3	2	1	2	2	2	2
Oligosaccharides (pot. sucrose)	1	1	-	1	-	-	1	1	1

At least one gene cluster encoding an ABC-transporter for the uptake of glycerol-3-P or maltose was found in all genomes, while all *L. hordei* and *L. nagelii* strains exhibited a complete cluster for an ABC-transporter for the uptake of nucleosides. Distributions and locus-tags of these transporters are listed in Appendix 16.

4.5.4.2 Central carbohydrate metabolism

All strains of *L. hordei* and *L. nagelii* encoded all enzymes involved in Embden-Meyerhof-Parnas (EMP) pathway, while this pathway was incomplete in *L. hilgardii* strains due to the lack of fructose-1,6-bisphosphate aldolase (E.C. 4.1.2.13). Moreover, *L. hilgardii* strains did not encode fructose-1,6-bisphatase (E.C. 3.1.3.11), 6-phosphofructokinase (E.C. 2.7.1.11) and 1-phosphofructokinase (E.C. 2.7.1.56) in contrast to *L. hordei* and *L. nagelii* strains. Additionally, both water kefir strains of *L. hilgardii* encoded for a pyruvate-P-dikinase (E.C. 2.7.9.1) and all *L. nagelii* strains encoded for a pyruvate, water dikinase (E.C. 2.7.9.2).

All strains possessed all enzymes involved in the oxidative part of pentose-phosphate pathway (PPP), as well as phosphoketolase pathway (PKP). However, only both water kefir strains of the species *L. hordei* and all three *L. nagelii* strains encoded a transketolase (E.C. 2.2.1.1), while none of the strains was found to exhibit a gene for transaldolase (E.C. 2.2.1.2). Additionally, all *L. hilgardii* and *L. nagelii* strains, as well as *L. hordei* TMW 1.1822 encoded for 2-keto-3-deoxy-6-P-gluconate (KDPG, E.C. 4.1.2.14) aldolase, the characteristic enzyme of Entner-

Doudoroff (ED) pathway. However, no gene encoding phosphogluconate dehydratase (E.C. 4.2.1.12) was found in the genomes of these strains. Nonetheless, *L. hordei* TMW 1.1822, *L. nagelii* TMW 1.1823 and *L. nagelii* TMW 1.1827 encoded for a galactonate dehydratase (E.C. 4.2.1.6) within the same gene cluster as KDPG-aldolase. Additionally, all *L. hilgardii* and all *L. nagelii* strains encoded for both, a gluconokinase (E.C. 2.7.1.12) and 2-dehydro-3-deoxygluconokinase (KDG, E.C. 2.7.1.45).

All strains of the species *L. nagelii* and *L. hilgardii* encoded all enzymes necessary for Leloir-pathway, while *L. nagelii* strains additionally exhibited all enzymes necessary for Tagatose-6-P-pathway. A β-galactosidase (E.C. 3.2.1.23) for the cleavage of lactose was found in both water kefir isolates of the species *L. hilgardii* and all strains of the species *L. nagelii*.

As sucrose is the main source of energy in water kefir, the predictively functional initial sucrose degradation was investigated more detailed. As stated several times above, all water kefir isolates, but not the typestrains originating from another source encoded a dextransucrase that enables extracellular sucrose degradation into fructose and glucose/ dextran. Moreover, all *L. hordei* strains encoded a putative GH32 β-fructosidase that may extracellularly cleave sucrose into glucose and fructose but may also degrade fructans. However, exact specificity was not derivable from sequence analysis alone. Intracellular sucrose degradation may further be achieved by sucrose-6-P-hydrolase (E.C. 3.2.1.26) that was encoded at least once by all *L. hordei* and *L. nagelii* strains and uses sucrose-6-P as substrate. In *L. hilgardii* strains, this un-phosphorylated sucrose is degraded by sucrose phosphorylase (E.C. 2.4.1.7). Moreover, all tested strains encoded at least one glucohydrolase that may also use sucrose as substrate. Although these enzymes were predicted to exhibit α-glucosidase activity, no further substrate-specificity could be derived from sequence analysis alone.

As shown in section 4.2, the ability to ferment L-arabinose and D-mannitol under acid formation were positively correlated to the isolation source water kefir. Therefore, the corresponding metabolic routes were investigated more detailed.

Both water kefir isolates of the species *L. hilgardii* encoded for several extracellular α-N-arabinofuranosidases (E.C. 3.2.1.55), an enzyme that degrades arabinans into L-arabinose. This enzyme was also encoded once by *L. nagelii* TMW 1.2352^{T}. L-arabinose may then be converted to L-ribulose by the enzyme L-arabinose isomerase (E.C. 5.3.1.4) that was encoded by the water kefir isolates of the species *L. hilgardii* and *L. nagelii*. Within the same gene cluster, a L-ribulokinase (E.C. 2.7.1.16) and L-ribulose-5-P 4-epimerase (E.C. 5.1.3.4) were encoded, respectively, that ultimately channel L-ribulose into PPP.

All strains of *L. hordei* and *L. nagelii,* but only the water kefir isolates of *L. hilgardii* encoded for at least one mannitol-1-P 5-dehydrogenase enzyme (E.C. 1.1.1.17) that mediates the interconversion of mannitol-1-P and NAD^+ to fructose-6-P and $NADH+H^+$. The tested strains did not encode mannitol-1-phosphatase (E.C. 3.1.3.22). However, an additional mannitol-1-P 5-dehydrogenase gene was found in water kefir borne *L. hilgardii* strains and all *L. nagelii* strains may potentially code for a mannitol-2-dehydrogenase (E.C. 1.1.1.67) instead. The corresponding orthogroups and locus-tags of all genes encoding enzymes of the mentioned pathways are listed in Appendix 17.

4.5.4.3 Pyruvate metabolism

As fermentative output is essentially influenced by the pathway that further metabolizes pyruvate, the presence of the corresponding routes was evaluated by genome analysis of *L. hilgardii*, *L. hordei* and *L. nagelii.* All strains exhibited at least one gene encoding for L-lactate dehydrogenase (E.C. 1.1.1.27) and D-lactate dehydrogenase (E.C. 1.1.1.28), respectively. Furthermore, all strains appeared to be capable of producing acetyl-CoA *via* pyruvate-dehydrogenase complex, but only *L. hordei* and *L. nagelii* strains encoded for a formate C-acetyltransferase (E.C. 2.3.1.54). None of the tested strains coded for pyruvate decarboxylase (E.C. 4.1.1.1). Acetyl-CoA may then react to acetyl-phosphate *via* phosphate-acetyltransferase (E.C. 2.3.1.8) that appeared to be present within all nine genomes. Additionally, acetyl-phosphate may directly come from pyruvate by means of pyruvate oxidase (E.C. 1.2.3.3) that was also encoded by all nine strains. Furthermore, acetyl-CoA may be converted to ethanol *via* acetaldehyde by the enzymes acetaldehyde-dehydrogenase (E.C. 1.2.1.10) and alcohol-dehydrogenase (E.C. 1.1.1.1). However, only a bifunctional acetaldehyde-CoA/alcohol-dehydrogenase was found within the genomes that may overtake both reactions.

Furthermore, all necessary enzymes for the conversion of pyruvate to 2,3-butanediol (acetolactate synthase, E.C. 2.2.1.6; acetolactate decarboxylase, E.C. 4.1.1.5 and butanediol dehydrogenase, E.C. 1.1.1.4) were present in all strains. By contrast, a gene encoding diacetyl reductase (E.C. 1.1.1.304) was not found in *L. hordei* TMW 1.1907 and TMW 1.2353^T, as well as *L. nagelii* TMW 1.2352^T. The locus-tags of all genes encoding the above-mentioned enzymes are listed in Appendix 18.

4.6 Behaviour of *L. hordei* TMW 1.1822 and *L. nagelii* TMW 1.1827 under dextran-forming conditions

In order to investigate the behaviour and metabolism of *L. hordei* TMW 1.1822 and *L. nagelii* TMW 1.1827 under dextran forming conditions (= in the presence of sucrose), the proteomic profiles of cell lysates and exoproteomes of both microorganisms were analysed after sucrose-treatment compared to glucose-treatment. Additionally, sugar consumption and acid formation, as well as the growth behaviour of both strains were investigated to support predictions made from proteomic analyses.

4.6.1 Proteomic analysis of cell lysates and exoproteomes

4.6.1.1 Differential proteomics of cell lysates

As stated in section 4.5.1, *L. hordei* TMW 1.1822 and *L. nagelii* TMW 1.1827 encoded 2461 and 2391 proteins within their respective functional proteomes. During proteomic analysis of the cell lysates of both microorganisms, 1361 proteins of *L. hordei* and 1384 proteins of *L. nagelii* were quantified by mass spectrometry (MS) according to the applied filtering criteria (Figure 31). According to differential expression analysis, 53 of these proteins appeared to be significantly differently abundant within the cellular proteomes of *L. hordei* when incubated in sucrose compared to glucose. Only 38 of such proteins could be found for *L. nagelii*. The *in silico* proteome of *L. hordei* exhibited about 1 % proteins that were predicted to be of extracellular nature. While this relative amount was constant among proteins quantified by MS, none of the differentially abundant proteins of the cellular proteomes of *L. hordei* was predicted to be secreted. Simultaneously, about 1 % of the *in silico* proteome of *L. nagelii* was predicted to be extracellular, however, only ~ 0.9 % of the proteins quantified by MS exhibited this trait. Surprisingly, about 8 % of the differentially abundant proteins were predictively secreted that were all found to be less abundant within the cellular proteomes of sucrose-treated cells compared to glucose-treated cultures.

As depicted in Figure 31 C + D, about 80 % of the differentially abundant proteins of *L. hordei* were assigned to the SEED category “carbohydrates”, while only ~ 43 % of the annotated proteins of *L. nagelii* accounted for this category. All significantly differentially abundant proteins of cellular proteomes are listed in Appendix 19 and Appendix 20.

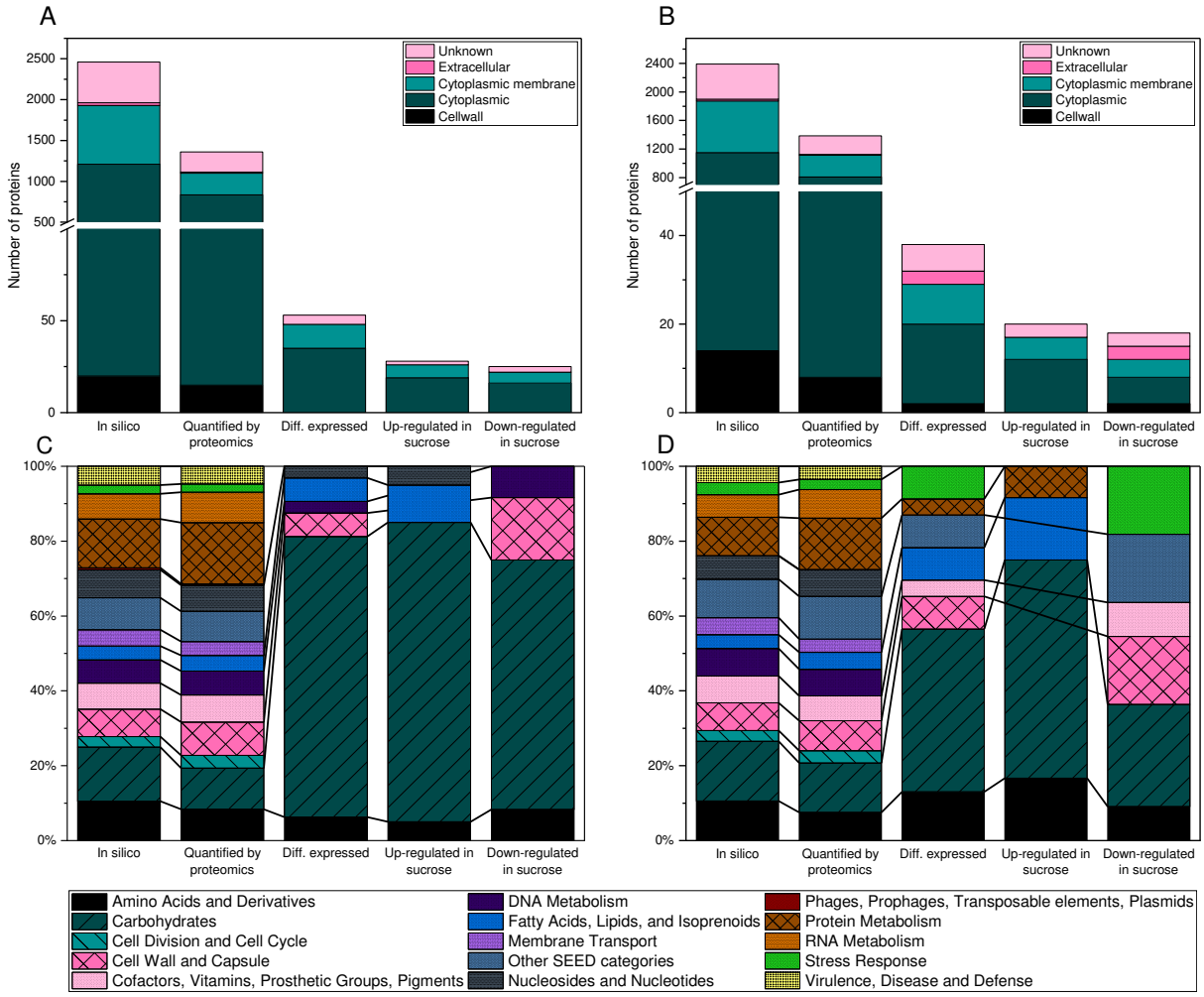

Figure 31 Comparison of the predicted functional proteomes (*in silico*) with protein sub-groups obtained from MS intensity statistical analysis of cellular proteomes of *L. hordei* TMW 1.1822 (A+C) and *L. nagelii* TMW 1.1827 (B+D). (**A+B**) Total protein counts of in silico predicted proteins, proteins quantified by proteomics (detected in four out of five replicates of at least one group), differentially expressed proteins and up- and down-regulated proteins in sucrose. Additionally, predicted subcellular localization of the respective proteins is shown. (**C+D**) Corresponding SEED category distributions. The SEED category proteome coverage was ~ 44 % for *L. hordei* TMW 1.1822 and ~ 45 % for *L. nagelii* TMW 1.1827. For reasons of clarity, the categories "Dormancy and Sporulation", "Metabolism of aromatic compounds", "Miscellaneous", "Motility and Chemotaxis", "Nitrogen metabolism", "Phosphorus metabolism", "Potassium metabolism", "Regulation and cell signalling", "Respiration" and "Sulfur metabolism" were summarized within "Other SEED categories".

Regarding the carbohydrate metabolism of *L. hordei* TMW 1.1822, several genes that were partially organized in gene clusters were found to be significantly differentially abundant (see Figure 32). This included pathways for the uptake and metabolism of sucrose, fructose, glucose, mannitol, glycerol and β-glucosides. Thus, several subunits of PTS^{fru}, PTS^{man}, PTS^{lac} and PTS^{scr} appeared to be significantly up-regulated, while a complete PTS^{man} and PTS^{glc} were significantly less abundant in the presence of sucrose. Moreover, a sucrose-specific MFS-transporter was significantly down-regulated in sucrose-treated cells, while subunits of an ABC-transporter specific for glycerol-3-P or maltose was significantly up-regulated. Among

proteins involved in EMP, 1-phosphofructokinase was significantly up-regulated in sucrose-treated cells, while glucose-6-P-isomerase and 6-phosphofructokinase were less abundant. Additionally, fructose-1,6-bisphosphatase was significantly up-regulated in the presence of sucrose. Apart from that, sucrose-6-P-hydrolase and mannitol-1-P 5-dehydrogenase were found to be significantly more abundant after sucrose-treatment, while two glucohydrolases with putative α-glucosidase activity were significantly less abundant. Additionally, two enzymes involved in glycerol metabolism, namely glycerol kinase (E.C. 2.7.1.30) and glycerol-3-P dehydrogenase (E.C. 1.1.5.3) were significantly up-regulated in sucrose-treated cells. Except for ribulose-3P-epimerase and transketolase, all enzymes involved in EMP, PPP and PKP pathways were quantified by proteomics, however, not influenced by the present carbon source. This also applied for both extracellular sucrose degrading enzymes, namely dextransucrase and β-fructosidase, respectively. Moreover, all enzymes that may participate in pyruvate degradation were quantified by proteomics, except for diacetyl reductase, while the alpha and beta E1 subunits of pyruvate dehydrogenase complex, as well as butanediol dehydrogenase were significantly up-regulated in sucrose-treated cells. Moreover, a GH25 muramidase was found to be significantly up-regulated in the presence of sucrose.

Regarding the carbohydrate metabolism of *L. nagelii* TMW 1.1827, several genes that were partially organized in gene clusters were found to be significantly differentially abundant (Figure 32). This included pathways for the uptake and metabolism of sucrose, fructose, glucose, mannitol, glycerol and β-glucosides. Thus, several subunits of PTS^{fru} and PTS^{scr} appeared to be significantly more abundant, when sucrose was present, while two subunits of a PTS^{man} and a PTS^{glc} were significantly less abundant. Like in *L. hordei,* a sucrose-specific MFS-transporter was significantly down-regulated in the presence of sucrose. All enzymes necessary for EMP-pathway were quantified by proteomics, however, glucose-6-P-isomerase was significantly less abundant in sucrose-treated cells, while 1-phosphofructokinase and fructose-1,6-bisphosphatase were significantly more abundant under this condition. Apart from transketolase, all enzymes involved in PPP and PKP were quantified by proteomics, but none of these proteins was differentially expressed/abundant. Regarding sucrose degradation, the expression of sucrose-6-P hydrolase was significantly up-regulated in the presence of sucrose. Dextransucrase was significantly down-regulated in the presence of sucrose. Similar to *L. hordei,* mannitol-1-P 5-dehydrogenase was significantly up-regulated in sucrose-treated cells of *L. nagelii*. All enzymes involved in different pathways of pyruvate degradation (see section 4.5.4) were quantified by proteomics, but were not significantly differentially expressed. Housekeeping proteins RNA polymerase sigma factor (rpoD), DNA gyrase subunits alpha and

beta (gyrA + gyrB) and the chaperones GroL, GroES, DnaJ and DnaK were not significantly differentially expressed in both microorganisms.

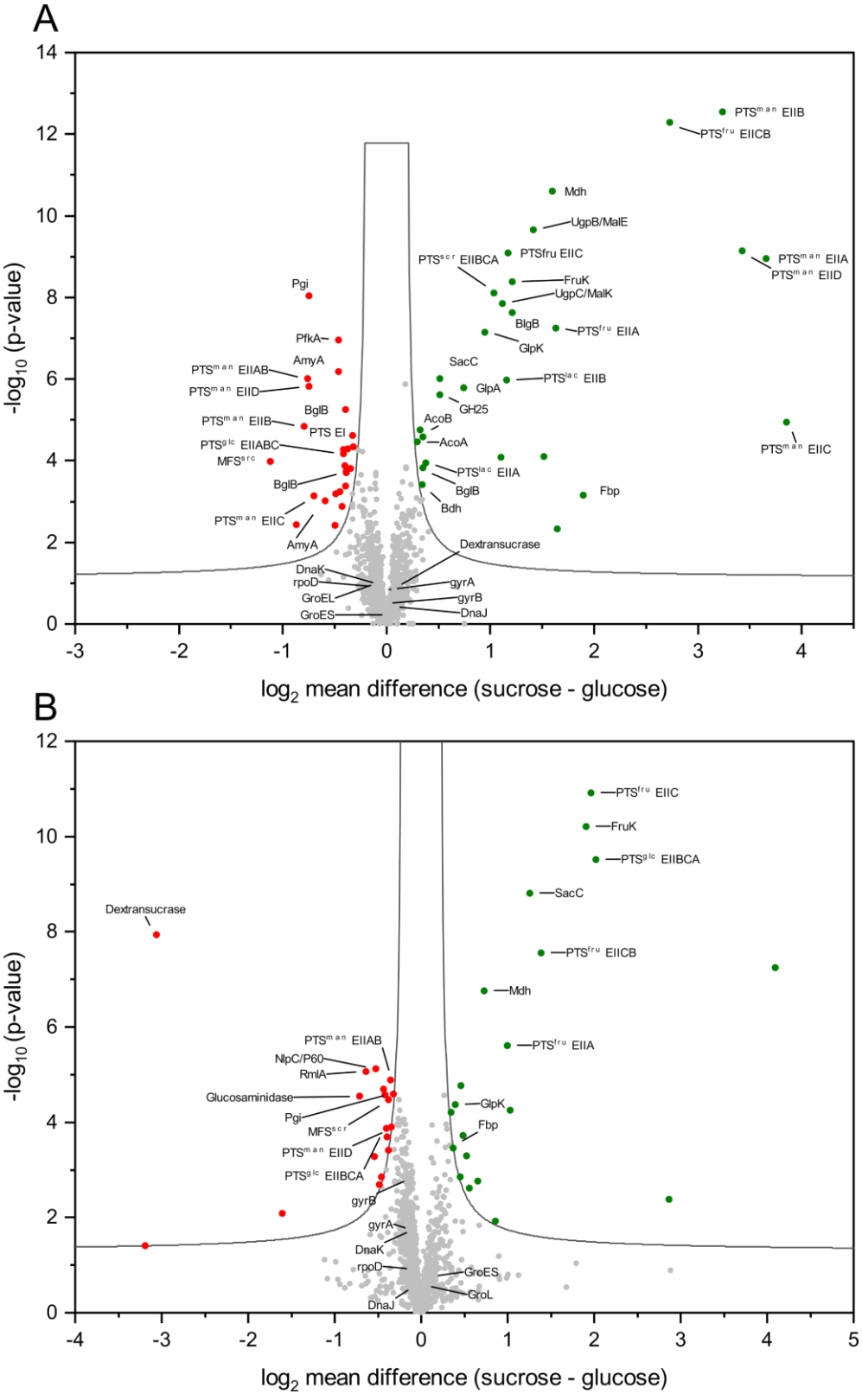

Figure 32 log2 fold changes (FC) plotted against -log10 p-values of proteins quantified by proteomics of cell lysates of *L. hordei* TMW 1.1822 (A) and *L. nagelii* TMW 1.1827 (B). Red = proteins significantly down-regulated in sucrose-supplemented medium, green = proteins significantly up-regulated in sucrose-supplemented medium. AcoA+AcoB = pyruvate dehydrogenase complex subunit E1, AmyA = glucohydrolase (putative α-glucosidase), Bdh = butanediol dehydrogenase, BglB = 6-P-β-glucosidase, Fpb = fructose-1,6-bisphosphatase, FlgJ = flagellar protein J/ cell wall hydrolase, FruK = 1-phosphofructokinase, GH25 = GH25 muramidase, GlpA = glycerol-3-P dehydrogenase, GlpK = glycerol kinase, gyrA+gyrB = DNA gyrase subunits, Mdh = mannitol-1-P 5-dehydrogenase, NlpC/P60 = NlpC/P60 domain containing protein, PfkA = 6-phosphofructokinase, Pgi =

glucose-6-P-isomerase, RpoD = RNA polymerase sigma factor, RmlA = glucose-1-P thymidylyltransferase, SacC = sucrose-6-P hydrolase, UgpB/MalE = ABC substrate-binding protein glycerol-3P/maltose specific, UgpC/MalK = ATP-binding protein glycerol-3P/maltose specific. DnaJ, DnaK, GroL, GroES = chaperones.

The ranking of all quantified proteins according to their iBAQ intensities furthermore provided the opportunity to compare absolute protein abundancies within a certain tested condition. As depicted in Figure 33, only proteins that participate in the carbohydrate metabolism of *L. hordei* TMW 1.1822 and *L. nagelii* TMW 1.1827, as well as other proteins relevant for further experiments were labelled. In *L. hordei,* most of the differentially expressed proteins appeared to remain within the same range of abundancy after sucrose-treatment, e.g. the significantly-down-regulated PTS^{man} was still of high abundancy in sucrose-treated cells. However, some proteins shifted more prominently. This was true for the significantly up-regulated PTS^{man}, mannitol-1-P 5-dehydrogenase, GH25-muramidase, fructose-1,6-bisphosphatase and one of the 6-P-β-glucosidases that were all shifted from mid- or low-range abundancy to high- or mid-range abundancy, respectively. In sucrose-treated cells, the sucrose-specific MFS-transporter changed from a mid-range abundancy to low-range abundancy. In general, the differentially expressed PTS transporters, as well as enzymes participating in glycolysis or mannitol-cycle were all of high abundancy independent of the present carbon source, while proteins involved in the degradation of di- and predictively oligosaccharides (e.g. sucrose-6-P hydrolase, 6-P-β-glucosidase, glucohydrolase), as well as of pyruvate degradation were rather of mid-range abundancy. Enzymes and transporters predictively involved in the uptake and metabolism of glycerol, as well as fructose-1,6-bisphosphatase were of mid- to low-range abundancy. The dextransucrase that was not significantly differentially expressed in *L. hordei* TMW 1.1822 appeared to be of high abundancy irrespective to the present carbon source, being in the range of common house-keeping proteins.

In *L. nagelii*, the most prominent shifts in protein abundancy were accomplished by significantly up-regulated PTS^{scr}, subunits of PTS^{fru}, 1-phosphofructokinase and sucrose-6-P hydrolase. By contrast, the dextransucrase that was significantly down-regulated after sucrose-treatment changed from being of high abundancy to a rather mid-range abundant protein. Similar to *L. hordei,* the differentially expressed PTS transporters, as well as enzymes participating in glycolysis and mannitol-cycle were of high abundancy in both conditions, while fructose-1,6-bisphosphatase was of low abundancy. Contrary to *L. hordei,* glycerol kinase that was significantly up-regulated in sucrose-treated cells of *L. nagelii* TMW 1.1827 was of mid-range abundancy in this strain.

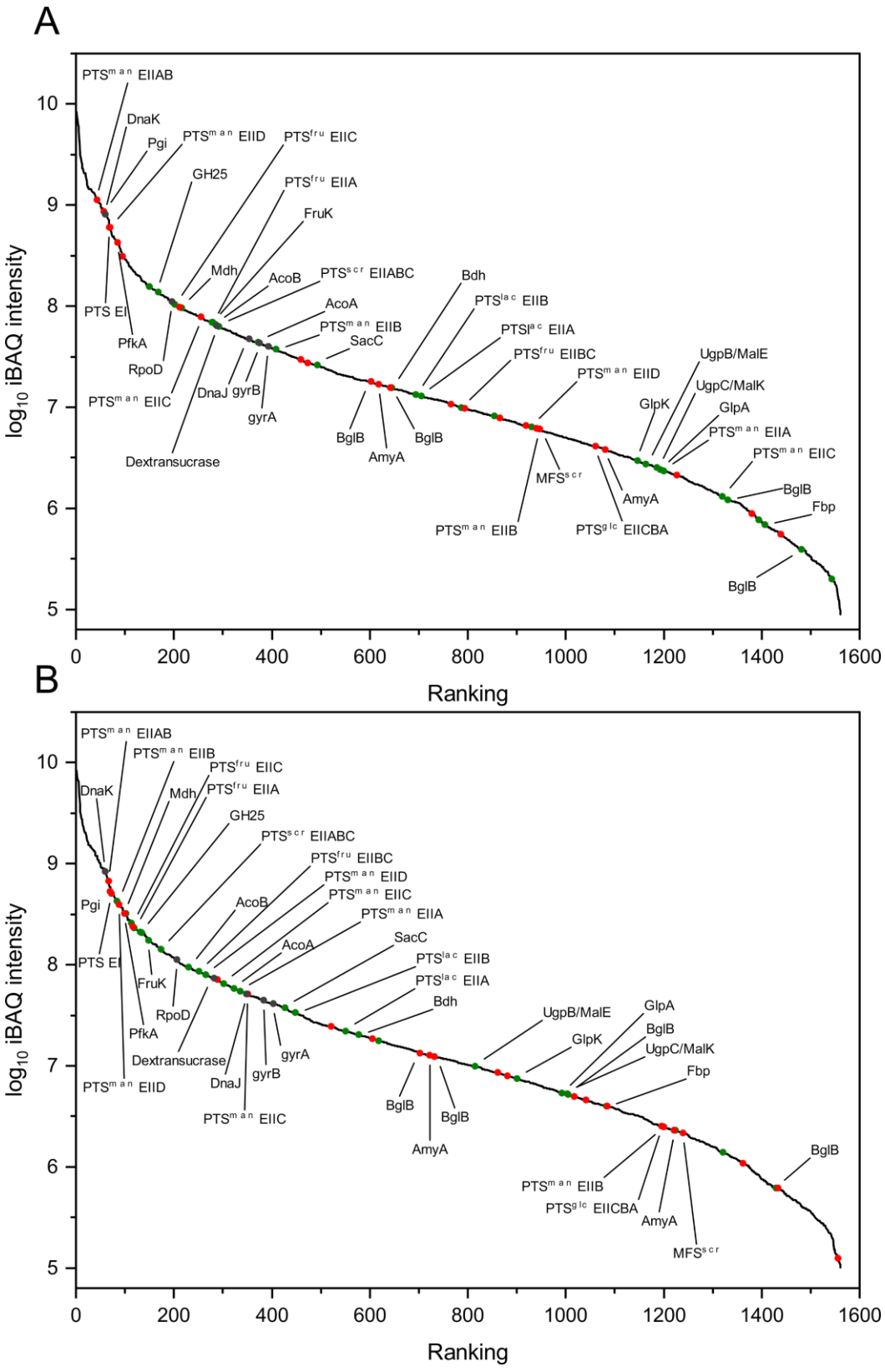
A
log10 iBAQ intensity
Ranking
PTSman EIIAB
DnaK
Pgi
PTSman EIID
PTSfru EIIC
GH25
PTSfru EIIA
FruK
Mdh
AcoB
PTSscr EIIABC
Bdh
PTSlac EIIB
AcoA
PTSman EIIB
PTSlac EIIA
SacC
PTSfru EIIBC
UgpB/MalE
PTSman EIID
UgpC/MalK
GlpK
GlpA
PTS EI
PfkA
PTSman EIIA
RpoD
PTSman EIIC
DnaJ
gyrB
gyrA
BglB
AmyA
BglB
Dextransucrase
MFSscr
AmyA
BglB
Fbp
PTSman EIIB
PTSglc EIICBA
BglB
B
log10 iBAQ intensity
Ranking
PTSman EIIAB
PTSman EIIB
PTSfru EIIC
DnaK
Mdh
PTSfru EIIA
GH25
PTSscr EIIABC
PTSfru EIIBC
PTSman EIID
PTSman EIIC
Pgi
AcoB
PTSman EIIA
SacC
AcoA
PTS EI
PTSlac EIIB
FruK
PTSlac EIIA
Bdh
RpoD
UgpB/MalE
GlpA
PfkA
GlpK
BglB
Dextransucrase
UgpC/MalK
gyrA
PTSman EIID
DnaJ
gyrB
Fbp
BglB
BglB
PTSman EIIC
AmyA
BglB
PTSman EIIB
PTSglc EIICBA
AmyA
MFSscr

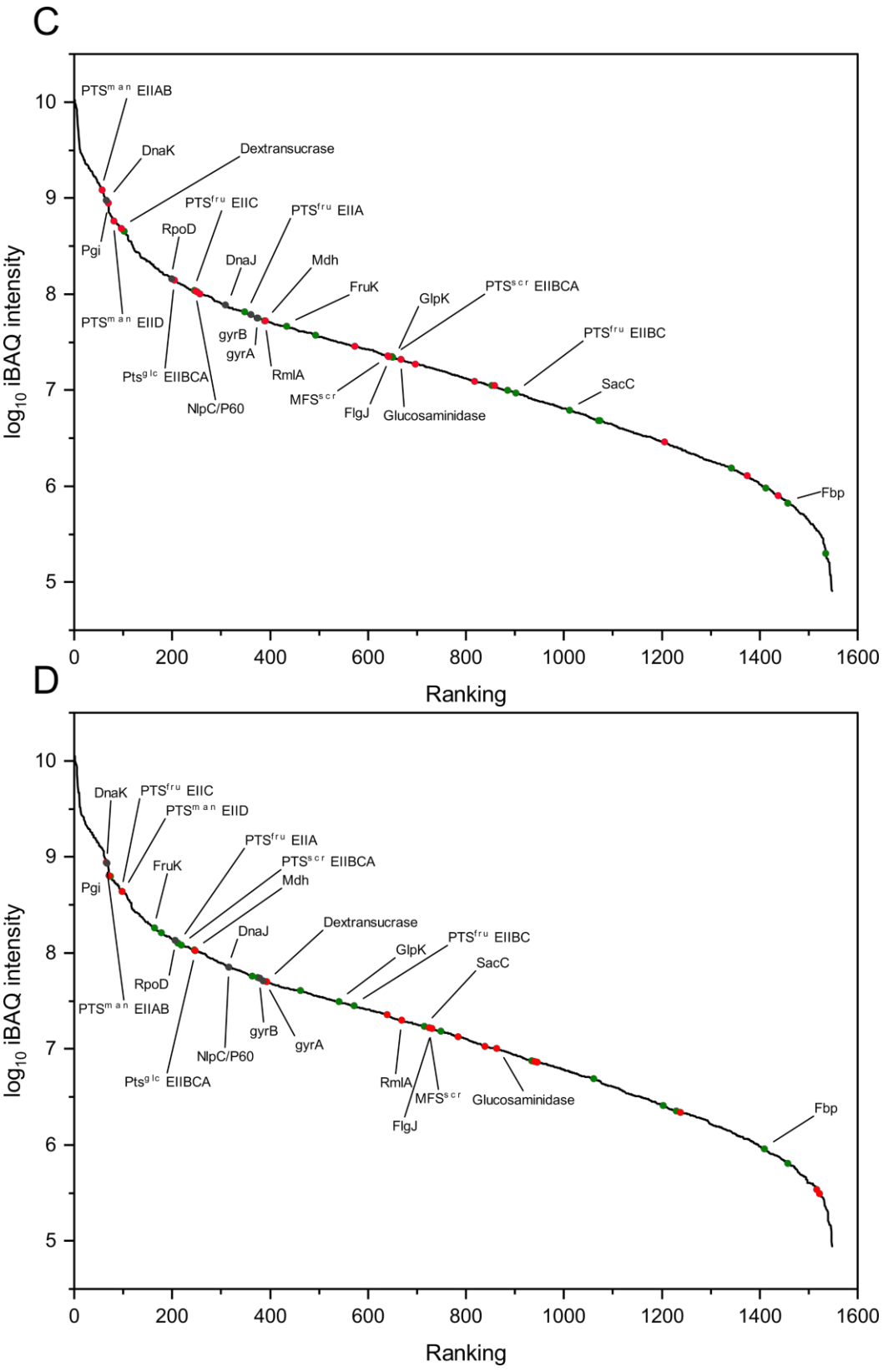

Figure 33 MS intensity ranking of quantified proteins within cellular proteomes of *L. hordei* TMW 1.1822 (A+B) and *L. nagelii* (C+D) after incubation in medium supplemented with glucose (A+C) or sucrose (B+D). Green = proteins significantly up-regulated in sucrose, red = proteins significantly down-regulated in sucrose, grey = not significantly differentially expressed. AcoA+AcoB = pyruvate dehydrogenase complex subunit E1, AmyA = glucohydrolase (putative α-glucosidase), Bdh = butanediol dehydrogenase, BglB = 6-P-β-glucosidase, Fpb = fructose-1,6-bisphosphatase, FlgJ = flagellar protein J/ cell wall hydrolase, FruK = 1-phosphofructokinase, GH25 = GH25 muramidase, GlpA = glycerol-3-P dehydrogenase, GlpK = glycerol kinase, gyrA+gyrB = DNA gyrase

subunits, Mdh = mannitol-1-P 5-dehydrogenase, NlpC/P60 = NlpC/P60 domain containing protein, PfkA = 6-phosphofructokinase, Pgi = glucose-6-P-isomerase, RmlA = glucose-1-P thymidylyltransferase, RpoD = RNA polymerase sigma factor, SacC = sucrose-6-P hydrolase, UgpB/MalE = ABC substrate-binding protein glycerol-3P/maltose specific, UgpC/MalK = ATP-binding protein glycerol-3P/maltose specific. DnaJ, DnaK, GroL, GroES = chaperones.

4.6.1.2 Differential proteomics of exoproteomes

Only very few proteins (a maximum of 8 proteins of *L. hordei* TMW 1.1822 and of 20 proteins of *L. nagelii* TMW 1.1827) were found in the un-inoculated medium samples (= negative control) that could be assigned to the respective *in silico* proteomes of *L. hordei* and *L. nagelii*, which may result from carry-over during preparative SDS-PAGE. Compared to the amount of quantified proteins within the cell lysates of both microorganisms, the amount of quantified proteins of the exoproteomes was distinctly lower. While the exoproteomes of *L. nagelii* TMW 1.1827 exhibited 579 proteins that matched the filtering criteria, the exoproteomes of *L. hordei* TMW 1.1822 exhibited only 271 different proteins (see Figure 34). Statistical analysis of the exoproteomes of *L. nagelii* furthermore revealed that only four of the quantified proteins were of significantly different abundancy after sucrose-treatment compared to glucose-treatment, of which only one protein was subjected for a decreased release in sucrose-supplemented medium. This protein was annotated as glucose-1-P thymidylyltransferase (2.7.7.24). Two of the other proteins were predicted to be of extracellular nature, however, only one protein, a predictive mannosyl-glycoprotein *endo*-β-N-acetylglucosaminidase (E.C. 3.2.1.96), was assigned to a SEED category, namely “stress response”. Additionally, a protein of unknown function and a predictive GH53 *endo*-1,4-β-galactosidase (E.C. 3.2.1.89) were subjected for significantly increased release after incubation in sucrose-supplemented medium.

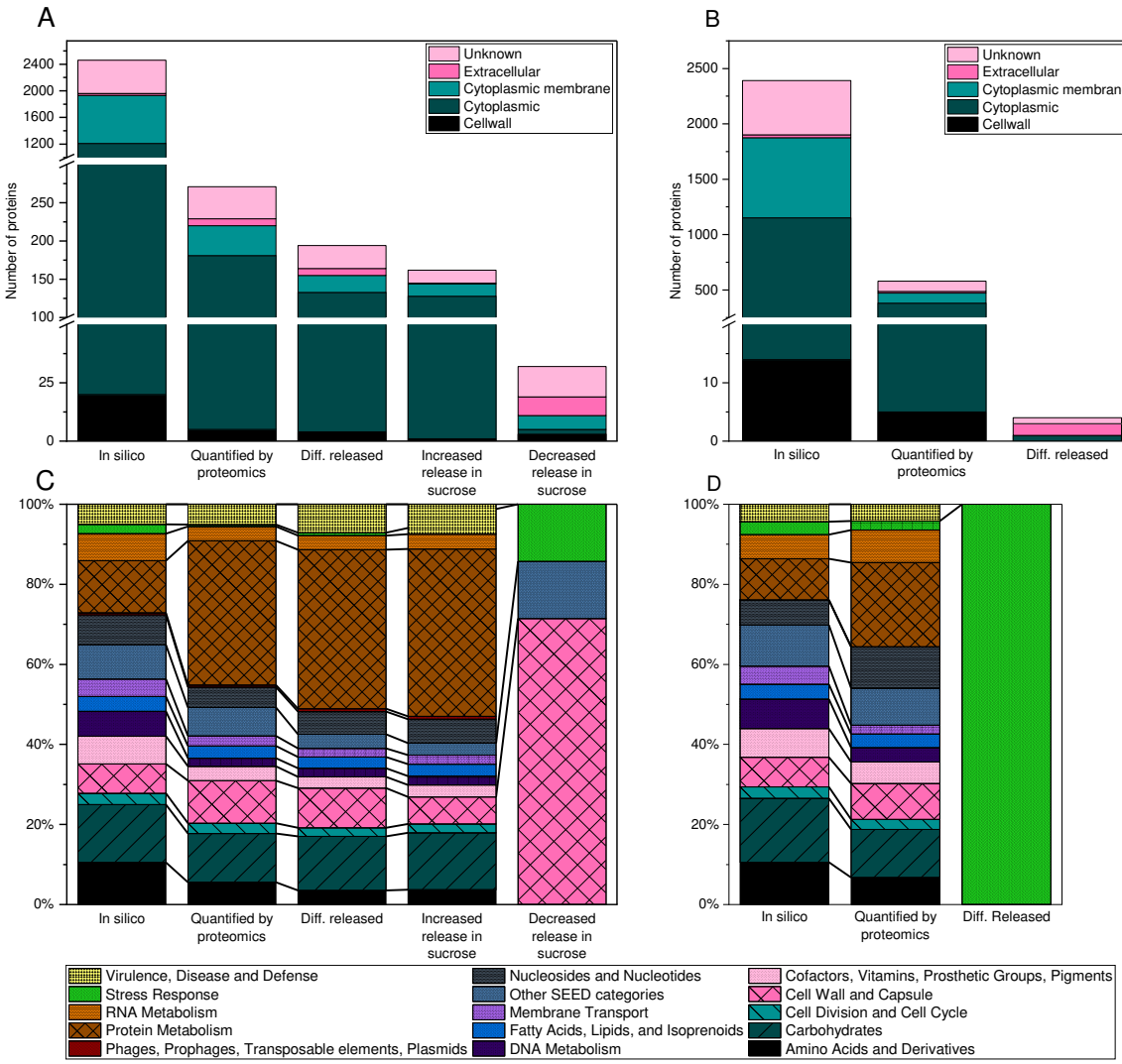

Figure 34 Comparison of the putative functional proteomes (in silico) with protein sub-groups obtained from MS intensity statistical analysis of exoproteomes of L. hordei TMW 1.1822 (A+C) and L. nagelii TMW 1.1827 (B+D). (A+B) Total protein counts of in silico predicted proteins, proteins quantified by proteomics (detected in four out of five replicates of at least one group), differentially expressed proteins and up- and down-regulated proteins in sucrose. Additionally, predicted subcellular localization of the respective proteins is shown. (**C+D**) Corresponding SEED category distributions. The SEED category proteome coverage was ~ 44 % for *L. hordei* TMW 1.1822 and ~ 45 % for *L. nagelii* TMW 1.1827. For reasons of clarity, the categories "Dormany and Sporulation", "Metabolism of aromatic compounds", "Miscellaneous", "Motility and Chemotaxis", "Nitrogen metabolism", "Phosphorus metabolism", "Potassium metabolism", "Regulation and cell signalling", "Respiration" and "Sulfur metabolism" were summarized within "Other SEED categories".

By contrast, a total number of 194 proteins were significantly differentially released by *L. hordei* after incubation in sucrose-supplemented medium. The majority of these proteins (= 162) appeared to be of higher abundancy within the exoproteomes of sucrose-treated cells, while only 32 proteins were affected by a decreased release compared to glucose-treated cells. About 42 % of increasingly released proteins were assigned to the SEED category "protein metabolism", followed by the "carbohydrate metabolism" category (~ 14 %)(Figure 34C) .

Surprisingly, about 80 % of the proteins that were of increased abundancy after sucrose-treatment were predicted to be of intracellular nature (Figure 34A). As such, 27 ribosomal proteins, two lactate dehydrogenases, four elongation factors (G, Ts, Tu, IF-3) and the housekeeping proteins DnaK and GroL appeared to be increasingly released in the presence of sucrose. This led to a significant enrichment of proteins that were summarized under the GO term "translation" (GO: 0006412, $p = 0.0375$, Table 18) among proteins that were significantly more released after sucrose-treatment. Furthermore, the putative extracellular β-fructosidase of *L. hordei* appeared to be released in higher amounts than in glucose-treated cells, an observation that could also be made for the dextransucrase. However, MS intensities of the dextransucrase appeared to be much higher than of the putative extracellular β-fructosidase.

The majority of the proteins that were significantly less abundant in the exoproteomes of sucrose-treated cells compared to glucose-treated ones belonged to SEED category "cell wall and capsule", including two flagellum-associated murein hydrolases (FlgJ-domain containing proteins, belonging to GH73) and two putative peptidoglycan endopeptidases containing an NlpC/P60 domain. As only seven of the 32 significantly less released proteins were assigned to a SEED category, GO analysis revealed the enrichment of flagellar proteins (GO: 0001539, $p = 8.9 \times 10^{-7}$) among decreasingly released proteins in the presence of sucrose (Table 18).

All significantly differentially released proteins within exoproteomes of *L. hordei* TMW 1.1822 and *L. nagelii* TMW 1.1827 are listed in Appendix 21 and Appendix 22.

Table 18 Significantly (Fisher´s exact p-value < 0.05) enriched gene ontologies (GO)(GO = biological process) among differentially released proteins within exoproteomes of glucose- and sucrose-treated cells of *L. hordei* TMW 1.1822. ↑ = increased release in sucrose, ↓ = decreased release in sucrose.

Regulation	GO ID	GO Term	Terms annotated	Significant terms	p-value
↑	GO:0006412	translation	67	52	0.0375
↓	GO:0001539	cilium or flagellum-dependent cell motility	7	6	8.90×10^{-7}
↓	GO:0030436	asexual sporulation	5	5	2.20×10^{-6}
↓	GO:0007059	chromosome segregation	2	2	0.0067
↓	GO:0030261	chromosome condensation	2	2	0.0067

4.6.1.3 Comparison of proteomic states of cell lysates and exoproteomes

A quantitative correlation of the exoproteomes and the cellular proteomes was examined to identify proteins that were significantly more concentrated in the exoproteomes than in the cellular proteomes and thus most likely proteins that were actively secreted. At least some of the proteins identified within the exoproteomes of *L. hordei* TMW 1.1822 and *L. nagelii* TMW

1.1827 exhibited comparable MS intensities relative to the corresponding proteins within the cellular proteomes (Figure 35). However, the relative abundance of most of the proteins within the exoproteomes was significantly different from that within the cell lysates (*L. hordei* glucose ~ 63 %, sucrose ~ 66 %; *L. nagelii* glucose ~ 91 %, sucrose ~ 92 %). Due to the high amounts of these proteins, only proteins that were subjected for directed release with high confidence (z-score difference exoproteome minus lysate ≥ 2.0) will be discussed further. In exoproteomes of *L. hordei* TMW 1.1822, 19 of such proteins were detected after glucose-treatment, while 22 of these proteins were detected after sucrose-treatment. Apart from two proteins of sucrose-treated cells, all these proteins were also found to be differentially released in the presence of sucrose compared to glucose. By contrast, none of the differentially released proteins of *L. nagelii* was among proteins that were subjected for directed release with high confidence. In exoproteomes of *L. nagelii*, six proteins were found after glucose-treatment und five proteins were found after sucrose-treatment that could be assigned to this category.

Regarding this group of released proteins, most of the proteins that were identified in the exoproteomes of *L. hordei* were flagellum-related in both conditions, which also applied for the NlpC/P60 domain-containing proteins. A similar, but less distinct result was obtained from the exoproteomes of *L. nagelii*. Additionally, the putative β-fructosidase and dextransucrase of *L. hordei* appeared to be subjected for directed release with high confidence in sucrose-treated cells. The *L. nagelii* dextransucrase was, however, predicted to be of significantly higher abundance within the exoproteomes of sucrose-treated cells than within the cellular proteomes, but with a z-score difference below 2.0.

A

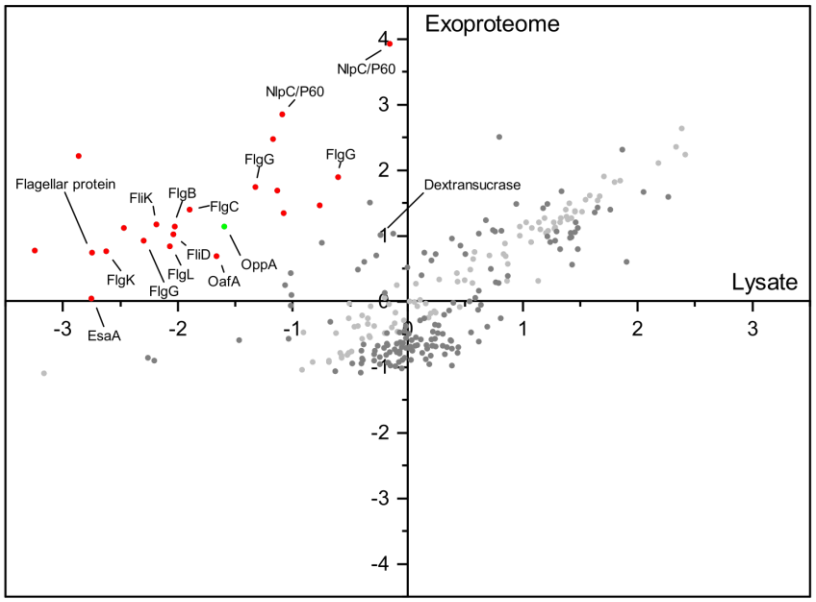
Exoproteome
Lysate
NlpC/P60
NlpC/P60
FlgG
FlgG
Flagellar protein
FliK
FlgB
FlgC
Dextransucrase
FliD
OppA
FlgK
FlgL
FlgG
OafA
EsaA

B

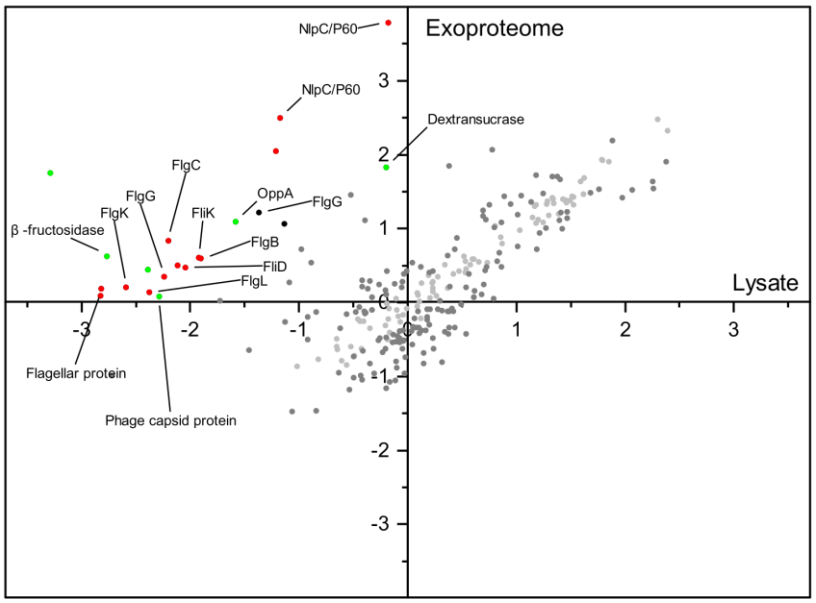
Exoproteome
Lysate
NlpC/P60
NlpC/P60
Dextransucrase
FlgC
FlgG
OppA
FlgG
FlgK
FliK
β -fructosidase
FlgB
FliD
FlgL
Flagellar protein
Phage capsid protein

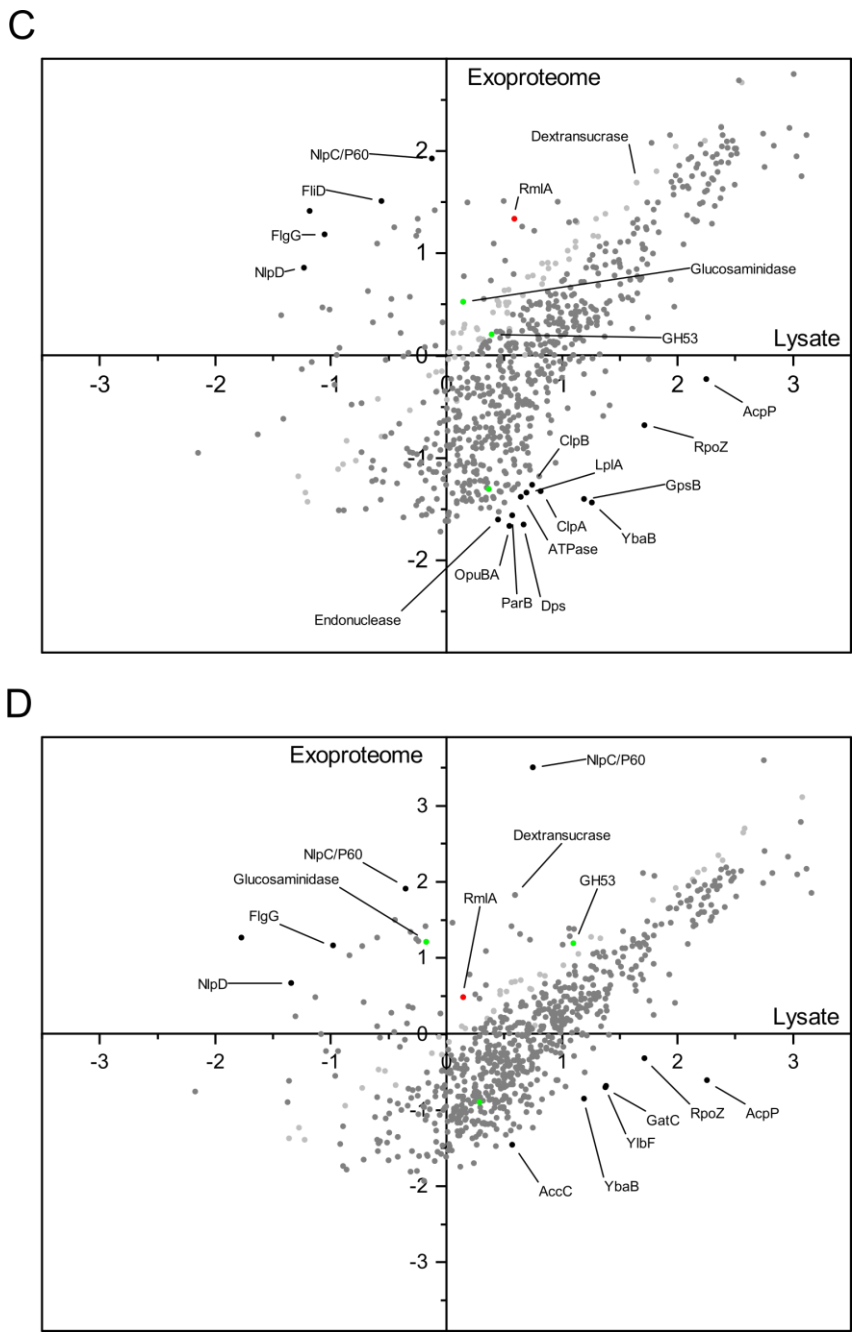

Figure 35 Comparison of abundances of proteins identified in cellular and extracellular proteomes in cultures of *L. hordei* TMW 1.1822 (A+B) and *L. nagelii* TMW 1.1827 (C+D) incubated in glucose (A+C) and sucrose (B+D). All log10-transformed iBAQ intensities were normalized by z-scoring. Light grey = proteins with similar relative abundance in cellular and extracellular proteomes; dark grey = proteins of significantly different relative abundancy (FDR ≤ 0.01, S0=0.1); black = proteins subjected for directed release with high confidence (z-score difference exoproteome−cellular proteome ≥ 2.0); red = proteins decreasingly released in the presence of sucrose; green = proteins increasingly released in the presence of sucrose. In *L. hordei*, all red and green coloured points overlay black points, while in *L. nagelii* none of the black points was differentially released. AccC = Acetyl-CoA carboxylase, AcpP = acyl-carrier protein, ClpA = ATP-dependent protease ATP-binding, ClpB = ATP-dependent chaperone, Dps = stationary phase protection protein, EsaA = type VII secretion protein, FlgB, FlgC, FlgG, FlgK, FliD, FliK = flagellar proteins, GatC = aspartyl/glutamyl-tRNA amidotransferase subunit C, GpsB = cell division protein, LplA = lipoate-protein ligase, NlpC/P60 = NlpC/P60 domain containing protein, NlpD = peptidoglycan endopeptidase activator protein, OafA = acetyltransferase, oppA = peptide ABC transporter substrate-binding, OpuBA = glycine/betaine ABC-transporter ATP-binding, ParB = chromosome partitioning protein, RmlA = glucose-1-P thymidylyltransferase, RpoZ = RNA-polymerase subunit ω, YbaB = DNA-binding protein.

4.6.2 SDS-PAGE and zymogram analysis of the exoproteomes

As exoproteome analysis revealed that most proteins identified within the supernatants of cultures of *L. hordei* TMW 1.1822 and *L. nagelii* TMW 1.1827 were annotated as cytoplasmic proteins, exoproteomic samples were subjected for SDS-PAGE and subsequent silver-staining of the gels. As shown in Figure 36A, the protein bands appeared well separated, while protein band patters were highly similar for both conditions. Moreover, proteomic analysis revealed the presence and regulation of several proteins that may putatively act as cell wall hydrolases, e.g. GH25 muramidase and FlgJ or NlpC/P60 domain-containing proteins in *L. hordei* TMW 1.1822 and NlpC/P60 domain-containing proteins and a putative glucosaminidase in *L. nagelii* TMW 1.1827. Therefore, exoproteomic samples were additionally subjected for SDS-PAGE on gels containing bacterial substrate (*M. luteus* TMW 2.96) and subsequent zymogram analysis. The stained gels showed one hydrolytic zone at ~ 110 kDa for supernatants of *L. hordei* that were treated with sucrose. However, it was not possible to assign a protein of the quantified exoproteome to this size. By contrast, supernatants of *L. nagelii* led to an identical band pattern for both conditions, showing two lytic zones between 130 – 250 kDa and one zone at ~ 70 kDa. The theoretical molecular weight of three different proteins within the exoproteomes of *L. nagelii* TMW 1.1827 that exhibit putative lytic activity fitted to the size of this lower band. Two of these proteins were found within one orthogroup and featured a GH25 muramidase domain (BSQ50_08465 and BSQ50_11560). An ortholog of the genes coding for these proteins appeared to be present in *L. hordei* TMW 1.1822 as well, which was significantly up-regulated in cellular proteomes of sucrose-treated cells (see section 4.6.1.1). Within the range of 130 – 250 kDa, only five proteins were quantified at all in exoproteomes of *L. nagelii*, while none of these proteins predictively exhibited a lytic function.

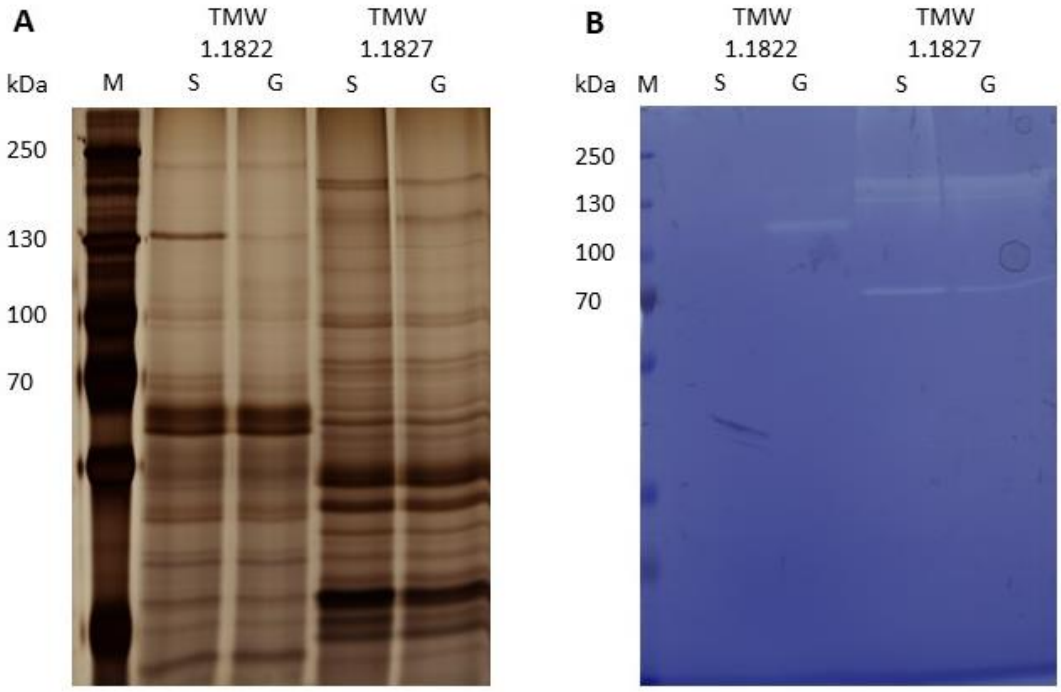

Figure 36 SDS-PAGE analysis of supernatants of *L. hordei* TMW 1.1822 and *L. nagelii* TMW 1.1827 incubated in either glucose (G) or sucrose (S) and subsequent silver staining (A) and zymogram analysis for the detection of lytic enzymes on gels containing dead cells of *M. luteus* TMW 2.96 (B).

4.6.3 Sugar consumption and acid formation of cells grown in either glucose or sucrose

The supernatants (= exoproteome samples) were subjected for HPLC analysis to investigate changes in metabolite formation due to sucrose treatment versus glucose treatment, as well as to follow sugar consumption. Within 2 h of incubation in glucose-supplemented medium, *L. hordei* consumed about 27 % of the available sugar, while *L. nagelii* consumed only ~ 21 % of glucose (Figure 37). However, within 2 h of incubation in sucrose-supplemented medium, *L. nagelii* degraded almost the entire sucrose (~ 97 %), while *L. hordei* degraded only ~ 77 % of sucrose. Simultaneously, *L. nagelii* formed more fructose (39.59 ± 1.73 mmol/L) than *L. hordei* (34.06 ± 0.78 mmol/L) upon sucrose degradation.

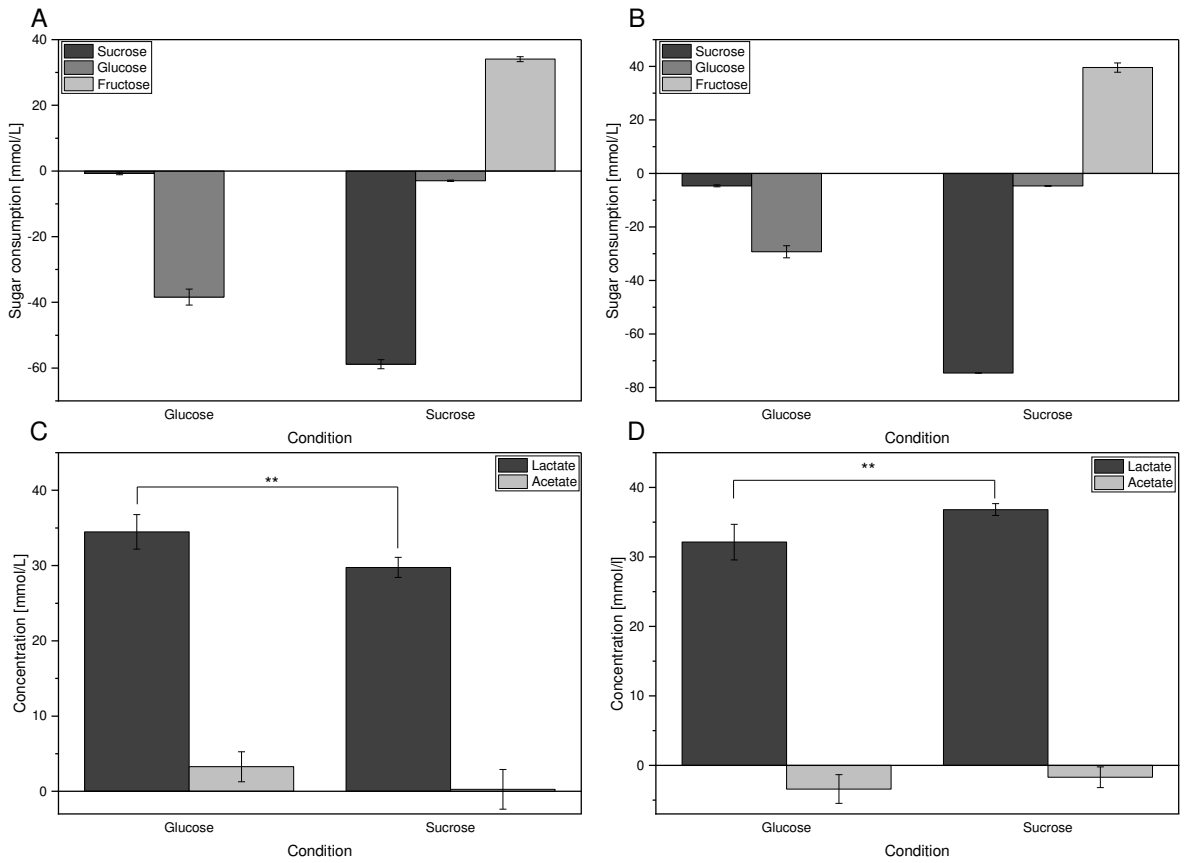

Figure 37 Sugar consumption (A+B) and acid formation (C+D) of L. hordei TMW 1.1822 (A+C) and L. nagelii TMW 1.1827 (B+D) within 2 h of incubation in glucose- or sucrose-supplemented medium. ** = $p \leq$ 0.01.

Moreover, *L. hordei* formed significantly more lactate upon glucose-treatment (34.47 ± 2.28 mmol/L) than within sucrose-supplemented medium (29.75 ± 1.33 mmol/L). Also, acetate was produced in higher amounts (3.27 ± 2.00 mmol/L) than in the presence of sucrose (0.27 ± 2.64 mmol/L), however, the difference appeared to be not statistically significant. By contrast, *L. nagelii* formed significantly more lactate in the presence of sucrose than in glucose-supplemented cultures (36.81 ± 0.85 and 32.13 ± 2.56 mmol/L). The amount of acetate appeared to be lower after 2 h of incubation than it was within the un-inoculated control samples. None of the two strains produced detectable amounts of ethanol or mannitol.

4.6.4 Growth characteristics in different sugars

In order to further investigate the behavior of *L. hordei* TMW 1.1822 and *L. nagelii* TMW 1.1827 in the presence of sucrose, their courses of growth, pH and redox-potential (ORP) were studied in media supplemented with either sucrose or glucose. Fructose and a mixture of glucose and fructose were additionally taken into account, as these sugars may emerge from

sucrose degradation upon extracellular dextransucrase or β-fructosidase activity. As shown in Figure 38, the growth of *L. hordei* did not appear to be influenced by the present carbon source. However, grofit analysis reported small, yet statistically significant differences in the lag-phases and maximum growth rates μ_{max} of this microorganism in different sugars. Thereby, the lag-phase appeared to be significantly prolonged in glucose compared to fructose and the mixture of both carbohydrates, while μ_{max} was significantly higher in fructose-supplemented cultures than in media with sucrose or a mixture of glucose and fructose. Also, acidification happened slightly faster in fructose and glucose than in sucrose or a mixture of glucose and fructose, however, final pH was comparable for all cultures (glucose 3.81 ± 0.01; fructose 3.72 ± 0.03; glucose + fructose 3.83 ± 0.02; sucrose 3.83 ± 0.00). The ORP of all cultures of *L. hordei* TMW 1.1822 decreased almost to 0 mV within ~ 20 h of incubation. Subsequently, the ORPs increased, while the smallest increase was detected for the sucrose-supplemented cultures. It was not possible to obtain growth curves of *L. nagelii* TMW 1.1827 using a plate-reader, as this device could not analyze the high OD_{590nm} that were detected for this strain. The growth behavior was thus recorded by manual OD_{590nm} measurements. However, the grofit package was not capable of analyzing the curves obtained by this method. Altogether, growth of *L. nagelii* appeared to be slower than of *L. hordei*, exhibiting longer lag-phases of almost 10 h, while entering stationary phase at ~ 25 h. By contrast, *L. hordei* reached its highest OD_{590nm} already after ~ 11 h of incubation in all cultures.

Growth of *L. nagelii* appeared to start slower in fructose- and glucose-supplemented cultures than in media with sucrose or a mixture of fructose and glucose. Nonetheless, glucose-supplemented cultures reached a comparable maximum OD_{590nm} as cultures with a mixture of glucose and fructose that exhibited the highest maximum OD_{590nm} after 25 h of incubation. Simultaneously, acidification of the culture broth happened slower in glucose- and fructose-supplemented cultures, reaching a state of constant pH after about 20 h of incubation. While cultures with a mixture of glucose and fructose entered this phase at ~ 21 h, sucrose-supplemented cultures showed no more considerable changes in pH after only 15 h. The final pH of sucrose-supplemented cultures was, however, higher than for the other cultures (glucose 3.70 ± 0.01; fructose 3.74 ± 0.02; glucose + fructose 3.72 ± 0.04; sucrose 3.84 ± 0.00). Furthermore, the ORP of cultures of *L. nagelii* decreased to about - 30 to - 50 mV within ~ 15 h of incubation before increasing again. However, the final ORPs of all cultures were lower than those of *L. hordei*, while the ORP of sucrose-supplemented cultures of *L. nagelii* stayed negative constantly.

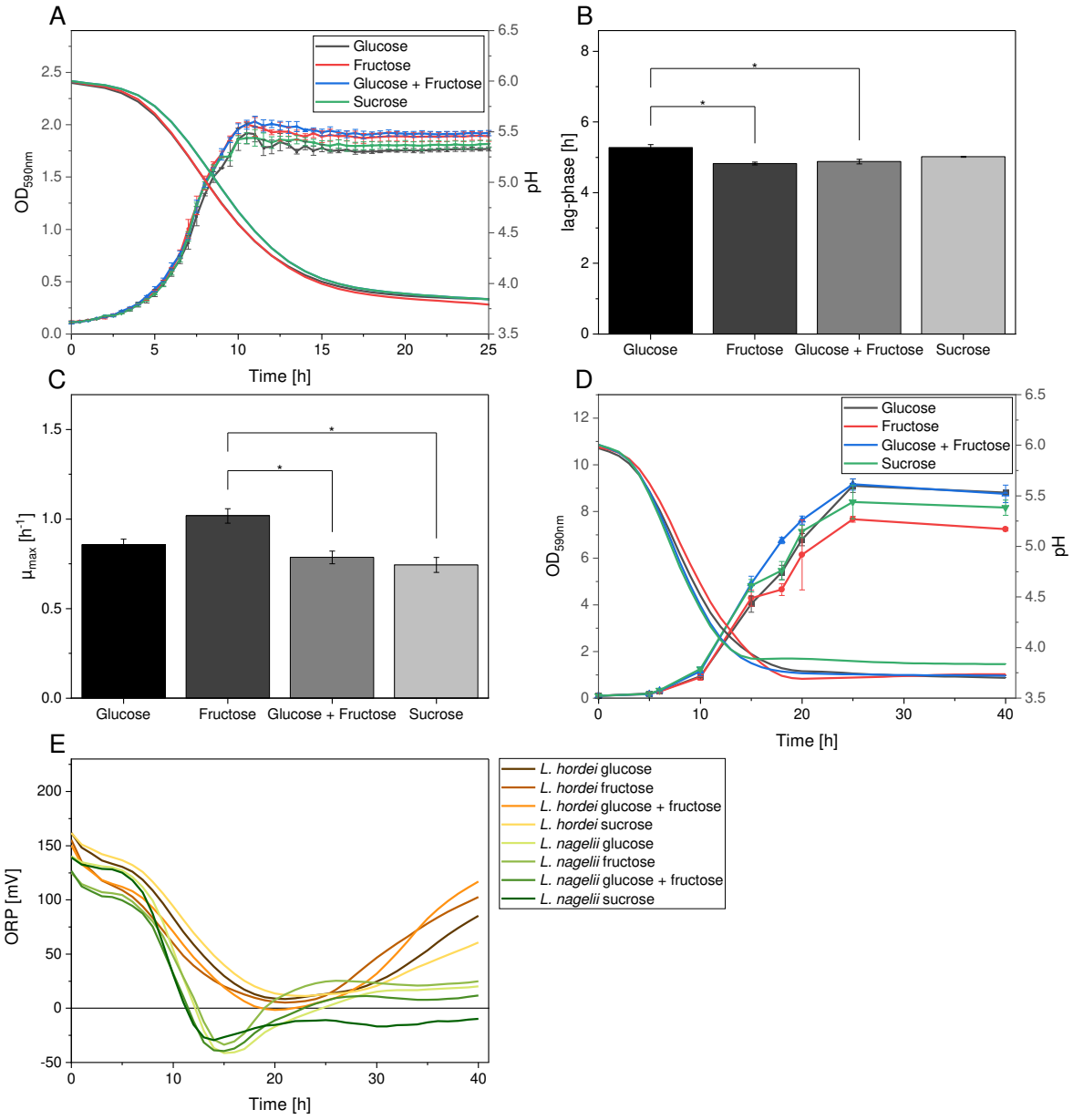

Figure 38 Growth characteristics of *L. hordei* TMW 1.1822 (A-C; E) and *L. nagelii* TMW 1.1827 (D + E) in different sugars. Panels A and D show growth curves obtained by OD measurements (lines with data points) and pH curves (continuous lines). Lag-phases (B) and maximum growth rates (C) of *L. hordei* in different cultures were calculated in R using grofit (Kahm *et al.*, 2010). Panel E depicts the ORP during microbial growth in different sugars.

Moreover, viable cells were counted within the cultures used for proteomic analysis. *L. hordei* exhibited comparable cell counts after incubation in glucose or sucrose for 2 h (glucose 8.3 ± 0.5 × 10^9 cfu/mL; sucrose 8.5 ± 0.8 × 10^9 cfu/mL) that appeared to be statistically not different ($p < 0.05$). By contrast, *L. nagelii* exhibited a significantly higher cell growth ($p = 0.005$) in sucrose-supplemented medium (glucose 5.7 ± 0.6 × 10^9 cfu/mL; sucrose 1.0 ± 0.2 × 10^{10}

cfu/mL), leading to higher cell counts than obtained by *L. hordei* in both conditions. Contrary, cell counts obtained in the presence of glucose were lower than of *L. hordei*.

5 Discussion

Despite their close phylogenetic relationship and common occurrence in water kefir *L. hordei* and *L. nagelii* express different relations to this habitat, which reside in their different functionalities, regulation and release of dextransucrases, their roles in biofilm formation and capabilities to colonize plant-derived habitats.

To weight these different relations to the water kefir habitat, the following theses can be derived from this work, which delineate the different roles and lifestyles of *L. hordei* and *L. nagelii* in water kefir:

***L. hordei* and *L. nagelii* isolates from water kefir harbour novel glucansucrases which deliver dextrans of the same dextran-type, but with different molecular and macromolecular architectures.**

- Sucrose is not only substrate but regulates dextransucrase expression or release in *L. nagelii* or *L. hordei*, respectively.
- Enzymatic activity of dextransucrases and amount of isolable dextran are predominantly dependent on the enzyme concentration.
- The processivity of these enzymes is mostly determined by the constitution of domain V, including the C-terminal glucan-binding domain, which is present only in *L. nagelii.*
- The highly efficient *L. nagelii* dextransucrase pre-synthesizes leucrose at the beginning of the reaction and may use it for dextran elongation after sucrose depletion.

***L. hordei* water kefir isolates appear as autochthonous to water kefir, while *L. nagelii* is an allochthonous contaminant expressing the ability to degrade plant-derived polysaccharides, and they persist due to their effective conversion of sucrose.**

- Water kefir-specific genomic traits include dextran formation and, predictively, catabolism of Amadori compounds like fructoselysine.
- Adaptation to the water kefir environment is predominantly found within carbohydrate metabolism related genes and each species developed its own adaptation strategy.
- *L. hordei* water kefir isolates were revealed as fructophilic water kefir specialists promoting proteinaceous biofilm formation above dextran biosynthesis, while *L. nagelii* appears prepared to colonize plant-derived habitats in general.

5.1 Identification and characterization of glucansucrases in LAB isolated from water kefir

5.1.1 Genome analysis of glucan-forming LAB reveals new types of GH70 enzymes

In a first step, LAB that were isolated from water kefir in previous studies (Gulitz *et al.*, 2011; Waldherr *et al.*, 2010), as well as some new water kefir isolates of the species *L. hordei* were re-evaluated for their EPS-forming capabilities on solid media containing sucrose. Additionally, the typestrains of *L. hilgardii, L. nagelii* (both isolated from wine (Douglas *et al.*, 1936; Edwards *et al.*, 2000)) and *L. hordei* (isolated from fermented barley (Rouse *et al.*, 2008) were analyzed. Except for *L. hilgardii* TMW 1.1819 and *L. nagelii* TMW 1.1825, all strains isolated from water kefir could produce EPS, which is in accordance with other studies (Côté *et al.*, 2013; Gulitz *et al.*, 2011). The fact that *L. hilgardii* TMW 1.1819 developed no mucous phenotype on sucrose-supplemented agar plates was unexpected, as this strain was described as strong EPS-producer in other studies (Eckel, 2020; Stadie, 2013). This finding will be discussed more detailed in section 5.2.1. Apart from strain *Lc. mesenteroides* TMW 2.1075, that produced a fructan, all strains synthesized a glucan-type EPS and were thus considered for further analysis. None of the typestrains produced detectable amounts of EPS on agar plates. Both, *L. hilgardii* and *L. hordei* did not produce EPS according to the original species descriptions of both species, indicating that this trait is only found in water kefir derived strains (Douglas *et al.*, 1936; Rouse *et al.*, 2008). By contrast, the *L. nagelii* typestrain was originally described to produce a dextran-type EPS from sucrose (Edwards *et al.*, 2000). This finding will be discussed more detailed in section 5.2.1.

Subsequently, strains of the species *Lc. citreum, Lc. mesenteroides, L. hilgardii, L. hordei, L. nagelii* and *L. satsumensis* were selected for whole genome sequencing. Within the WGSs of all strains isolated from water kefir, at least one glucansucrase gene could be identified, indicating that glucan-formation of these strains is linked to the expression of these genes. As described for other strains of the genus *Leuconostoc*, the water kefir isolates encoded several different glucansucrases (Amari *et al.*, 2015; Bounaix *et al.*, 2010a; Passerini *et al.*, 2015). Thereby, *Lc. mesenteroides* TMW 2.1073 and TMW 2.1195 featured two glucansucrase genes, while *Lc. citreum* TMW 2.1194 exhibited four different glucansucrases. Moreover, dsr2135 of *Lc. citreum* TMW 2.1194 comprised two GH70 catalytic domains, a property that is characteristic for the large branching sucrase found in several *Leuconostoc* strains (Bozonnet *et al.*, 2002; Passerini *et al.*, 2015). Strains of the genus *Leuconostoc* are commonly isolated from highly diverse environments, such as packaged meat, dairy products and raw or processed plant materials (Back, 1981; Juffs *et al.*, 1975; Korkeala *et al.*, 1988; Mundt *et al.*, 1967).

Nonetheless, they were firstly described as being responsible for the spoilage of sugar cane, as they are able to grow and form EPS in this sucrose-rich environment (Tilbury, 1975; Van Tiegham, 1878). The expression of several different glucansucrases may thus reflect their general adaptation to habitats rich in sucrose, as it is the case for water kefir.

With *L. satsumensis* TMW 1.1829, a fourth strain could be identified encoding four different glucansucrase genes. Côté *et al.* (2013) investigated the glucan-forming capabilities of several *L. satsumensis* strains from water kefir and could show that different types of α-glucans were produced at once that were identified as dextrans. Considering that glucansucrases are known to be only capable of synthesizing one type of glycosidic linkage in addition to the one found in the polysaccharide backbone, more than one glucansucrase must have been responsible for this result (Leemhuis *et al.*, 2013b). The findings from the genomic investigation of *L. satsumensis* TMW 1.1829 may thus provide an explanation for the results achieved by Côté *et al.* (2013). By contrast, *L. hilgardii* TMW 1.2196 and TMW 1.828, *L. hordei* TMW 1.1907 and TMW 1.1822, as well as *L. nagelii* TMW 1.1823 and TMW 1.1827 featured only one glucansucrase gene.

Amino acid sequence analysis of the identified glucansucrases revealed a high diversity regarding domain architecture (Figure 5). Apart from dsr2135 of *Lc. citreum* TMW 2.1194, all glucansucrases featured only one characteristic GH70 catalytic domain. Moreover, at least one glucan-binding domain could be identified in the C-terminal region of all glucansucrases except for dsr7775 and dsr11535 of both *L. hordei* strains and dsr8475 of *L. satsumensis* TMW1.1829 lacking this region. However, these glucansucrases exhibited a glucan-binding domain within their N-terminal variable regions, as it was also the case for other glucansucrases, e.g. those of *L. nagelii* TMW 1.1823 and TMW 1.1827. None of the identified glucansucrases was predicted to have a LPxTG cell wall anchor, indicating their free secretion into the environment. However, it has been proposed that glucan-binding domains may mediate non-covalent attachment of the glucansucrases to the cell surface (Olvera *et al.*, 2007). Analysis of the N-terminal region furthermore revealed the presence of a KxYKxGKxW-type signal peptide in some of the identified glucansucrases. So far, this peptide has not been studied in detail, but is described as a novel form of signal motif occurring in Gram-positive bacteria that facilitates secretion by an accessory Sec-system rather than by the canonical Sec-system (Bensing *et al.*, 2014).

However, not all of the identified glucansucrases appeared to have a signal peptide, including those of both *L. hordei* strains, which has already been reported for other glucansucrases, such as dextransucrase dsrA from *Lc. mesenteroides* NRRL B-1299 (Monchois *et al.*, 1996).

Therefore, release of these glucansucrases into the extracellular environment may follow a non-classical secretory pathway different from glucansucrases carrying a signal peptide.

The identified glucansucrases were compared to already described glucansucrases to find potentially novel enzymes (Figure 6). Due to the variable domain architecture, reasonable alignments may only arise from sequence comparisons of the GH70 catalytic domains that were shown to determine product specificity regarding linkage type (Leemhuis *et al.*, 2012). Apart from dsr10980 encoded by *Lc. mesenteroides* TMW 2.1073 that appeared to be different from currently known glucansucrases, all enzymes identified within the genomes of *Leuconostoc* strains exhibited high similarity with already known glucansucrases within this genus. Among strains of the *Lactobacillaceae* family, amino acid sequences appeared to be highly similar within one species, indicating that these enzymes may have co-evolved with the respective species. Both *L. hilgardii* glucansucrases clustered together with the one from *Lentilactobacillus parabuchneri*, a close relative of the species *L. hilgardii* (Zheng *et al.*, 2020). However, if this glucansucrase either co-evolved together with both species or was acquired independently from each other remains speculative. The glucansucrases of *L. satsumensis, L. hordei* and *L. nagelii* were shown to be only distantly related to yet known GH70 enzymes and were thus considered potentially novel types of glucansucrases. While dsr4425 and dsr12020 of *L. satsumensis* TMW 1.1829 exhibited some similarity with the glucansucrases of the *L. hilgardii* strains, dsr8475 clustered together with both *L. hordei* glucansucrases. Dsr0880 of *L. satsumensis* was shown to be more distantly related to the glucansucrases of *L. hordei* and *L. nagelii*. Although *L. hilgardii* was proposed to be the polysaccharide-producer during granule formation (Pidoux, 1989), the presented results hint at a similar role of the *L. satsumensis* glucansucrases that appeared to be closely related to the *L. hilgardii* glucansucrase. In contrast to the species *L. hilgardii, L. hordei* (and in this study also *L. nagelii*), glucan-formation in *L. satsumensis* was not restricted to the strains isolated from water kefir. *L. satsumensis* has been isolated from various beverage fermentations, such as water kefir, shochu, a traditional Japanese beverage made from rice, barley, sweet potato or brown sugar, and boza, made from maize, wheat or millet. All of these substrates are rich in carbohydrates, where sucrose concentrations were reported to be higher than 5 %. It is thus not surprising that the *L. satsumensis* strains isolated so far are equipped with GH70 enzymes to survive in such environments (Angelescu *et al.*, 2019; Côté *et al.*, 2013; Endo *et al.*, 2005; Zorba *et al.*, 2003). The identified glucansucrases of *L. hordei* and *L. nagelii* were found in a separate sub-cluster among already characterized GH70 enzymes. Therefore, both enzymes were considerably new types of glucansucrases, while being closely related to each other. Both species were shown to

fermentatively produce a dextran-type α-glucan (Xu *et al.*, 2018), which was confirmed with the isolated enzymes during this study. The dextransucrases of these two species were subsequently characterized in more detail.

Altogether, the glucansucrases identified within LAB from water kefir showed a high diversity. The shaping of this two-phase beverage by glucan formation is hence independent on one specific dextransucrase but more likely a process involving several different such enzymes. Moreover, the presence of different types of glucans (Fels *et al.*, 2018) is therefore attributable to the diversity of dextransucrases found among the water kefir strains, while a cooperative synthesis of polysaccharides by different sucrases cannot be excluded, as all glucansucrases are predictively extracellular.

5.1.2 Sucrose induces release of dextransucrase differentially in *L. hordei* TMW 1.1822 and *L. nagelii* TMW 1.1827

As the dextransucrases of neither *L. hordei* TMW 1.1822 nor *L. nagelii* TMW 1.1827 were found to have a cell wall anchor, both dextransucrases were predicted to be freely released into the extracellular environment. Therefore, dextransucrases of both microorganisms were yielded in a buffered cell suspension and supernatants were subsequently applied for SDS-PAGE (Figure 8). The protein bands identified by activity staining matched the predicted molecular weights of both dextransucrases and therefore the range of other known GH70 enzymes (Meng *et al.*, 2016). This staining could furthermore show that both enzymes were functionally expressed and released into the supernatant. The *L. nagelii* dextransucrases was detectable in supernatants independently of supplemented sucrose, whereas the *L. hordei* dextransucrases was only released in the presence of sucrose. Noticeably, *L. hordei* accumulates its dextransucrases intracellularly and releases it only if sucrose is present in the extracellular environment (Figure 9). This may result from different mechanisms in secretion or recognition as extracellular proteins, which are implied by the absence and presence of predictable signal peptides in both enzymes.

Surprisingly, the activity staining of the *L. nagelii* supernatant led to the visualization of several protein bands despite coding for only one dextransucrase. Using the SignalP 4.1 tool, a putative N-terminal cleavage site could be identified cutting the signal peptide after efficient translocation. However, as the distance between both proteins seems to be > 3 kDa, which is the predicted molecular weight difference between the N-terminally cleaved and the non-cleaved protein, it is unlikely that the protein band pattern is a result of post-translocational cleavage. This was furthermore corroborated by the results obtained from the SDS-PAGE

analysis of the *L. hilgardii* TMW 1.828 glucansucrase, which features the same type of signal peptide, but only led to one activity-stained protein band (Figure 9). Comparison of the amino acid sequences of *L. nagelii* and *L. hilgardii* revealed the presence of serine- and threonine-rich repeats within the N-terminal region of *L. nagelii* (Appendix 2) that were absent in *L. hilgardii*. These serine-rich repeats have also been described for other proteins exhibiting the KxYKxGKxW-type signal peptide, while serine- and threonine-rich repeats are frequently associated with heavily glycosylated proteins (Bensing *et al.*, 2014; Gagic *et al.*, 2013). Therefore, the supernatants of *L. nagelii* obtained in the absence of sucrose were subjected for another SDS-PAGE analysis following glycoprotein staining (Figure 9). The staining appeared to be positive for both bands of the *L. nagelii* dextransucrases, suggesting that this specific band pattern is a result of different degrees of glycosylation. Glycosylation of the dextransucrases may also be a critical factor for α-glucan synthesis during water kefir fermentation. Yeasts are not only part of the autochthonus water kefir microbiota, but also known for the release of extracellular proteases (Gulitz *et al.*, 2011; Ogrydziak, 1993; Stadie *et al.*, 2013). Glycosylation may protect the dextransucrases from proteolytic digestion (Langsford *et al.*, 1987), enabling stable polysaccharide formation within the water kefir environment. Moreover, this post-translational modification could only be shown for the *L. nagelii* dextransucrases. However, the other dextransucrases cannot be precluded from being glycosylated as well, as a negative result from glycoprotein staining may also be a result of the low sensitivity of the assay (~ 1 mg/mL glycoprotein, according to the manufacturer).

Although different degrees of glycosylation may be a reasonable explanation of the obtained band pattern of the *L. nagelii* dextransucrases, later-on analysis of this enzyme being heterologously expressed in *E. coli* revealed an identical protein band pattern, but with additional bands that are most likely attributed to a higher concentration of dextransucrases applied to the gel (Figure 15). By contrast, a truncated variant of the enzyme lacking the C-terminal glucan-binding domain led to only one protein band at the size of the lower two main bands of the full-length protein. Although protein glycosylation has been described for some *E. coli* strains (Charbonneau *et al.*, 2007; Reidl *et al.*, 2009), it appears currently more likely that the protein band patterns are caused by different conformations of the enzyme. This is further supported by the fact that the suspectedly glycosylated serine- and threonine-rich repeat region is still intact in the truncated variant. Indeed, crystal structure analyses of *L. reuteri* GTF180-ΔN and *Lc. mesenteroides* NRRL B-1299 ΔN123-GBD-CD2 showed that glucansucrases may exist in different conformations. This was shown to be mediated by flexibility between domains IV and V, which leads to rotation of domain V and thus to a more compact structure of the

enzyme (Brison *et al.*, 2012; Pijning *et al.*, 2014). Thereby, it can be hypothesized that the C-terminal region of the *L. nagelii* dextransucrases enables the protein to fold into different conformations, leading to the characteristic pattern on SDS-gels.

5.1.3 Concentration and domain-architecture of *L. hordei* and *L. nagelii* dextransucrases mediate differences in activity and dextran structure

The dextransucrases of both, *L. hordei* TMW 1.1822 and *L. nagelii* TMW 1.1827, were obtained in buffered cell suspensions containing sucrose to induce release of the *L. hordei* glucansucrase. The pH optimum of both native extracellular dextransucrases was shown to be at pH ~ 5.0, while the temperature optimum was at 35 °C (Figure 10), being in the range of other GH70 enzymes (Côté *et al.*, 2012; Kim *et al.*, 2010; Rühmkorf *et al.*, 2013; Waldherr *et al.*, 2010). Furthermore, both enzymes exhibited a slight increase in activity at 70 °C. However, this may rather be an unspecific reaction, as enzymes of mesophilic bacteria are commonly sensitive to heat denaturation (Kristjánsson *et al.*, 1991; Ratkowsky *et al.*, 2005).

A similar result was obtained from the heterologously expressed variants of the *L. nagelii* dextransucrase, although the truncated variant dsr3510ΔC-term was active only over a narrow range of pH values and temperatures with optima at pH 4.5 and 30 °C (25 °C at pH 5.0)(Figure 16). It was furthermore necessary to incubate assays with this variant for a longer time, as overall enzyme activity was low. This indicates that the glucan-binding domain that eventually folds into domain V is necessary for a stable overall enzyme activity of the *L. nagelii* dextransucrases, including integrity of the enzyme over a broad range of conditions. Furthermore, it could be shown that the presence of Ca^{2+} had a beneficial effect on enzyme activity in both heterologously expressed variants, while copper ions effected enzyme activity adversely (Figure 17). A similar effect was observed for other glucansucrases (Kralj *et al.*, 2004; Rühmkorf *et al.*, 2013). The calcium ion is proposed to form or stabilize the acceptor binding site of the enzyme (Ito *et al.*, 2011). Ca^{2+} improved the enzyme activity more drastically in the truncated variant than the full-length enzyme, implying that the truncated variant profits more from a stabilizing effect of the metal ion. This is in accordance with the hypothesis inferred above, proposing that enzymatic activity of the truncated variant suffers from a reduced stability due to the lack of the C-terminal domain. Noticeably, the native enzymes of both, *L. hordei* TMW 1.1822 and *L. nagelii* TMW 1.1827, maintained their activity over a broad range of pH and temperatures despite the absence of external calcium. In order to chelate the metal ion during growth in culture broth and thus prior to export of the protein into the extracellular environment, the protein has to be folded at least partially within the cell. However, protein

translocation by (accessory) Sec-systems is known to occur in un-folded state (Bensing *et al.*, 2014), which is why it is more likely that insertion of a Ca^{2+} ion happens post-translocationally. Cell-wall associated lipoteichoic acids that are exclusively found in gram-positive bacteria are known to bind divalent cations (Lambert *et al.*, 1975) and may, therefore, contribute to the incorporation of calcium into the native dextransucrases after translocation.
Both native dextransucrases, as well as the heterologously expressed enzymes were shown to fit the model of Michaelis-Menten kinetics. The Michaelis constants of both, the native and heterologously expressed enzymes, appeared to be within the range of other glucansucrases (Brison *et al.*, 2012; Côté *et al.*, 2012; Kim *et al.*, 2010; Waldherr *et al.*, 2010). The v_{max} of all four enzymes was quite variable, however, as the specific concentration of the dextransucrases was not known, this may also be a result of different enzyme concentrations.

The native extracellular dextransucrase reactions of both, *L. hordei* TMW 1.1822 and *L. nagelii* TMW 1.1827, were monitored over 24 h and glucans obtained after 24 h were subsequently analysed (Figure 11). At equal reaction conditions, the native *L. nagelii* dextransucrases synthesized a higher amount of dextran after 24 h of production, which was due to its significantly higher volumetric total and transglycosylation activity in comparison to the dextransucrases released by *L. hordei.* Remarkably, the dextransucrases released by *L. nagelii* consumed the total sucrose within the first 10 min of incubation implying its high efficiency at the applied conditions. Since both dextransucrases were used as a crude protein extract, the amount of dextransucrase released into the buffer may have varied between *L. hordei* and *L. nagelii*. By tendency, the dextransucrase from *L. nagelii* was indeed released in higher amounts into the environment, as diverse staining approaches (Coomassie staining) empirically revealed more intense bands for this enzyme in comparison to the dextransucrase released by *L. hordei.* Therefore, both enzyme extracts were subsequently applied at varying dilutions (Figure 14). The dilution of the *L. hordei* dextransucrase led to a stepwise decrease in overall activity and transferase rate, while the amount of released glucose was decreasing less drastically. This ultimately led to a decreasing amount of predicted dextran, converging with the amount of effectively isolated dextran. Therefore, these results indicate that less enzyme produces less dextran, but with a higher processivity leading to a proportionately higher amount of high molecular weight dextran. Nonetheless, it is important to note that an extracellular enzyme with putative β-fructosidase activity was predicted from the genome of *L. hordei* TMW 1.1822 that was later-on shown to be significantly more released when cells were incubated in sucrose-supplemented medium. This enzyme may contribute to the hydrolysis of sucrose and thus to a

relatively smaller transferase rate compared to *L. nagelii* TMW 1.1827. However, it remains unclear if this enzyme is also expressed and released in buffered cell suspensions, while the overall lower activity towards sucrose is not explained by the presence of this enzyme.

By contrast, overall activity, transferase rates and isolated amounts of dextran of the *L. nagelii* dextransucrase only decreased, once the enzyme extract was 10-fold diluted. This indicated that less enzyme can form the same amount of dextran, but more slowly, which was furthermore supported by the result that v_{max} linearly decreased with increasing dilution of the *L. nagelii* enzyme extract (Figure 21). By contrast, K_M stayed constant for all dilutions, excluding the presence of any metabolic waste products within the supernatants of *L. nagelii*, which may otherwise explain this effect. However, the assumption of less enzyme forming the same amount of dextran more slowly only appeared to be true until a critical concentration of the *L. nagelii* dextransucrase. Once, this dilution is reached, the predicted amount of dextran converged with the effectively isolated amount of dextran, which was similar to observations made for the *L. hordei* enzyme extracts. Hence, the *L. nagelii* dextransucrase seems to be released in considerably higher amounts than the *L. hordei* sucrase, while a decreased loss of dextrans with DP < 20 during dialysis is concomitant with a higher processivity at lower enzyme concentrations of both dextransucrases.

Additionally, enzymes are also influenced by the pH, temperature, salt concentration and other factors, why both dextransucrases could have also exhibited different folding and concomitant stability at the applied conditions (Leemhuis *et al.*, 2013b; Prechtl *et al.*, 2018b; Rühmkorf *et al.*, 2013). While exhibiting a highly homologous catalytic domain, the dextransucrase released by *L. nagelii* is distinctly larger in size especially due to an additional C-terminal glucan-binding domain. This difference could result in altered foldings and different transglycosylation activities, as glucan-binding domains can influence the ratio between hydrolysis and transglycosylation in other glucansucrases (Kralj *et al.*, 2004; Lis *et al.*, 1995). A higher transglycosylation rate is, however, not necessarily correlated with the DP of the synthesized glucan and rather reflects the productivity of the enzyme. The obtained results suggest that the comparatively higher transglycosylation rate of the glucansucrase released by *L. nagelii* could be responsible for the synthesis of higher molecular weight dextran. Differences in polymer size may have been also influenced by differing enzyme concentrations, as already described for other glucansucrases (Falconer *et al.*, 2011). Although some variations in polymer size could be shown to reside in the applied amount of enzyme, the *L. nagelii* dextransucrase synthesized dextrans of comparably higher molecular weights and rms radii at all enzyme concentrations. This suggests an overall higher processivity of the *L. nagelii* dextransucrase most likely caused

by differences in domain V, which is altered by the presence or absence of a C-terminal glucan-binding domain and was recently shown to mediate processivity in GH70 enzymes (Claverie *et al.*, 2020).

Furthermore, the additional glucan-binding domain of the *L. nagelii* dextransucrase did not alter the basic dextran type, as a comparable structural composition was detected by methylation analysis and because identical oligosaccharide fragments were obtained after *endo*-dextranase digestion of both dextrans (Figure 12). Nonetheless, varying portions of enzymatically liberated oligosaccharides were detected, which indicates differences in the structural architecture of the polysaccharides, namely the side-chain length. This is characteristic for GH70 enzymes, as the linkage type was found to be determined by the conformation of the acceptor binding site, which resides within the catalytic core of the enzymes (Leemhuis *et al.*, 2012; Meng *et al.*, 2014). Furthermore, comparable results of molecular structural analysis were also shown from previous studies on dextrans, which were produced by fermentation with *L. nagelii* TMW 1.1827 and *L. hordei* TMW 1.1822, respectively (Xu *et al.*, 2018). The basic dextran types of both dextransucrases are thus not influenced by surrounding reaction conditions, as the fermentation process leads to continuous changes in reaction conditions. Due to the structural similarity regarding methylation analysis and enzymatic fingerprinting of the dextrans produced by *L. hordei* and *L. nagelii*, both dextrans may not be distinguishable, when directly isolated from a water kefir fermentation. Recently, the *L. hordei* dextran was shown to constitute a colloidal cloud-forming suspension in aqueous systems (Eckel *et al.*, 2019), while dextrans of *L. nagelii* may exhibit similar properties, as implied from experiments on this dextransucrase (Figure 22C). This is of high importance for the beverage industry, which seeks natural agents generating stable turbidity of beverages. Hence, it appears likely that both microorganisms contribute more to the formation of the naturally stable turbid aqueous phase rather than granule formation, however, it remains unknown if the environmental conditions during water kefir fermentation, e.g. low amounts of ethanol or presence of other enzymes, may affect the synthesis or constitution of the dextrans.

In order to elucidate the role of the C-terminal glucan-binding domain in the *L. nagelii* dextransucrase, which otherwise exhibits a similar domain architecture to the *L. hordei* dextransucrase, two variants of the *L. nagelii* dextransucrase were expressed in *E. coli*: the full-length enzyme and a C-terminally truncated variant of the enzyme (Figure 18). As it was not possible to purify the enzyme without complete loss of activity, possibly due to the harsh conditions applied during the purification process (e.g. high pH and salt concentration), the

enzyme variants were used in different concentrations. Thereby, it could be shown that the overall and transferase activities, as well as the isolated amount of dextran of the full-length enzyme stayed constant until a 4-fold dilution and decreased at a 10-fold dilution, similar to that of the native *L. nagelii* dextransucrase. By contrast, the overall and transferase activities, as well as the isolated amount of dextran continuously decreased with increasing dilution of the truncated variant, similar to the native *L. hordei* dextransucrase. However, the undiluted truncated variant exhibited a similar overall and transferase activity and produced even higher amounts of dextran as the full-length enzyme did until a 4-fold dilution. This clearly implies that overall and transferase activities are strongly influenced by the applied enzyme concentration rather than by the presence or absence of the C-terminal glucan-binding domain and thus lead to the synthesis of different amounts of dextran. Moreover, these results confirm the hypothesis that – until a critical enzyme concentration is reached – less enzyme can form comparable amounts of dextran, but more slowly. The results from AF4 measurements furthermore showed that the enzyme concentration only had a minor effect on the polymer size, while the full-length enzyme produced consistently larger molecules than the truncated enzyme. Therefore, it can be concluded that the higher processivity of the native *L. nagelii* dextransucrase resides in an altered domain V, which is due to the presence of an additional C-terminal glucan-binding domain. Nonetheless, larger polysaccharides can also be synthesized by higher concentrations of *L. hordei* dextransucrase and thus a higher transferase activity.

Furthermore, the additional glucan-binding domain and the potentially resulting differences in protein folding did not influence the molecular structural architecture of the synthesized dextran, as portions of different oligosaccharides liberated by *endo*-dextranase digestions were comparable for the full-length enzyme and the truncated variant. Simultaneously, these fine structures were not influenced by the applied enzyme concentration. Despite being not directly involved in substrate- or acceptor-binding, several more distantly located amino acid residues have been identified to influence the linkage pattern of synthesized dextrans (Funane *et al.*, 2005; Irague *et al.*, 2011). These residues may either be directly involved in shaping the active site or influence those residues by steric interactions (Kirby *et al.*, 2008). The *L. hordei* and *L. nagelii* dextransucrases were shown to be conserved with regards to the amino acid sequences involved in substrate and direct acceptor binding, however, only ~ 76 % of the amino acids within the catalytic domain were identical. Therefore, the reason for the differences in the molecular architecture of the dextrans synthesized by native dextransucrases of *L. hordei* and *L. nagelii* remains unclear.

5.1.4 Highly efficient native dextransucrase of *L. nagelii* TMW 1.1827 further elongates dextran after sucrose depletion

Previously, it was demonstrated that the dextransucrase of *L. nagelii* TMW 1.1827 can be released into a buffer system to obtain cell-free enzyme extracts. It was further shown that the *L. nagelii* dextransucrase is detectable in the extracellular environment irrespective of the presence of sucrose. However, it remained unknown whether more extracellular dextransucrase (activity) is present in the presence of sucrose. Furthermore, the pH decreased from pH 6.5 to 5.0 in buffers with sucrose during incubation of *L. nagelii* TMW 1.1827, while in cell suspensions without sucrose the initial pH was retained over 3 h of incubation, indicating the metabolic activity of *L. nagelii* in sucrose-supplemented buffers. Moreover, incubation in sucrose supplemented buffers led to an increase in viable cell counts, while staying constant in buffers without sucrose. As this may affect the totally released protein amounts, the release experiments in buffered cell suspensions were conducted at three different initial pH values, with and without the addition of sucrose, respectively (Figure 20). The total protein amount was low for all samples (max. about 220µg/mL), but it increased with increasing initial pH, which may *inter alia* result from physical effects between cell wall and proteins, e.g. coulomb repulsion, as more proteins become negatively charged with increasing pH (Zhou *et al.*, 2018). Concurrently, the protein amounts varied only slightly between release conditions with and without the addition of sucrose. This clearly implies that the possible cell growth and metabolic activity of *L. nagelii* in buffers with sucrose had no significant influence on the released overall protein amounts. Moreover, similar protein patterns were obtained under both test conditions indicating that the release of most of the proteins detected in the supernatants were not directly related to the presence of sucrose. Although the highest total protein amounts were measured at an initial pH of 6.5, the final dextran yields decreased slightly with increasing initial pH when sucrose was present in the cell suspensions, while averaged volumetric activities were comparable for all samples. As discussed above, different amounts of dextransucrase may be capable of producing the same amount of dextran, but more slowly, which is why enzyme concentrations released at different initial pH may not be estimated from this experiment. Nonetheless, higher amounts of enzyme may also lead to an extended formation of smaller oligosaccharides that are subsequently lost during dialysis and thus not isolated, as already shown by other studies (Falconer *et al.*, 2011; Kim *et al.*, 2003). Slight differences in enzyme concentration may thus explain the minimal increase in isolated dextran with decreasing initial pH. By contrast, the amounts of isolated dextran and volumetric activities slightly increased with increasing release pH at release conditions without sucrose. These differences in

volumetric dextransucrase activity were bigger at release conditions without sucrose and may be due to higher amounts of freely released dextransucrase with increasing initial pH. However, this effect may be masked at release in sucrose-supplemented buffers as sucrose apparently boosted release of dextransucrase (activity) into the extracellular milieu. Therefore, the initial pH of buffered cell suspensions only had a minor impact on the amount of dextransucrase release, as it was already shown for *L. hordei* (Schmid *et al.*, 2019). These findings thus indicate that dextransucrase release in the presence of sucrose is comparable to that of *L. hordei* TMW 1.1822, which accumulates its dextransucrase intracellularly and only releases it in the presence of sucrose. In contrast to *L. hordei*, *L. nagelii* released at least some dextransucrases into the extracellular milieu in the absence of sucrose. Therefore, some dextransucrases may be displayed on the cell surface and may more easily become solubilized and released with increasing extracellular pH. To investigate whether this was a result of different enzyme concentrations, the *L. nagelii* dextransucrase obtained in the presence of sucrose was applied at different concentrations as already discussed in section 5.1.3. Even a 10-fold dilution of the enzyme extract could not resemble the low yields from enzyme extracts obtained in the absence of sucrose. This suggests that the buffer supernatant contained only traces of free dextransucrase in the absence of sucrose. Apart from that, other studies controversially discussed the necessity of "primer" dextran for an efficient dextransucrase reaction (Germaine *et al.*, 1974; Kingston *et al.*, 2002; V. Monchois *et al.*, 1998; Monchois *et al.*, 1997; Monchois *et al.*, 1996). While this was already present after buffered cell suspension with sucrose, no "primer" dextran was synthesized in the absence of sucrose prior to starting the cell-free reaction and hence may have caused the large differences in volumetric activity and isolated dextran. Nonetheless, the high extracellular overall dextransucrase activity released in the presence of sucrose, which enables the conversion of 0.2 M sucrose within 10 min of incubation, may help *L. nagelii* to gradually colonize habitats being rich in this sugar, e.g. plants or fermented foods such as water kefir, once the sugar is detected. Like other members of the genus *Liquorilactobacillus*, e.g. *L. sucicola*, *L. hordei* or *L. mali*, extracellular glucan synthesis from sucrose appears to be a decisive trait to subsist in such environments (Carr *et al.*, 1970; Irisawa *et al.*, 2009; Zheng *et al.*, 2020). Moreover, glycosyltransferases have been shown not only to contribute to the carbohydrate metabolism and formation of extracellular polysaccharides in certain LAB like *L. reuteri* but may also be involved in auto-aggregation of the cells leading to the formation of floating biofilms (Schwab *et al.*, 2007; Walter *et al.*, 2008). The presence of extracellular dextransucrase in buffers without sucrose may thus hint at a similar role in *L. nagelii* that requires additional elucidation.

In order to gain further insights into the complex processes of native dextran formation of *L. nagelii* TMW 1.1827, an additional approach was applied. Dextransucrase containing supernatants were obtained at pH 6.5 in sucrose-supplemented buffers and extracellular dextran production was monitored over time (Figure 22). As discussed in section 5.1.3, the total amount of sucrose was already consumed within the first 10 min of incubation, while neither fructose release nor formation of isolable high molecular weight dextran were completed at this point of time. Hence, the fructose moiety of sucrose remained bound and non-detectable. As sucrose and fructose can act as acceptors during the early phase of the dextransucrase reaction, this reaction likely took place (Cheetham *et al.*, 1991; Moulis *et al.*, 2006). This type of transglycosylation was reported to be especially favoured at the start of the reaction, leading to the formation of higher amounts of disaccharides and short-chain oligosaccharides in a non-processive mode. Once, a critical chain length is reached, the reaction switches to a processive mechanism that is mediated by domain V, holding the growing polysaccharide chain (Claverie *et al.*, 2020; Moulis *et al.*, 2006; Tsuchiya *et al.*, 1953). Nonetheless, the difference between isolated dextran recovered after 10 min and 24 h of production, respectively, was ~ 8.4 g/L, which corresponds to ~ 51 mM glucose and may correspond to the still increasing amount of released fructose despite sucrose depletion. Besides other acceptors, the glucose moiety from sucrose may also be transferred onto fructose, leading to the formation of sucrose or sucrose isomers, such as leucrose or palatinose (Koepsell *et al.*, 1953; Moulis *et al.*, 2006; Robyt *et al.*, 1978) that appeared to be present at all timepoints during dextran formation. Notably, there was no detectable sucrose left after 10 min of incubation, while the decrease in leucrose concentrations was higher than the increase of glucose concentrations over time. This strongly suggests that leucrose serves as substrate for further dextran formation or elongation of IMOs in supernatants of *L. nagelii*. However, the use of leucrose as a substrate for dextran formation has not been reported so far, while information on enzymatic leucrose conversion is generally scarce. Although strongly suggested, it is thus not possible to exclude the presence of other extracellular enzymes than the dextransucrase acting on leucrose from WGS analysis. The fast conversion of sucrose to leucrose at the beginning of the water kefir fermentation may furthermore avoid sucrose degradation of other inhabiting microorganisms that cannot use leucrose. Additionally, the disaccharide is extremely resistant to acid hydrolysis (Bailey *et al.*, 1959) and may hence contribute to further dextran formation after pH decrease during fermentations with LAB. Moreover, Binder *et al.* (1983) postulated that glucansucrases from *Lc. mesenteroides* NRRL B-512F and *Streptococcus mutans* 6715 utilize isomaltotriose to form glucose and isomaltotetraose in the absence of sucrose, while this type of reaction occurred

more slowly than sucrose conversion. It is thus possible that a similar reaction took place during native extracellular dextran formation in *L. nagelii* TMW 1.1827. Nonetheless, the peak intensities of neither isomaltose nor isomaltotriose increased between 10 min and 24 h of incubation, which may contradict against this type of reaction occurring here. However, only few studies discussed disproportionation reactions of glucansucrases so far (Binder *et al.*, 1983; López-Munguía *et al.*, 1993) that were already studied in detail for other polymerizing enzymes such as levansucrases and inulosucrases (Ozimek *et al.*, 2006). Therefore, further studies are needed to investigate a possible utilization of short IMOs as glucosyl-donors during dextran synthesis in supernatants of *L. nagelii* TMW 1.1827. Furthermore, the structural analysis of the dextrans recovered at different production times indicated an increase in the degree of branching over time. As the maxima of distributions of rms radii were shifted to smaller radii with increasing production time, a comparatively higher portion of more branched and presumably more compact dextran molecules was increasingly formed. As a type of acceptor reaction during dextran synthesis, branching may also depend on the sterical properties of its glucosyl-donor within the active site of the enzyme. Both, leucrose and IMOs are sterically different to sucrose, while their role as substrates for further dextran synthesis in supernatants of *L. nagelii* TMW 1.1827 is strongly indicated from these results. However, as dextrans with higher rms radii were still present after 24 h of incubation, short IMOs that were possibly lost during dialysis after 10 min of incubation may rather act as acceptors for further dextran synthesis than high molecular weight dextrans.

5.1.5 Conclusions I: Shaping of the water kefir habitat by glucansucrases is functionally diverse

Several LAB isolated from water kefir were shown to produce glucans from sucrose, which was attributable to the presence and putative expression of one or more glucansucrase genes in these microorganisms. Bioinformatic analysis of these genes revealed a high interspecies and in the case of *Leuconostoc* strains also intraspecies diversity of these enzymes regarding amino acid sequence of the catalytic domain, as well as overall domain architecture. Therefore, water kefir borne LAB shape the two-phase beverage differently due to their diverse glucansucrase equipment. A comparison with already known GH70 enzymes furthermore confirmed the presence of novel types of glucansucrases within the water kefir microbiota. The two novel and closely related dextransucrases of *L. hordei* TMW 1.1822 and *L. nagelii* TMW 1.1827 were subsequently analysed in more detail. In the presence of sucrose, both microorganisms released their dextransucrase in high amounts, although the results indicate a distinctly higher amount

of freely released dextransucrase in supernatants of *L. nagelii* TMW 1.1827. However, in the absence of sucrose, only the *L. nagelii* dextransucrase could be identified in the extracellular environment, which is most likely due to different secretion (recognition) mechanisms, as the *L. hordei* dextransucrase featured no known type of signal motif. Nonetheless, even *L. nagelii* appeared to release comparatively low amounts of dextransucrase (activity) in the absence of sucrose.

The relatively low overall and transglycosylation activity of the *L. hordei* dextransucrase is most likely attributable to a lower concentration of released dextransucrase. While the applied enzyme concentration appeared to subsidiary influence the processivity and thus the amount of isolable dextran and polymer size, processivity was largely dependent on the properties of domain V, which is constituted of an additional C-terminal domain in the case of *L. nagelii* compared to *L. hordei*. Furthermore, the catalytic domains of their dextransucrases determine the produced dextran type, which is identical regarding methylation analysis and enzymatic fingerprinting. However, differences in the molecular architecture of these dextrans are most likely due to amino acid substitutions apart from substrate- and acceptor-binding sites within the GH70 catalytic domain.

Moreover, a detailed characterization of the native extracellular dextransucrase of *L. nagelii* revealed that the initial pH of buffered cell suspensions only had a minor impact on the amount of released dextransucrase (activity). The results furthermore highlight the high overall and transglycosylation activity found within the supernatants of *L. nagelii*. Herein, the hypothesized utilization of leucrose (and possibly also short IMOs) after sucrose depletion coincides with the formation of higher portions of more branched dextran molecules.

In conclusion, this study gives new molecular insights into how *L. hordei* and *L. nagelii* naturally produce dextrans and, thereby, contribute to water kefir formation.

5.2 Adaptation of *L. hilgardii*, *L. hordei* and *L. nagelii* to the water kefir environment

5.2.1 Manifestations of genetic adaptations are species-specific, while dextran formation and predictive catabolism of Amadori products are water kefir-specific traits

Bacterial genomes are constantly evolving structures, as gene content and genetic organization may result from strong evolutionary pressure towards optimal growth in their respective habitats (Casjens, 1998). Also LAB from fermented foods have been shown to underlie these processes, especially due to the fact that many microbial consortia are carried on to the next fermentation cycle by back-slopping, which may promote genetic drift (Kirchberger *et al.*,

2020; Teusink *et al.*, 2017). Strains of the species *L. hilgardii, L. hordei* and *L. nagelii* are stable parts of the water kefir microbiota (Gulitz *et al.*, 2013; Gulitz *et al.*, 2011; Laureys *et al.*, 2014; Pidoux, 1989; Verce *et al.*, 2019). However, all three species have also been isolated from different sources. *L. hilgardii* and *L. nagelii* were originally isolated from wine (Douglas *et al.*, 1936; Edwards *et al.*, 2000), which generally resembles the water kefir environment as a fruit-based fermentation in the presence of yeasts. However, wine exhibits a distinctly higher amount of alcohol and was shown to contain high amounts of polyphenols that may have antimicrobial potential (Boban *et al.*, 2010). *L. hordei* was originally isolated from partially fermented barley, which offers very low concentrations of mono- and disaccharides, but high amounts of polysaccharides, such as starch and β-glucan (Henry, 1988; Rouse *et al.*, 2008). Therefore, the water kefir isolates of all three species may have to face different environmental challenges than the ones isolated from different sources and thus underlie different selective pressure. In order to collect new insights into the formation of water kefir, the genetic adaptation of the water kefir isolates was investigated regarding genomic arrangement and water kefir specific traits. Herein, the results from ANI value analysis showed that the water kefir strains are more closely related to each other than to the strain isolated from a different source, respectively, despite being isolated from different water kefir consortia. This already indicates that the water kefir strains genetically diverged from the other strains, while developing into inhabitants of the water kefir microbiota. This was, however, less drastic for the *L. nagelii* strains than for the other two species, indicating that *L. nagelii* strains have either been part of the water kefir consortium for a shorter period of time or genetic properties enable the species to equally grow well in water kefir and wine. This was furthermore supported by collinearity analysis of this species, as only minor genomic rearrangements were found among these strains, while larger differing regions were assigned to the insertion of prophage sequences. By contrast, the genomes of the three *L. hordei* strains were subjected for more drastic genomic rearrangements, when water kefir strains were compared with the typestrain. This suggests that the strains diverged a longer time ago and subsequently adapted to their respective habitats. The genetic rearrangement especially applied for the region encoding the dextransucrase. However, it was not possible to derive a specific function of the proteins encoded within close proximity to the dextransucrase. Furthermore, it remains unknown if the surrounding genes of the dextransucrase are functionally linked to it or if the dextransucrase is generally located in a region of high plasticity in *L. hordei*. The latter option is, hence, more likely, as dextransucrases were proposed to be transcribed monocistronically, although polycistronic transcription has also been observed (Nácher-Vázquez *et al.*, 2017; Quirasco *et al.*, 1999).

Genetic loci of the dextransucrases appeared to be highly different among *L. hordei* and *L. nagelii*. A comparison of *L. hordei* TMW 1.1822 and *L. nagelii* TMW 1.1827 revealed that the *L. hordei* dextransucrase was indeed localized in a segment that exhibited no collinearity with the *L. nagelii* chromosome. In contrast, the *L. nagelii* dextransucrase was located at a genomic site that was not subjected for extensive rearrangements, as this locus appeared to be present in *L. hordei* and was highly similar to that in the typestrain. The latter one differed only by four genes within the water kefir strains of *L. nagelii* and nine genes within the genome of the typestrain, encoding a type I restriction modification system. Interestingly, the typestrain was originally described to produce dextran on sucrose-containing agar plates (Edwards *et al.*, 2000), a property that appeared to be absent during the current study, although this strain was freshly acquired from the German collection of microorganisms (DSMZ). Neither PCR-analysis, nor analysis of the two genomes that were available for this strain could reveal the presence of a dextransucrase gene. Therefore, it must be concluded that dextran production is not strictly a water kefir specific trait in *L. nagelii*, although it remains unknown, how the typestrain hast lost the ability to form this polysaccharide. Provided that the typestrain actually produced a dextran-type polysaccharide, the evolution of the dextransucrase locus must have undergone a two-step process. This includes loss of the dextransucrase, as well as the three other genes located there, and insertion of the restriction modification system. It is also possible, that the water kefir strains lost the restriction modification system at this locus. At least the restriction modification system exhibited transposable elements in its down-stream region, hinting at a putative transposition event of this segment. In general, these results are in accordance with the literature, where genetic loci of dextransucrases were described to be quite diverse, as they have been shown to be located at different chromosomal positions, plasmids and even within prophage regions (Amari *et al.*, 2015; Nácher-Vázquez *et al.*, 2017; Passerini *et al.*, 2015; Prechtl *et al.*, 2018a). This furthermore suggests that dextransucrases can generally be acquired through horizontal gene transfer by conjugation and transduction and thus improve the fitness of a species in a certain habitat. The expression of a dextransucrase indeed appears to be a decisive trait within the sucrose-rich water kefir environment, as all *L. hordei* and *L. nagelii* isolates were shown to encode a dextransucrase specific for the respective species, although *L. nagelii* TMW 1.1825 appeared to have lost the ability to produce dextrans by a mutation within the catalytic core of the enzyme. However, due to the lack of further genome sequences or even strains of these species isolated from different sources, it is not possible to evaluate if the dextransucrase has originally been a characteristic of the whole species or has been acquired during adaptation to certain niches.

In *L. hilgardii*, no genetic localization of the dextransucrase could be derived from WGSs, as this gene was the sole one on a contig in both sequenced strains. Furthermore, no dextransucrase gene could be identified within the WGS of the typestrain, which was confirmed by PCR analysis. Nonetheless, effective dextran production appeared to be quite versatile among the water kefir isolates, as some strains did not produce EPS despite being described as strong EPS-producers in other studies. PCR-analysis of genomic and plasmid DNA furthermore suggests that the dextransucrase is located on a plasmid in *L. hilgardii* strains that may get lost from time to time and thus produces EPS-negative mutants. Commonly, plasmids are maintained especially under selective pressure, while loss of plasmids is often attributable to collisions of the replication and transcription machineries (Helmrich *et al.*, 2013; Wein *et al.*, 2019). However, it remains to be elucidated if plasmid loss in *L. hilgardii* happens more often under certain conditions (e.g. presence or absence of sucrose) and, if this is a common trait of all *L. hilgardii* strains isolated from water kefir. As such, it may be an interesting "regulation" of dextran-production during water kefir formation, as *L. hilgardii* was proposed to produce the main polysaccharide found within the water kefir grains (Fels *et al.*, 2018; Pidoux, 1989).
Due to the lack of dextransucrase sequences within the genomes of the typestrains isolated from wine and malted barley, the presence of such genes within the water kefir isolates appeared to be a specific trait in this environment. Indeed, dextransucrase expression may be a decisive characteristic within the water kefir milieu, ensuring efficient extracellular sucrose degradation. Furthermore, the synthesized polysaccharides present a stable matrix, where the microorganisms can attach to and thus avoid being washed away during back-slopping of the grains. Moreover, the polysaccharide matrix holds the members of the water kefir microbiota in tight proximity to enable lossless cross-feeding (Stadie *et al.*, 2013).

Nonetheless, WGS comparisons revealed the presence of further genes characteristic for the water kefir isolates of the species *L. hilgardii, L. hordei* and *L. nagelii* that were all located within one conserved gene cluster (Figure 29). At least in *L. hordei* TMW 1.1822, *L. nagelii* TMW 1.1823 and TMW 1.1827, this gene cluster is part of a plasmid that was found to be shared among these strains. This was not surprising, as plasmids are well-known carriers of genes that confer niche adaptation (Davray *et al.*, 2020). Nonetheless, also both water kefir borne *L. hilgardii* strains, as well as *L. hordei* TMW 1.1907 featured this gene cluster that was conserved with regards to genetic organization among all analysed strains. However, it remains unknown if the gene cluster is also located on plasmids in these three strains. From BLAST analysis, this gene cluster was predicted to enable the transport and metabolization of

fructoselysine, an amino sugar that arises from the initial phase of the Maillard reaction between a reducing sugar (i.e. glucose) and protein-bound or free lysine. Metabolic pathways for the break-down of these stable Amadori intermediates can be found in all kingdoms of life involving different enzymes (Deppe *et al.*, 2011a; Yaylayan *et al.*, 1994). However, in prokaryotes only few examples have been studied in detail so far. In *E. coli*, a fructoselysine-6 kinase was shown to phosphorylate the fructosamine at the 6th carbon to generate fructoselysine-6-P that is subsequently split into glucose-6-P and lysine by fructoselysine-6-P deglycase. A putative transporter for the import of fructosamine was also found to be located within this operon (Wiame *et al.*, 2002). Therefore, *E. coli* is able to degrade fructoselysine from glycated proteins of undigested foods. As resorption of fructosamines by the human mucosa is very limited, this trait may provide some advantages in the environment of the human gut (Erbersdobler *et al.*, 2001). A similar operon was described in *B. subtilis*. In contrast to *E. coli*, the fructoselysine-6 kinase homologue of *B. subtilis* exhibited a broader specificity rather acting on α-glycated amino acids than on fructose-ε-lysine (Wiame *et al.*, 2004). As Amadori products are generally known to be formed non-enzymatically during heating, e.g. during processing of food products (Erbersdobler *et al.*, 2001), it appears rather unreasonable that *B. subtilis*, a common soil bacterium, can degrade these compounds. However, it has been shown that Maillard reactions take place in humus and to a rather large extend in rotting fruits and vegetables, suggesting that degradation of Amadori products is a decisive trait of *B. subtilis* to colonize and subsist in these environments (Nursten, 2005; Shallenberger, 1974). Literature on amino acid and protein glycation in plants is generally underrepresented compared to literature on these reactions in mammals, possibly due to the deleterious health-effects of these compounds that are eventually formed in, e.g. hyperglycemic patients. Nonetheless, Amadori products like fructoselysine were shown to be formed spontaneously by condensation of the sugar with the amino acid at high concentrations of both compounds and are thus abundant in plant materials (Bilova *et al.*, 2016). Therefore, it is most likely that these compounds originate from the dried fruits added to the water kefir fermentation, while the catabolism of the same may contribute to the survival of these microorganisms in this harsh environment that is – apart from sucrose – low in nutrients. A similar niche adaptation was also reported for a lineage of *L. curvatus* stains isolated from plant habitats (Terán *et al.*, 2018). During the current study, all investigated strains were, however, isolated from plant-related habitats, which is why a putative catabolism of Amadori products rather reflects an adaptation highly specific for the water kefir environment than a general adaptation to plant habitats. Moreover, the responsible operon of *L. curvatus* largely differed from that of *E. coli* and *B. subtilis*, exhibiting higher similarity with

that described for *E. faecium*. This operon included a Man-family PTS most likely involved in the uptake of fructosamines. Furthermore, the putative fructoselysine-6-P deglycase homologue of *E. faecium* was in fact shown to be a glucoselysine-6-P deglycase. This operon appeared to be widespread among gram-positive and -negative bacteria, including *Listeria monocytogenes* and *Salmonella enterica* serovar *typhimurium* (Miller *et al.*, 2015; Terán *et al.*, 2018; Wiame *et al.*, 2005; Yang *et al.*, 2008). A further bioinformatic analysis of the water kefir strains revealed the presence of this operon also in *L. hordei* TMW 1.1822, which appeared to be a strain-specific trait that was plasmid-encoded like the other fructoselysine gene cluster. Therefore, this strain codes for two of these gene clusters.
Nonetheless, the disruption of the gene clusters of *L. hilgardii* TMW 1.828 and TMW 1.2196, *L. hordei* TMW 1.1822 and *L. nagelii* TMW 1.1827 by transposases may leave the operons unfunctional in these strains. Therefore, it remains to be elucidated if the water kefir isolates are actually capable of using Amadori products as growth substrate and, if this trait harbours advantages during growth in water kefir fermentations.

A general analysis of the pan-, core- and accessory genomes of all *L. hilgardii, L. hordei* and *L. nagelii* strains furthermore revealed that most functional categories of SEED-based and TIGRFAM annotations stayed relatively constant between pan- and coregenome. Nonetheless, the proportion of functional categories involved in protein metabolism (both TIGRFAM and SEED-based annotations) was higher within the coregenome. This suggests that only little adaptation to the water kefir environment occurred here, which may be due to a similar supply with amino acids and peptides within the isolation sources of the investigated strains. By contrast, functional annotations related to energy/carbohydrate metabolism, as well as to transport proteins appeared to be underrepresented within the coregenome, indicating that the water kefir strains especially adapted their uptake and metabolism of carbohydrates to this environment. Nonetheless, only six genes were identified to be specific for the water kefir isolates that were already discussed above. This implies that adaptations of the uptake and metabolism of carbohydrates are possibly species-specific. Therefore, a detailed analysis of these metabolic routes may give new insights into the species-specific adaptation to the water kefir environment and may furthermore predict reactions that may occur in addition or competition to the dextransucrase reaction.

5.2.2 Genetic adaptations within the carbohydrate metabolism reveal the nature of *L. hordei, L. nagelii* and *L. hilgardii*

In general, only few of the PTS identified within the genomes of the investigated strains could be assigned to transport a specific compound. In some cases it was, however, possible to predict a specific function by the analysis of the genetic environment of a certain PTS, e.g. the Man-family PTS most likely involved in fructoselysine uptake in *L. hordei* TMW 1.1822, as discussed above. Nonetheless, sorting the annotated PTS into families gave at least a hint, which compounds may be transported by a certain PTS. It was most prominent that all *L. hilgardii* strains only encoded a small number of complete PTS compared to *L. hordei* and *L. nagelii*, being in accordance with the general assumption that heterofermentative LAB exhibit a reduced content of these transporters (Zheng *et al.*, 2015). Besides sucrose uptake, only one complete Man-Family PTS was found in *L. hilgardii* strains, which is most likely specific for the uptake of fructose and/or glucose according to API-test results. By contrast, *L. hordei* and *L. nagelii* strains encoded complete PTS for the uptake of fructose, glucose, sucrose, N-acetylglucosamine, sorbose, mannose, mannitol, β-glucosides and lactose or cellobiose. Most of these carbohydrates were furthermore confirmed to be effectively metabolized upon acid formation indicating that the predicted PTS were intact. None of the tested strains catabolized lactose, suggesting that the predicted Lac-family PTS are rather involved in the uptake of cellobiose. Furthermore, the metabolism of sorbose appeared to be a trait specific for the species *L. nagelii* and rather reflects the ability of this species to survive in various plant habitats. This also applied for the species-specific Gut-family PTS that may confer sorbitol uptake in *L. nagelii.* Furthermore, all *L. nagelii* strains, as well as *L. hordei* TMW 1.1822 exhibited two complete Gat-family PTS that were predicted to import galactitol or galactose. While *L. nagelii* strains showed a positive API-test result on galactose, none of the *L. hordei* strains could metabolize this sugar. Together with the fact that no complete orthologues were found among the Gat-family PTS of *L. nagelii* strains and *L. hordei* TMW 1.1822, these PTS may exhibit different specificities in *L. hordei*. In general, the distribution of PTS was more versatile in *L. hordei* strains than in *L. nagelii* strains, corroborating the hypothesis that water kefir borne *L. hordei* strains diverged more drastically from the strain isolated from malted barley than it was the case for the *L. nagelii* strains. In the PTS mediated uptake of carbohydrates, this particularly manifested in the higher number of Man-family and Glc-family PTS of water kefir *L. hordei* strains. However, due to the lack of information on specificity of these transporters, it remains to be elucidated whether this multitude of PTS reflects adaptation to substrates found within the water kefir environment.

By contrast, *L. hilgardii* exhibited a high number of different MFS-transporters compared to *L. hordei* and *L. nagelii*, possibly substituting the lack of PTS within these strains. These transporters were predicted to transport fucose, rhamnose, glucose, arabinose, xylose, galactose, melibiose, lactose and/ or raffinose. Under the applied incubation conditions of the API-test stripes, none of the strains was shown to ferment fucose or lactose. Rhamnose was only metabolized by *L. nagelii* strains and most of the water kefir borne *L. hordei* strains, indicating that these transporters are rather involved in the uptake of glucose in *L. hilgardii.* L-arabinose was only metabolized by water kefir borne *L. nagelii* and *L. hilgardii* strains, while xylose was fermented by all *L. hilgardii* strains and galactose by all *L. nagelii* and *L. hilgardii* strains. This suggests that arabinose/xylose/galactose MFS-transporters are specific for one of these substrates, respectively, while L-arabinose degradation appeared to be a decisive trait of some water kefir microorganisms and will be discussed in more detail later-on. The α-galactoside melibiose was fermented by all *L. hilgardii* strains. Melibiose rarely occurs in nature and is commonly found as degradation product of raffinose (Mital *et al.*, 1973). It was thus surprising that raffinose was not metabolized by the *L. hilgardii* strains investigated during this study, while raffinose was reported to induce dextransucrase expression and/or release in *L. hilgardii* TMW 1.828 (Waldherr *et al.*, 2010). In general, analysis of the MFS-transporter distribution led to the same conclusion as already stated for the PTS of *L. nagelii* strains. Among *L. hilgardii* strains, the most prominent difference was observed for the reduced number of MFS-transporters within the water kefir borne strains, participating in the metabolism of arabinose, xylose or galactose. All these genes were found to be orthologous, which particularly exacerbates the assignment of a certain transporter to a specific physiological function. Moreover, water kefir borne *L. hilgardii* strains exhibited a higher number of sucrose-specific MFS-transporters, possibly reflecting an adaptation to the sucrose-rich water kefir environment. The genomes of all strains encoded several ABC-transporters that were predicted to transport either maltose or glycerol-3-P. Due to a general lack in information on glycerol-3-P specific ABC-transporters in LAB, a more detailed prediction on the specificity of these transporters cannot be made. Investigations on gram-negative bacteria like *E. coli*, however, have shown that glycerol-3-P is only metabolized under certain conditions, such as phosphate starvation (Wuttge *et al.*, 2012). By contrast, maltose appeared to be metabolized by almost all tested strains. Maltose is a common non-PTS sugar and import is highly regulated by inducer exclusion, when glucose or other rapidly metabolized substrates are present (Monedero *et al.*, 2008; Postma *et al.*, 1993). Therefore, one of the predicted ABC-transporters is most likely involved in the uptake of this sugar.

Members of the species *L. hordei* and *L. nagelii* encoded all enzymes necessary for EMP and PKP pathways. Therefore, *L. hordei* and *L. nagelii* could be considered as facultatively heterofermentative, despite being originally described as homofermentative LAB (Edwards *et al.*, 2000; Rouse *et al.*, 2008). A similar observation was made for *Lactococcus lactis*, which showed a homolactic fermentation profile in the presence of several PTS sugars and a mixed acid fermentation from non-PTS sugars (Bolotin *et al.*, 2001). Moreover, *Lactiplantibacillus plantarum* exhibited a heterofermentative phenotype only at extremely low substrate availability (Teusink *et al.*, 2006). Further examples are given within the literature, stating that shifts between homo- and heterofermentative pathways are determined by the ratio of NAD^+/NADH, ATP/ADP, or fructose-1,6-bisphosphate and triose phosphate concentrations (Crow *et al.*, 1977; Garrigues *et al.*, 1997; Melchiorsen *et al.*, 2002; Palmfeldt *et al.*, 2004; Thomas *et al.*, 1979). The PKP may furthermore provide an advantage within the water kefir environment, as gluconate may be formed by other members of the consortium (e.g. acetic acid bacteria) and subsequently fed into this pathway by *L. hordei* and *L. nagelii*. However, only *L. nagelii* strains encoded a gluconokinase for intracellular phosphorylation of this substrate. No habitat-specific differences were observed regarding the presence or absence of enzymes involved in EMP and PKP, respectively. The non-oxidative part of the PPP of both species was incomplete by the lack of transaldolase, interrupting the link to glycolysis. However, this does not hinder the generation of $NADPH/H^+$ within the oxidative part, as well as interconversion of ribose-5-P, glycerinaldehyde-3-P, xylulose-5-P and erythrose-4-P that are essential for the formation of other important compounds, such as vitamins, amino acids and nucleotides. Moreover, transketolase (and transaldolase) are essential for the homofermentative conversion of pentoses to pyruvate (Zheng *et al.*, 2015). Besides transaldolase, the *L. hordei* typestrain additionally lacked transketolase, while both water kefir strains yet featured two genes coding for this enzyme. This suggests that the rudimental interconversion reactions catalysed by transketolase may be essential for *L. hordei* to subsist within the water kefir environment.

By contrast, *L. hilgardii* strains were confirmed to follow an obligate heterofermentative lifestyle. By the lack of fructose-1,6-bP-aldolase and 6-phosphofructokinase, these strains are not able to degrade hexoses *via* EMP pathway. Instead, they can metabolize hexoses *via* PKP. Neither transketolase nor transaldolase were present within the genomes of all investigated *L. hilgardii* strains. Additionally, all strains encoded a gluconokinase in order to feed gluconate into the central carbohydrate metabolism, which was confirmed by positive API-test results.

Apart from β-galactosidase, which was absent in the genome of the *L. hilgardii* typestrain, all *L. hilgardii* and *L. nagelii* strains encoded all enzymes involved in the degradation of lactose

and galactose *via* Leloir-pathway. At least galactose was shown to be effectively metabolized by these strains. In nature, galactose is commonly bound within α- and β-galacto-oligosaccharides. The most widespread galacto-oligosacharide is represented by lactose that is present in milk of mammals (Gänzle *et al.*, 2008). Moreover, galactose may also arise from the degradation of plant derived oligo- and polysaccharides like arabinogalactans, raffinose or melibiose (Belitz *et al.*, 2009), which is why an efficient galactose metabolism is not a hallmark for an exclusive adaptation of LAB to the fermentation of milk, but additionally to plant-derived habitats. In addition to Leloir-pathway, all *L. nagelii* strains encoded all proteins involved in Tagatose-6-P-pathway. Interestingly, the *L. nagelii* typestrain appeared to possess all genes coding for Leloir- and Tagatose-6-P-pathway at least twice, suggesting that the water kefir isolates were subjected for evolutionary reduction of these genes. This indicates that galactose or galacto-oligosaccharide metabolism only plays a minor role for *L. nagelii* in the water kefir environment.

In contrast, an efficient metabolism of the most abundant carbohydrate within water kefir fermentations is an advantageous trait (Gulitz *et al.*, 2011; Laureys *et al.*, 2014). Herein, sucrose metabolism of water kefir LAB already occurs within the extracellular milieu by the help of GH70 enzymes that form extracellular polysaccharides upon simultaneous fructose release. These enzymes were shown to be dextransucrases in *L. hilgardii* (Waldherr *et al.*, 2010), *L. nagelii* and *L. hordei* and appeared to be only present within the genomes of the water kefir isolates of these species, reflecting the adaptation to the sucrose-rich environment. The released fructose may subsequently be fed into the central carbohydrate metabolism by PTS-import. Furthermore, all *L. hordei* strains encoded a predictively extracellular β-fructosidase, which may cleave sucrose into glucose and fructose. Additionally, this enzyme may potentially degrade fructans which may be an advantageous trait within the water kefir environment, as fructan-producing LAB and acetic acid bacteria were shown to be present in the consortia (Jakob *et al.*, 2020; Paludan-Müller *et al.*, 2002). Moreover, all investigated strains exhibited MFS-transporters and PTS specific for the uptake of sucrose. All *L. hordei* and *L. nagelii* strains encoded for at least one sucrose-6-P hydrolase that splits the phosphorylated sucrose imported by PTS into fructose and glucose-6-P, while this enzyme was absent in *L. hilgardii*. This was compensated by sucrose phosphorylase in *L. hilgardii* strains, indicating that sucrose import is rather mediated by MFS-transporters in this species, while PTS mediated import is favoured in *L. hordei* and *L. nagelii*.

Since fermentation of mannitol and arabinose were significantly correlated with the isolation source water kefir, metabolism of these compounds was investigated by WGS analysis.

Arabinose metabolism appeared to be particularly important for the water kefir isolates of the species *L. hilgardii*, as these strains encoded L-arabinose isomerase and several GH43 arabinofuranosidases for the extracellular break-down of arabinoxylans and arabinogalactans that may originate from plant material, such as the dried fruits added to the water kefir fermentation (Belitz *et al.*, 2009). Nonetheless, also other members of the water kefir consortium may profit from extracellular degradation of complex polysaccharides by enzymes of *L. hilgardii.* This may enable *L. nagelii* strains to ferment arabinose, a proficiency that was limited to the water kefir isolates of this species, while the typestrain lacked the necessary enzymes for this metabolic route.

All water kefir borne *L. hilgardii, L. hordei* and *L. nagelii* could grow on mannitol as sole carbon source, while the *L. hilgardii* typestrain did not. Mannitol was shown to be present during water kefir fermentation, which is most likely due to the metabolic activity of yeasts (Gonçalves *et al.*, 2019; Onishi *et al.*, 1968). In *L. hordei* and *L. nagelii*, the sugar alcohol may be imported into the cell *via* PTS upon simultaneous phosphorylation. Subsequently, mannitol-1-P 5-dehydroganese converts mannitol-1-P to fructose-6-P and thus feeds the central carbohydrate metabolism. Furthermore, mannitol-1-P 5-dehydrogenase may not only contribute to mannitol degradation, but it may also use fructose-6-P to form mannitol-1-P upon NAD^+ regeneration. Also, in both water kefir borne *L. hilgardii* strains a protein was annotated as mannitol-1-P 5-dehydrogenase, however, this enzyme exhibited only slight similarity to the *L. hordei* and *L. nagelii* proteins. A subsequent BLAST analysis of the *L. hilgardii* enzymes, as well as bioinformatic investigation of the conserved domains, suggested that this enzyme may instead act as mannitol-dehydrogenase, which would explain why Verce *et al.* (2019) proposed that *L. hilgardii* produces mannitol itself. Surprisingly, OrthoFinder analysis revealed the presence of an orthologous gene within all three *L. nagelii* strains, while the presence of mannitol-2-dehydrogenase in homofermentative (or facultative heterofermentative) LAB is rather uncommon (Zheng *et al.*, 2015). Nonetheless, from sequence analysis alone it cannot be concluded whether this enzyme is a mannitol-1-P 5-dehydrogenase or a mannitol-2-dehydrogenase.

In order to predict the metabolic output and, how this may change under certain conditions, pyruvate degradation was analysed by comparative genomics, as it was already done for the carbohydrate metabolism. As expected, all strains featured several copies of lactate dehydrogenase to regenerate NAD^+ upon pyruvate reduction. Moreover, all strains can predictively form acetolactate that is either converted to acetoin by acetolactate decarboxylase

or non-enzymatically to diacetyl in the presence of oxygen. At this stage, both, acetoin and diacetyl may be excreted from the cells. Eventually, diacetyl is converted to acetoin upon NAD^+ recycling, while acetoin may be further reduced to 2,3-butanediol, yielding another NAD^+. Originally, it was proposed that two enzymes are necessary for the conversion of diacetyl to 2,3-butanediol. However, both steps may be catalysed by the same enzyme: either diacetyl/acetoin reductase or butanediol dehydrogenase (Hugenholtz, 1993). In general, all strains can form acetate and ethanol as metabolic end products, as predicted from WGS analysis. In a first step, pyruvate has to be converted into acetyl-CoA, which may be achieved by either pyruvate-dehydrogenase complex or pyruvate-formate lyase. Expectedly, none of the *L. hilgardii* strains encoded for the latter enzyme, as it is commonly described for obligate heterofermentative LAB (Zheng *et al.*, 2015). By contrast, all *L. hordei* and *L. nagelii* strains exhibited several copies of this gene and are thus capable of switching from homofermentative to a mixed acid fermentation. The formed acetyl-CoA may subsequently be converted to ethanol by a bifunctional acetaldehyde/alcohol dehydrogenase that is encoded by all investigated strains and may contribute to NAD^+ regeneration. While *L. hilgardii* is commonly described to produce ethanol (Dicks *et al.*, 2009), this has not been shown for *L. hordei* or *L. nagelii* so far. Furthermore, phosphate-acetyltransferase may convert acetyl-CoA to acetylphosphate that may additionally originate from PKP and is subsequently metabolized into acetate by acetate kinase, yielding ATP. In general, no prominent species-specific differences could be observed between water kefir isolates and the typestrains, respectively, regarding genetic equipment for pyruvate degradation.

5.2.3 The presence of sucrose regulates more than dextransucrase release in *L. hordei* TMW 1.1822 and *L. nagelii* TMW 1.1827

This work demonstrates that sucrose is not only substrate for the dextransucrases of the water kefir lactobacilli but can also have a regulatory function. For a better understanding of such a function in different dextran producers of the water kefir consortium and as a prerequisite for their application in other plant-derived fermentations, the behavior of *L. hordei* TMW 1.1822 and *L. nagelii* TMW 1.1827 was studied in the presence of sucrose compared to glucose in a proteomic study.

5.2.3.1 Sucrose facilitates dextransucrase release differently in *L. hordei* TMW 1.1822 and *L. nagelii* TMW 1.1827

While in *Leuconostoc* species, the expression of dextransucrases was reported to be most often specifically stimulated by its substrate sucrose, many other LABs express their dextransucrases independently of this sugar (Årsköld *et al.*, 2007; Bounaix *et al.*, 2010b; Prechtl *et al.*, 2018a; Quirasco *et al.*, 1999; Schwab *et al.*, 2007). This could also be observed for the *L. hordei* TMW 1.1822 dextransucrase, suggesting sucrose-independent expression (Figure 32). By contrast, the *L. nagelii* TMW 1.1827 dextransucrase was significantly less abundant in cell lysates in the presence of sucrose. Furthermore, it was demonstrated by mass spectrometry that the dextransucrase is among the most abundant proteins in cells grown on glucose as well as sucrose-supplemented media in both microorganisms and dextransucrase is equally abundant as common housekeeping proteins, like RNA polymerase sigma factor RpoD (Figure 33). Additionally, investigations of the exoproteomes of *L. hordei* TMW1.1822 could demonstrate that the release of this enzyme is induced by sucrose, which confirmed the assumptions that intracellular dextransucrase accumulation occurs independently of the present carbon source and experiences boosted release only in the presence of sucrose. The significantly higher relative abundance of the dextransucrase in sucrose-supplemented culture supernatants compared to the related cell lysates furthermore supported the assumption of directed release in the presence of sucrose despite the absence of a known type of signal peptide (Figure 35). The analysis of the exoproteomic MS-intensities revealed that the dextransucrase was among the 20 most abundant proteins in sucrose-supplemented cultures.

In this study, a similar mechanism of sucrose-induced boosted release was proposed for the *L. nagelii* dextransucrase, however, exoproteomic analysis indicated no significant increase in dextransucrase concentration in supernatants after sucrose-treatment, although a slightly higher MS-intensity of the dextransucrase was detected. Nonetheless, a significantly higher relative abundance of the dextransucrase in sucrose-supplemented culture supernatants compared to the related cell lysates indicated that dextransucrase is actually subjected for directed release in the presence of sucrose (Figure 35). Therefore, the significantly reduced presence of dextransucrase within the cell lysates of *L. nagelii* may rather be an effect of enzyme release than of down-regulated expression. Nonetheless, this does not explain why dextransucrase is among the most abundant proteins within the exoproteomes of *L. nagelii* TMW 1.1827 in both tested conditions (Figure 33), although supernatants obtained in the absence of sucrose exhibited much lower dextransucrase activities in other experiments, which were shown to be dependent on enzyme concentration. The reduced activities in these supernatants may thus be explained by the

absence of "primer" dextran that was shown to enhance activity in *S. mutans, L. reuteri* and *L. curvatus* dextransucrases, when cells were grown in the absence of sucrose (Germaine *et al.*, 1974; Kingston *et al.*, 2002; Rühmkorf *et al.*, 2013), as already discussed in section 5.1.4. However, adverse effects were described for other dextransucrases (V. Monchois *et al.*, 1998; Monchois *et al.*, 1997; Monchois *et al.*, 1996). Moreover, protein glycosylation that was shown for the *L. nagelii* dextransucrase (Figure 9), as well as dextran bound to the enzyme may have led to results during proteomic analysis that do not reflect the actual amount of dextransucrase present within cell lysates and supernatants, as glycosylation is known to protect proteins from proteolytic digestion (Langsford *et al.*, 1987). This is corroborated by the fact that dextransucrase protein bands were empirically less abundant on a Coomassie-stained SDS-gel, when supernatants were obtained in the absence of sucrose in previous experiments (Figure 19). However, it remains unknown if a similar effect is obtained from cells in the presence of glucose, as protein concentrations of the exoproteomic samples were too low to visualize differences in dextransucrase concentrations on SDS-gels.

Similar to the results from *L. hordei* proteomic analysis, dextransucrase was among the most abundant proteins detected within the supernatants of *L. nagelii* and is therefore likely responsible for most of the extracellular sucrose turnover in both microorganisms, leading to dextran formation upon simultaneous fructose release, which is subsequently metabolized. The resulting biofilm formation may protect the microorganisms against desiccation along with surface adhesion, helping *L. hordei* and *L. nagelii* to gradually colonize habitats rich in sucrose, e.g., plants or fermented foods such as water kefir, once the sugar is detected. Therefore, efficient extracellular sucrose degradation upon simultaneous exopolysaccharide formation appears to be a decisive trait to subsist in such environments, as it was also shown for other members of the genus *Liquorilactobacillus*, such as *L. sucicola* and *L. mali* (formerly *Lactobacillus sucicola* and *mali* (Zheng *et al.*, 2020)) (Carr *et al.*, 1970; Irisawa *et al.*, 2009).

5.2.3.2 Sucrose regulates intracellular carbohydrate metabolism similarly in *L. hordei* TMW 1.1822 and *L. nagelii* TMW 1.1827

In general, carbohydrate metabolism appeared to be regulated quite similar in both tested microorganisms, as shown in Figure 39. The switch from glucose to sucrose as sole carbon source led to the up-regulation of fructose-specific transporters of the PTS^{fru} and in *L. hordei* additionally PTS^{man} families. This indicates enhanced uptake of fructose, which was previously released during the extracellular dextransucrase reaction. Correspondingly, 1-phosphofructokinase was up-regulated in sucrose, enabling the efficient processing of 1-

phosphorylated fructose to fructose-1,6-bisphosphate, which is an early intermediate of glycolysis. This is in good agreement with a down-regulation of glucose-6-P isomerase and in *L. hordei* additionally 6-phosphofructokinase that are both necessary to channel glucose into the EMP. Nonetheless, a Man-family PTS was significantly down-regulated in the presence of sucrose in both strains. It is thus likely that this PTS is involved in the uptake of compounds related to glucose metabolism, as it was shown for other lactobacilli (Yebra *et al.*, 2006).
Furthermore, the enzyme fructose-1,6-bisphosphatase was significantly up-regulated in sucrose, which is a central enzyme of gluconeogenesis. Therefore, *L. hordei* TMW 1.1822 and *L. nagelii* TMW 1.1827 fill their fructose-6-P pools. While the activity of fructose-1,6-bisphosphatase is highly regulated itself, its substrate fructose-1,6-bP is involved in the regulation of several other processes, including activation of carbon catabolite repression (Deutscher *et al.*, 2006; Hines *et al.*, 2007; Lu *et al.*, 2018). Reducing the fructose-1,6-bP pools may hence contribute to switching between different carbohydrate sources.

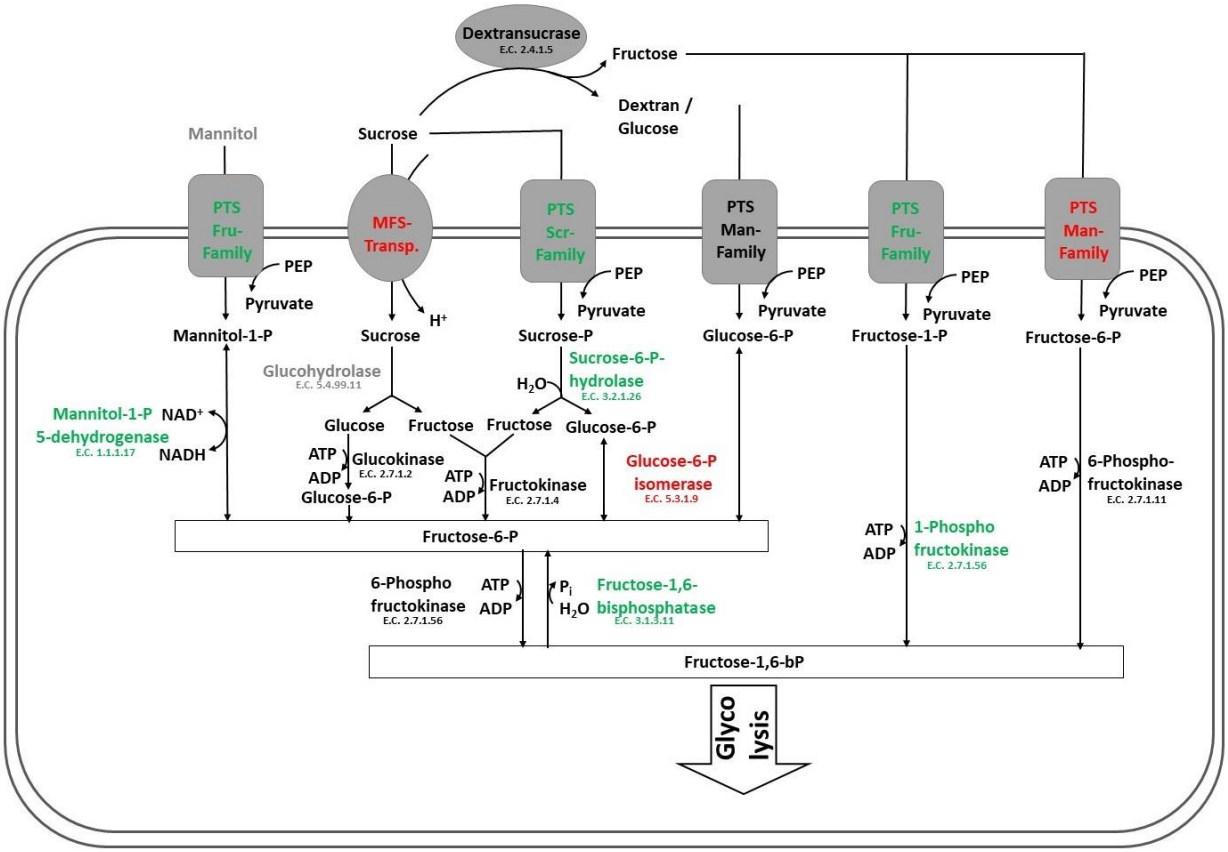

Figure 39 Initial carbohydrate metabolism of *L. hordei* TMW 1.1822 and *L. nagelii* TMW 1.1827 regulated in the presence of sucrose compared to glucose. Only proteins with similar regulation in *L. hordei* and *L. nagelii* are marked in colour. Green = proteins with higher abundance in sucrose-supplemented medium, red = proteins with decreased abundance in sucrose-supplemented medium compared to glucose, grey = it is unknown if this enzyme actually catalyses this reaction. Mannitol is also written in grey, as mannitol import is predictively possible, but this compound was not present in culture media used for the proteomic experiments.

In addition, glycerol kinase and in *L. hordei* additionally glycerol-3-P dehydrogenase were up-regulated in sucrose-treated cells, yielding dihydroxyacetone phosphate, which can either react during glycolysis or to glyceraldehyde-3-P. None of the investigated strains expressed transketolase, which is why glyceraldehyde-3-P cannot be channeled into the non-oxidative part of PPP. Otherwise, together with fructose-6-P, the glyceraldehyde-3-P may be used by transketolase to yield xylulose-5-P and erythrose-4-P, which would link carbohydrate metabolism to the synthesis of other compounds, respectively, e.g., nucleotides, vitamins and certain amino acids. In general, glycerol catabolism of some LAB cannot be excluded within the water kefir environment, as it was postulated that yeasts may form glycerol during fermentation (Verce *et al.*, 2019). Moreover, in both, *L. hordei* TMW 1.1822 and *L. nagelii* TMW 1.1827, several orthologues of a putative glycerol transporter were found, however, basal expression was only detected in *L. nagelii*. Looking at the raw proteomic data furthermore revealed that this transporter was detected in some replicates of the *L. hordei* proteomes, but with extremely low MS-intensities. Once inside the cell, glycerol may be converted by the phosphorylation pathway starting with the glycerol kinase reaction upon ATP consumption. Two options of further glycerol-3-P degradation were observed in LAB: glycerol-3-P dehydrogenase yields dihydroxyacetone-P by reduction of quinone, while glycerol-3-P oxidase needs oxygen as oxidant, forming hydrogen peroxide (Condon, 1987; Doi, 2019; Koditschek *et al.*, 1969). However, both of these enzymes are closely related and sequence analysis alone did not reveal, which of these enzymes is encoded by *L. hordei* and *L. nagelii*, although glycerol-3-P oxidase is more widespread among LAB (Doi, 2019). Furthermore, it is important to note that glycerol metabolism is tightly controlled by LAB, especially when other nutrients are present. Thus, it has been shown that expression of the relevant genes is suppressed by the absence of glycerol and oxygen in *Enterococcus faecalis* and *B. subtilis* (Darbon *et al.*, 2002; Doi, 2015; Vesić *et al.*, 2013). Furthermore, transcription of the relevant genes was significantly suppressed by the presence of glucose, which is regulated by carbon catabolite control protein A (Charrier *et al.*, 1997; Darbon *et al.*, 2002; De Fátima Alvarez *et al.*, 2004). Therefore, the upregulation of glycerol kinase and glycerol-3-P dehydrogenase/oxidase in the presence of sucrose may rather reflect a glucose-induced down-regulation. Furthermore, none of the *L. hordei* and *L. nagelii* strains could metabolize glycerol upon acid formation, which was most likely due to the fact that the API-tests were conducted under micro-oxic conditions by overlaying the cultures with paraffin oil, although *L. hordei* and *L. nagelii* may have needed oxygen for the glycerol-3-P oxidase reaction. Moreover, possible carbon catabolite repression may suppress glycerol metabolism during water kefir fermentation until preferred substrates

are consumed. The higher abundance of enzymes involved in glycerol metabolism in the presence of sucrose, as well as predictively lower amounts of fructose-1,6-bP indicate that transcriptional repression of these enzymes is linked to the presence of glucose but not sucrose. Altogether, the results relating to the effects of sucrose on the initial carbohydrate metabolism of *L. hordei* TMW 1.1822 suggest that fructose is rather metabolized than glucose in sucrose-treated cells, although glucose may also be released by hydrolysis from the extracellular dextransucrase reaction. This is further supported by the results from growth experiments in different sugars, where the lag-phase of *L. hordei* was the shortest in fructose, although the lag-phase of other sugar combinations that included fructose was not significantly different. By contrast, the lag-phase of cells grown in glucose was significantly longer. Furthermore, maximum growth rates were highest in fructose, while all sugar combinations that included glucose had (significantly) lower maximum growth rates, which was possibly due to catabolite repression of other sugar-converting enzymes in the presence of glucose. Taken together, these results hint at the fructophilic nature of *L. hordei* TMW 1.1822, once more emphasizing the adaptation of this microorganism to the fruit-based fermentation of water kefir. Although these experiments clearly showed that other sugars than glucose had an enhancing effect on growth and metabolism of *L. hordei* TMW 1.1822, this difference was not observable from cell counts in glucose and sucrose-treated cells after 2 h of incubation. However, the microorganism was grown in glucose until mid-exponential growth phase and *L. hordei* may have possibly needed some time to adapt its metabolism from glucose to sucrose. This assumption also applies for the consumption of sugars, as well as the production of acids, in the same samples. Within 2 h of incubation, 27% of glucose was consumed, while already 77% of sucrose was split. As *L. hordei* intracellularly accumulates its dextransucrase and releases it immediately once its substrate is detected, the microorganism is optimally prepared for rapid extracellular sucrose degradation. However, the products formed during this reaction were not consumed within 2 h of incubation. Under the assumption that sucrose is exclusively converted by the extracellular dextransucrase reaction, only 32% of the released fructose would have been metabolized at this point in time. Moreover, significantly more lactate was formed in glucose-treated cells within 2 h of incubation, which may be due to an enhanced formation of acetyl-CoA in sucrose-treated cells, suggested from significantly higher amounts of pyruvate dehydrogenase subunits in this condition. In *L. nagelii* TMW 1.1827 only ~ 21 % of glucose were consumed at this point of time, while almost no sucrose was left, which is most likely due to the high overall activity of the extracellular *L. nagelii* dextransucrase. Assuming that sucrose is only converted by extracellular dextransucrase, already 47 % of the released fructose may be consumed after 2 h.

These results are furthermore in accordance with the different cell counts obtained from both investigated strains, as glucose-treatment of *L. nagelii* led to lower cell counts than in *L. hordei,* while sucrose-treatment led to a significantly higher cell count of *L. nagelii*. As other growth experiments of *L. nagelii* revealed that fructose exhibits slightly adverse effects on growth of *L. nagelii,* sucrose itself may be the preferred substrate for this strain. Nonetheless, an increased growth rate may furthermore arise from potentially beneficial effects of the synthesized dextran rather than from intracellular sucrose metabolism. Looking at the ORP-curves of both, *L. hordei* and *L. nagelii,* cultures grown in the presence of sucrose could maintain a low ORP, while this was not the case in the absence of sucrose. This may be correlated with the synthesis of dextran, as this polymer is known to lower the diffusion of oxygen (Ju *et al.*, 1986). Both species were originally described as facultative anaerobe microorganisms (Edwards *et al.*, 2000; Rouse *et al.*, 2008), which is why they may profit from the reduced presence of oxygen. A similar observation was made for *Lc. mesenteroides* BD3749, which was shown to alleviate oxygen-related stress by the up-regulation of a dextransucrase and subsequent formation of EPS (Yan *et al.*, 2016). Additionally, *L. nagelii* TMW 1.1827 produced significantly more lactate in the presence of sucrose, which may be a result of the increased growth and concomitant metabolic activity in this condition. In the presence of sucrose, a switch from homo-lactic to mixed acid formation could thus not be observed in both *L. hordei* and *L. nagelii.* It has long been a matter of discussion, why facultative heterofermentative LAB rather produce lactate than acetate, despite generating an additional ATP. Besides the already discussed homeostasis of redox-balance, the production of lactic acid may acidify the surrounding environment faster than acetic acid, due to a lower pK_a of lactic acid and the necessity of three enzymatic steps (when resulting from EMP) compared to only one in lactic acid formation. A faster acidification of the environment may subsequently hinder other microorganisms to grow and is thus decisive in competition for nutrients (Teusink *et al.*, 2017). In *L. hordei* TMW 1.1822 (Schmid *et al.*, 2019), as well as *L. nagelii* TMW 1.1827, the pH has only a minor effect on the released amount of dextransucrase (activity). The optimum pH for dextransucrase productivity, however, was shown to be at ~ pH 5.0 for both enzymes, which is why rapid acidification faster generates the optimal environment for this enzyme.

Apart from that, a sucrose-specific PTS was up-regulated in sucrose-treated cells of both, *L. hordei* and *L. nagelii*, which shows that not all of the supplied sucrose is used by the extracellular dextransucrase. Within the same gene cluster, the up-regulated sucrose-6-P hydrolase ensures metabolism of internalized and phosphorylated sucrose, cleaving it into glucose-6-P and fructose. By contrast, a sucrose-specific MFS transporter was significantly

down-regulated in sucrose, suggesting that *L. hordei* and *L. nagelii* adjust their sucrose uptake, which may also be dependent on the concentration of this substrate (Figure 32). This may help the microorganisms to avoid intracellular dextran formation by not yet released dextransucrase, which may lead to cell lysis. Within the same gene cluster, a glucohydrolase with putative α-glucosidase activity was significantly down-regulated in *L. hordei* TMW 1.1822. α-glucosidases represent a heterogeneous group of enzymes with a large range of substrate specificities, including sucrose isomerase. Sucrose isomerases catalyze the conversion of sucrose into isomaltulose or trehalulose, while sucrose hydrolysis may also occur to some extent (Goulter *et al.*, 2012). The conversion to sucrose isomers would hence contribute to the prevention of cell lysis due to intracellular dextran formation. However, sucrose isomerases have not been described in LAB so far, which is why such an activity of the predicted glucohydrolases remains speculative. Oligo-1,6-glucosidases also belong to this group, which are capable of dextran degradation (Møller *et al.*, 2012). As both differentially expressed glucohydrolases with putative α-glucosidase activity were not identifiable in exoproteomes of *L. hordei* TMW 1.1822, extracellular dextran hydrolysis is unlikely. However, both enzymes may be involved in the intracellular metabolism of short-chain IMOs, which are produced during the early steps of dextran formation (Moulis *et al.*, 2006). Nonetheless, both proteins were significantly down-regulated in sucrose, which is contrary to similar enzymes in other LAB (Møller *et al.*, 2012; Prechtl *et al.*, 2018a). This may hint at a divergent role of these enzymes in the carbohydrate metabolism of *L. hordei* TMW 1.1822, which remains to be elucidated. This also applies for a putative extracellular β-fructosidase that was not significantly differentially expressed in cell lysates but was certainly more released in the presence of sucrose. Regarding the application of *L. hordei* TMW 1.1822 in plant-based food fermentations aiming at the *in situ* production of dextran, this enzyme may appear as a competing reaction to dextran production. However, the dextransucrase was shown to be of distinctly higher abundance than the β-fructosidase (Figure 33), implying that this enzyme plays only a minor role in extracellular sucrose degradation. Furthermore, this particular β-fructosidase exhibits a C-terminal LPxTG motif, indicating its covalent attachment to the cell surface of *L. hordei* TMW 1.1822. However, harsh cell separation techniques, such as centrifugation, may have led the enzyme to be lost from the cell wall. Moreover, this enzyme might also act as a fructan hydrolase, which would exhibit additional advantages for *L. hordei* to survive in the water kefir environment, as already discussed above. Fructose or smaller fructooligosaccharides may then be efficiently imported by the fructose- or sucrose-specific PTS, repsectively, as it was reported for *Lactiplantibacillus plantarum* (Saulnier *et al.*, 2007).

Additionally, a gene cluster involved in the uptake and metabolism of mannitol was significantly up-regulated in sucrose. As there was certainly no extracellular mannitol detectable in un-fermented MRS media, the PTS was in this experiment more likely utilized for fructose uptake in *L. hordei* and *L. nagelii*. By contrast, the mannitol-1-P 5-dehydrogenase may not only contribute to mannitol degradation, but it may also use fructose-6-P to form mannitol-1-P upon NAD^+ regeneration. However, no mannitol was detectable in culture supernatants of both, *L. hordei* TMW 1.1822 and *L. nagelii* TMW 1.1827, which would have been of additional nutritional value for products fermented with these microorganisms, as mannitol can be applied as a low-calorie sweetener with health-promoting effects (Wisselink *et al.*, 2002). Nonetheless, the sugar alcohol is a well-known compatible solute, protecting the organisms against a number of stress situations, such as high osmotic pressure. The intracellular accumulation of mannitol was, therefore, reported to maintain cell turgor at low water activity (Kets *et al.*, 1996) (Efiuvwevwere *et al.*, 1999). However, due to the lack of mannitol-1-phosphatase, *L. hordei* and *L. nagelii* are not capable of producing un-phosphorylated mannitol. Moreover, the additional gene found in *L. nagelii* TMW 1.1827, probably encoding a mannitol-2-dehydrogenase appeared to be silent and thus not expressed. Whether the intracellular accumulation of mannitol-1-P has the same protecting effect in environmental stress situations remains to be elucidated. This is in good agreement with other homofermentative (or facultative heterofermentative) LAB, among which extracellularly detectable mannitol formation is rather uncommon (Wisselink *et al.*, 2002). Furthermore, the mannitol operon was reported to be sensitive to catabolite repression. When rapidly degradable carbohydrates such as glucose are internalized by their PTS, the mannitol operon is no longer stimulated (Henstra *et al.*, 2000; Henstra *et al.*, 1999). Therefore, the results of the differential proteomic analysis of *L. hordei* and *L. nagelii* may rather reflect glucose-induced down-regulation than sucrose-induced up-regulation of the expression of these gene clusters. This may also apply for the differentially expressed PTS^{Glc} and in *L. hordei* additionally phospho-β-glucosidases. From amino acid sequence analysis, it was not possible to derive the substrate specificity of these proteins. However, β-glucosides are often hydrolysis products of plant material, and efficient uptake and metabolic mechanism of these substrates would not be surprising in plant-adapted *L. hordei* TMW 1.1822 and *L. nagelii* TMW 1.1827.

Butanediol dehydrogenase was significantly up-regulated in sucrose-treated *L. hordei* and may therefore contribute to NAD^+ recycling upon reduced lactate formation, which was already discussed above. This proteomic change was also observable in a previous study as a result of co-cultivation with water kefir-borne *Saccharomyces cerevisiae* TMW 3.221 and is thus not

exclusively induced by sucrose treatment (D. Xu *et al.*, 2019b). Therefore, the buttery and fruity aroma of 2,3-butanediol in water kefir may *vice versa* not only come from co-cultivation of *L. hordei* with yeasts but also from the presence of sucrose.

5.2.3.3 Sucrose promotes proteinaceous biofilm formation by *L. hordei* TMW 1.1822, while leaving *L. nagelii* TMW 1.1827 exoproteomes rather unaffected

The proteomic analysis of culture supernatants of *L. hordei* TMW 1.1822 revealed that the majority of the significantly differentially released proteins were predicted to be located in the cytoplasm. Sucrose is known to be osmotically active on LAB (Papadimitriou *et al.*, 2016) and may have thus led to cell lysis of at least a fraction of the culture. Moreover, as sucrose can enter cells of *L. hordei* by MFS transporters, leaving the sugar un-phosphorylated, intracellular dextran formation may cause cell lysis. However, as cell counts for glucose and sucrose-treated cells were similar after plating on agar, sucrose appeared to have no significant (osmo-)lytic effect on *L. hordei* TMW 1.1822. Only a small fraction (~ 20%) of the quantified cellular proteome was also specifically quantified in the exoproteomes of glucose and sucrose-treated cells, which is an additional argument against significant amounts of cell lysis. This clearly indicates that the majority of cells of *L. hordei* stayed intact during incubation in sucrose. The comparative analysis of MS-intensities supported this suggestion, as it revealed that, in both conditions, around two thirds of the proteins were of significantly different abundances in cell lysates and exoproteomes (Figure 35). Among these proteins, the dextransucrase and the putative β-fructosidase were of distinctly different abundances in exoproteomes compared to cell lysates when cells were treated with sucrose. Still, in glucose and sucrose-treated cells, proteins exhibiting an NlpC/P60 domain were actively released into the extracellular milieu, while being significantly less present in sucrose-treated cells than in glucose-treated cells. This domain is frequently found in bacterial peptidoglycan hydrolases (Vermassen *et al.*, 2019). The role of these proteins will be further discussed in the next section. Interestingly, after glucose as well as sucrose-treatment, flagellar proteins were detected in distinctly higher abundance in exoproteomes than in cellular proteomes of *L. hordei*, while being significantly less present in sucrose-treated cells than in glucose-treated cells. Although the species *L. hordei* was originally believed to be non-motile, it was recently shown that *L. hordei* and other Liquorilactobacilli, such as *L. nagelii* and *L. mali*, exhibit a complete motility operon (Cousin *et al.*, 2015; Rouse *et al.*, 2008). This operon is also present in *L. hordei* TMW 1.1822 (BSQ40_10755 - BSQ_11055) and *L. nagelii* TMW 1.1827 (BSQ50_10965 - BSQ_11180). The expression of the majority of these genes may enable motility in *L. hordei* TMW 1.1822, which appeared to

be regulated by the present carbon source. The decreased release of these proteins in the presence of sucrose may thus hint at reduced motility under biofilm formation conditions (= in the presence of sucrose), as it was reported for *B. subtilits* (Vlamakis *et al.*, 2013). Moreover, flagellar proteins of other LAB were reported to exhibit an immunomodulatory effect (Neville *et al.*, 2012), which was observed to be a beneficial health effect of water kefir consumption (Sharifi *et al.*, 2017). From SEED-based analysis as well as GO enrichment analysis, it could be shown that the majority of proteins that were increasingly released by *L. hordei* in the presence of sucrose were related to protein metabolism and translation. However, these proteins were not found to be among the proteins that were actively released with high confidence (z-score difference exoproteome vs. cell lysate $\geq$ 2.0), although many of them were still of distinctly different abundance in exoproteomes than in cell lysates. Even though it was postulated above that cell lysis did not happen to a significant extent, when sucrose was present, this increased release of intracellular proteins may still have been an effect of high abundances of these proteins within the cellular proteomes and may thus point at a leakage of sucrose-treated cells. However, it was frequently reported that intracellular proteins, such as elongation factors, molecular chaperones (e.g., GroL, DnaK), ribosomal proteins, glycolytic enzymes (e.g., glucose-6-phosphate isomerase, glycerinaldehyde-3-P dehydrogenase, phosphoglycerate mutase, enolase) and pyruvate degrading enzymes (e.g., lactate dehydrogenase), among others, can overtake other functions when released into the extracellular milieu, mostly acting as adhesion factors (Celebioglu *et al.*, 2017; De Angelis *et al.*, 2016; Espino *et al.*, 2015; Peng *et al.*, 2018; Waśko *et al.*, 2014). Glycosyltransferases, involved in exopolysaccharide synthesis from sucrose, were also shown to mediate cell aggregation and are thus responsible for the formation of floating biofilms in *L. reuteri* (Walter *et al.*, 2008). After sucrose treatment, the exoproteome of *L. hordei* TMW 1.1822 indeed showed an increase in a multitude of such proteins, indicating that sucrose-induced biofilm formation in *L. hordei*, which was thought to be mainly composed of the EPS dextran, is additionally mediated by released cytoplasmic proteins. This may furthermore play a role in the persistence of *L. hordei* within the water kefir environment, as the abundance of sucrose may constantly trigger the release of such proteins and thus help *L. hordei* to adhere to other inhabiting microorganisms or the kefir granules. In exoproteomes of *L. nagelii*, a distinctly higher number of proteins was identified, however, more than 90 % of these proteins were found to be of significantly higher or lower relative abundancy than within cellular proteomes of *L. nagelii*, indicating their directed release or retention. Only four proteins were shown to be of significantly different abundance in exoproteomes of sucrose- compared to glucose-treated cells. This implies that *L. nagelii* TMW

1.1827 does not alter its exoproteome to the same extent as *L. hordei* TMW 1.1822 does in reaction to sucrose. Among the significantly more released proteins, an enzyme predictively belonging to GH53 was found. So far, the only known specificity of GH53 enzymes is acting as β-1,4-galactanase, hydrolyzing galactans and arabinogalactans from plant material (Belitz *et al.*, 2009; Böger *et al.*, 2019; Hinz *et al.*, 2005; Le Nours *et al.*, 2009). Therefore, the presence of sucrose may also stimulate degradation of plant material in *L. nagelii* TMW 1.1827, which may contribute to gradual colonization of plant-environments. Apart from that, the composition of proteins that were released with high confidence in *L. nagelii* was similar to that in *L. hordei*, showing the presence of flagellar proteins, as well as enzymes carrying NlpC/P60 domains. In contrast to *L. hordei*, the abundance of these proteins was, however, not influenced by the present carbon source.

Altogether, these analyses showed that exoproteomes of *L. hordei* TMW 1.1822 underwent a drastic change under dextran- and thus biofilm-forming conditions in the presence sucrose. By contrast, exoproteomes of *L. nagelii* varied only slightly, when switching from glucose to sucrose. The results hence indicate that *L. hordei* strains are more specialized to live in the water kefir environment not only on a genetic basis, but also due to regulatory mechanisms in the presence of sucrose. By contrast, *L. nagelii* appeared adapted to various plant habitats, being rather unperturbed by the presence of sucrose.

5.2.3.4 *L. hordei* TMW 1.1822 and *L. nagelii* TMW 1.1827 release predictively cell-wall active enzymes

The differential proteomic analysis of cell lysates revealed up-regulated expression of a predicted GH25 muramidase in sucrose-treated cells of *L. hordei* TMW 1.1822 compared to glucose-treated cells. This was also observed for the analysis of exoproteomes, where it appeared to be increasingly released in the presence of sucrose. Proteins containing a GH25 muramidase domain were shown to cleave the β-(1→4) glycosidic bond between N-acetylglucosamine and N-acetylmuramic acid of bacterial peptidoglycans in *Lentilactobacillus buchneri* (formerly *Lactobacillus buchneri* (Zheng *et al.*, 2020)) (Anzengruber *et al.*, 2014). However, no lytic activity could be observed from supernatants of *L. hordei* TMW 1.1822 when treated with sucrose, indicating that this enzyme has no or little hydrolytic activity against the cell wall of *M. luteus* or released amount of this enzyme was too low for visualization by zymogram analysis. By contrast, supernatants of glucose-treated cells led to formation of a lytic zone of around 110 kDa during zymogram analysis, indicating the presence of a lytic enzyme (Figure 36). In the exoproteomes of glucose-treated cells, several proteins annotated as

flagellum-associated mureinhydrolases (flgJ) and proteins exhibiting an NlpC/P60 domain were found in significantly higher amounts than in sucrose-treated cells. FlgJ is a cell wall active enzyme which is necessary for cell envelope remodelling during flagellar rod assembly (Herlihey *et al.*, 2014), which is in good agreement with the increased release of a multitude of flagellar proteins in glucose-treated cells. However, flgJ has not been studied in LAB so far, leaving its lytic role in *L. hordei* TMW 1.1822 speculative. By contrast, NlpC/P60 domain-containing proteins were characterized as γ-D-Glu-diaminoacid endopeptidases, involved in cell division and autolysis of LAB (Claes *et al.*, 2012; Regulski *et al.*, 2012; Rolain *et al.*, 2012). However, in *L. hordei* TMW1.1822, the theoretical molecular weight of both NlpC/P60 domain-containing proteins was 41 and 44 kDa, respectively, not resembling the lytic band of 110 kDa. This may hint at the presence of an additional lytic enzyme in glucose-treated cells which may have not been quantified during proteomic analysis. Furthermore, SDS-PAGE was performed under non-denaturing conditions, which is why the lytic band may also have been caused by a multimeric enzyme. By contrast, supernatants of *L. nagelii* TMW 1.1827 obtained in the presence of glucose and sucrose led to three lytic bands within this analysis. None of the protein bands with a predictively higher molecular weight could be assigned to a protein released in the presence of both sugars. The lower band, however, represented a protein of ~ 70 kDa, which matched the *L. nagelii* GH25 muramidase (BSQ50_08465 and BSQ50_11560) that appeared to be an orthologue of the above-mentioned *L. hordei* GH25 muramidase. The release of such lytic enzymes may help *L. hordei* and *L. nagelii* to compete for nutrients in challenging environments, such as water kefir.

5.2.4 Conclusions II: Adaptation and metabolic strategies of *L. hordei, L. nagelii* and *L. hilgardii* to persist in and contribute to water kefir formation

Strains of the species *L. hilgardii, L. hordei* and *L. nagelii* are frequently isolated from water kefir, but were originally obtained from other habitats. Comparative genomic analysis of these strains could show that all water kefir isolates genetically diverged from their relatives being isolated from differed habitats, confirming that the hypothesized adaptation indeed happened. However, this was found to be less drastic for strains of the species *L. nagelii,* indicating that this species has either been part of the water kefir consortium for a shorter period of time or environmental challenges in water kefir and wine are coped equally by this species. The most prominent differences between water kefir isolates and the respective typestrains arose from the presence of a dextransucrase gene, enabling efficient extracellular sucrose conversion, and a (or two in *L. hordei*) gene cluster predictively involved in the uptake and metabolization of

Amadori products, e.g. fructoselysine, which may originate from the dried fruits added to water kefir fermentations. Therefore, both water kefir specific traits may help the microorganisms to subsist in the harsh water kefir environment, being poor in nutrients other than sucrose, by rapid sucrose turnover and assimilation of rather uncommon compounds.

Additionally, it could be shown that protein metabolism is left rather un-affected by adaptation to the water kefir environment, while species-specific differences in carbohydrate uptake and metabolism were predicted. Regarding carbohydrate uptake, water kefir borne strains of the species *L. hordei* encoded a distinctly higher number of Glc- and Man-family PTS than the strain originally isolated from malted barley, indicating that β-glucosides, as well as sugars imported by PTS^{man}, e.g. fructose, glucose, N-acetylglucosamine or mannose, play an imported role for these strains to subsist in the water kefir environment. No habitat-specific differences were observed for the abundance of proteins involved in EMP and PKP, which is why the species *L. hordei* may rather be considered facultatively heterofermentative. Nonetheless, the typestrain lacked transketolase in addition to transaldolase, suggesting that the rudimental interconversion reactions catalysed by transketolase are essential for the water kefir strains. No differences in PTS-dependent uptake of carbohydrates could be observed among the *L. nagelii* strains, while minor differences resided within the abundance of carbohydrate-related MFS-transporters. Thereby a higher number of arabinose/xylose/galactose transporters and a lower number of melibiose/lactose/raffinose transporters in water kefir borne strains suggested that monosaccharides are either preferred by these strains or present in higher abundancy within the water kefir environment. This may possibly be due to the expression and release of GH53 enzymes or the presence of other microorganisms degrading higher plant-derived polysaccharides, such as *L. hilgardii*. Furthermore, this was corroborated by the fact that only water kefir borne *L. nagelii* strains were able to metabolize arabinose, which was already indicated from WGS analysis. Galactose, which may also originate from degraded plant material, was suggested to play only a minor role in the metabolism of water kefir derived isolates, due to the distinctly reduced number of enzymes involved in Leloir- and Tagatose-6-P-pathways. Like *L. hordei,* all strains of the species *L. nagelii* encoded all enzymes necessary for EMP and PKP, implying a facultative heterofermentative lifestyle. No water kefir related differences were observed for EMP, PKP and possible pyruvate degradation routes. A somewhat inverse adaptation strategy was exhibited by water kefir borne *L. hilgardii* strains that encoded a reduced number of arabinose/xylose/galactose MFS-transporters and a higher number of melibiose/lactose/raffinose transporters, indicating that this species is more adapted to the fermentation of plant-derived oligosaccharides. Furthermore, the higher number of

sucrose-specific MFS-transporters reflected the adaptation of these strains to the sucrose-rich water kefir environment. The absence of certain key enzymes confirmed the obligate heterofermentative nature of all members of the species *L. hilgardii* and no habitat-specific differences were observed. The most prominent differences of water kefir borne *L. hilgardii* strains compared to the one isolated from wine were observed in the presence of a high number of arabinofuranosidases that may extracellularly degrade plant-derived arabinoxylans and arabinogalactans thus contributing to the liberation of arabinose, xylose and galactose. Furthermore, the wine-isolate could not grow on mannitol as sole carbon source, which is most likely due to the absence of mannitol-1-P 5-dehydrogenase/mannitol-2-dehydrogenase in this strain.

Taken together, water kefir borne strains of the species *L. hilgardii, L. hordei* and *L. nagelii* developed different strategies apart from efficient sucrose metabolism in order to subsist in the water kefir environment, which is attributable to the utilization of diverse sugars and sugar alcohols that may originate from plant-material or yeast metabolism. Overall genomic differences were, however, most distinct in water kefir borne *L. hordei* strains compared to their typestrain counterpart, indicating that *L. hordei* developed into an autochthonous water kefir specialist. Both other species appeared to be prepared for the colonization of various plant-derived compounds on a genetic basis.

Furthermore, the elaborated knowledge on the carbohydrate metabolism of water kefir borne *L. hordei* and *L. nagelii* laid the basis for a subsequent proteomic experiment, which should enlighten the response of both species to the main substrate of water kefir fermentation that is sucrose. As both species are furthermore promising candidates for the use as starter cultures in plant-based food fermentations due to their dextran-forming capabilities, the proteomic experiment should furthermore give new insights into which reactions may occur in addition or competition to the dextransucrase reaction. Therefore, the proteomic experiment confirmed the results obtained during investigation of the *L. hordei* dextransucrase, showing that it is accumulated intracellularly and only released in the presence of sucrose. By contrast, the proteomic results of *L. nagelii* contradicted those obtained from prior experiments, as the abundance of the extracellular dextransucrase was independent from the present carbon source, while being significantly less present in cellular proteomes after sucrose-treatment. However, it remains unknown if this is due to protein glycosylation or putative requirement of “primer” dextran. Furthermore, it could be shown that the dextransucrase is among the most abundant proteins in exoproteomes of both species, when sucrose was present, suggesting that it is responsible for most of the extracellular sucrose-turnover. In *L. hordei* TMW 1.1822 an

additional extracellular potentially sucrose-degrading enzyme appeared to be up-regulated in the presence of sucrose. The β-fructosidase may additionally cleave sucrose into glucose and fructose, which should be taken into account when *L. hordei* is applied as starter culture aiming at the *in situ* formation of dextran. Moreover, the effects of sucrose-treatment on the central carbohydrate metabolism of *L. hordei* TMW 1.1822 and *L. nagelii* TMW 1.1827 were shown to be similar, though *L. nagelii* appeared to be slightly less affected. Herein, transporters and enzymes channeling fructose into EMP were significantly more abundant in the presence of sucrose, while transporters and enzymes involved in glucose uptake and metabolism were significantly less abundant. This is in good agreement with an efficient sucrose-degradation by extracellular dextransucrase, which forms polysaccharide upon fructose release. Furthermore, sucrose is metabolized intracellularly in addition to extracellular dextransucrase reaction. The higher abundance of enzymes involved in the metabolism of glycerol and mannitol in the presence of sucrose is most likely due to carbon catabolite repression in the presence of glucose. Additionally, *L. hordei* was shown to exhibit an up-regulated butanediol-dehydrogenase, as well as pyruvate dehydrogenase in the presence of sucrose, which is in agreement with a reduced lactate formation, despite similar growth in glucose and sucrose. In *L. nagelii* TMW 1.1827, the enhanced production of lactic acid was most likely attributable to a significantly increased growth and concomitant higher metabolic activity in the presence of sucrose. Therefore, the results of the proteomic investigation, as well as the growth experiments in different sugars pointed at a fructophilic nature of *L. hordei*, while *L. nagelii* appeared to prefer sucrose as substrate. Nonetheless, the increased growth of *L. nagelii* in sucrose-supplemented media may also result from the potentially beneficial effects of the simultaneously formed polysaccharide.

Investigations of the exoproteomes furthermore revealed that in both strains the majority of identified proteins was predicted to be cytoplasmic, although most of these proteins were proposed to be subjected for a directed release. Sucrose had only a minor effect on the exoproteomes of *L. nagelii*. Nonetheless, a putative GH53 β-galactanase was significantly more abundant in the presence of sucrose, enabling degradation of plant-derived galactans and arabinogalactans. The presence of sucrose may thus stimulate *L. nagelii* to gradually colonize plant-habitats. By contrast, the presence of sucrose had a much larger impact on the exoproteomes of *L. hordei.* This corroborates the hypothesis from WGS comparison, in which adaptation to the sucrose-rich water kefir environment is less distinct in *L. nagelii* than in *L. hordei*, which may be due to the fact that water kefir and wine represent more similar environments than water kefir and malted barley. The concomitant release of predictively

intracellular proteins by *L. hordei* under dextran-forming conditions may furthermore contribute to biofilm and - in the case of water kefir - to granule formation, as these "moonlighting" proteins may confer adhesion. Furthermore, in supernatants of both, *L. hordei* and *L. nagelii*, the presence of flagellar proteins could be demonstrated, indicating that both strains may be motile, which may be regulated in *L. hordei* under dextran-forming conditions. The release of potentially lytic enzymes by *L. hordei* and *L. nagelii* may enable both microorganisms to compete for nutrients when other microorganisms are present.

Taken together, the results from comparative genomics and proteomic experiments give new insights into the similar and distinct strategies of the investigated microorganisms to adapt and contribute to water kefir fermentation.

6 Summary

In the present work, LAB isolated from water kefir were probed for their mechanisms of persistence in the water kefir, their active contributions to the shaping of this environment and their exploitability for novel applications. The selected LAB were subjected for whole genome sequencing and the resulting WGS were searched for the presence of sequences encoding the enzymes responsible for glucan synthesis. Thereby, it could be shown that all strains encoded one or more predictively extracellular sucrases of the GH70 family that were highly diverse, explaining the diversity of different glucans in water kefir. A comparison of the amino acid sequences of these enzymes subsequently revealed the novelty of the glucansucrases encoded by strains of the species *L. hordei* and *L. nagelii*, while being closely related with each other. Therefore, the traditionally fermented beverage proved to be a reservoir for different and actually new glucansucrases encoded by LAB. In further analyses, the *L. hordei* and *L. nagelii* glucansucrases were shown to be effectively expresses and released into the extracellular environment, where they produce dextran-type glucans with branches in *O*3 position. Despite exhibiting a highly similar catalytic domain, which is most likely responsible for the production of dextrans with identical structural components, differences were observed in the release of the enzyme, as well as in overall and transglycosylation activities, processivity and abundancy of structural elements of the synthesized dextrans. Herein, *L. hordei* could be shown to accumulate its dextransucrase intracellularly, which was exclusively released in the presence of sucrose. By contrast, the *L. nagelii* dextransucrase was present in supernatants irrespective of the present carbon source, however, in the absence of sucrose a distinctly lower amount of extracellular dextransucrase (activity) was observed. These results may have arisen from different secretion mechanisms or signals, as suggested from the absence and presence of known types of signal peptides. While supernatants of *L. nagelii* exhibited an extremely high overall and transglycosylation activity, which already consumed the total amount of sucrose (200 mM) within the first 10 min of incubation, supernatants of *L. hordei* exhibited a distinctly lower overall and transglycosylation activity. These differences were shown to be most likely attributable to a lower concentration of native dextransucrase within the supernatants of *L. hordei* compared to *L. nagelii*. To some extent, the enzyme concentration may furthermore influence the processivity of the enzyme, forming higher amounts of isolable dextran, when more enzyme is present. However, comparative analysis of native enzymes and heterologously expressed variants, lacking the C-terminal glucan-binding domain that was additionally present in the *L. nagelii* dextransucrase, showed that processivity of these enzymes is mostly determined by the constitution of domain V, including this C-terminal glucan-binding domain.

Therefore, the native extracellular dextransucrase of *L. nagelii* produces more isolable dextran with higher molecular weight and rms radius than the native extracellular dextransucrase of *L. hordei*. Differences in the molecular architecture were demonstrated to reside in the abundancies of structural elements that attributed to different branch lengths of the polysaccharides produced by native dextransucrases of *L. hordei* and *L. nagelii*, which is most likely due to differences in amino acid composition within the catalytic domain that are more distantly located to the substrate binding sites.

More detailed investigations of the highly efficient native extracellular *L. nagelii* dextransucrase furthermore revealed that less dextransucrase may form the same amount of dextran, but more slowly, until a critical concentration of enzyme is reached. The ongoing formation of high molecular weight dextran upon simultaneous fructose release after sucrose depletion was shown to come along with proportionately more branched dextrans. Simultaneously, the amount of leucrose pre-synthesized at early steps of the dextransucrase reaction, decreased and may thus contribute to further dextran elongation after sucrose depletion.

In a second part of this work, WGS of *L. hilgardii, L. hordei* and *L. nagelii* were compared with strains of these species that were isolated from different sources. Thereby, two water kefir specific genomic traits could be identified, namely dextran formation and predicted catabolism of Amadori products like fructoselysine. Further WGS comparisons revealed that specific adaptation to the water kefir environment predominantly resides within the carbohydrate metabolism of these species, however, each species evolved a separate strategy to subsist in this habitat. Herein, water kefir borne *L. hordei* strains encoded a higher number of transporters specific for the uptake of fructose, glucose, β-glucosides, N-acetylglucosamine and mannose, as well as transketolase enabling rudimental interconversion reactions of the non-oxidative PPP. By contrast, water kefir borne *L. nagelii* strains were shown to ferment plant-derived monosaccharides, such as arabinose. Both, *L. hordei* and *L. nagelii*, encoded all enzymes necessary for EMP and PKP, suggesting them to be facultatively heterofermentative instead of strictly homofermentative. *L. hilgardii* is an obligately heterofermentative microorganism showing extensive genomic differences within the uptake and metabolism of carbohydrates compared to *L. hordei* and *L. nagelii*. Nonetheless, adaptation of the water kefir borne strains was shown to be similar to that of the *L. nagelii* strains, as degradation of plant-derived polysaccharides, such as arabinoxylans and arabinogalactans was predicted from these genomes. Additionally, water kefir borne *L. hilgardii* strains exhibited a higher number of sucrose-specific transporters and could grow on mannitol as sole carbon source.

The elaborated knowledge on the carbohydrate metabolism subsequently laid the basis for investigations on the proteomic states of water kefir borne *L. hordei* TMW 1.1822 and *L. nagelii* TMW 1.1827 in the presence of sucrose. In general, the change from glucose to sucrose affected *L. hordei* more drastically than *L. nagelii*, especially within the exoproteomes. Nonetheless, the carbohydrate metabolism was regulated similarly for both strains, as enzymes for the uptake and metabolism of fructose and sucrose were significantly more abundant in sucrose-treated cells, while proteins involved in the uptake and metabolism of glucose were significantly less abundant. This is most likely a result of the fructose that is released during extracellular dextran synthesis. The proteomic analysis furthermore confirmed that *L. hordei* accumulates its dextransucrase and releases it in high amounts, once sucrose is present. Expression and release of the *L. nagelii* dextransucrase was proposed to be similar than in *L. hordei* with regards to the presence of sucrose and pH, however, proteomic investigation of cell lysates and exoproteomes revealed contradictive results. Moreover, proteomic analysis together with growth experiments pointed at a fructophilic nature of *L. hordei,* while *L. nagelii* performed best in the presence of sucrose, which may *inter alia* come from beneficial effects of the synthesized dextran on fitness of this strain. Furthermore, sucrose appeared to induce the release of enzymes involved in degradation of plant-material in *L. nagelii* that may help these strains to colonize plant-related habitats. In *L. hordei*, a multitude of predictively intracellular proteins was released in the presence of sucrose, suggesting that biofilms of this species also exhibit a proteinaceous component in addition to dextran. These experiments furthermore revealed the presence (and regulation) of extracellular proteins involved in motility and cell wall hydrolysis.

In conclusion, the present study identified and characterized native extracellular dextran formation by water kefir borne LAB *L. hordei* TMW 1.1822 and *L. nagelii* TMW 1.1827, which may also be transferrable to other strains of these species, as well as the molecular processes involved in dextran synthesis during water kefir fermentation. Moreover, this study identified water kefir specific traits and extensively discussed the diverse adaptation strategies of inhabiting LAB, while further elucidating the behavior of *L. hordei* and *L. nagelii* under dextran-forming conditions. Therefore, these findings generate a basis for sophisticated exploitations of these microorganism as starter cultures in food-fermentations and give new insights into the complex formation of the traditional beverage water kefir.

7 Zusammenfassung

In der vorliegenden Arbeit wurden Milchsäurebakterien hinsichtlich der zugrundeliegenden Mechanismen ihrer Beständigkeit im Wasserkefir, ihrem Beitrag zur Gestaltung dieser Umgebung und ihrer Anwendbarkeit in neuartigen Lebensmittelfermentationen untersucht. Die ausgewählten Milchsäurebakterien wurden genom-sequenziert und auf die Anwesenheit von für die Glucansynthese verantwortlichen Enzymen hin überprüft. Dabei konnte gezeigt werden, dass alle Glucan-bildenden Stämme eine oder mehrere möglicherweise extrazelluläre Sucrasen der GH70 Familie kodieren. Die hohe Diversität der identifizierten Enzyme erklärt vermutlich die Vielfalt an Glucanen, die im Wasserkefir zu finden sind. Ein Aminosäuresequenz-basierter Vergleich dieser Enzyme mit bereits bekannten Enzymen dieser Familie zeigte nachfolgend, dass die von *L. hordei* und *L. nagelii* kodierten Glucansucrasen neuartig und gleichzeitig nahe verwandt sind. Hierbei konnte bereits darauf geschlossen werden, dass Wasserkefir in der Tat ein interessantes Reservoir zur Untersuchung neuartiger Glucansucrasen aus Milchsäurebakterien darstellt. Weitere Analysen zeigten, dass *L. hordei* und *L. nagelii* ihre jeweiligen Glucansucrasen tatsächlich exprimierten und in das extrazelluläre Milieu freisetzten, wo sie dann ein Glucan des Dextrantyps mit Verzweigungen an Position *O*3 bildeten. Die katalytische Domäne dieser zwei Dextransucrasen ist sehr ähnlich, wodurch vermutlich die identischen strukturellen Einheiten der gebildeten Dextrane erklärbar sind. Trotzdem wurde beobachtet, dass sich die beiden Enzyme hinsichtlich ihrer Freisetzung in die Umgebung, sowie der allgemeinen und transglycosylierenden Aktivität, ihrer Prozessivität und hinsichtlich der relativen Abundanz verschiedener Strukturelemente im gebildeten Dextran unterscheiden. Dabei akkumulierte *L. hordei* die Dextransucrase intrazellulär und setzte sie nur in Gegenwart von Saccharose frei. In Überständen von *L. nagelii* Kulturen konnte die Dextransucrase jedoch unabhängig von der vorliegenden Kohlenstoffquelle nachgewiesen werden, obwohl in der Abwesenheit von Saccharose nur eine sehr geringe Menge an Dextransucrase (-aktivität) vorlag. Diese Ergebnisse könnten durch unterschiedliche Sekretions-signale oder -mechanismen hervorgerufen worden sein, was in dem Vorhandensein eines Signalpeptids begründet sein könnte. Des Weiteren war in Überständen von *L. nagelii* Kulturen eine sehr viel höhere Gesamt- als auch Transglycosylierungsaktivität messbar als in Überständen von *L. hordei*, die bereits innerhalb von 10 Min Inkubation die komplette zur Verfügung gestellte Saccharose (200 mM) aufbrauchte. Diese Unterschiede wurden im weiteren Verlauf einer geringeren Konzentration an Dextransucrase in den Überständen von *L. hordei* zugeschrieben. Es konnte außerdem gezeigt werden, dass die Enzymkonzentration zu einem gewissen Grad die Prozessivität der Dextranbildung beeinflusst, wodurch mit mehr Enzym folglich eine größere

Menge isolierbaren Dextrans gebildet wird. Um weitere Klarheit über die Prozessivität dieser Enzyme zu erlangen, wurden zwei Varianten der *L. nagelii* Dextransucrase heterolog exprimiert: eine komplette Variante und eine, die um die C-terminale Glucan-bindende Domäne verkürzt wurde, die in der *L. hordei* Dextransucrase nicht vorhanden war. Ein Vergleich dieser Enzyme zeigte, dass die Prozessivitätsunterschiede der *L. nagelii* und *L. hordei* Dextransucrasen primär in der Struktur von Domäne V begründet liegt, die mitunter durch das Vorhandensein der C-terminalen Glucan-bindenden Domäne geformt wird. Durch die andere Beschaffenheit von Domäne V konnte die native *L. nagelii* Dextransucrase größere Mengen an isolierbarem Dextran mit größerem Molekulargewicht und rms Radius produzieren. Zusätzlich konnte gezeigt werden, dass sich die Dextrane der beiden Mikroorganismen in der Häufigkeit unterschiedlich langer Seitenketten unterscheiden. Da dieser Unterschied weder durch unterschiedliche Enzymkonzentrationen noch durch die zusätzliche Glucan-bindende Domäne der *L. nagelii* Sucrase erklärbar war, muss darauf geschlossen werden, dass kleine Unterschiede in der Aminosäuresequenz der katalytischen Domäne, die sich vermutlich nicht in direkter Umgebung der Substratbindestellen befinden, hierfür verantwortlich sind.

Genauere Untersuchungen der hoch-effizienten nativen *L. nagelii* Dextransucrase zeigten darüber hinaus, dass weniger Enzym dieselbe Menge an Dextran bilden kann, wenn auch langsamer und nur bis zu einer kritischen Enzymkonzentration. Obwohl die gesamte Menge an Saccharose bereits nach 10 Min aufgebraucht war, lief die Bildung hochmolekularen Dextrans, sowie die gleichzeitige Freisetzung von Fruktose weiter. Dies ging einher mit der Bildung von Dextranen, die vergleichsweise mehr Verzweigungen aufwiesen. Gleichzeitig nahm die Konzentration an Leucrose, die während der frühen Reaktionen der Dextranbildung gebildet wurde, wieder ab, sodass darauf geschlossen werden konnte, dass dieses Disaccharid nach Umsetzung der Saccharose für die fortlaufende Polysaccharid-Elongation verantwortlich ist.

In dem zweiten Teil dieser Arbeit wurden WGS von Stämmen der Spezies *L. hilgardii, L. hordei* und *L. nagelii* verglichen mit Stämmen derselben Spezies, die zuvor aus anderen Habitaten isoliert wurden. Dadurch konnten zwei Wasserkefir-spezifische genomische Eigenschaften festgestellt werden: die Bildung von Dextran mittels Dextransucrase und die mögliche Verstoffwechselung von Amadori-Produkten, wie z.B. Fruktoselysin. Weiterführende Genomanalysen zeigten außerdem, dass spezifische Anpassungen an das Wasserkefirmilieu hauptsächlich im Kohlenhydratmetabolismus dieser drei Spezies begründet liegen und, dass jede dieser Spezies eine eigene Strategie der Anpassung entwickelt hat. Wasserkefirstämme der Spezies *L. hordei* zeigten dabei eine höhere Anzahl an kompletten Transportern für die Aufnahme von Fruktose, Glukose, β-Glukosiden, N-Acetylglucosamin

und Mannose. Darüber hinaus kodierten die Wasserkefirstämme im Gegensatz zum Typstamm für das Enzym Transketolase, sodass die rudimentären Umwandlungsreaktionen des nicht-oxidativen PPP ablaufen können. Die Wasserkefirstämme der Spezies *L. nagelii* konnten Monosaccharide aus Pflanzen, wie z.B. Arabinose, fermentieren. Sowohl Stämme der Spezies *L. hordei,* als auch *L. nagelii* kodierten für alle Enzyme des EMP und PKP, weshalb sie fakultativ heterofermentativ einzuordnen sind. Stämme der Spezies *L. hilgardii* sind dagegen obligat heterofermentativ, worin die großen Unterschiede in Transport und Metabolismus von Kohlenhydraten im Vergleich zu *L. hordei* and *L. nagelii* begründet liegen. Trotzdem erschien die Anpassung der *L. hilgardii* Wasserkefirstämme ähnlich zu denen der Spezies *L. nagelii*, da Genomanalysen den Abbau und Metabolismus von Pflanzen-assoziierten Polysacchariden, wie z.B. Arabinoxylanen oder Arabinogalactanen, vorhersagten. Zusätzlich besaßen die Wasserkefirstämme eine größere Anzahl an Saccharose-spezifischen Transportern und konnten auf Mannitol als alleinige Kohlenhydratquelle wachsen.

Das somit erarbeitete Wissen über den Kohlenhydratmetabolismus dieser Mikroorganismen diente folglich als Basis für Untersuchungen von durch Saccharose ausgelösten proteomischen Unterschieden in den zwei Wasserkefirstämmen *L. hordei* TMW 1.1822 und *L. nagelii* TMW 1.1827. Allgemein konnte festgestellt werden, dass die Umstellung von Glukose auf Saccharose das Proteom von *L. hordei* deutlich mehr beeinflusste als das Proteom von *L. nagelii*, was besonders auf die Exoproteome zutraf. Der Kohlenhydratmetabolismus beider Stämme war vergleichbar reguliert, da Enzyme für die Aufnahme und den Metabolismus von Fruktose signifikant abundanter und von Glukose signifikant weniger abundant in Gegenwart von Saccharose waren. Dieses Ergebnis ist vermutlich auf die durch die Dextransucrasereaktion freigesetzte Fruktose zurückzuführen. Die proteomischen Analysen konnten des Weiteren bestätigen, dass *L. hordei* die Dextransucrase intrazellulär akkumuliert und sie in Gegenwart von Saccharose in großen Mengen freisetzt. Die vorherigen Ergebnisse zur Freisetzung der *L. nagelii* Dextransucrase konnten in diesem Experiment jedoch nicht bestätigt werden. Zusammen mit Ergebnissen von Wachstumsexperimenten in verschiedenen Zuckern, zeigte die Proteomanalyse von *L. hordei* TMW 1.1822 dessen potentiell fruktophile Natur auf, während *L. nagelii* TMW 1.1827 das beste Wachstum in Saccharose-supplementierten Medien zeigte. Dies könnte auf zusätzlich begünstigende Effekte des Dextrans auf die Fitness dieses Mikroorganismus zurückzuführen sein. Des Weiteren induzierte die Anwesenheit von Saccharose die vermehrte Freisetzung eines Enzymes, das möglicherweise zum Abbau von Pflanzenpolysacchariden beiträgt und somit dazu, dass *L. nagelii* Pflanzen-nahe Habitate besiedeln kann. In Exoproteomen von *L. hordei* konnte in Gegenwart von Saccharose eine

vermehrte Freisetzung von intrazellulären Proteinen nachgewiesen werden, was darauf hindeutet, dass Biofilme dieser Spezies zusätzlich zur Dextrankomponente eine Proteinkomponente aufweisen. Außerdem konnte dieses Experiment zeigen, dass in Überständen von *L. hordei* TMW 1.1822 und *L. nagelii* TMW 1.1827 Proteine anwesend (und reguliert) sind, die zur Motilität und Hydrolyse von Zellwänden beitragen.

In der vorliegenden Studie wurde die native extrazelluläre Dextranbildung der aus Wasserkefir isolierten Stämme *L. hordei* TMW 1.1822 und *L. nagelii* TMW 1.1827 identifiziert und charakterisiert, was möglicherweise auch auf andere Stämme dieser beiden Spezies als auch die molekularen Prozesse der Dextranbildung im Wasserkefir übertragbar ist. Darüber hinaus wurden spezifische Charakteristika der aus Wasserkefir stammenden Isolate der Spezies *L. hilgardii, L. hordei* und *L. nagelii* identifiziert und ihre verschiedenen Anpassungsstrategien an diese Umgebung diskutiert. Außerdem wurde das Verhalten von *L. hordei* TMW 1.1822 und *L. nagelii* TMW 1.1827 unter Dextran-bildenden Umständen untersucht. Die erreichten Ergebnisse können als Basis für eine biotechnologische Nutzung dieser Stämme in neuartigen Lebensmittelfermentationen genutzt werden. Zusammenfassend konnten während dieser Arbeit neue Erkenntnisse über die komplexe Bildung des traditionell fermentierten Getränks Wasserkefir gewonnen werden.

8 References

Abo, H., Matsumura, T., Kodama, T., Ohta, H., Fukui, K., Kato, K., *et al.* (1991). Peptide sequences for sucrose splitting and glucan binding within *Streptococcus sobrinus* glucosyltransferase (water-insoluble glucan synthetase). *Journal of bacteriology, 173*(3), 989-996. doi:10.1128/jb.173.3.989-996.1991

Albenne, C., Skov, L. K., Mirza, O., Gajhede, M., Feller, G., D'Amico, S., *et al.* (2004). Molecular basis of the amylose-like polymer formation catalyzed by *Neisseria polysaccharea* amylosucrase *Journal of Biological Chemistry, 279*(1), 726-734. doi:10.1074/jbc.M309891200

Alexa A., & J., R. (2020). topGO: Enrichment Analysis for Gene Ontology. (Version 2.40.0).

Altschul, S. F., Gish, W., Miller, W., Myers, E. W., & Lipman, D. J. (1990). Basic local alignment search tool. *Journal of Molecular Biology, 215*(3), 403-410. doi:10.1016/S0022-2836(05)80360-2

Amari, M., Valérie, G., Robert, H., Morel, S., Moulis, C., Gabriel, B., *et al.* (2015). Overview of the glucansucrase equipment of *Leuconostoc citreum* LBAE-E16 and LBAE-C11, two strains isolated from sourdough. *FEMS Microbiology Letters, 362*(1), 1-8. doi:10.1093/femsle/fnu024

Angelescu, I.-R., Zamfir, M., Stancu, M.-M., & Grosu-Tudor, S.-S. (2019). Identification and probiotic properties of lactobacilli isolated from two different fermented beverages. *Annals of Microbiology, 69*(13), 1557-1565. doi:10.1007/s13213-019-01540-0

Anzengruber, J., Courtin, P., Claes, I. J. J., Debreczeny, M., Hofbauer, S., Obinger, C., *et al.* (2014). Biochemical characterization of the major N-acetylmuramidase from *Lactobacillus buchneri*. *Microbiology (Reading, England), 160*(Pt 8), 1807-1819. doi:10.1099/mic.0.078162-0

Ardö, Y. (2006). Flavour formation by amino acid catabolism. *Biotechnology Advances, 24*(2), 238-242. doi:10.1016/j.biotechadv.2005.11.005

Argimón, S., Alekseyenko, A. V., DeSalle, R., & Caufield, P. W. (2013). Phylogenetic analysis of glucosyltransferases and implications for the coevolution of mutans streptococci with their mammalian hosts. *PLOS ONE, 8*(2), e56305. doi:10.1371/journal.pone.0056305

Arndt, D., Grant, J. R., Marcu, A., Sajed, T., Pon, A., Liang, Y., *et al.* (2016). PHASTER: a better, faster version of the PHAST phage search tool. *Nucleic Acids Research, 44*(W1), W16-W21. doi:10.1093/nar/gkw387

Årsköld, E., Svensson, M., Grage, H., Roos, S., Rådström, P., & van Niel, E. W. J. (2007). Environmental influences on exopolysaccharide formation in *Lactobacillus reuter*i ATCC 55730. *International Journal of Food Microbiology, 116*(1), 159-167. doi:10.1016/j.ijfoodmicro.2006.12.010

Ashburner, M., Ball, C. A., Blake, J. A., Botstein, D., Butler, H., Cherry, J. M., *et al.* (2000). Gene ontology: tool for the unification of biology. The Gene Ontology Consortium. *Nature genetics, 25*(1), 25-29. doi:10.1038/75556

Asioli, D., Aschemann-Witzel, J., Caputo, V., Vecchio, R., Annunziata, A., Næs, T., *et al.* (2017). Making sense of the "clean label" trends: A review of consumer food choice behavior and discussion of industry implications. *Food Research International, 99*, 58-71. doi:10.1016/j.foodres.2017.07.022

Azaïs-Braesco, V., Bresson, J. L., Guarner, F., & Corthier, G. (2010). Not all lactic acid bacteria are probiotics, …but some are. *British Journal of Nutrition, 103*(7), 1079-1081. doi:10.1017/S0007114510000723

Aziz, R. K., Bartels, D., Best, A. A., DeJongh, M., Disz, T., Edwards, R. A., *et al.* (2008). The RAST Server: Rapid Annotations using Subsystems Technology. *BMC Genomics, 9*(1), 75. doi:10.1186/1471-2164-9-75

Back, W. (1981). Schädliche Mikroorganismen in Fruchtsäften, Fruchtnektaren und süßen, alkoholfreien Erfrischungsgetränken. *Brauwelt, 121*, 43-48.

Bailey, R. W., & Bourne, E. J. (1959). Formation of leucrose in dextran-producing cultures of *Streptococcus bovis*. *Nature, 184*(4690), 904-905. doi:10.1038/184904b0

Bankevich, A., Nurk, S., Antipov, D., Gurevich, A. A., Dvorkin, M., Kulikov, A. S., *et al.* (2012). SPAdes: a new genome assembly algorithm and its applications to single-cell sequencing. *Journal of computational biology : a journal of computational molecular cell biology, 19*(5), 455-477. doi:10.1089/cmb.2012.0021

Barends, T. R. M., Bultema, J. B., Kaper, T., van der Maarel, M. J. E. C., Dijkhuizen, L., & Dijkstra, B. W. (2007). Three-way stabilization of the covalent intermediate in amylomaltase, an α-amylase-like transglycosylase. *Journal of Biological Chemistry, 282*(23), 17242-17249. doi:10.1074/jbc.M701444200

Bartowsky, E. J., & Henschke, P. A. (2008). Acetic acid bacteria spoilage of bottled red wine - a review. *International Journal of Food Microbiology, 125*(1), 60-70. doi:10.1016/j.ijfoodmicro.2007.10.016

Belitz, H.-D., Grosch, W., & Schieberle, P. (2009). *Food chemistry* (4 ed.). Heidelberg: Springer.

Bensing, B. A., Seepersaud, R., Yen, Y. T., & Sullam, P. M. (2014). Selective transport by SecA2: an expanding family of customized motor proteins. *Biochimica et biophysica acta, 1843*(8), 1674-1686. doi:10.1016/j.bbamcr.2013.10.019

Besrour-Aouam, N., Mohedano, M. L., Fhoula, I., Zarour, K., Najjari, A., Aznar, R., *et al.* (2019). Different modes of regulation of the expression of dextransucrase in *Leuconostoc lactis* AV1n and *Lactobacillus sakei* MN1. *Frontiers in Microbiology, 10*(959). doi:10.3389/fmicb.2019.00959

Bilova, T., Lukasheva, E., Brauch, D., Greifenhagen, U., Paudel, G., Tarakhovskaya, E., *et al.* (2016). A snapshot of the plant glycated proteome: Structural, functional and mechanistic aspects. *The Journal of biological chemistry, 291*(14), 7621-7636. doi:10.1074/jbc.M115.678581

Binder, T. P., Côté, G. L., & Robyt, J. F. (1983). Disproportionation reactions catalyzed by *Leuconostoc* and *Streptococcus* glucansucrases. *Carbohydrate Research, 124*(2), 275-286. doi:10.1016/0008-6215(83)88463-8

Bittner, M., de Souza, A. C., Brozova, M., Matoulkova, D., Dias, D. R., & Branyik, T. (2016). Adhesion of anaerobic beer spoilage bacteria *Megasphaera cerevisiae* and *Pectinatus frisingensis* to stainless steel. *LWT, 70*, 148-154. doi:10.1016/j.lwt.2016.02.044

Bivolarski, V., Vasileva, T., Gabriel, V., & Iliev, I. (2018). Synthesis of glucooligosaccharides with prebiotic potential by glucansucrase URE 13-300 acceptor reactions with maltose, raffinose and lactose. *Engineering in life sciences, 18*(12), 904-913. doi:10.1002/elsc.201800047

Blum, H., Beier, H., & Gross, H. J. (1987). Improved silver staining of plant proteins, RNA and DNA in polyacrylamide gels. *Electrophoresis, 8*(2), 93-99. doi:10.1002/elps.1150080203

Boban, N., Tonkic, M., Budimir, D., Modun, D., Sutlovic, D., Punda-Polic, V.*, et al.* (2010). Antimicrobial effects of wine: Separating the role of polyphenols, pH, ethanol, and other wine components. *Journal of Food Science, 75*(5), M322-M326. doi:10.1111/j.1750-3841.2010.01622.x

Bockwoldt, J. A., Stahl, L., Ehrmann, M. A., Vogel, R. F., & Jakob, F. (2020). Persistence and β-glucan formation of beer-spoiling lactic acid bacteria in wheat and rye sourdoughs. *Food Microbiology, 91*, 103539. doi:10.1016/j.fm.2020.103539

Böger, M., Hekelaar, J., van Leeuwen, S. S., Dijkhuizen, L., & Lammerts van Bueren, A. (2019). Structural and functional characterization of a family GH53 β-1,4-galactanase from *Bacteroides thetaiotaomicron* that facilitates degradation of prebiotic galactooligosaccharides. *Journal of Structural Biology, 205*(1), 1-10. doi:10.1016/j.jsb.2018.12.002

Bolotin, A., Wincker, P., Mauger, S., Jaillon, O., Malarme, K., Weissenbach, J.*, et al.* (2001). The complete genome sequence of the lactic acid bacterium *Lactococcus lactis* ssp. *lactis* IL1403. *Genome research, 11*(5), 731-753.

Bounaix, M.-S., Gabriel, V., Robert, H., Morel, S., Remaud-Siméon, M., Gabriel, B.*, et al.* (2010a). Characterization of glucan-producing *Leuconostoc* strains isolated from sourdough. *International Journal of Food Microbiology, 144*(1), 1-9. doi:10.1016/j.ijfoodmicro.2010.05.026

Bounaix, M.-S., Robert, H., Gabriel, V., Morel, S., Remaud-Siméon, M., Gabriel, B.*, et al.* (2010b). Characterization of dextran-producing *Weissella* strains isolated from sourdoughs and evidence of constitutive dextransucrase expression. *FEMS Microbiology Letters, 311*(1), 18-26. doi:10.1111/j.1574-6968.2010.02067.x

Bozonnet, S., Dols-Laffargue, M., Fabre, E., Pizzut, S., Remaud-Simeon, M., Monsan, P.*, et al.* (2002). Molecular characterization of DSR-E, an alpha-1,2 linkage-synthesizing dextransucrase with two catalytic domains. *Journal of bacteriology, 184*(20), 5753-5761. doi:10.1128/jb.184.20.5753-5761.2002

Bradford, M. M. (1976). A rapid and sensitive method for the quantitation of microgram quantities of protein utilizing the principle of protein-dye binding. *Analytical Biochemistry, 72*(1), 248-254. doi:10.1016/0003-2697(76)90527-3

Brison, Y., Malbert, Y., Czaplicki, G., Mourey, L., Remaud-Simeon, M., & Tranier, S. (2016). Structural insights into the carbohydrate binding ability of an α-(1→2) branching sucrase from glycoside hydrolase family 70. *Journal of Biological Chemistry, 291*(14), 7527-7540. doi:10.1074/jbc.M115.688796

Brison, Y., Pijning, T., Malbert, Y., Fabre, É., Mourey, L., Morel, S.*, et al.* (2012). Functional and structural characterization of α-(1->2) branching sucrase derived from DSR-E glucansucrase. *The Journal of biological chemistry, 287*(11), 7915-7924. doi:10.1074/jbc.M111.305078

Camacho, C., Coulouris, G., Avagyan, V., Ma, N., Papadopoulos, J., Bealer, K.*, et al.* (2009). BLAST+: architecture and applications. *BMC Bioinformatics, 10*(1), 421. doi:10.1186/1471-2105-10-421

Cantarel, B. L., Coutinho, P. M., Rancurel, C., Bernard, T., Lombard, V., & Henrissat, B. (2009). The Carbohydrate-Active EnZymes database (CAZy): an expert resource for glycogenomics. *Nucleic Acids Research, 37*(Database issue), D233-D238. doi:10.1093/nar/gkn663

Carattoli, A., Zankari, E., García-Fernández, A., Voldby Larsen, M., Lund, O., Villa, L.*, et al.* (2014). In silico detection and typing of plasmids using PlasmidFinder and plasmid multilocus sequence typing. *Antimicrobial agents and chemotherapy, 58*(7), 3895-3903. doi:10.1128/AAC.02412-14

Carr, J. G., & Davies, P. A. (1970). Homofermentative Lactobacilli of Ciders including *Lactobacillus mali* nov. spec. *Journal of Applied Bacteriology, 33*(4), 768-774. doi:10.1111/j.1365-2672.1970.tb02261.x

Casjens, S. (1998). The diverse and dynamic structure of bacterial genomes. *Annual Review of Genetics, 32*(1), 339-377. doi:10.1146/annurev.genet.32.1.339

Celebioglu, H. U., Olesen, S. V., Prehn, K., Lahtinen, S. J., Brix, S., Abou Hachem, M.*, et al.* (2017). Mucin- and carbohydrate-stimulated adhesion and subproteome changes of the probiotic bacterium *Lactobacillus acidophilus* NCFM. *Journal of Proteomics, 163*, 102-110. doi:10.1016/j.jprot.2017.05.015

Charbonneau, M.-È., Girard, V., Nikolakakis, A., Campos, M., Berthiaume, F., Dumas, F.*, et al.* (2007). O-Linked glycosylation ensures the normal conformation of the autotransporter adhesin involved in diffuse adherence. *Journal of bacteriology, 189*(24), 8880. doi:10.1128/JB.00969-07

Charrier, V., Buckley, E., Parsonage, D., Galinier, A., Darbon, E., Jaquinod, M.*, et al.* (1997). Cloning and sequencing of two Enterococcal glpK genes and regulation of the encoded glycerol kinases by phosphoenolpyruvate-dependent, phosphotransferase system-catalyzed phosphorylation of a single histidyl residue *Journal of Biological Chemistry, 272*(22), 14166-14174. doi:10.1074/jbc.272.22.14166

Cheetham, N. W. H., Slodki, M. E., & Walker, G. J. (1991). Structure of the linear, low molecular weight dextran synthesized by α-D-glucosyltransferase (GTF-S3) of *Streptococcus sobrinus*. *Carbohydrate Polymers, 16*(4), 341-353. doi:10.1016/0144-8617(91)90053-F

Choi, H., Kim, Y.-W., Hwang, I., Kim, J., & Yoon, S. (2012). Evaluation of *Leuconostoc citreum* HO12 and *Weissella koreensis* HO20 isolated from kimchi as a starter culture for whole wheat sourdough. *Food Chemistry, 134*(4), 2208-2216. doi:10.1016/j.foodchem.2012.04.047

Claes, I. J. J., Schoofs, G., Regulski, K., Courtin, P., Chapot-Chartier, M.-P., Rolain, T.*, et al.* (2012). Genetic and biochemical characterization of the cell wall hydrolase activity of the major secreted protein of *Lactobacillus rhamnosus* GG. *PLOS ONE, 7*(2), e31588-e31588. doi:10.1371/journal.pone.0031588

Claverie, M., Cioci, G., Vuillemin, M., Bondy, P., Remaud-Simeon, M., & Moulis, C. (2020). Processivity of dextransucrases synthesizing very-high-molar-mass dextran is mediated by sugar-binding pockets in domain V. *Journal of Biological Chemistry, 295*(17), 5602-5613. doi:10.1074/jbc.RA119.011995

Condon, S. (1987). Responses of lactic acid bacteria to oxygen. *FEMS Microbiology Reviews, 3*(3), 269-280. doi:10.1111/j.1574-6968.1987.tb02465.x

Côté, G. L. (2009). Acceptor products of alternansucrase with gentiobiose. Production of novel oligosaccharides for food and feed and elimination of bitterness. *Carbohydrate Research, 344*(2), 187-190. doi:10.1016/j.carres.2008.10.017

Côté, G. L., Dunlap, C. A., & Vermillion, K. E. (2009). Glucosylation of raffinose via alternansucrase acceptor reactions. *Carbohydrate Research, 344*(15), 1951-1959. doi:10.1016/j.carres.2009.06.023

Côté, G. L., & Leathers, T. D. (2005). A method for surveying and classifying *Leuconostoc* spp. glucansucrases according to strain-dependent acceptor product patterns. *Journal of Industrial Microbiology and Biotechnology, 32*(2), 53-60. doi:10.1007/s10295-004-0194-x

Côté, G. L., & Skory, C. D. (2012). Cloning, expression, and characterization of an insoluble glucan-producing glucansucrase from *Leuconostoc mesenteroides* NRRL B-1118. *Applied Microbiology and Biotechnology, 93*(6), 2387-2394. doi:10.1007/s00253-011-3562-2

Côté, G. L., Skory, C. D., Unser, S. M., & Rich, J. O. (2013). The production of glucans via glucansucrases from *Lactobacillus satsumensis* isolated from a fermented beverage starter culture. *Applied Microbiology and Biotechnology, 97*(16), 7265-7273. doi:10.1007/s00253-012-4606-y

Cousin, F. J., Lynch, S. M., Harris, H. M. B., McCann, A., Lynch, D. B., Neville, B. A.*, et al.* (2015). Detection and genomic characterization of motility in *Lactobacillus curvatus*: Confirmation of motility in a species outside the *Lactobacillus salivarius* clade. *Applied and Environmental Microbiology, 81*(4), 1297. doi:10.1128/AEM.03594-14

Cox, J., & Mann, M. (2008). MaxQuant enables high peptide identification rates, individualized ppb-range mass accuracies and proteome-wide protein quantification. *Nature Biotechnology, 26*(12), 1367-1372. doi:10.1038/nbt.1511

Cox, J., Neuhauser, N., Michalski, A., Scheltema, R. A., Olsen, J. V., & Mann, M. (2011). Andromeda: a peptide search engine integrated into the MaxQuant environment. *Journal of proteome research, 10*(4), 1794-1805.

Craig, W. J. (2010). Nutrition concerns and health effects of vegetarian diets. *Nutrition in Clinical Practice, 25*(6), 613-620. doi:10.1177/0884533610385707

Crow, V. L., & Pritchard, G. G. (1977). Fructose 1,6-diphosphate-activated L-lactate dehydrogenase from *Streptococcus lactis*: kinetic properties and factors affecting activation. *Journal of bacteriology, 131*(1), 82.

Darbon, E., Servant, P., Poncet, S., & Deutscher, J. (2002). Antitermination by GlpP, catabolite repression via CcpA and inducer exclusion triggered by P~GlpK dephosphorylation control Bacillus subtilis glpFK expression. *Molecular Microbiology, 43*(4), 1039-1052. doi:10.1046/j.1365-2958.2002.02800.x

Darling, A. C. E., Mau, B., Blattner, F. R., & Perna, N. T. (2004). Mauve: multiple alignment of conserved genomic sequence with rearrangements. *Genome research, 14*(7), 1394-1403. doi:10.1101/gr.2289704

Davray, D., Deo, D., & Kulkarni, R. (2020). Plasmids encode niche-specific traits in *Lactobacillaceae*. *Microbial Genomics*. doi:10.1099/mgen.0.000472

De Angelis, M., Calasso, M., Cavallo, N., Di Cagno, R., & Gobbetti, M. (2016). Functional proteomics within the genus *Lactobacillus*. *PROTEOMICS, 16*(6), 946-962. doi:10.1002/pmic.201500117

De Fátima Alvarez, M., Medina, R., Pasteris, S. E., Strasser de Saad, A. M., & Sesma, F. (2004). Glycerol metabolism of *Lactobacillus rhamnosus* ATCC 7469: cloning and expression of two glycerol kinase genes. *Microbial Physiology, 7*(4), 170-181. doi:10.1159/000079826

De Man, J. C., Rogosa, M., & Sharpe, M. E. (1960). A medium for the cultivation of lactobacilli. *Journal of Applied Bacteriology, 23*(1), 130-135. doi:10.1111/j.1365-2672.1960.tb00188.x

De Vuyst, L., & Degeest, B. (1999). Heteropolysaccharides from lactic acid bacteria. *FEMS Microbiology Reviews, 23*(2), 153-177. doi:10.1111/j.1574-6976.1999.tb00395.x

De Vuyst, L., & Leroy, F. (2007). Bacteriocins from lactic acid bacteria: Production, purification, and food applications. *Microbial Physiology, 13*(4), 194-199. doi:10.1159/000104752

Demuth, K., Jördening, H.-J., & Buchholz, K. (2002). Oligosaccharide synthesis by dextransucrase: new unconventional acceptors. *Carbohydrate Research, 337*(20), 1811-1820. doi:10.1016/S0008-6215(02)00272-0

Deppe, V. M., Bongaerts, J., O'Connell, T., Maurer, K.-H., & Meinhardt, F. (2011a). Enzymatic deglycation of Amadori products in bacteria: mechanisms, occurrence and physiological functions. *Applied Microbiology and Biotechnology, 90*(2), 399-406. doi:10.1007/s00253-010-3083-4

Deppe, V. M., Klatte, S., Bongaerts, J., Maurer, K.-H., O'Connell, T., & Meinhardt, F. (2011b). Genetic control of amadori product degradation in *Bacillus subtilis* via regulation of frlBONMD expression by FrlR. *Applied and Environmental Microbiology, 77*(9), 2839-2846. doi:10.1128/AEM.02515-10

Dertli, E., Colquhoun, I. J., Gunning, A. P., Bongaerts, R. J., Le Gall, G., Bonev, B. B.*, et al.* (2013). Structure and biosynthesis of two exopolysaccharides produced by *Lactobacillus johnsonii* FI9785*. *Journal of Biological Chemistry, 288*(44), 31938-31951. doi:10.1074/jbc.M113.507418

Deutscher, J., Francke, C., & Postma, P. W. (2006). How phosphotransferase system-related protein phosphorylation regulates carbohydrate metabolism in bacteria. *Microbiology and Molecular Biology Reviews, 70*(4), 939. doi:10.1128/MMBR.00024-06

Devulapalle, K. S., Goodman, S. D., Gao, Q., Hemsley, A., & Mooser, G. (1997). Knowledge-based model of a glucosyltransferase from the oral bacterial group of mutans streptococci. *Protein Science, 6*(12), 2489-2493. doi:10.1002/pro.5560061201

Dicks, L. M., & Endo, A. (2009). Taxonomic status of lactic acid bacteria in wine and key characteristics to differentiate species. *South African journal of enology and viticulture, 30*(1), 72-90.

Dimopoulou, M., Vuillemin, M., Campbell-Sills, H., Lucas, P. M., Ballestra, P., Miot-Sertier, C.*, et al.* (2014). Exopolysaccharide (EPS) synthesis by *Oenococcus oeni*: From genes to phenotypes. *PLOS ONE, 9*(6), e98898. doi:10.1371/journal.pone.0098898

Doi, Y. (2015). L-lactate production from biodiesel-derived crude glycerol by metabolically engineered *Enterococcus faecalis*: cytotoxic evaluation of biodiesel waste and development of a glycerol-inducible gene expression system. *Applied and Environmental Microbiology, 81*(6), 2082. doi:10.1128/AEM.03418-14

Doi, Y. (2019). Glycerol metabolism and its regulation in lactic acid bacteria. *Applied Microbiology and Biotechnology, 103*(13), 5079-5093. doi:10.1007/s00253-019-09830-y

Donlan, R. M. (2002). Biofilms: microbial life on surfaces. *Emerging infectious diseases, 8*(9), 881-890. doi:10.3201/eid0809.020063

Douglas, H. C., & Cruess, W. V. (1936). A Lactobacillus from California wine: *Lactobacillus hilgardii*. *Journal of Food Science, 1*(2), 113-119. doi:10.1111/j.1365-2621.1936.tb17774.x

Eckel, V. (2020). *Lifestyle and functional properties of lactobacilli and bifidobacteria in water kefir.* (Dissertation), Technical University Munich, Munich.

Eckel, V., & Vogel, R. (2020a). Genomic and physiological insights into the lifestyle of *Bifidobacterium* species from water kefir. *Archives of Microbiology, 202*(7), 1627-1637. doi:10.1007/s00203-020-01870-7

Eckel, V., Vogel, R. F., & Jakob, F. (2019). *In situ* production and characterization of cloud forming dextrans in fruit-juices. *International Journal of Food Microbiology, 306*, 108261. doi:10.1016/j.ijfoodmicro.2019.108261

Eckel, V., Ziegler, L.-M., Vogel, R., & Ehrmann, M. (2020b). *Bifidobacterium tibiigranuli* sp. nov. isolated from homemade water kefir. *International Journal of Systematic and Evolutionary Microbiology, 70*(3), 1562-1570. doi:10.1099/ijsem.0.003936

Edwards, C. G., Collins, M. D., Lawson, P. A., & Rodriguez, A. V. (2000). *Lactobacillus nagelii* sp. nov., an organism isolated from a partially fermented wine. *International Journal of Systematic and Evolutionary Microbiology, 50*(2), 699-702. doi:10.1099/00207713-50-2-699

Efiuvwevwere, B. J. O., Gorris, L. G. M., Smid, E. J., & Kets, E. P. W. (1999). Mannitol-enhanced survival of *Lactococcus lactis* subjected to drying. *Applied Microbiology and Biotechnology, 51*(1), 100-104. doi:10.1007/s002530051369

Emms, D. M., & Kelly, S. (2019). OrthoFinder: phylogenetic orthology inference for comparative genomics. *Genome Biology, 20*(1), 238. doi:10.1186/s13059-019-1832-y

Endo, A., & Okada, S. (2005). *Lactobacillus satsumensis* sp. nov., isolated from mashes of shochu, a traditional Japanese distilled spirit made from fermented rice and other starchy materials. *International Journal of Systematic and Evolutionary Microbiology, 55*(1), 83-85. doi:10.1099/ijs.0.63248-0

Engel, K.-H., Vogel, R. F., Knorr, D., Habermeyer, M., Kochte-Clemens, B., & Eisenbrand, G. (2011). The role of the concept of "history of safe use" in the safety assessment of novel foods and novel food ingredients. Opinion of the Senate Commission on Food Safety (SKLM) of the German Research Foundation (DFG). *Molecular Nutrition & Food Research, 55*(6), 957-963. doi:10.1002/mnfr.201100206

Erbersdobler, H. F., & Faist, V. (2001). Metabolic transit of Amadori products. *Food / Nahrung, 45*(3), 177-181. doi:10.1002/1521-3803(20010601)45:3<177::AID-FOOD177>3.0.CO;2-A

Espino, E., Koskenniemi, K., Mato-Rodriguez, L., Nyman, T. A., Reunanen, J., Koponen, J.*, et al.* (2015). Uncovering surface-exposed antigens of *Lactobacillus rhamnosus* by cell shaving proteomics and two-dimensional immunoblotting. *Journal of proteome research, 14*(2), 1010-1024. doi:10.1021/pr501041a

Falconer, D. J., Mukerjea, R., & Robyt, J. F. (2011). Biosynthesis of dextrans with different molecular weights by selecting the concentration of *Leuconostoc mesenteroides* B-512FMC dextransucrase, the sucrose concentration, and the temperature. *Carbohydrate Research, 346*(2), 280-284. doi:10.1016/j.carres.2010.10.024

Fehér, A., Gazdecki, M., Véha, M., Szakály, M., & Szakály, Z. (2020). A comprehensive review of the benefits of and the barriers to the switch to a plant-based diet. *Sustainability, 12*(10). doi:10.3390/su12104136

Fels, L., Jakob, F., Vogel, R. F., & Wefers, D. (2018). Structural characterization of the exopolysaccharides from water kefir. *Carbohydrate Polymers, 189*, 296-303. doi:10.1016/j.carbpol.2018.02.037

Felsenstein, J. (1981). Evolutionary trees from DNA sequences: A maximum likelihood approach. *Journal of Molecular Evolution, 17*(6), 368-376. doi:10.1007/BF01734359

Fernández-Tornero, C., López, R., García, E., Giménez-Gallego, G., & Romero, A. (2001). A novel solenoid fold in the cell wall anchoring domain of the pneumococcal virulence factor LytA. *Nature Structural Biology, 8*(12), 1020-1024. doi:10.1038/nsb724

Finkenstadt, V. L., Côté, G. L., & Willett, J. L. (2011). Corrosion protection of low-carbon steel using exopolysaccharide coatings from *Leuconostoc mesenteroides*. *Biotechnology Letters, 33*(6), 1093-1100. doi:10.1007/s10529-011-0539-2

Fiorda, F. A., de Melo Pereira, G. V., Thomaz-Soccol, V., Rakshit, S. K., Pagnoncelli, M. G. B., Vandenberghe, L. P. d. S., *et al.* (2017). Microbiological, biochemical, and functional aspects of sugary kefir fermentation - A review. *Food Microbiology, 66*, 86-95. doi:10.1016/j.fm.2017.04.004

Flemming, H.-C., & Wingender, J. (2010). The biofilm matrix. *Nature Reviews Microbiology, 8*(9), 623-633. doi:10.1038/nrmicro2415

Forssten, S. D., Björklund, M., & Ouwehand, A. C. (2010). *Streptococcus mutans*, caries and simulation models. *Nutrients, 2*(3). doi:10.3390/nu2030290

Fostier, J., Proost, S., Dhoedt, B., Saeys, Y., Demeester, P., Van de Peer, Y., *et al.* (2011). A greedy, graph-based algorithm for the alignment of multiple homologous gene lists. *Bioinformatics, 27*(6), 749-756. doi:10.1093/bioinformatics/btr008

Frank, A., & Pevzner, P. (2005). PepNovo: de novo peptide sequencing via probabilistic network modeling. *Analytical Chemistry, 77*(4), 964-973. doi:10.1021/ac048788h

Fraunhofer, M. E., Geissler, A. J., Wefers, D., Bunzel, M., Jakob, F., & Vogel, R. F. (2018). Characterization of β-glucan formation by *Lactobacillus brevis* TMW 1.2112 isolated from slimy spoiled beer. *International Journal of Biological Macromolecules, 107*, 874-881. doi:10.1016/j.ijbiomac.2017.09.063

Freitas, F., Alves, V. D., & Reis, M. A. M. (2011). Advances in bacterial exopolysaccharides: from production to biotechnological applications. *Trends in Biotechnology, 29*(8), 388-398. doi:10.1016/j.tibtech.2011.03.008

Frohberg, C., & Pilling, J. (2009). Germany Patent No.: B. C. AG.

Funane, K., Ishii, T., Ono, H., & Kobayashi, M. (2005). Changes in linkage pattern of glucan products induced by substitution of Lys residues in the dextransucrase. *FEBS Letters, 579*(21), 4739-4745. doi:10.1016/j.febslet.2005.07.050

Funane, K., Ookura, T., & Kobayashi, M. (1998). Glucan binding regions of dextransucrase from *Leuconostoc mesenteroides* NRRL B-512F. *Bioscience, Biotechnology, and Biochemistry, 62*(1), 123-127. doi:10.1271/bbb.62.123

Gagic, D., Wen, W., Collett, M. A., & Rakonjac, J. (2013). Unique secreted-surface protein complex of *Lactobacillus rhamnosus*, identified by phage display. *MicrobiologyOpen, 2*(1), 1-17. doi:10.1002/mbo3.53

Galié, S., García-Gutiérrez, C., Miguélez, E. M., Villar, C. J., & Lombó, F. (2018). Biofilms in the food industry: health aspects and control methods. *Frontiers in Microbiology, 9*, 898-898. doi:10.3389/fmicb.2018.00898

Galle, S., Schwab, C., Arendt, E., & Gänzle, M. (2010). Exopolysaccharide-forming *Weissella* strains as starter cultures for sorghum and wheat sourdoughs. *Journal of Agricultural and Food Chemistry, 58*(9), 5834-5841. doi:10.1021/jf1002683

Galle, S., Schwab, C., Bello, F. D., Coffey, A., Gänzle, M., & Arendt, E. (2012). Comparison of the impact of dextran and reuteran on the quality of wheat sourdough bread. *Journal of Cereal Science, 56*(3), 531-537. doi:10.1016/j.jcs.2012.07.001

Gangoiti, J., Pijning, T., & Dijkhuizen, L. (2018). Biotechnological potential of novel glycoside hydrolase family 70 enzymes synthesizing α-glucans from starch and sucrose. *Biotechnology Advances, 36*(1), 196-207. doi:10.1016/j.biotechadv.2017.11.001

Gangoiti, J., van Leeuwen, S. S., Gerwig, G. J., Duboux, S., Vafiadi, C., Pijning, T., *et al.* (2017). 4,3-α-Glucanotransferase, a novel reaction specificity in glycoside hydrolase family 70 and clan GH-H. *Scientific Reports, 7*(1), 39761. doi:10.1038/srep39761

Gänzle, M. G., Haase, G., & Jelen, P. (2008). Lactose: Crystallization, hydrolysis and value-added derivatives. *International Dairy Journal, 18*(7), 685-694. doi:10.1016/j.idairyj.2008.03.003

Gardy, J. L., Laird, M. R., Chen, F., Rey, S., Walsh, C. J., Ester, M., *et al.* (2005). PSORTb v.2.0: Expanded prediction of bacterial protein subcellular localization and insights gained from comparative proteome analysis. *Bioinformatics, 21*(5), 617-623. doi:10.1093/bioinformatics/bti057

Garrigues, C., Loubiere, P., Lindley, N. D., & Cocaign-Bousquet, M. (1997). Control of the shift from homolactic acid to mixed-acid fermentation in *Lactococcus lactis*: predominant role of the NADH/NAD+ ratio. *Journal of bacteriology, 179*(17), 5282. doi:10.1128/jb.179.17.5282-5287.1997

Germaine, G. R., Chludzinski, A. M., & Schachtele, C. F. (1974). *Streptococcus mutans* dextransucrase: requirement for primer dextran. *Journal of bacteriology, 120*(1), 287-294. doi:10.1128/JB.120.1.287-294.1974

Gibson, G. R., & Roberfroid, M. B. (1995). Dietary modulation of the human colonic microbiota: Introducing the concept of prebiotics. *The Journal of Nutrition, 125*(6), 1401-1412. doi:10.1093/jn/125.6.1401

Giraffa, G. (2004). Studying the dynamics of microbial populations during food fermentation. *FEMS Microbiology Reviews, 28*(2), 251-260. doi:10.1016/j.femsre.2003.10.005

Golowczyc, M. A., Mobili, P., Garrote, G. L., Abraham, A. G., & De Antoni, G. L. (2007). Protective action of *Lactobacillus kefir* carrying S-layer protein against *Salmonella enterica* serovar *enteritidis*. *International Journal of Food Microbiology, 118*(3), 264-273. doi:10.1016/j.ijfoodmicro.2007.07.042

Gonçalves, C., Ferreira, C., Gonçalves, L. G., Turner, D. L., Leandro, M. J., Salema-Oom, M., *et al.* (2019). A new pathway for mannitol metabolism in yeasts suggests a link to the evolution of alcoholic fermentation. *Frontiers in Microbiology, 10*, 2510-2510. doi:10.3389/fmicb.2019.02510

Goris, J., Konstantinidis, K. T., Klappenbach, J. A., Coenye, T., Vandamme, P., & Tiedje, J. M. (2007). DNA–DNA hybridization values and their relationship to whole-genome sequence similarities. *International Journal of Systematic and Evolutionary Microbiology, 57*(1), 81-91. doi:10.1099/ijs.0.64483-0

Goulter, K. C., Hashimi, S. M., & Birch, R. G. (2012). Microbial sucrose isomerases: Producing organisms, genes and enzymes. *Enzyme and Microbial Technology, 50*(1), 57-64. doi:10.1016/j.enzmictec.2011.09.011

Grobben, G. J., Smith, M. R., Sikkema, J., & de Bont, J. A. M. (1996). Influence of fructose and glucose on the production of exopolysaccharides and the activities of enzymes involved in the sugar metabolism and the synthesis of sugar nucleotides in *Lactobacillus delbrueckii* subsp. *bulgaricus* NCFB 2772. *Applied Microbiology and Biotechnology, 46*(3), 279-284. doi:10.1007/s002530050817

Gulitz, A. (2013). *Analysis of the diversity of water kefir microbiota by culture-dependent and -independent approaches.* (Dissertation), Technical University Munich, Munich.

Gulitz, A., Stadie, J., Ehrmann, M. A., Ludwig, W., & Vogel, R. F. (2013). Comparative phylobiomic analysis of the bacterial community of water kefir by 16S rRNA gene amplicon sequencing and ARDRA analysis. *Journal of Applied Microbiology, 114*(4), 1082-1091. doi:10.1111/jam.12124

Gulitz, A., Stadie, J., Wenning, M., Ehrmann, M. A., & Vogel, R. F. (2011). The microbial diversity of water kefir. *International Journal of Food Microbiology, 151*(3), 284-288. doi:10.1016/j.ijfoodmicro.2011.09.016

Hector, S., Willard, K., Bauer, R., Mulako, I., Slabbert, E., Kossmann, J., *et al.* (2015). Diverse exopolysaccharide producing bacteria isolated from milled sugarcane: implications for cane spoilage and sucrose yield. *PLOS ONE, 10*(12), e0145487-e0145487. doi:10.1371/journal.pone.0145487

Heinze, S., Zimmermann, K., Ludwig, C., Heinzlmeir, S., Schwarz, W. H., Zverlov, V. V., *et al.* (2018). Evaluation of promoter sequences for the secretory production of a Clostridium thermocellum cellulase in Paenibacillus polymyxa. *Applied Microbiology and Biotechnology, 102*(23), 10147-10159. doi:10.1007/s00253-018-9369-7

Hellmuth, H., Wittrock, S., Kralj, S., Dijkhuizen, L., Hofer, B., & Seibel, J. (2008). Engineering the glucansucrase GTFR enzyme reaction and glycosidic bond specificity: toward tailor-made polymer and oligosaccharide products. *Biochemistry, 47*(25), 6678-6684. doi:10.1021/bi800563r

Helmrich, A., Ballarino, M., Nudler, E., & Tora, L. (2013). Transcription-replication encounters, consequences and genomic instability. *Nature Structural & Molecular Biology, 20*(4), 412-418. doi:10.1038/nsmb.2543

Henry, R. J. (1988). The carbohydrates of barley grains - a review. *Journal of the Institute of Brewing, 94*(2), 71-78. doi:10.1002/j.2050-0416.1988.tb04560.x

Henstra, S. A., Duurkens, R. H., & Robillard, G. T. (2000). Multiple phosphorylation events regulate the activity of the mannitol transcriptional regulator MtlR of the *Bacillus stearothermophilus* phosphoenolpyruvate-dependent mannitol phosphotransferase system. *Journal of Biological Chemistry, 275*(10), 7037-7044. doi:10.1074/jbc.275.10.7037

Henstra, S. A., Tuinhof, M., Duurkens, R. H., & Robillard, G. T. (1999). The *Bacillus stearothermophilus* mannitol regulator, MtlR, of the phosphotransferase system. *Journal of Biological Chemistry, 274*(8), 4754-4763. doi:10.1074/jbc.274.8.4754

Herlihey, F. A., Moynihan, P. J., & Clarke, A. J. (2014). The essential protein for bacterial flagella formation FlgJ functions as a β-N-acetylglucosaminidase. *Journal of Biological Chemistry, 289*(45), 31029-31042. doi:10.1074/jbc.M114.603944

Hilbig, J., Hildebrandt, L., Herrmann, K., Weiss, J., & Loeffler, M. (2020). Influence of homopolysaccharide-producing lactic acid bacteria on the spreadability of raw fermented sausages (onion mettwurst). *Journal of Food Science, 85*(2), 289-297. doi:10.1111/1750-3841.15010

Hines, J. K., Fromm, H. J., & Honzatko, R. B. (2007). Structures of activated fructose-1,6-bisphosphatase from *Escherichia coli*: Coordinate regulation of bacterial metabolism and the conservation of the R-state. *Journal of Biological Chemistry, 282*(16), 11696-11704. doi:10.1074/jbc.M611104200

Hinz, S. W. A., Pastink, M. I., van den Broek, L. A. M., Vincken, J.-P., & Voragen, A. G. J. (2005). *Bifidobacterium longum* endogalactanase liberates galactotriose from type I galactans. *Applied and Environmental Microbiology, 71*(9), 5501-5510. doi:10.1128/AEM.71.9.5501-5510.2005

Hoshino, T., Fujiwara, T., & Kawabata, S. (2012). Evolution of cariogenic character in *Streptococcus mutans*: horizontal transmission of glycosyl hydrolase family 70 genes. *Scientific Reports, 2*(1), 518. doi:10.1038/srep00518

Howard, J. M., Ebert, R. V., Bloom, W. L., & Sloan, M. H. (1959). The present status of dextran as a plasma expander. *The American Journal of Surgery, 97*(5), 593-596. doi:10.1016/0002-9610(59)90251-X

Hugenholtz, J. (1993). Citrate metabolism in lactic acid bacteria. *FEMS Microbiology Reviews, 12*(1-3), 165-178. doi:10.1111/j.1574-6976.1993.tb00017.x

Hugenholtz, J. (2008). The lactic acid bacterium as a cell factory for food ingredient production. *International Dairy Journal, 18*(5), 466-475. doi:10.1016/j.idairyj.2007.11.015

Hugenschmidt, S., Schwenninger, S. M., Gnehm, N., & Lacroix, C. (2010). Screening of a natural biodiversity of lactic and propionic acid bacteria for folate and vitamin B12 production in supplemented whey permeate. *International Dairy Journal, 20*(12), 852-857. doi:10.1016/j.idairyj.2010.05.005

Hughes, D. (1995). Animal welfare. *British Food Journal, 97*(10), 3-7. doi:10.1108/00070709510104529

Huptas, C., Scherer, S., & Wenning, M. (2016). Optimized Illumina PCR-free library preparation for bacterial whole genome sequencing and analysis of factors influencing *de novo* assembly. *BMC research notes, 9*, 269. doi:10.1186/s13104-016-2072-9

Ibarburu, I., Soria-Díaz, M. E., Rodríguez-Carvajal, M. A., Velasco, S. E., Tejero-Mateo, P., Gil-Serrano, A. M.*, et al.* (2007). Growth and exopolysaccharide (EPS) production by *Oenococcus oeni* I4 and structural characterization of their EPSs. *Journal of Applied Microbiology, 103*(2), 477-486. doi:10.1111/j.1365-2672.2006.03266.x

Imeson, A. (2010). *Food stabilizers, thickeners and gelling agents*. Chichester, UK: Wiley-Blackwell Publishing Ltd.

Irague, R., Massou, S., Moulis, C., Saurel, O., Milon, A., Monsan, P.*, et al.* (2011). NMR-based structural glycomics for high-throughput screening of carbohydrate-active enzyme specificity. *Analytical Chemistry, 83*(4), 1202-1206. doi:10.1021/ac1032148

Irisawa, T., & Okada, S. (2009). *Lactobacillus sucicola* sp. nov., a motile lactic acid bacterium isolated from oak tree (*Quercus* sp.) sap. *International Journal of Systematic and Evolutionary Microbiology, 59*(11), 2662-2665. doi:10.1099/ijs.0.006478-0

Ito, K., Ito, S., Shimamura, T., Weyand, S., Kawarasaki, Y., Misaka, T.*, et al.* (2011). Crystal structure of glucansucrase from the dental caries pathogen *Streptococcus mutans*. *Journal of Molecular Biology, 408*(2), 177-186. doi:10.1016/j.jmb.2011.02.028

Jakob, F., Gebrande, C., Bichler, R. M., & Vogel, R. F. (2020). Insights into the pH-dependent, extracellular sucrose utilization and concomitant levan formation by *Gluconobacter albidus* TMW 2.1191. *Antonie van Leeuwenhoek, 113*(7), 863-873. doi:10.1007/s10482-020-01397-3

Jakob, F., Meißner, D., & Vogel, R. F. (2012). Comparison of novel GH 68 levansucrases of levan-overproducing *Gluconobacter* species. *Acetic Acid Bacteria, 1*(1), e2. doi:10.4081/aab.2012.e2

Janeček, Š., Svensson, B., & Russell, R. R. B. (2000). Location of repeat elements in glucansucrases of Leuconostoc and Streptococcus species. *FEMS Microbiology Letters, 192*(1), 53-57. doi:10.1111/j.1574-6968.2000.tb09358.x

Jones, D. T., Taylor, W. R., & Thornton, J. M. (1992). The rapid generation of mutation data matrices from protein sequences. *Bioinformatics, 8*(3), 275-282. doi:10.1093/bioinformatics/8.3.275

Ju, L.-K., & Ho, C. S. (1986). The measurement of oxygen diffusion coefficients in polymeric solutions. *Chemical Engineering Science, 41*(3), 579-589. doi:10.1016/0009-2509(86)87040-3

Juffs, H. S., & Babel, F. J. (1975). Inhibition of psychrotrophic bacteria by lactic cultures in milk stored at low temperature. *Journal of Dairy Science, 58*(11), 1612-1619. doi:10.3168/jds.S0022-0302(75)84759-X

Kahm, M., Hasenbrink, G., Lichtenberg-Frate, H., Ludwig, J., & Kschischo, M. (2010). Grofit: Fitting biological growth curves. *Nature Precedings*. doi:10.1038/npre.2010.4508.1

Karatan, E., & Watnick, P. (2009). Signals, regulatory networks, and materials that build and break bacterial biofilms. *Microbiology and Molecular Biology Reviews, 73*(2), 310. doi:10.1128/MMBR.00041-08

Kebler, L. F. (1921). California bees. *The Journal of the American Pharmaceutical Association (1912), 10*(12), 939-943.

Kets, E. P., Galinski, E. A., de Wit, M., de Bont, J. A., & Heipieper, H. J. (1996). Mannitol, a novel bacterial compatible solute in *Pseudomonas putida* S12. *Journal of bacteriology, 178*(23), 6665-6670. doi:10.1128/jb.178.23.6665-6670.1996

Kim, D., & Robyt, J. F. (1994). Production and selection of mutants of *Leuconostoc mesenteroides* constitutive for glucansucrases. *Enzyme and Microbial Technology, 16*(8), 659-664. doi:10.1016/0141-0229(94)90086-8

Kim, D., Robyt, J. F., Lee, S.-Y., Lee, J.-H., & Kim, Y.-M. (2003). Dextran molecular size and degree of branching as a function of sucrose concentration, pH, and temperature of reaction of *Leuconostoc mesenteroides* B-512FMCM dextransucrase. *Carbohydrate Research, 338*(11), 1183-1189. doi:10.1016/s0008-6215(03)00148-4

Kim, M., Jang, J.-K., & Park, Y.-S. (2021). Production optimization, structural analysis, and prebiotic- and anti-inflammatory effects of gluco-oligosaccharides produced by *Leuconostoc lactis* SBC001. *Microorganisms, 9*(1). doi:10.3390/microorganisms9010200

Kim, M. J., Seo, H. N., Hwang, T. S., Lee, S. H., & Park, D. H. (2008). Characterization of exopolysaccharide (EPS) produced by *Weissella hellenica* SKkimchi3 isolated from kimchi. *The Journal of Microbiology, 46*(5), 535-541. doi:10.1007/s12275-008-0134-y

Kim, Y.-M., Yeon, M. J., Choi, N.-S., Chang, Y.-H., Jung, M. Y., Song, J. J., *et al.* (2010). Purification and characterization of a novel glucansucrase from *Leuconostoc lactis* EG001. *Microbiological Research, 165*(5), 384-391. doi:10.1016/j.micres.2009.08.005

Kingston, K. B., Allen, D. M., & Jacques, N. A. (2002). Role of the C-terminal YG repeats of the primer-dependent streptococcal glucosyltransferase, GtfJ, in binding to dextran and mutan. *Microbiology, 148*(2), 549-558. doi:10.1099/00221287-148-2-549

Kirby, A. J., & Hollfelder, F. (2008). Enzymes under the nanoscope. *Nature, 456*(7218), 45-47. doi:10.1038/456045a

Kirchberger, P. C., Schmidt, M. L., & Ochman, H. (2020). The ingenuity of bacterial genomes. *Annual Review of Microbiology, 74*(1), 815-834. doi:10.1146/annurev-micro-020518-115822

Koditschek, L. K., & Umbreit, W. W. (1969). α-Glycerophosphate oxidase in *Streptococcus faecium* F 24. *Journal of bacteriology, 98*(3), 1063.

Koepsell, H. J., Tsuchiya, H. M., Hellman, N. N., Kazenko, A., Hoffman, C. A., Sharpe, E. S., *et al.* (1953). Enzymatic synthesis of dextran: acceptor specificity and chain initiation. *Journal of Biological Chemistry, 200*(2), 793-801.

Koh, W. Y., Utra, U., Ahmad, R., Rather, I. A., & Park, Y.-H. (2018). Evaluation of probiotic potential and anti-hyperglycemic properties of a novel *Lactobacillus* strain isolated from water kefir grains. *Food Science and Biotechnology, 27*(5), 1369-1376. doi:10.1007/s10068-018-0360-y

Kolde, R. (2018). pheatmaps: pretty heatmaps (Version 1.0.12) [R-package].

Korkeala, H., Suortti, T., & Mäkelä, P. (1988). Ropy slime formation in vacuum-packed cooked meat products caused by homofermentative lactobacilli and a *Leuconostoc* species. *International Journal of Food Microbiology, 7*(4), 339-347. doi:10.1016/0168-1605(88)90060-8

Kralj, S., Grijpstra, P., van Leeuwen, S. S., Leemhuis, H., Dobruchowska, J. M., van der Kaaij, R. M., *et al.* (2011). 4,6-α-glucanotransferase, a novel enzyme that structurally and functionally provides an evolutionary link between glycoside hydrolase enzyme families 13 and 70. *Applied and Environmental Microbiology, 77*(22), 8154. doi:10.1128/AEM.05735-11

Kralj, S., van Geel-Schutten, G. H., van der Maarel, M. J. E. C., & Dijkhuizen, L. (2004). Biochemical and molecular characterization of *Lactobacillus reuteri* 121 reuteransucrase. *Microbiology, 150*(7), 2099-2112. doi:10.1099/mic.0.27105-0

Kralj, S., van Geel-Schutten, I. G. H., Faber, E. J., van der Maarel, M. J. E. C., & Dijkhuizen, L. (2005). Rational transformation of *Lactobacillus reuteri* 121 reuteransucrase into a dextransucrase. *Biochemistry, 44*(25), 9206-9216. doi:10.1021/bi050447q

Krassowski, M. (2021). ComplexUpset (Version 1.1.0) [R-package].

Kristjánsson, M. M., & Kinsella, J. E. (1991). Protein and enzyme stability: Structural, thermodynamic, and experimental aspects. In J. E. Kinsella (Ed.), *Advances in Food and Nutrition Research* (Vol. 35, pp. 237-316): Academic Press.

Krzywinski, M. I., Schein, J. E., Birol, I., Connors, J., Gascoyne, R., Horsman, D., *et al.* (2009). Circos: An information aesthetic for comparative genomics. *Genome research*. doi:10.1101/gr.092759.109

Kubota, H., Senda, S., Tokuda, H., Uchiyama, H., & Nomura, N. (2009). Stress resistance of biofilm and planktonic *Lactobacillus plantarum* subsp. *plantarum* JCM 1149. *Food Microbiology, 26*(6), 592-597. doi:10.1016/j.fm.2009.04.001

Kumar, S., Stecher, G., & Tamura, K. (2016). MEGA7: molecular evolutionary genetics analysis version 7.0 for bigger datasets. *Molecular Biology and Evolution, 33*(7), 1870-1874. doi:10.1093/molbev/msw054

Kushner, S. R. (1978). An improved method for transformation of Escherichia coli with ColE1-derived plasmids. *Genetic Engineering, Elsevier, 173*, 17-23.

Kwon, M., Hussain, M. S., & Oh, D. H. (2017). Biofilm formation of *Bacillus cereus* under food-processing-related conditions. *Food Science and Biotechnology, 26*(4), 1103-1111. doi:10.1007/s10068-017-0129-8

Laemmli, U. K. (1970). Cleavage of structural proteins during the assembly of the head of bacteriophage T4. *Nature, 227*(5259), 680-685. doi:10.1038/227680a0

Lambert, P. A., Hancock, I. C., & Baddiley, J. (1975). The interaction of magnesium ions with teichoic acid. *The Biochemical journal, 149*(3), 519-524. doi:10.1042/bj1490519

Langsford, M. L., Gilkes, N. R., Singh, B., Moser, B., Miller, R. C., Warren, R. A. J.*, et al.* (1987). Glycosylation of bacterial cellulases prevents proteolytic cleavage between functional domains. *FEBS Letters, 225*(1-2), 163-167. doi:10.1016/0014-5793(87)81150-X

Lapasin, R., & Pricl, S. (1995). Industrial applications of polysaccharides. In R. Lapasin & S. Pricl (Eds.), *Rheology of industrial polysaccharides: Theory and applications* (pp. 134-161). Boston, MA: Springer US.

Laureys, D., Aerts, M., Vandamme, P., & De Vuyst, L. (2018). Oxygen and diverse nutrients influence the water kefir fermentation process. *Food Microbiology, 73*, 351-361. doi:10.1016/j.fm.2018.02.007

Laureys, D., Cnockaert, M., De Vuyst, L., & Vandamme, P. (2016). *Bifidobacterium aquikefiri* sp. nov., isolated from water kefir. *International Journal of Systematic and Evolutionary Microbiology, 66*(3), 1281-1286. doi:10.1099/ijsem.0.000877

Laureys, D., & De Vuyst, L. (2014). Microbial species diversity, community dynamics, and metabolite kinetics of water kefir fermentation. *Applied and Environmental Microbiology, 80*(8), 2564-2572. doi:10.1128/AEM.03978-13

Laureys, D., & De Vuyst, L. (2017). The water kefir grain inoculum determines the characteristics of the resulting water kefir fermentation process. *Journal of Applied Microbiology, 122*(3), 719-732. doi:10.1111/jam.13370

Le Nours, J., De Maria, L., Welner, D., Jørgensen, C. T., Christensen, L. L. H., Borchert, T. V.*, et al.* (2009). Investigating the binding of β-1,4-galactan to *Bacillus licheniformis* β-1,4-galactanase by crystallography and computational modeling. *Proteins: Structure, Function, and Bioinformatics, 75*(4), 977-989. doi:10.1002/prot.22310

LeBlanc, J. G., Laiño, J. E., del Valle, M. J., Vannini, V., van Sinderen, D., Taranto, M. P.*, et al.* (2011). B-Group vitamin production by lactic acid bacteria – current knowledge and potential applications. *Journal of Applied Microbiology, 111*(6), 1297-1309. doi:10.1111/j.1365-2672.2011.05157.x

Lee, S., Park, J., Jang, J.-K., Lee, B.-H., & Park, Y.-S. (2019). Structural analysis of gluco-oligosaccharides produced by *Leuconostoc lactis* and their prebiotic effect. *Molecules, 24*(21). doi:10.3390/molecules24213998

Leemhuis, H., Dijkman, W. P., Dobruchowska, J. M., Pijning, T., Grijpstra, P., Kralj, S.*, et al.* (2013a). 4,6-alpha-glucanotransferase activity occurs more widespread in Lactobacillus strains and constitutes a separate GH70 subfamily. *Appl Microbiol Biotechnol, 97*(1), 181-193. doi:10.1007/s00253-012-3943-1

Leemhuis, H., Pijning, T., Dobruchowska, J. M., Dijkstra, B. W., & Dijkhuizen, L. (2012). Glycosidic bond specificity of glucansucrases: on the role of acceptor substrate binding residues. *Biocatalysis and Biotransformation, 30*(3), 366-376. doi:10.3109/10242422.2012.676301

Leemhuis, H., Pijning, T., Dobruchowska, J. M., van Leeuwen, S. S., Kralj, S., Dijkstra, B. W.*, et al.* (2013b). Glucansucrases: three-dimensional structures, reactions, mechanism, alpha-glucan analysis and their implications in biotechnology and food applications. *Journal of Biotechnology, 163*(2), 250-272. doi:10.1016/j.jbiotec.2012.06.037

Leite, A. M. O., Miguel, M. A. L., Peixoto, R. S., Ruas-Madiedo, P., Paschoalin, V. M. F., Mayo, B.*, et al.* (2015). Probiotic potential of selected lactic acid bacteria strains isolated from Brazilian kefir grains. *Journal of Dairy Science, 98*(6), 3622-3632. doi:10.3168/jds.2014-9265

Lembo, F. L., Longo, P. L., Ota-Tsuzuki, C., Rodrigues, C. R. M. D., & Mayer, M. P. A. (2007). Genotypic and phenotypic analysis of *Streptococcus mutans* from different oral cavity sites of caries-free and caries-active children. *Oral Microbiology and Immunology, 22*(5), 313-319. doi:10.1111/j.1399-302X.2007.00361.x

Lepeuple, A.-S., Van Gemert, E., & Chapot-Chartier, M.-P. (1998). Analysis of the bacteriolytic enzymes of the autolytic *Lactococcus lactis* subsp. *cremoris* strain AM2 by renaturing polyacrylamide gel electrophoresis: Identification of a prophage-encoded enzyme. *Applied and Environmental Microbiology, 64*(11), 4142. doi:10.1128/AEM.64.11.4142-4148.1998

Leroy, F., & De Vuyst, L. (2004). Lactic acid bacteria as functional starter cultures for the food fermentation industry. *Trends in Food Science & Technology, 15*(2), 67-78. doi:10.1016/j.tifs.2003.09.004

Lis, M., Shiroza, T., & Kuramitsu, H. K. (1995). Role of C-terminal direct repeating units of the *Streptococcus mutans* glucosyltransferase-S in glucan binding. *Applied and Environmental Microbiology, 61*(5), 2040-2042. doi:10.1128/AEM.61.5.2040-2042.1995

López-Munguía, A., Pelenc, V., Remaud, M., Biton, J., Michel, J. M., Lang, C.*, et al.* (1993). Production and purification of alternansucrase, a glucosyltransferase from *Leuconostoc*

*mesenteroide*s NRRL B-1355, for the synthesis of oligoalternans. *Enzyme and Microbial Technology, 15*(1), 77-85. doi:10.1016/0141-0229(93)90120-Q

Lu, Y., Song, S., Tian, H., Yu, H., Zhao, J., & Chen, C. (2018). Functional analysis of the role of CcpA in *Lactobacillus plantarum* grown on fructooligosaccharides or glucose: a transcriptomic perspective. *Microbial Cell Factories, 17*(1), 201. doi:10.1186/s12934-018-1050-4

Lutz, L. (1899). *Recherches biologiques sur la constitution du Tibi* (Vol. 15). France: Bulletin de la Société Mycologique.

Lynch, K. M., McSweeney, P. L. H., Arendt, E. K., Uniacke-Lowe, T., Galle, S., & Coffey, A. (2014). Isolation and characterisation of exopolysaccharide-producing *Weissella* and *Lactobacillus* and their application as adjunct cultures in Cheddar cheese. *International Dairy Journal, 34*(1), 125-134. doi:10.1016/j.idairyj.2013.07.013

MacGregor, E. A., Janeček, Š., & Svensson, B. (2001). Relationship of sequence and structure to specificity in the α-amylase family of enzymes. *Biochimica et Biophysica Acta (BBA) - Protein Structure and Molecular Enzymology, 1546*(1), 1-20. doi:10.1016/S0167-4838(00)00302-2

MacGregor, E. A., Jespersen, H. M., & Svensson, B. (1996). A circularly permuted α-amylase-type α/β-barrel structure in glucan-synthesizing glucosyltransferases. *FEBS Letters, 378*(3), 263-266. doi:10.1016/0014-5793(95)01428-4

Madigan, M. T., & Martinko, J. M. (2009). *Brock Mikrobiologie* (11 ed.): Pearson Education, Inc.

Mäkeläinen, H., Hasselwander, O., Rautonen, N., & Ouwehand, A. C. (2009). Panose, a new prebiotic candidate. *Letters in Applied Microbiology, 49*(6), 666-672. doi:10.1111/j.1472-765x.2009.02698.x

Marsh, A. J., O'Sullivan, O., Hill, C., Ross, R. P., & Cotter, P. D. (2013). Sequence-based analysis of the microbial composition of water kefir from multiple sources. *FEMS Microbiology Letters, 348*(1), 79-85. doi:10.1111/1574-6968.12248

Martinez-Villaluenga, C., Peñas, E., & Frias, J. (2017). Chapter 2 - Bioactive peptides in fermented foods: Production and evidence for health effects. In J. Frias, C. Martinez-Villaluenga, & E. Peñas (Eds.), *Fermented Foods in Health and Disease Prevention* (pp. 23-47). Boston: Academic Press.

Masuda, M., Ide, M., Utsumi, H., Niiro, T., Shimamura, Y., & Murata, M. (2012). Production potency of folate, vitamin B12, and thiamine by lactic acid bacteria isolated from japanese pickles. *Bioscience, Biotechnology, and Biochemistry, 76*(11), 2061-2067. doi:10.1271/bbb.120414

Maurice, N. M., Bedi, B., & Sadikot, R. T. (2018). *Pseudomonas aeruginosa* biofilms: host response and clinical implications in lung infections. *American journal of respiratory cell and molecular biology, 58*(4), 428-439. doi:10.1165/rcmb.2017-0321TR

Mayer, M. J., D'Amato, A., Colquhoun, I. J., Le Gall, G., & Narbad, A. (2020). Identification of genes required for glucan exopolysaccharide production in *Lactobacillus johnsonii* suggests a novel biosynthesis mechanism. *Applied and Environmental Microbiology, 86*(8), e02808-02819. doi:10.1128/AEM.02808-19

Melchiorsen, R. C., Jokumsen, V. K., Villadsen, J., Israelsen, H., & Arnau, J. (2002). The level of pyruvate-formate lyase controls the shift from homolactic to mixed-acid product formation in *Lactococcus lactis*. *Applied Microbiology and Biotechnology, 58*(3), 338-344. doi:10.1007/s00253-001-0892-5

Meng, X., Dobruchowska, J. M., Pijning, T., López, C. A., Kamerling, J. P., & Dijkhuizen, L. (2014). Residue Leu940 has a crucial role in the linkage and reaction specificity of the glucansucrase GTF180 of the probiotic bacterium *Lactobacillus reuteri* 180. *Journal of Biological Chemistry, 289*(47), 32773-32782. doi:10.1074/jbc.M114.602524

Meng, X., Gangoiti, J., Bai, Y., Pijning, T., Van Leeuwen, S. S., & Dijkhuizen, L. (2016). Structure-function relationships of family GH70 glucansucrase and 4,6-alpha-glucanotransferase enzymes, and their evolutionary relationships with family GH13 enzymes. *Cell Mol Life Sci, 73*(14), 2681-2706. doi:10.1007/s00018-016-2245-7

Mestrom, L., Przypis, M., Kowalczykiewicz, D., Pollender, A., Kumpf, A., Marsden, S. R.*, et al.* (2019). Leloir glycosyltransferases in applied biocatalysis: A multidisciplinary approach. *International journal of molecular sciences, 20*(21), 5263. doi:10.3390/ijms20215263

Miller, A. W., & Robyt, J. F. (1986). Detection of dextransucrase and levansucrase on polyacrylamide gels by the periodic acid-Schiff stain: Staining artifacts and their prevention. *Analytical Biochemistry, 156*(2), 357-363. doi:10.1016/0003-2697(86)90266-6

Miller, K. A., Phillips, R. S., Kilgore, P. B., Smith, G. L., & Hoover, T. R. (2015). A mannose family phosphotransferase system permease and associated enzymes are required for utilization of fructoselysine and glucoselysine in *Salmonella enterica* serovar *typhimurium*. *Journal of bacteriology, 197*(17), 2831-2839. doi:10.1128/JB.00339-15

Mital, B. K., Shallenberger, R. S., & Steinkraus, K. H. (1973). Alpha-glactosidase activity of lactobacilli. *Applied microbiology, 26*(5), 783-788.

Møller, M. S., Fredslund, F., Majumder, A., Nakai, H., Poulsen, J.-C. N., Lo Leggio, L.*, et al.* (2012). Enzymology and structure of the GH13_31 glucan 1,6-α-glucosidase that confers isomaltooligosaccharide utilization in the probiotic *Lactobacillus acidophilus* NCFM. *Journal of bacteriology, 194*(16), 4249-4259. doi:10.1128/JB.00622-12

Monchois, V., Remaud-Simeon, M., Monsan, P., & Willemot, R. M. (1998). Cloning and sequencing of a gene coding for an extracellular dextransucrase (DSRB) from *Leuconostoc mesenteroides* NRRL B-1299 synthesizing only a alpha (1-6) glucan. *FEMS Microbiology Letters, 159*(2), 307-315. doi:10.1111/j.1574-6968.1998.tb12876.x

Monchois, V., Remaud-Simeon, M., Russell, R. R. B., Monsan, P., & Willemot, R. M. (1997). Characterization of *Leuconostoc mesenteroides* NRRL B-512F dextransucrase (DSRS)

and identification of amino-acid residues playing a key role in enzyme activity. *Applied Microbiology and Biotechnology, 48*(4), 465-472. doi:10.1007/s002530051081

Monchois, V., Reverte, A., Remaud-Simeon, M., Monsan, P., & Willemot, R.-M. (1998). Effect of *Leuconostoc mesenteroides* NRRL B-512F dextransucrase carboxy-terminal deletions on dextran and oligosaccharide synthesis. *Applied and Environmental Microbiology, 64*(5), 1644-1649.

Monchois, V., Willemot, R.-M., & Monsan, P. (1999). Glucansucrases: mechanism of action and structure–function relationships. *FEMS Microbiology Reviews, 23*(2), 131-151. doi:10.1111/j.1574-6976.1999.tb00394.x

Monchois, V., Willemot, R.-M., Remaud-Simeon, M., Croux, C., & Monsan, P. (1996). Cloning and sequencing of a gene coding for a novel dextransucrase from *Leuconostoc mesenteroides* NRRL B-1299 synthesizing only α(1–6) and α(1–3) linkages. *Gene, 182*(1), 23-32. doi:10.1016/S0378-1119(96)00443-X

Monedero, V., Yebra, M. J., Poncet, S., & Deutscher, J. (2008). Maltose transport in *Lactobacillus casei* and its regulation by inducer exclusion. *Research in Microbiology, 159*(2), 94-102. doi:10.1016/j.resmic.2007.10.002

Monsan, P., Bozonnet, S., Albenne, C., Joucla, G., Willemot, R.-M., & Remaud-Siméon, M. (2001). Homopolysaccharides from lactic acid bacteria. *International Dairy Journal, 11*(9), 675-685. doi:10.1016/S0958-6946(01)00113-3

Monsan, P., Remaud-Siméon, M., & André, I. (2010). Transglucosidases as efficient tools for oligosaccharide and glucoconjugate synthesis. *Current Opinion in Microbiology, 13*(3), 293-300. doi:10.1016/j.mib.2010.03.002

Mooser, G. (1992). Glycosidases and glycosyltransferases. In D. S. Sigman (Ed.), *The Enzymes* (Vol. 20, pp. 187-233): Academic Press.

Mooser, G., Hefta, S. A., Paxton, R. J., Shively, J. E., & Lee, T. D. (1991). Isolation and sequence of an active-site peptide containing a catalytic aspartic acid from two *Streptococcus sobrinus* alpha-glucosyltransferases. *Journal of Biological Chemistry, 266*(14), 8916-8922. doi:10.1016/S0021-9258(18)31531-X

Mooser, G., & Iwaoka, K. R. (1989). Sucrose 6-alpha-D-glucosyltransferase from *Streptococcus sobrinus*: characterization of a glucosyl-enzyme complex. *Biochemistry, 28*(2), 443-449. doi:10.1021/bi00428a006

Moreira, M. E. C., Santos, M. H. D., Zolini, G. P. P., Wouters, A. T. B., Carvalho, J. C. T., & Schneedorf, J. M. (2008). Anti-inflammatory and cicatrizing activities of a carbohydrate fraction isolated from sugary kefir. *Journal of Medicinal Food, 11*(2), 356-361. doi:10.1089/jmf.2007.329

Moulis, C., Joucla, G., Harrison, D., Fabre, E., Potocki-Veronese, G., Monsan, P.*, et al.* (2006). Understanding the polymerization mechanism of glycoside-hydrolase family 70 glucansucrases. *Journal of Biological Chemistry, 281*(42), 31254-31267. doi:10.1016/S0021-9258(19)84038-3

Mukaka, M. M. (2012). Statistics corner: A guide to appropriate use of correlation coefficient in medical research. *Malawi medical journal : the journal of Medical Association of Malawi, 24*(3), 69-71.

Mulcahy, L. R., Isabella, V. M., & Lewis, K. (2014). *Pseudomonas aeruginosa* biofilms in disease. *Microbial ecology, 68*(1), 1-12. doi:10.1007/s00248-013-0297-x

Mundt, J. O., Graham, W. F., & McCarty, I. E. (1967). Spherical lactic acid-producing bacteria of southern-grown raw and processed vegetables. *Applied microbiology, 15*(6), 1303-1308.

Münkel, F., Bechtner, J., Eckel, V., Fischer, A., Herbi, F., Jakob, F.*, et al.* (2019). Detailed structural characterization of glucans produced by glucansucrases from *Leuconostoc citreum* TMW 2.1194. *Journal of Agricultural and Food Chemistry, 67*(24), 6856-6866. doi:10.1021/acs.jafc.9b01822

Nácher-Vázquez, M., Ruiz-Masó, J. A., Mohedano, M. L., del Solar, G., Aznar, R., & López, P. (2017). Dextransucrase expression is concomitant with that of replication and maintenance functions of the pMN1 plasmid in *Lactobacillus sakei* MN1. *Frontiers in Microbiology, 8*, 2281.

Naessens, M., Cerdobbel, A., Soetaert, W., & Vandamme, E. J. (2005). *Leuconostoc* dextransucrase and dextran: production, properties and applications. *Journal of Chemical Technology & Biotechnology, 80*(8), 845-860. doi:10.1002/jctb.1322

Neville, B. A., Forde, B. M., Claesson, M. J., Darby, T., Coghlan, A., Nally, K.*, et al.* (2012). Characterization of pro-inflammatory flagellin proteins produced by *Lactobacillus ruminis* and related motile *Lactobacilli*. *PLOS ONE, 7*(7), e40592. doi:10.1371/journal.pone.0040592

Nilsson, L. (2013). Separation and characterization of food macromolecules using field-flow fractionation: A review. *Food Hydrocolloids, 30*(1), 1-11. doi:10.1016/j.foodhyd.2012.04.007

Nursten, H. E. (2005). *The Maillard reaction: chemistry, biochemistry and implications*: Royal Society of Chemistry.

Nwodo, U. U., Green, E., & Okoh, A. I. (2012). Bacterial exopolysaccharides: functionality and prospects. *International journal of molecular sciences, 13*(11), 14002-14015. doi:10.3390/ijms131114002

Ogrydziak, D. M. (1993). Yeast extracellular proteases. *Critical Reviews in Biotechnology, 13*(1), 1-55. doi:10.3109/07388559309069197

Olvera, C., Fernández-Vázquez, J. L., Ledezma-Candanoza, L., & López-Munguía, A. (2007). Role of the C-terminal region of dextransucrase from *Leuconostoc mesenteroides* IBT-PQ in cell anchoring. *Microbiology, 153*(12), 3994-4002. doi:10.1099/mic.0.2007/008854-0

Onishi, H., & Suzuki, T. (1968). Production of D-mannitol and glycerol by yeasts. *Applied microbiology, 16*(12), 1847-1852.

Ortiz, M. E., Bleckwedel, J., Raya, R. R., & Mozzi, F. (2013). Biotechnological and in situ food production of polyols by lactic acid bacteria. *Applied Microbiology and Biotechnology, 97*(11), 4713-4726. doi:10.1007/s00253-013-4884-z

Overbeek, R., Olson, R., Pusch, G. D., Olsen, G. J., Davis, J. J., Disz, T.*, et al.* (2014). The SEED and the Rapid Annotation of microbial genomes using Subsystems Technology (RAST). *Nucleic Acids Research, 42*(Database issue), D206-D214. doi:10.1093/nar/gkt1226

Ozimek, L. K., Kralj, S., van der Maarel, M. J. E. C., & Dijkhuizen, L. (2006). The levansucrase and inulosucrase enzymes of *Lactobacillus reuteri* 121 catalyse processive and non-processive transglycosylation reactions. *Microbiology, 152*(4), 1187-1196. doi:10.1099/mic.0.28484-0

Palmfeldt, J., Paese, M., Hahn-Hägerdal, B., & van Niel, E. W. J. (2004). The pool of ADP and ATP regulates anaerobic product formation in resting cells of *Lactococcus lactis*. *Applied and Environmental Microbiology, 70*(9), 5477. doi:10.1128/AEM.70.9.5477-5484.2004

Paludan-Müller, C., Gram, L., & Rattray, F. P. (2002). Purification and characterisation of an extracellular fructan beta-fructosidase from a *Lactobacillus pentosus* strain isolated from fermented fish. *Systematic and Applied Microbiology, 25*(1), 13-20.

Pan, Y.-J., Lin, T.-L., Chen, C.-T., Chen, Y.-Y., Hsieh, P.-F., Hsu, C.-R.*, et al.* (2015). Genetic analysis of capsular polysaccharide synthesis gene clusters in 79 capsular types of *Klebsiella spp. Scientific Reports, 5*(1), 15573. doi:10.1038/srep15573

Paniagua-Michel, J. d. J., Olmos-Soto, J., & Morales-Guerrero, E. R. (2014). Algal and microbial exopolysaccharides: new insights as biosurfactants and bioemulsifiers. In S.-K. Kim (Ed.), *Advances in Food and Nutrition Research* (Vol. 73, pp. 221-257): Academic Press.

Papadimitriou, K., Alegría, Á., Bron, P. A., de Angelis, M., Gobbetti, M., Kleerebezem, M.*, et al.* (2016). Stress physiology of lactic acid bacteria. *Microbiology and molecular biology reviews : MMBR, 80*(3), 837-890. doi:10.1128/MMBR.00076-15

Parolis, L. A. S., Parolis, H., Kenne, L., Meldal, M., & Bock, K. (1998). The extracellular polysaccharide of *Pichia* (*Hansenula*) *holstii* NRRL Y-2448: the phosphorylated side chains. *Carbohydrate Research, 309*(1), 77-87. doi:10.1016/S0008-6215(98)00101-3

Passerini, D., Vuillemin, M., Ufarté, L., Morel, S., Loux, V., Fontagné-Faucher, C.*, et al.* (2015). Inventory of the GH70 enzymes encoded by *Leuconostoc citreum* NRRL B-1299 – identification of three novel α-transglucosylases. *The FEBS Journal, 282*(11), 2115-2130. doi:10.1111/febs.13261

Pasteur, L. (1861). Sur la fermentation visqueuse et la fermentation butyrique. *Bulletin de la Société Chimique de Paris, 11*, 30-31.

Peleg, A. Y., & Hooper, D. C. (2010). Hospital-acquired infections due to gram-negative bacteria. *The New England journal of medicine, 362*(19), 1804-1813. doi:10.1056/NEJMra0904124

Peng, Z., Vogel, R. F., Ehrmann, M. A., & Xiong, T. (2018). Identification and characterization of adhesion proteins in *lactobacilli* targeting actin as receptor. *Molecular and cellular probes, 37*, 60-63. doi:10.1016/j.mcp.2017.08.002

Perkins, D. N., Pappin, D. J. C., Creasy, D. M., & Cottrell, J. S. (1999). Probability-based protein identification by searching sequence databases using mass spectrometry data. *Electrophoresis, 20*(18), 3551-3567. doi:10.1002/(SICI)1522-2683(19991201)20:18<3551::AID-ELPS3551>3.0.CO;2-2

Petersen, T. N., Brunak, S., von Heijne, G., & Nielsen, H. (2011). SignalP 4.0: discriminating signal peptides from transmembrane regions. *Nature Methods, 8*(10), 785-786. doi:10.1038/nmeth.1701

Pidoux, M. (1989). The microbial flora of sugary kefir grain (the gingerbeer plant): biosynthesis of the grain from *Lactobacillus hilgardii* producing a polysaccharide gel. *MIRCEN journal of applied microbiology and biotechnology, 5*(2), 223-238. doi:10.1007/BF01741847

Pijning, T., Vujičić-Žagar, A., Kralj, S., Dijkhuizen, L., & Dijkstra, B. W. (2014). Flexibility of truncated and full-length glucansucrase GTF180 enzymes from *Lactobacillus reuteri* 180. *The FEBS Journal, 281*(9), 2159-2171. doi:10.1111/febs.12769

Postma, P. W., Lengeler, J. W., & Jacobson, G. R. (1993). Phosphoenolpyruvate:carbohydrate phosphotransferase systems of bacteria. *Microbiological Reviews, 57*(3), 543.

Prechtl, R. M., Janßen, D., Behr, J., Ludwig, C., Küster, B., Vogel, R. F.*, et al.* (2018a). Sucrose-induced proteomic response and carbohydrate utilization of *Lactobacillus sakei* TMW 1.411 during dextran formation. *Frontiers in Microbiology, 9*(2796). doi:10.3389/fmicb.2018.02796

Prechtl, R. M., Wefers, D., Jakob, F., & Vogel, R. F. (2018b). Cold and salt stress modulate amount, molecular and macromolecular structure of a *Lactobacillus sakei* dextran. *Food Hydrocolloids, 82*, 73-81. doi:10.1016/j.foodhyd.2018.04.003

Proost, S., Fostier, J., De Witte, D., Dhoedt, B., Demeester, P., Van de Peer, Y.*, et al.* (2012). i-ADHoRe 3.0--fast and sensitive detection of genomic homology in extremely large data sets. *Nucleic Acids Research, 40*(2), e11-e11. doi:10.1093/nar/gkr955

Quirasco, M., López-Munguía, A., Remaud-Simeon, M., Monsan, P., & Farrés, A. (1999). Induction and transcription studies of the dextransucrase gene in *Leuconostoc mesenteroides* NRRL B-512F. *Applied and Environmental Microbiology, 65*(12), 5504-5509. doi:10.1128/AEM.65.12.5504-5509.1999

Rabelo, M. C., Honorato, T. L., Gonçalves, L. R. B., Pinto, G. A. S., & Rodrigues, S. (2006). Enzymatic synthesis of prebiotic oligosaccharides. *Applied Biochemistry and Biotechnology, 133*(1), 31. doi:10.1385/ABAB:133:1:31

Ratkowsky, D. A., Olley, J., & Ross, T. (2005). Unifying temperature effects on the growth rate of bacteria and the stability of globular proteins. *Journal of Theoretical Biology, 233*(3), 351-362. doi:10.1016/j.jtbi.2004.10.016

Regulski, K., Courtin, P., Meyrand, M., Claes, I. J. J., Lebeer, S., Vanderleyden, J.*, et al.* (2012). Analysis of the peptidoglycan hydrolase complement of *Lactobacillus casei* and characterization of the major γ-D-glutamyl-L-lysyl-endopeptidase. *PLOS ONE, 7*(2), e32301. doi:10.1371/journal.pone.0032301

Rehm, B. H. A. (2010). Bacterial polymers: biosynthesis, modifications and applications. *Nature Reviews Microbiology, 8*(8), 578-592. doi:10.1038/nrmicro2354

Reidl, S., Lehmann, A., Schiller, R., Salam Khan, A., & Dobrindt, U. (2009). Impact of O-glycosylation on the molecular and cellular adhesion properties of the *Escherichia coli* autotransporter protein Ag43. *International Journal of Medical Microbiology, 299*(6), 389-401. doi:10.1016/j.ijmm.2009.01.001

Remaud-Simeon, M., Willemot, R.-M., Sarçabal, P., Potocki de Montalk, G., & Monsan, P. (2000). Glucansucrases: molecular engineering and oligosaccharide synthesis. *Journal of Molecular Catalysis B: Enzymatic, 10*(1), 117-128. doi:10.1016/S1381-1177(00)00119-3

Revelle, W. R. (2020). psych: procedures for psychological, psychometric, and personality research (Version 2.0.12) [R-package]. Northwestern University, Evanston, Illinois.

Richter, M., Rosselló-Móra, R., Oliver Glöckner, F., & Peplies, J. (2015). JSpeciesWS: a web server for prokaryotic species circumscription based on pairwise genome comparison. *Bioinformatics, 32*(6), 929-931. doi:10.1093/bioinformatics/btv681

Riedl, R., Dünzer, N., Michel, M., Jacob, F., & Hutzler, M. (2019). Beer enemy number one: genetic diversity, physiology and biofilm formation of *Lactobacillus brevis*. *Journal of the Institute of Brewing, 125*(2), 250-260. doi:10.1002/jib.553

Robyt, J. F., & Walseth, T. F. (1978). The mechanism of acceptor reactions of *Leuconostoc mesenteroides* B-512F dextransucrase. *Carbohydrate Research, 61*(1), 433-445. doi:10.1016/S0008-6215(00)84503-6

Rodrigues, K. L., Araújo, T. H., Schneedorf, J. M., Ferreira, C. d. S., Moraes, G. d. O. I., Coimbra, R. S.*, et al.* (2016). A novel beer fermented by kefir enhances anti-inflammatory and anti-ulcerogenic activities found isolated in its constituents. *Journal of Functional Foods, 21*, 58-69. doi:10.1016/j.jff.2015.11.035

Rolain, T., Bernard, E., Courtin, P., Bron, P. A., Kleerebezem, M., Chapot-Chartier, M.-P.*, et al.* (2012). Identification of key peptidoglycan hydrolases for morphogenesis, autolysis, and peptidoglycan composition of *Lactobacillus plantarum* WCFS1. *Microbial Cell Factories, 11*(1), 137. doi:10.1186/1475-2859-11-137

Rotz, C. A., Montes, F., & Chianese, D. S. (2010). The carbon footprint of dairy production systems through partial life cycle assessment. *Journal of Dairy Science, 93*(3), 1266-1282. doi:10.3168/jds.2009-2162

Rouse, S., Canchaya, C., & van Sinderen, D. (2008). *Lactobacillus hordei* sp. nov., a bacteriocinogenic strain isolated from malted barley. *International Journal of Systematic and Evolutionary Microbiology, 58*(9), 2013-2017. doi:10.1099/ijs.0.65584-0

Ruas-Madiedo, P., & de los Reyes-Gavilán, C. G. (2005). Invited review: Methods for the screening, isolation, and characterization of exopolysaccharides produced by lactic acid bacteria. *Journal of Dairy Science, 88*(3), 843-856. doi:10.3168/jds.S0022-0302(05)72750-8

Rübsam, H., Krottenthaler, M., Gastl, M., & Becker, T. (2012). An overview of separation methods in starch analysis: The importance of size exclusion chromatography and field flow fractionation. *Starch - Stärke, 64*(9), 683-695. doi:10.1002/star.201100188

Rühmkorf, C., Bork, C., Mischnick, P., Rübsam, H., Becker, T., & Vogel, R. F. (2013). Identification of *Lactobacillus curvatus* TMW 1.624 dextransucrase and comparative characterization with *Lactobacillus reuteri* TMW 1.106 and *Lactobacillus animalis* TMW 1.971 dextransucrases. *Food Microbiology, 34*(1), 52-61. doi:10.1016/j.fm.2012.11.002

Rühmkorf, C., Rübsam, H., Becker, T., Bork, C., Voiges, K., Mischnick, P.*, et al.* (2012). Effect of structurally different microbial homoexopolysaccharides on the quality of gluten-free bread. *European Food Research and Technology, 235*(1), 139-146. doi:10.1007/s00217-012-1746-3

Ruiz-Herrera, J. (1991). Biosynthesis of β-glucans in fungi. *Antonie van Leeuwenhoek, 60*(2), 73-81. doi:10.1007/BF00572695

Rycroft, C. E., Jones, M. R., Gibson, G. R., & Rastall, R. A. (2001). Fermentation properties of gentio-oligosaccharides. *Letters in Applied Microbiology, 32*(3), 156-161. doi:10.1046/j.1472-765x.2001.00875.x

Saiki, R. K., Gelfand, D. H., Stoffel, S., Scharf, S. J., Higuchi, R., Horn, G. T.*, et al.* (1988). Primer-directed enzymatic amplification of DNA with a thermostable DNA polymerase. *Science, 239*(4839), 487. doi:10.1126/science.239.4839.487

Sambrook, J., Fritsch, E. F., & Maniatis, T. (1989). *Molecular cloning: a laboratory manual* (2 ed.). Cold spring harbor, NY: Cold spring harbor laboratory press.

Santos, A. L. S. D., Galdino, A. C. M., Mello, T. P. d., Ramos, L. d. S., Branquinha, M. H., Bolognese, A. M.*, et al.* (2018). What are the advantages of living in a community? A microbial biofilm perspective! *Memorias do Instituto Oswaldo Cruz, 113*(9), e180212-e180212. doi:10.1590/0074-02760180212

Sanz, M. L., Côté, G. L., Gibson, G. R., & Rastall, R. A. (2005). Prebiotic properties of alternansucrase maltose-acceptor oligosaccharides. *Journal of Agricultural and Food Chemistry, 53*(15), 5911-5916. doi:10.1021/jf050344e

Sanz, M. L., Côté, G. L., Gibson, G. R., & Rastall, R. A. (2006). Selective fermentation of gentiobiose-derived oligosaccharides by human gut bacteria and influence of molecular

weight. *FEMS Microbiology Ecology, 56*(3), 383-388. doi:10.1111/j.1574-6941.2006.00075.x

Sarbini, S. R., Kolida, S., Deaville, E. R., Gibson, G. R., & Rastall, R. A. (2014). Potential of novel dextran oligosaccharides as prebiotics for obesity management through in vitro experimentation. *British Journal of Nutrition, 112*(8), 1303-1314. doi:10.1017/S0007114514002177

Saulnier, D. M. A., Molenaar, D., de Vos, W. M., Gibson, G. R., & Kolida, S. (2007). Identification of prebiotic fructooligosaccharide metabolism in *Lactobacillus plantarum* WCFS1 through microarrays. *Applied and Environmental Microbiology, 73*(6), 1753-1765. doi:10.1128/AEM.01151-06

Schmid, J. (2018). Recent insights in microbial exopolysaccharide biosynthesis and engineering strategies. *Current Opinion in Biotechnology, 53*, 130-136. doi:10.1016/j.copbio.2018.01.005

Schmid, J., Bechtner, J., Vogel, R. F., & Jakob, F. (2019). A systematic approach to study the pH-dependent release, productivity and product specificity of dextransucrases. *Microbial Cell Factories, 18*(1), 153. doi:10.1186/s12934-019-1208-8

Schmid, J., Sieber, V., & Rehm, B. (2015). Bacterial exopolysaccharides: biosynthesis pathways and engineering strategies. *Frontiers in Microbiology, 6*, 496. doi:10.3389/fmicb.2015.00496

Schwab, C., Walter, J., Tannock, G. W., Vogel, R. F., & Gänzle, M. G. (2007). Sucrose utilization and impact of sucrose on glycosyltransferase expression in *Lactobacillus reuteri*. *Systematic and Applied Microbiology, 30*(6), 433-443. doi:10.1016/j.syapm.2007.03.007

Selbmann, L., Stingele, F., & Petruccioli, M. (2003). Exopolysaccharide production by filamentous fungi: the example of *Botryosphaeria rhodina*. *Antonie van Leeuwenhoek, 84*(2), 135-145. doi:10.1023/A:1025421401536

Selengut, J. D., Haft, D. H., Davidsen, T., Ganapathy, A., Gwinn-Giglio, M., Nelson, W. C.*, et al.* (2007). TIGRFAMs and genome properties: tools for the assignment of molecular function and biological process in prokaryotic genomes. *Nucleic Acids Research, 35*(Database issue), D260-D264. doi:10.1093/nar/gkl1043

Seo, E.-S., Kang, J., Lee, J.-H., Kim, G.-E., Kim, G. J., & Kim, D. (2009). Synthesis and characterization of hydroquinone glucoside using *Leuconostoc mesenteroides* dextransucrase. *Enzyme and Microbial Technology, 45*(5), 355-360. doi:10.1016/j.enzmictec.2009.07.011

Seo, E.-S., Nam, S.-H., Kang, H.-K., Cho, J.-Y., Lee, H.-S., Ryu, H.-W.*, et al.* (2007). Synthesis of thermo- and acid-stable novel oligosaccharides by using dextransucrase with high concentration of sucrose. *Enzyme and Microbial Technology, 40*(5), 1117-1123. doi:10.1016/j.enzmictec.2006.08.017

Shallenberger, R. (1974). Occurrence of various sugars in foods. *Sugars in Nutrition. HL Sipple & KW McNutt, eds*.

Sharifi, M., Moridnia, A., Mortazavi, D., Salehi, M., Bagheri, M., & Sheikhi, A. (2017). Kefir: a powerful probiotics with anticancer properties. *Medical Oncology, 34*(11), 183. doi:10.1007/s12032-017-1044-9

Sharma, D., Misba, L., & Khan, A. U. (2019). Antibiotics versus biofilm: an emerging battleground in microbial communities. *Antimicrobial Resistance & Infection Control, 8*(1), 76. doi:10.1186/s13756-019-0533-3

Shevchenko, A., Tomas, H., Havli, J., Olsen, J. V., & Mann, M. (2006). In-gel digestion for mass spectrometric characterization of proteins and proteomes. *Nature Protocols, 1*(6), 2856-2860. doi:10.1038/nprot.2006.468

Siakotos, A. N., & Rouser, G. (1965). Analytical separation of nonlipid water soluble substances and gangliosides from other lipids by dextran gel column chromatography. *Journal of the American Oil Chemists Society, 42*(11), 913-919. doi:10.1007/BF02632444

Sidebotham, R. L. (1974). Dextrans. In R. S. Tipson & D. Horton (Eds.), *Advances in Carbohydrate Chemistry and Biochemistry* (Vol. 30, pp. 371-444): Academic Press.

Sloan, A. E. (2018). *Top10 Functional food trends*. Retrieved from Chicago, IL:

Stadie, J. (2013). *Metabolic activity and symbiotic interaction of bacteria and yeasts in water kefir.* (Dissertation), Technical University, Munich.

Stadie, J., Gulitz, A., Ehrmann, M. A., & Vogel, R. F. (2013). Metabolic activity and symbiotic interactions of lactic acid bacteria and yeasts isolated from water kefir. *Food Microbiology, 35*(2), 92-98. doi:10.1016/j.fm.2013.03.009

Stam, M. R., Danchin, E. G. J., Rancurel, C., Coutinho, P. M., & Henrissat, B. (2006). Dividing the large glycoside hydrolase family 13 into subfamilies: towards improved functional annotations of α-amylase-related proteins. *Protein Engineering, Design and Selection, 19*(12), 555-562. doi:10.1093/protein/gzl044

Stasinopoulos, S. J., Fisher, P. R., Stone, B. A., & Stanisich, V. A. (1999). Detection of two loci involved in (1→3)-β-glucan (curdlan) biosynthesis by *Agrobacterium* sp. ATCC31749, and comparative sequence analysis of the putative curdlan synthase gene. *Glycobiology, 9*(1), 31-41. doi:10.1093/glycob/9.1.31

Sullivan, M. J., Petty, N. K., & Beatson, S. A. (2011). Easyfig: a genome comparison visualizer. *Bioinformatics (Oxford, England), 27*(7), 1009-1010. doi:10.1093/bioinformatics/btr039

Sutherland, I. W. (1972). Bacterial Exopolysaccharides. In A. H. Rose & D. W. Tempest (Eds.), *Advances in Microbial Physiology* (Vol. 8, pp. 143-213): Academic Press.

Sutherland, I. W. (2001). The biofilm matrix - an immobilized but dynamic microbial environment. *Trends in Microbiology, 9*(5), 222-227. doi:10.1016/S0966-842X(01)02012-1

Sweet, D. P., Shapiro, R. H., & Albersheim, P. (1975). Quantitative analysis by various g.l.c. response-factor theories for partially methylated and partially ethylated alditol acetates. *Carbohydrate Research, 40*(2), 217-225. doi:10.1016/S0008-6215(00)82604-X

Taggart, P., & Mitchell, J. R. (2009). Starch. In G. O. Phillips & P. A. Williams (Eds.), *Handbook of Hydrocolloids (Second Edition)* (pp. 108-141): Woodhead Publishing.

Terán, L. C., Coeuret, G., Raya, R., Zagorec, M., Champomier-Vergès, M.-C., & Chaillou, S. (2018). Phylogenomic analysis of *Lactobacillus curvatus* reveals two lineages distinguished by genes for fermenting plant-derived carbohydrates. *Genome biology and evolution, 10*(6), 1516-1525. doi:10.1093/gbe/evy106

Teusink, B., & Molenaar, D. (2017). Systems biology of lactic acid bacteria: For food and thought. *Current Opinion in Systems Biology, 6*, 7-13. doi:10.1016/j.coisb.2017.07.005

Teusink, B., Wiersma, A., Molenaar, D., Francke, C., de Vos, W. M., Siezen, R. J.*, et al.* (2006). Analysis of growth of *Lactobacillus plantarum* WCFS1 on a complex medium using a genome-scale metabolic model. *Journal of Biological Chemistry, 281*(52), 40041-40048. doi:10.1074/jbc.M606263200

Thomas, T. D., Ellwood, D. C., & Longyear, V. M. C. (1979). Change from homo- to heterolactic fermentation by *Streptococcus lactis* resulting from glucose limitation in anaerobic chemostat cultures. *Journal of bacteriology, 138*(1), 109.

Thompson, J. D., Gibson, T. J., & Higgins, D. G. (2003). Multiple sequence alignment using ClustalW and ClustalX. *Current Protocols in Bioinformatics, 00*(1), 2.3.1-2.3.22. doi:10.1002/0471250953.bi0203s00

Tilbury, R. H. (1975). *Occurrence and effects of lactic acid bacteria in the sugar industry.* Paper presented at the Lactic acid bacteria in beverages and food: proceedings of a symposium.

Torino, M., Font de Valdez, G., & Mozzi, F. (2015). Biopolymers from lactic acid bacteria. Novel applications in foods and beverages. *Frontiers in Microbiology, 6*(834). doi:10.3389/fmicb.2015.00834

Tsuchiya, H. M., Hellman, N. N., & Koepsell, H. J. (1953). Factors effecting molecular weight of enzymatically synthesized dextran. *Journal of the American Chemical Society, 75*(3), 757-758. doi:10.1021/ja01099a521

Tyanova, S., Temu, T., Sinitcyn, P., Carlson, A., Hein, M. Y., Geiger, T.*, et al.* (2016). The Perseus computational platform for comprehensive analysis of (prote)omics data. *Nature Methods, 13*(9), 731-740. doi:10.1038/nmeth.3901

Ua-Arak, T., Jakob, F., & Vogel, R. F. (2016). Characterization of growth and exopolysaccharide production of selected acetic acid bacteria in buckwheat sourdoughs. *International Journal of Food Microbiology, 239*, 103-112. doi:10.1016/j.ijfoodmicro.2016.04.009

Ua-Arak, T., Jakob, F., & Vogel, R. F. (2017a). Fermentation pH modulates the size distributions and functional properties of *Gluconobacter albidus* TMW 2.1191 levan. *Frontiers in Microbiology, 8*, 807-807. doi:10.3389/fmicb.2017.00807

Ua-Arak, T., Jakob, F., & Vogel, R. F. (2017b). Influence of levan-producing acetic acid bacteria on buckwheat-sourdough breads. *Food Microbiology, 65*, 95-104. doi:10.1016/j.fm.2017.02.002

Usbeck, J. C., Kern, C. C., Vogel, R. F., & Behr, J. (2013). Optimization of experimental and modelling parameters for the differentiation of beverage spoiling yeasts by Matrix-Assisted-Laser-Desorption/Ionization–Time-of-Flight Mass Spectrometry (MALDI–TOF MS) in response to varying growth conditions. *Food Microbiology, 36*(2), 379-387. doi:10.1016/j.fm.2013.07.004

van Hijum, S. A. F. T., Kralj, S., Ozimek, L. K., Dijkhuizen, L., & van Geel-Schutten, I. G. H. (2006). Structure-function relationships of glucansucrase and fructansucrase enzymes from lactic acid bacteria. *Microbiology and molecular biology reviews : MMBR, 70*(1), 157-176. doi:10.1128/MMBR.70.1.157-176.2006

van Leeuwen, S. S., Kralj, S., Eeuwema, W., Gerwig, G. J., Dijkhuizen, L., & Kamerling, J. P. (2009). Structural characterization of bioengineered α-D-glucans produced by mutant glucansucrase GTF180 enzymes of *Lactobacillus reuteri* strain 180. *Biomacromolecules, 10*(3), 580-588. doi:10.1021/bm801240r

Van Tiegham, P. (1878). Sur la gomme de sucrerie. *Annales des sciences naturelles botanique, 6*(7), 180.

Varshosaz, J. (2012). Dextran conjugates in drug delivery. *Expert Opinion on Drug Delivery, 9*(5), 509-523. doi:10.1517/17425247.2012.673580

Velásquez-Riaño, M., & Bojacá, V. (2017). Production of bacterial cellulose from alternative low-cost substrates. *Cellulose, 24*(7), 2677-2698. doi:10.1007/s10570-017-1309-7

Velázquez-Hernández, M. L., Baizabal-Aguirre, V. M., Bravo-Patiño, A., Cajero-Juárez, M., Chávez-Moctezuma, M. P., & Valdez-Alarcón, J. J. (2009). Microbial fructosyltransferases and the role of fructans. *Journal of Applied Microbiology, 106*(6), 1763-1778. doi:10.1111/j.1365-2672.2008.04120.x

Verce, M., De Vuyst, L., & Weckx, S. (2019). Shotgun metagenomics of a water kefir fermentation ecosystem reveals a novel *Oenococcus* species. *Frontiers in Microbiology, 10*, 479.

Vermassen, A., Leroy, S., Talon, R., Provot, C., Popowska, M., & Desvaux, M. (2019). Cell wall hydrolases in bacteria: insight on the diversity of cell wall amidases, glycosidases and peptidases toward peptidoglycan. *Frontiers in Microbiology, 10*, 331.

Vesić, D., & Kristich, C. J. (2013). A Rex family transcriptional repressor influences H_2O_2 accumulation by *Enterococcus faecalis*. *Journal of bacteriology, 195*(8), 1815. doi:10.1128/JB.02135-12

Viswanathan, A. (1999). Effect of degree of substitution of octenyl succinate starch on the emulsification activity on different oil phases. *Journal of environmental polymer degradation, 7*(4), 191-196. doi:10.1023/A:1022830715565

Vlamakis, H., Chai, Y., Beauregard, P., Losick, R., & Kolter, R. (2013). Sticking together: building a biofilm the *Bacillus subtilis* way. *Nature reviews. Microbiology, 11*(3), 157-168. doi:10.1038/nrmicro2960

Vujičić-Žagar, A., Pijning, T., Kralj, S., López, C. A., Eeuwema, W., Dijkhuizen, L.*, et al.* (2010). Crystal structure of a 117 kDa glucansucrase fragment provides insight into evolution and product specificity of GH70 enzymes. *Proceedings of the National Academy of Sciences, 107*(50), 21406. doi:10.1073/pnas.1007531107

Waldherr, F. W., Doll, V. M., Meissner, D., & Vogel, R. F. (2010). Identification and characterization of a glucan-producing enzyme from *Lactobacillus hilgardii* TMW 1.828 involved in granule formation of water kefir. *Food Microbiology, 27*(5), 672-678. doi:10.1016/j.fm.2010.03.013

Walter, J., Schwab, C., Loach, D. M., Gänzle, M. G., & Tannock, G. W. (2008). Glucosyltransferase A (GtfA) and inulosucrase (Inu) of *Lactobacillus reuteri* TMW1.106 contribute to cell aggregation, in vitro biofilm formation, and colonization of the mouse gastrointestinal tract. *Microbiology, 154*(1), 72-80. doi:10.1099/mic.0.2007/010637-0

Walton, K. W. (1952). The biological behaviour of a new synthetic anticoagulant (dextran sulphate) possessing heparin-like properties. *British journal of pharmacology and chemotherapy, 7*(3), 370-391. doi:10.1111/j.1476-5381.1952.tb00705.x

Wang, B., Song, Q., Zhao, F., Zhang, L., Han, Y., & Zhou, Z. (2019). Isolation and characterization of dextran produced by *Lactobacillus sakei* L3 from Hubei sausage. *Carbohydrate Polymers, 223*, 115111. doi:10.1016/j.carbpol.2019.115111

Ward, H. M. (1892). The ginger-beer plant, and the organisms composing it: A contribution to the study of fermentation-yeasts and bacteria. *Philosophical Transactions of the Royal Society of London. B, 183*, 125-197.

Waśko, A., Polak-Berecka, M., Paduch, R., & Jóźwiak, K. (2014). The effect of moonlighting proteins on the adhesion and aggregation ability of *Lactobacillus helveticus*. *Anaerobe, 30*, 161-168. doi:10.1016/j.anaerobe.2014.10.002

Wefers, D., & Bunzel, M. (2015). Characterization of dietary fiber polysaccharides from dehulled common buckwheat (*Fagopyrum esculentum*) seeds. *Cereal Chemistry, 92*(6), 598-603. doi:10.1094/CCHEM-03-15-0056-R

Wein, T., Hülter, N. F., Mizrahi, I., & Dagan, T. (2019). Emergence of plasmid stability under non-selective conditions maintains antibiotic resistance. *Nature Communications, 10*(1), 2595. doi:10.1038/s41467-019-10600-7

Welman, A. D., & Maddox, I. S. (2003). Exopolysaccharides from lactic acid bacteria: perspectives and challenges. *Trends in Biotechnology, 21*(6), 269-274. doi:10.1016/S0167-7799(03)00107-0

Werning, M. L., Ibarburu, I., DueÑAs, M. T., Irastorza, A. N. A., Navas, J., & LÓPez, P. (2006). *Pediococcus parvulus* gtf gene encoding the GTF glycosyltransferase and its application for specific PCR detection of β-d-glucan–producing bacteria in foods and beverages. *Journal of Food Protection, 69*(1), 161-169. doi:10.4315/0362-028X-69.1.161

Wiame, E., Delpierre, G., Collard, F., & Van Schaftingen, E. (2002). Identification of a pathway for the utilization of the Amadori product fructoselysine in *Escherichia coli*. *The Journal of biological chemistry, 277*(45), 42523-42529. doi:10.1074/jbc.m200863200

Wiame, E., Duquenne, A., Delpierre, G., & Van Schaftingen, E. (2004). Identification of enzymes acting on α-glycated amino acids in *Bacillus subtilis*. *FEBS Letters, 577*(3), 469-472. doi:10.1016/j.febslet.2004.10.049

Wiame, E., Lamosa, P., Santos, H., & Van Schaftingen, E. (2005). Identification of glucoselysine-6-phosphate deglycase, an enzyme involved in the metabolism of the fructation product glucoselysine. *The Biochemical journal, 392*(Pt 2), 263-269. doi:10.1042/BJ20051183

Wickramasinghe, N. N., Ravensdale, J. T., Coorey, R., Dykes, G. A., & Scott Chandry, P. (2019). *In situ* characterisation of biofilms formed by psychrotrophic meat spoilage pseudomonads. *Biofouling, 35*(8), 840-855. doi:10.1080/08927014.2019.1669021

Williams, J. G. K., Kubelik, A. R., Livak, K. J., Rafalski, J. A., & Tingey, S. V. (1990). DNA polymorphisms amplified by arbitrary primers are useful as genetic markers. *Nucleic Acids Research, 18*(22), 6531-6535. doi:10.1093/nar/18.22.6531

Willis, L. M., & Whitfield, C. (2013). Structure, biosynthesis, and function of bacterial capsular polysaccharides synthesized by ABC transporter-dependent pathways. *Carbohydrate Research, 378*, 35-44. doi:10.1016/j.carres.2013.05.007

Wingender, J., Neu, T. R., & Flemming, H.-C. (1999). What are bacterial extracellular polymeric substances? In J. Wingender, T. R. Neu, & H.-C. Flemming (Eds.), *Microbial extracellular polymeric substances: characterization, structure and function* (pp. 1-19). Berlin, Heidelberg: Springer Berlin Heidelberg.

Wisselink, H. W., Weusthuis, R. A., Eggink, G., Hugenholtz, J., & Grobben, G. J. (2002). Mannitol production by lactic acid bacteria: a review. *International Dairy Journal, 12*(2), 151-161. doi:10.1016/S0958-6946(01)00153-4

Wolter, A., Hager, A.-S., Zannini, E., Czerny, M., & Arendt, E. K. (2014a). Influence of dextran-producing *Weissella cibaria* on baking properties and sensory profile of gluten-free and wheat breads. *International Journal of Food Microbiology, 172*, 83-91. doi:10.1016/j.ijfoodmicro.2013.11.015

Wolter, A., Hager, A. S., Zannini, E., Galle, S., Gänzle, M. G., Waters, D. M., *et al.* (2014b). Evaluation of exopolysaccharide producing *Weissella cibaria* MG1 strain for the production of sourdough from various flours. *Food Microbiology, 37*, 44-50. doi:10.1016/j.fm.2013.06.009

Wong, H. C., Fear, A. L., Calhoon, R. D., Eichinger, G. H., Mayer, R., Amikam, D., *et al.* (1990). Genetic organization of the cellulose synthase operon in *Acetobacter xylinum*. *Proceedings of the National Academy of Sciences, 87*(20), 8130. doi:10.1073/pnas.87.20.8130

Wright, M. H., Adelskov, J., & Greene, A. C. (2017). Bacterial DNA extraction using individual enzymes and phenol/chloroform separation. *Journal of microbiology & biology education, 18*(2), 18.12.48. doi:10.1128/jmbe.v18i2.1348

Wuttge, S., Bommer, M., Jäger, F., Martins, B. M., Jacob, S., Licht, A., *et al.* (2012). Determinants of substrate specificity and biochemical properties of the sn-glycerol-3-phosphate ATP binding cassette transporter (UgpB–AEC2) of *Escherichia coli*. *Molecular Microbiology, 86*(4), 908-920. doi:10.1111/mmi.12025

Xavier, J. B., & Foster, K. R. (2007). Cooperation and conflict in microbial biofilms. *Proceedings of the National Academy of Sciences, 104*(3), 876. doi:10.1073/pnas.0607651104

Xu, D. (2019). *Interaction between Lactobacillus hordei, Lactobacillus nagelii and Saccharomyces cerevisiae isolates from water kefir.* (Dissertation), Technical University Munich, Munich.

Xu, D., Bechtner, J., Behr, J., Eisenbach, L., Geißler, A. J., & Vogel, R. F. (2019a). Lifestyle of *Lactobacillus hordei* isolated from water kefir based on genomic, proteomic and physiological characterization. *International Journal of Food Microbiology, 290*, 141-149. doi:10.1016/j.ijfoodmicro.2018.10.004

Xu, D., Behr, J., Geißler, A. J., Bechtner, J., Ludwig, C., & Vogel, R. F. (2019b). Label-free quantitative proteomic analysis reveals the lifestyle of *Lactobacillus hordei* in the presence of *Sacchromyces cerevisiae*. *International Journal of Food Microbiology, 294*, 18-26. doi:10.1016/j.ijfoodmicro.2019.01.010

Xu, D., Fels, L., Wefers, D., Behr, J., Jakob, F., & Vogel, R. F. (2018). *Lactobacillus hordei* dextrans induce *Saccharomyces cerevisiae* aggregation and network formation on hydrophilic surfaces. *International Journal of Biological Macromolecules, 115*, 236-242. doi:10.1016/j.ijbiomac.2018.04.068

Xu, W., Ni, D., Zhang, W., Guang, C., Zhang, T., & Mu, W. (2019). Recent advances in levansucrase and inulosucrase: evolution, characteristics, and application. *Critical Reviews in Food Science and Nutrition, 59*(22), 3630-3647. doi:10.1080/10408398.2018.1506421

Yan, M., Han, J., Xu, X., Liu, L., Gao, C., Zheng, H., *et al.* (2016). Gsy, a novel glucansucrase from *Leuconostoc mesenteroides*, mediates the formation of cell aggregates in response to oxidative stress. *Scientific Reports, 6*(1), 38122. doi:10.1038/srep38122

Yang, Q., & Sze, S.-H. (2008). Large-scale analysis of gene clustering in bacteria. *Genome research, 18*(6), 949-956. doi:10.1101/gr.072322.107

Yang, Y., Peng, Q., Guo, Y., Han, Y., Xiao, H., & Zhou, Z. (2015). Isolation and characterization of dextran produced by *Leuconostoc citreum* NM105 from manchurian sauerkraut. *Carbohydrate Polymers, 133*, 365-372. doi:10.1016/j.carbpol.2015.07.061

Yaylayan, V. A., Huyghues-Despointes, A., & Feather, M. S. (1994). Chemistry of Amadori rearrangement products: Analysis, synthesis, kinetics, reactions, and spectroscopic properties. *Critical Reviews in Food Science and Nutrition, 34*(4), 321-369. doi:10.1080/10408399409527667

Yebra, M. J., Monedero, V., Zúñiga, M., Deutscher, J., & Pérez-Martínez, G. (2006). Molecular analysis of the glucose-specific phosphoenolpyruvate:sugar phosphotransferase system from *Lactobacillus casei* and its links with the control of sugar metabolism. *Microbiology, 152*(1), 95-104. doi:10.1099/mic.0.28293-0

Younes, M., Aggett, P., Aguilar, F., Crebelli, R., Filipič, M., Frutos, M. J.*, et al.* (2018). Re-evaluation of carrageenan (E 407) and processed Eucheuma seaweed (E 407a) as food additives. *EFSA Journal, 16*(4), e05238. doi:10.2903/j.efsa.2018.5238

Yu, N. Y., Wagner, J. R., Laird, M. R., Melli, G., Rey, S., Lo, R.*, et al.* (2010). PSORTb 3.0: improved protein subcellular localization prediction with refined localization subcategories and predictive capabilities for all prokaryotes. *Bioinformatics (Oxford, England), 26*(13), 1608-1615. doi:10.1093/bioinformatics/btq249

Yuryev, V., Tomasik, P., & Bertoft, E. (2007). *Starch: Achievements in understanding of structure and functionality*. New York: Nova Science Publishers.

Zacharius, R. M., Zell, T. E., Morrison, J. H., & Woodlock, J. J. (1969). Glycoprotein staining following electrophoresis on acrylamide gels. *Analytical Biochemistry, 30*(1), 148-152. doi:10.1016/0003-2697(69)90383-2

Zannini, E., Waters, D. M., Coffey, A., & Arendt, E. K. (2016). Production, properties, and industrial food application of lactic acid bacteria-derived exopolysaccharides. *Applied Microbiology and Biotechnology, 100*(3), 1121-1135. doi:10.1007/s00253-015-7172-2

Zhao, H., Xia, J., Wang, J., Yan, X., Wang, C., Lei, T.*, et al.* (2018). Production of bacterial cellulose using polysaccharide fermentation wastewater as inexpensive nutrient sources. *Biotechnology & Biotechnological Equipment, 32*(2), 350-356. doi:10.1080/13102818.2017.1418673

Zheng, J., Ruan, L., Sun, M., & Gänzle, M. (2015). A genomic view of Lactobacilli and Pediococci demonstrates that phylogeny matches ecology and physiology. *Applied and Environmental Microbiology, 81*(20), 7233. doi:10.1128/AEM.02116-15

Zheng, J., Wittouck, S., Salvetti, E., Franz, C. M. A. P., Harris, H. M. B., Mattarelli, P.*, et al.* (2020). A taxonomic note on the genus Lactobacillus: Description of 23 novel genera, emended description of the genus Lactobacillus Beijerinck 1901, and union of Lactobacillaceae and Leuconostocaceae. *International Journal of Systematic and Evolutionary Microbiology, 70*(4), 2782-2858. doi:10.1099/ijsem.0.004107

Zhou, H.-X., & Pang, X. (2018). Electrostatic interactions in protein structure, folding, binding, and condensation. *Chemical reviews, 118*(4), 1691-1741. doi:10.1021/acs.chemrev.7b00305

Zhu, F., Du, B., & Xu, B. (2016). A critical review on production and industrial applications of beta-glucans. *Food Hydrocolloids, 52*, 275-288. doi:10.1016/j.foodhyd.2015.07.003

Zorba, M., Hancioglu, O., Genc, M., Karapinar, M., & Ova, G. (2003). The use of starter cultures in the fermentation of boza, a traditional Turkish beverage. *Process Biochemistry, 38*(10), 1405-1411. doi:10.1016/S0032-9592(03)00033-5

9 Appendix

Appendix 1 Amino acid sequence of the *L. hordei* TMW 1.1822 dextransucrase. Blue = serine and threonine residues, red = conserved sequence motifs harbouring the substrate-binding sites.

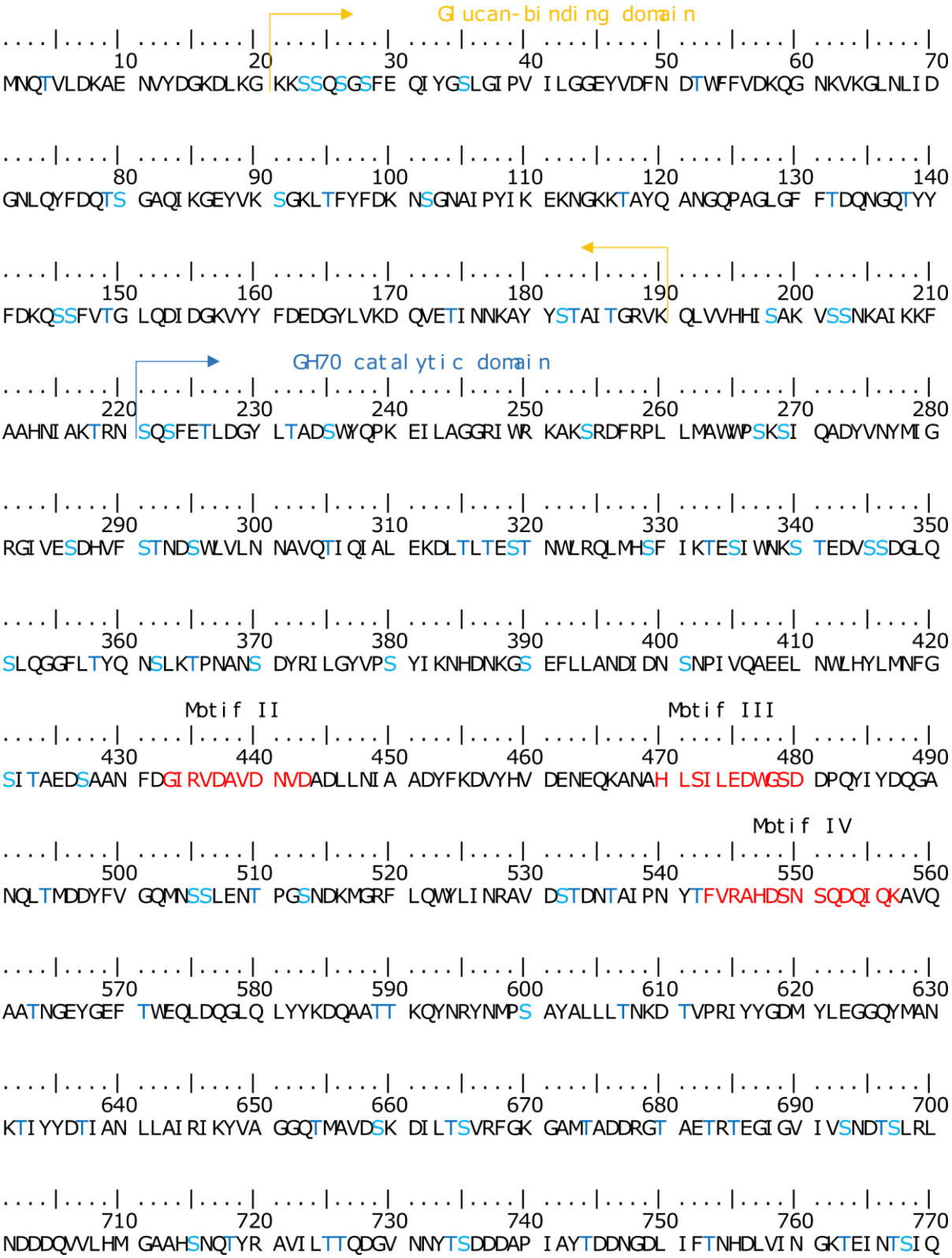

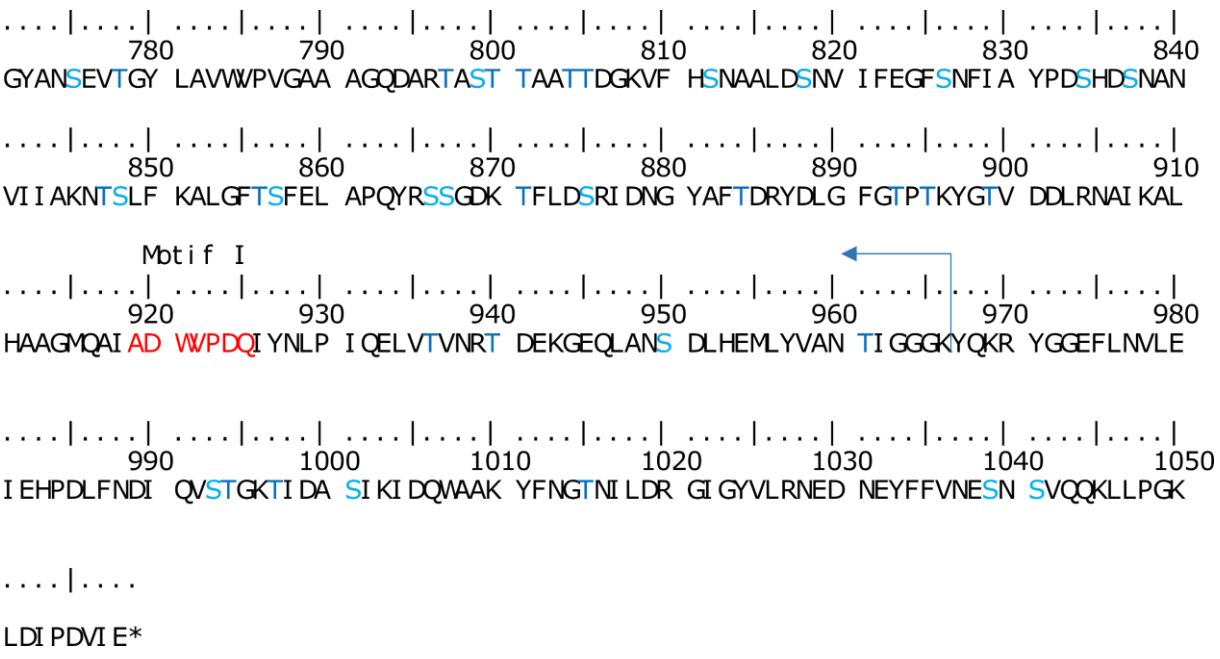
780 790 800 810 820 830 840
GYANSEVTGY LAVWVPVGAA AGQDARTAST TAATTDGKVF HSNAALDSNV IFEGFSNFIA YPDSHDSNAN
850 860 870 880 890 900 910
VIIAKNTSLF KALGFTSFEL APQYRSSGDK TFLDSRIDNG YAFTDRYDLG FGTPTKYGTV DDLRNAIKAL
Motif I
920 930 940 950 960 970 980
HAAGMQAIAD WVPDQIYNLP IQELVTVNRT DEKGEQLANS DLHEMLYVAN TIGGGKYQKR YGGEFLNVLE
990 1000 1010 1020 1030 1040 1050
IEHPDLFNDI QVSTGKTIDA SIKIDQWAAK YFNGTNILDR GIGYVLRNED NEYFFVNESN SVQQKLLPGK
LDIPDVIE*

Appendix 2 Amino acid sequence of the *L. nagelii* TMW 1.1827 dextransucrase. Blue = serine and threonine residues, red = conserved sequence motifs harbouring the substrate-binding sites, green = signal peptide.

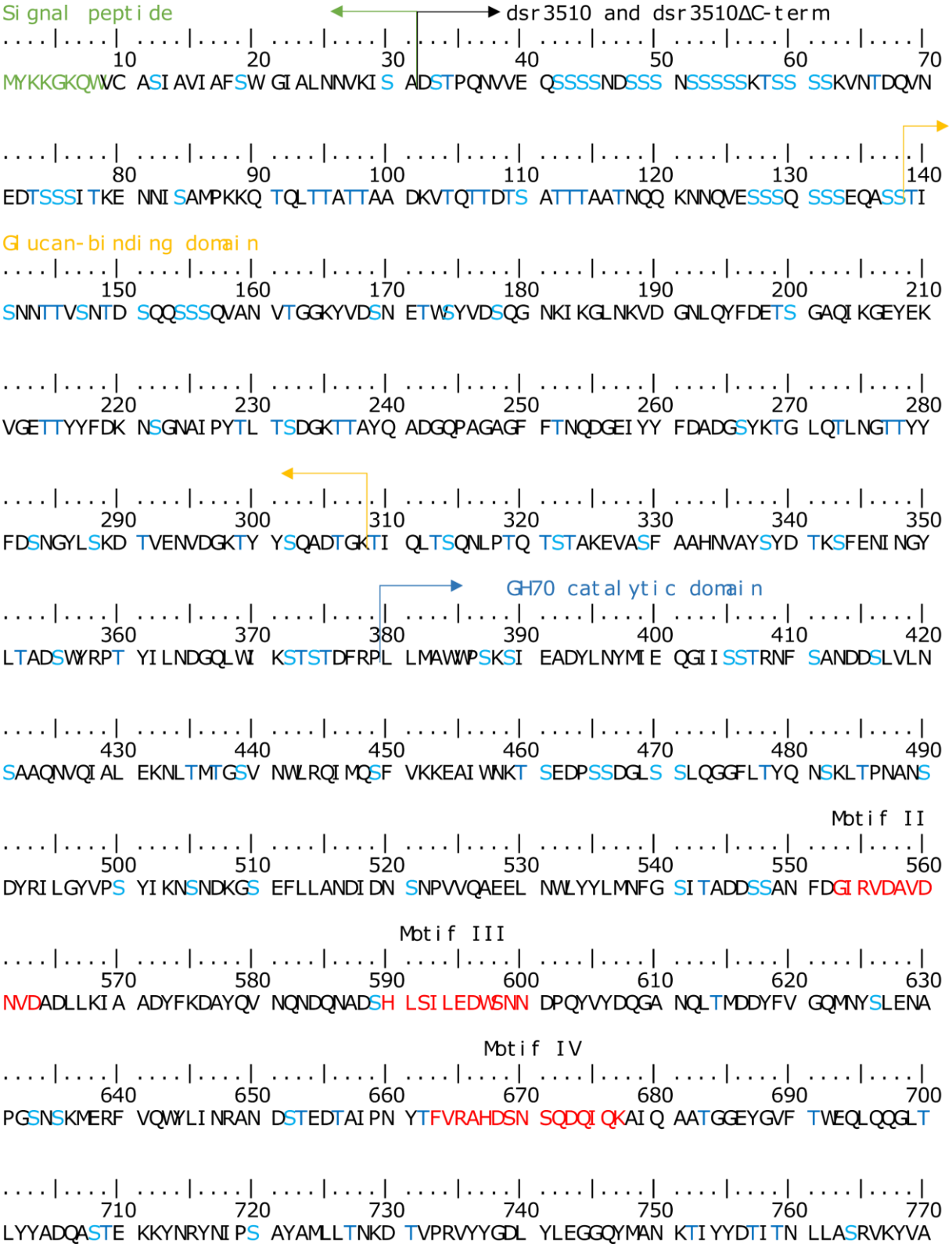

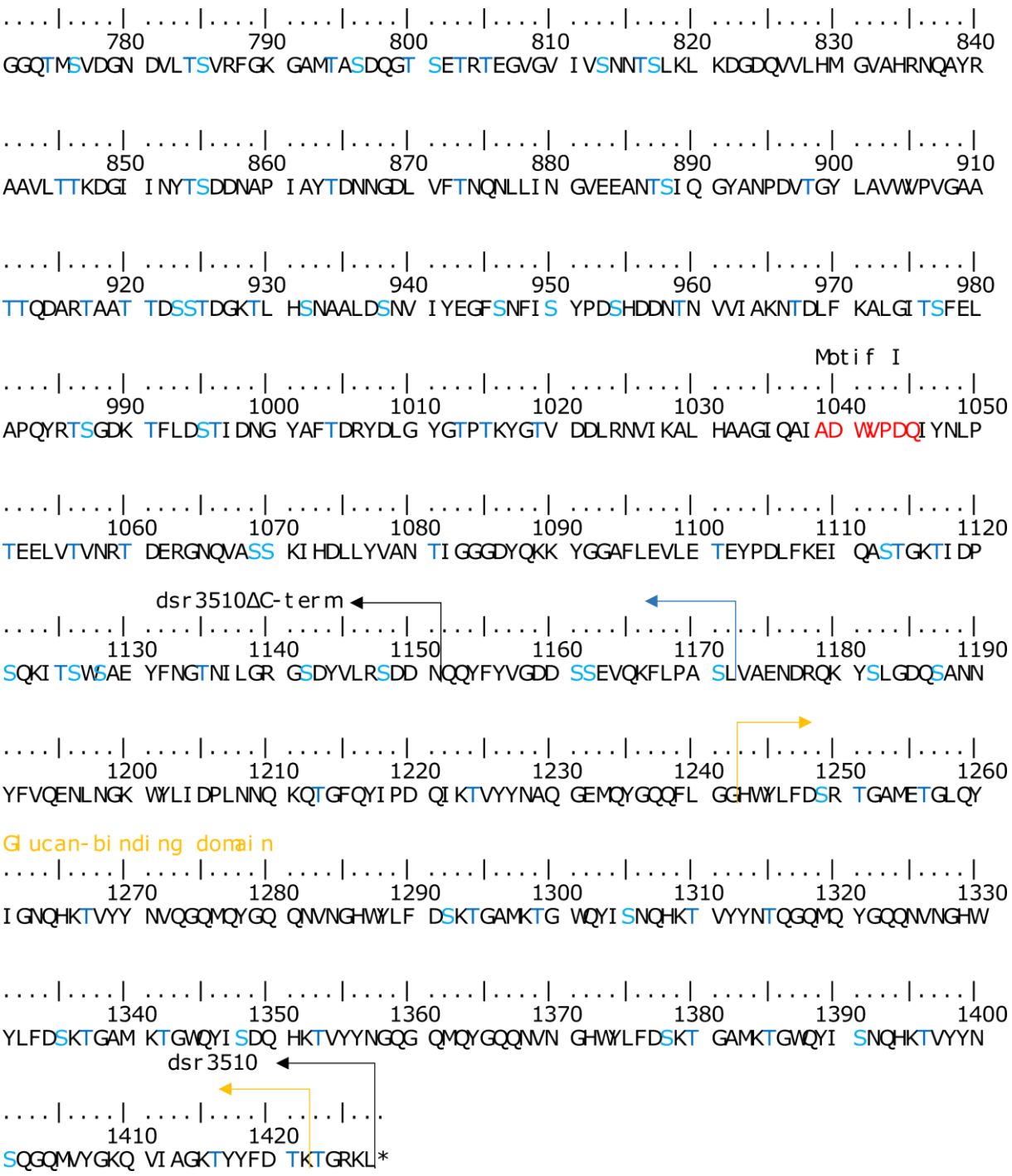
780 790 800 810 820 830 840
GGQTMSVDGN DVLTSVRFGK GAMTASDQGT SETRTEGVGV IVSNNTSLKL KDGDQVVLHM GVAHRNQAYR
850 860 870 880 890 900 910
AAVLTTKDGI INYTSDDNAP IAYTDNNGDL VFTNQNLLIN GVEEANTSIQ GYANPDVTGY LAVVWPVGAA
920 930 940 950 960 970 980
TTQDARTAAT TDSSTDGKTL HSNAALDSNV IYEGFSNFIS YPDSHDDNTN VVIAKNTDLF KALGITSFEL
Motif I
990 1000 1010 1020 1030 1040 1050
APQYRTSGDK TFLDSTIDNG YAFTDRYDLG YGTPTKYGTV DDLRNVIKAL HAAGIQAIAD VWPDQIYNLP
1060 1070 1080 1090 1100 1110 1120
TEELVTVNRT DERGNQVASS KIHDLLYVAN TIGGGDYQKK YGGAFLEVLE TEYPDLFKEI QASTGKTIDP
dsr3510ΔC-term
1130 1140 1150 1160 1170 1180 1190
SQKITSWSAE YFNGTNILGR GSDYVLRSDD NQQYFYVGDD SSEVQKFLPA SLVAENDRQK YSLGDQSANN
1200 1210 1220 1230 1240 1250 1260
YFVQENLNGK WYLIDPLNNQ KQTGFQYIPD QIKTVYYNAQ GEMQYGQQFL GGHWYLFDSR TGAMETGLQY
Glucan-binding domain
1270 1280 1290 1300 1310 1320 1330
IGNQHKTVYY NVQGQMQYGQ QNVNGHWYLF DSKTGAMKTG WQYISNQHKT VYYNTQGQMQ YGQQNVNGHW
1340 1350 1360 1370 1380 1390 1400
YLFDSKTGAM KTGWQYISDQ HKTVYYNGQG QMQYGQQNVN GHWYLFDSKT GAMKTGWQYI SNQHKTVYYN
dsr3510
1410 1420
SQGQMVYGKQ VIAGKTYYFD TKTGRKL*

Appendix 3 Correlation coefficients and corresponding p-values of Spearman´s rank correlation analysis on the API-test results with the isolation source water kefir. No correlation analysis could be performed for substrates that were not fermented by any strain (= n.a.).

Substrate	Correlation coefficient	p-value
glycerol	n.a.	n.a.
erythritol	n.a.	n.a.
D-arabinose	n.a.	n.a.
L-arabinose	0.517	0.016
D-ribose	n.a.	n.a.
D-xylose	-0.181	0.433
L-xylose	n.a.	n.a.
D-adonitol	n.a.	n.a.
methyl-beta-D-xylopyranoside	n.a.	n.a.
D-galactose	-0.106	0.647
D-glucose	n.a.	n.a.
D-fructose	n.a.	n.a.
D-mannose	0.181	0.433
L-sorbose	0.106	0.647
L-rhamnose	0.279	0.221
dulcitol	n.a.	n.a.
inositol	n.a.	n.a.
D-mannitol	0.645	0.002
D-sorbitol	0.106	0.647
methyl-alpha-D-mannopyranoside	0.167	0.470
methyl-alpha-D-glucopyranoside	n.a.	n.a.
N-acetylglucosamine	0.181	0.433
amygdalin	0.181	0.433
arbutin	0.181	0.433
esculin	0.181	0.433
salicin	0.181	0.433
D-cellobiose	0.181	0.433
D-maltose	-0.141	0.541
D-lactose	n.a.	n.a.
D-melibiose	-0.181	0.433
D-sucrose	0.354	0.116
D-trehalose	0.224	0.330
inulin	0.181	0.433
D-melezitose	n.a.	1.000
D-raffinose	-0.224	0.330
starch	n.a.	n.a.
glycogen	n.a.	n.a.
xylitol	n.a.	n.a.
gentibiose	0.181	0.433
D-turanose	0.224	0.330
D-lyxose	n.a.	n.a.
D-tagatose	-0.354	0.116
D-fucose	n.a.	n.a.

L-fucose	n.a.	n.a.
D-arabitol	n.a.	n.a.
L-arabitol	n.a.	n.a.
potassium gluconate	-0.181	0.433
potassium 2-ketogluconate	0.141	0.541
potassium 5-ketagluconate	-0.304	0.180

Appendix 4 Volumetric acitivities of the native extracellular dextransucrases of *L. hordei* TMW 1.1822 and *L. nagelii* TMW 1.1827 depending on the sucrose concentration.

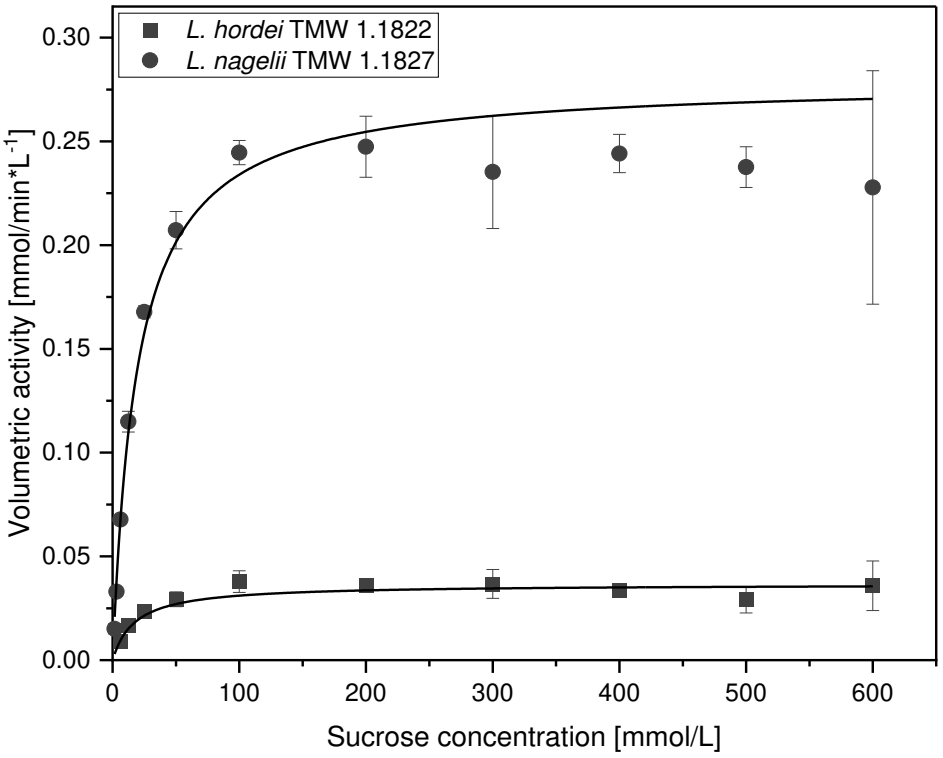

Appendix 5 Table of p-values representing statistical significance regarding isolated and predicted amounts of dextran and respective average molecular weights (M_w) and average rms radii (R_w) as obtained from comparison of dextrans produced by distinct amounts of enzyme extracts of *L. hordei* TMW 1.1822 and *L. nagelii* TMW 1.1827. - = no significant difference, light gray = $0.05 > p > 0.01$; gray = $0.01 \geq p > 0.001$; dark gray = $p \leq 0.001$.

Dextran isolated	1.1822-1X	1.1822-2X	1.1822-4X	1.1822-10X	1.1827-1X	1.1827-2X	1.1827-4X	1.1827-10X
1.1822-1X	-	< 0.001	< 0.001	< 0.001	0.002	< 0.001	< 0.001	0.007
1.1822-2X	< 0.001	-	< 0.001	< 0.001	< 0.001	< 0.001	< 0.001	< 0.001
1.1822-4X	< 0.001	< 0.001	-	0.001	< 0.001	< 0.001	< 0.001	< 0.001
1.1822-10X	< 0.001	< 0.001	0.001	-	< 0.001	< 0.001	< 0.001	< 0.001
1.1827-1X	0.002	< 0.001	< 0.001	< 0.001	-	-	-	0.029
1.1827-2X	< 0.001	< 0.001	< 0.001	< 0.001	-	-	-	0.008
1.1827-4X	< 0.001	< 0.001	< 0.001	< 0.001	-	-	-	0.003
1.1827-10X	0.007	< 0.001	< 0.001	< 0.001	0.029	0.008	0.003	-
Dextran predicted	1.1822-1X	1.1822-2X	1.1822-4X	1.1822-10X	1.1827-1X	1.1827-2X	1.1827-4X	1.1827-10X
1.1822-1X	-	< 0.001	< 0.001	< 0.001	0.001	0.002	< 0.001	0.004
1.1822-2X	< 0.001	-	< 0.001	< 0.001	< 0.001	< 0.001	< 0.001	< 0.001
1.1822-4X	< 0.001	< 0.001	-	< 0.001	< 0.001	< 0.001	< 0.001	< 0.001
1.1822-10X	< 0.001	< 0.001	< 0.001	-	< 0.001	< 0.001	< 0.001	< 0.001
1.1827-1X	0.001	< 0.001	< 0.001	< 0.001	-	-	-	0.003
1.1827-2X	0.002	< 0.001	< 0.001	< 0.001	-	-	-	0.005
1.1827-4X	< 0.001	< 0.001	< 0.001	< 0.001	-	-	-	< 0.001
1.1827-10X	0.004	< 0.001	< 0.001	< 0.001	0.003	0.005	< 0.001	-
R_w	1.1822-1X	1.1822-2X	1.1822-4X	1.1822-10X	1.1827-1X	1.1827-2X	1.1827-4X	1.1827-10X
1.1822-1X	-	0.048	0.032	0.005	0.005	0.001	0.006	< 0.001
1.1822-2X	0.048	-	-	0.004	0.010	< 0.001	0.007	< 0.001
1.1822-4X	0.032	-	-	-	-	-	-	0.046
1.1822-10X	0.005	0.004	-	-	0.031	< 0.001	-	< 0.001
1.1827-1X	0.005	0.010	-	0.031	-	-	0.032	-
1.1827-2X	0.001	< 0.001	-	< 0.001	-	-	0.001	0.004
1.1827-4X	0.006	0.007	-	-	0.032	0.001	-	< 0.001
1.1827-10X	< 0.001	< 0.001	0.046	< 0.001	-	0.004	< 0.001	-
M_w	1.1822-1X	1.1822-2X	1.1822-4X	1.1822-10X	1.1827-1X	1.1827-2X	1.1827-4X	1.1827-10X
1.1822-1X	-	0.006	0.012	-	0.006	0.002	< 0.001	0.001
1.1822-2X	0.006	-	-	-	-	-	-	0.012
1.1822-4X	0.012	-	-	-	-	-	-	0.012
1.1822-10X	-	-	-	-	-	-	-	0.011
1.1827-1X	0.006	-	-	-	-	-	-	-
1.1827-2X	0.002	-	-	-	-	-	-	0.016
1.1827-4X	< 0.001	-	-	-	-	-	-	0.011
1.1827-10X	0.001	0.012	0.012	0.011	-	0.016	0.011	-

Appendix 6 Table of p-values representing statistical significance regarding isolated and predicted amounts of dextran and respective average molecular weights (M_w) and average rms radii (R_w) as obtained from comparison of dextrans produced by distinct amounts of enzyme extracts of the heterologously expressed dextransucrase variants dsr3510 and dsr3510ΔC-term. - = no significant difference, light gray = $0.05 > p > 0.01$; gray = $0.01 \geq p > 0.001$; dark gray = $p \leq 0.001$.

Dextran isolated	**dsr3510ΔC-term 1X**	**dsr3510ΔC-term 2X**	**dsr3510ΔC-term 4X**	**dsr3510ΔC-term 10X**	**dsr3510 1X**	**dsr3510 2X**	**dsr3510 4X**	**dsr3510 10X**
dsr3510ΔC-term 1X	-	0.039	0.003	<0.001	<0.001	<0.001	<0.001	<0.001
dsr3510ΔC-term 2X	0.039	-	0.038	0.001	0.254	0.527	0.529	0.033
dsr3510ΔC-term 4X	0.003	0.038	-	0.011	0.008	0.012	0.012	0.528
dsr3510ΔC-term 10X	<0.001	0.001	0.011	-	<0.001	<0.001	<0.001	0.002
dsr3510 1X	<0.001	0.254	0.008	<0.001	-	0.048	0.066	0.002
dsr3510 2X	<0.001	0.527	0.012	<0.001	0.048	-	1.000	0.004
dsr3510 4X	0.001	0.529	0.012	<0.001	0.066	1.000	-	0.004
dsr3510 10X	0.001	0.033	0.528	0.002	0.002	0.004	0.004	-
Dextran predicted	**dsr3510ΔC-term 1X**	**dsr3510ΔC-term 2X**	**dsr3510ΔC-term 4X**	**dsr3510ΔC-term 10X**	**dsr3510 1X**	**dsr3510 2X**	**dsr3510 4X**	**dsr3510 10X**
dsr3510ΔC-term 1X	-	0.142	0.001	<0.001	0.644	0.880	0.510	0.005
dsr3510ΔC-term 2X	0.142	-	0.046	0.003	0.108	0.149	0.101	0.126
dsr3510ΔC-term 4X	0.001	0.046	-	0.007	0.001	0.001	0.001	0.361
dsr3510ΔC-term 10X	<0.001	0.003	0.007	-	<0.001	<0.001	<0.001	0.005
dsr3510 1X	0.644	0.108	0.001	<0.001	-	0.457	0.640	0.004
dsr3510 2X	0.880	0.149	0.001	<0.001	0.457	-	0.397	0.005
dsr3510 4X	0.510	0.101	0.001	<0.001	0.640	0.397	-	0.004
dsr3510 10X	0.005	0.126	0.361	0.005	0.004	0.005	0.004	-
R_w	**dsr3510ΔC-term 1X**	**dsr3510ΔC-term 2X**	**dsr3510ΔC-term 4X**	**dsr3510ΔC-term 10X**	**dsr3510 1X**	**dsr3510 2X**	**dsr3510 4X**	**dsr3510 10X**
dsr3510ΔC-term 1X	-	0.136	0.051	0.003	<0.001	<0.001	<0.001	<0.001
dsr3510ΔC-term 2X	0.136	-	0.616	0.106	0.002	<0.001	<0.001	0.001
dsr3510ΔC-term 4X	0.051	0.616	-	0.173	0.001	<0.001	<0.001	0.001
dsr3510ΔC-term 10X	0.003	0.106	0.173	-	<0.001	<0.001	<0.001	0.001
dsr3510 1X	<0.001	0.002	0.001	<0.001	-	0.002	0.001	0.010
dsr3510 2X	<0.001	<0.001	<0.001	<0.001	0.002	-	0.069	0.122
dsr3510 4X	<0.001	<0.001	<0.001	<0.001	0.001	0.069	-	0.304
dsr3510 10X	<0.001	0.001	0.001	0.001	0.010	0.122	0.304	-
M_w	**dsr3510ΔC-term 1X**	**dsr3510ΔC-term 2X**	**dsr3510ΔC-term 4X**	**dsr3510ΔC-term 10X**	**dsr3510 1X**	**dsr3510 2X**	**dsr3510 4X**	**dsr3510 10X**
dsr3510ΔC-term 1X	-	0.234	0.186	0.002	0.002	<0.001	<0.001	0.001
dsr3510ΔC-term 2X	0.234	-	0.007	<0.001	0.001	<0.001	<0.001	<0.001
dsr3510ΔC-term 4X	0.186	0.007	-	0.001	0.002	<0.001	<0.001	0.001
dsr3510ΔC-term 10X	0.002	<0.001	0.001	-	0.076	0.004	0.005	0.002
dsr3510 1X	0.002	0.001	0.002	0.076	-	0.065	0.063	0.006
dsr3510 2X	<0.001	<0.001	<0.001	0.004	0.065	-	0.908	0.015

dsr3510 4X	<0.001	<0.001	<0.001	0.005	0.063	0.908	-	0.017
dsr3510 10X	0.001	<0.001	0.001	0.002	0.006	0.015	0.017	-

Appendix 7 *Endo*-dextranase fingerprints of dextrans obtained with 4-fold and 10-fold dilutions of the enzyme extracts of the heterologously expressed dextransucrase variants dsr3510 and dsr3510ΔC-term in comparison with the dextrans obtained with native dextransucrase-containing secretomes of *L. hordei* TMW 1.1822 and *L. nagelii* TMW 1.1827.

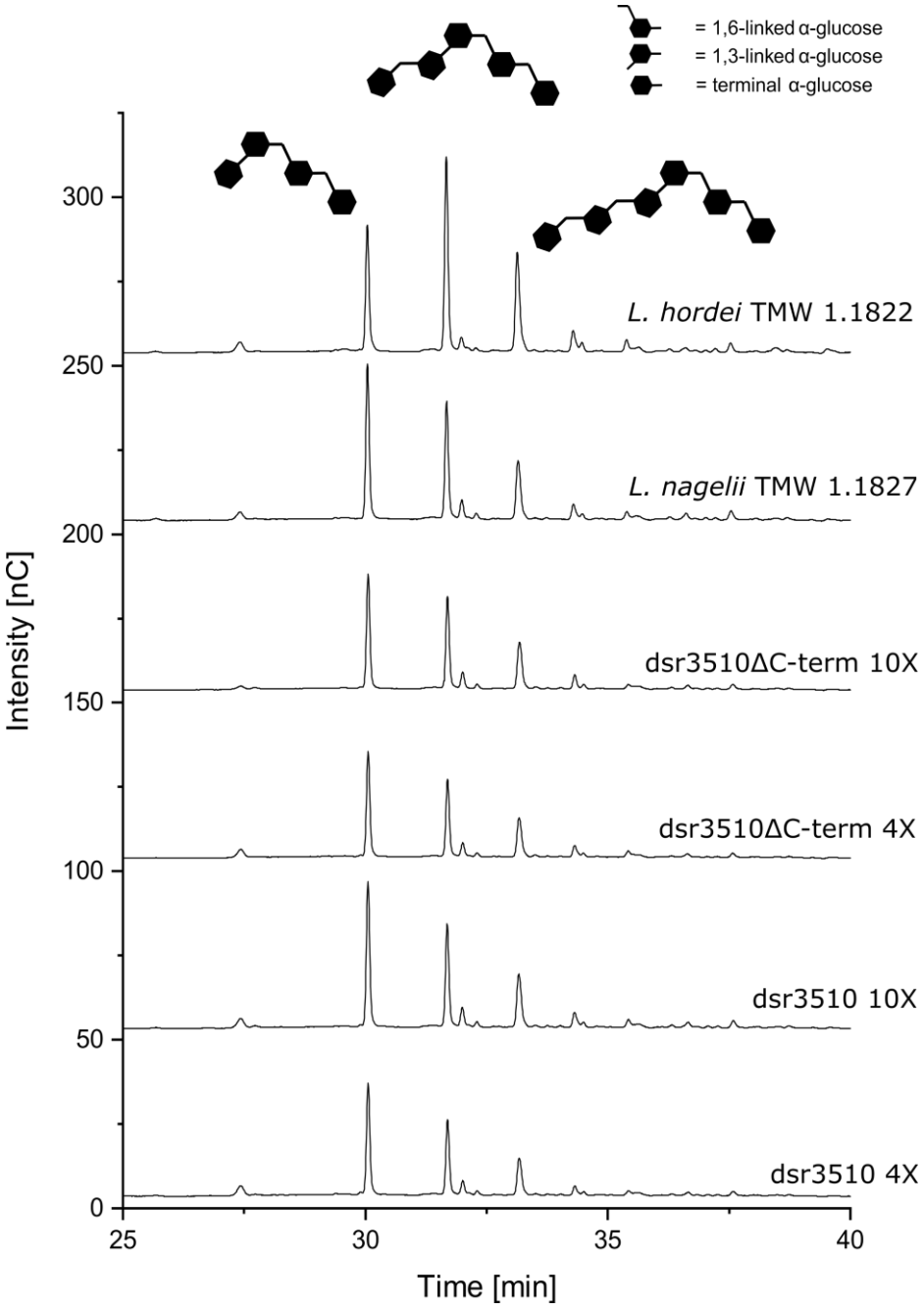

Appendix 8 Table of p-values representing statistical significance regarding volumetric activity and isolated amounts of dextran as determined from native extracellular dextransucrase reaction of the *L. nagelii* TMW 1.1827 dextransucrase obtained at different initial pH and in the presence or absence of sucrose. Light gray = $0.05 > p > 0.01$; gray = $0.01 \geq p > 0.001$; dark gray = $p \leq 0.001$.

Volumetric activity	pH 5.5 + sucrose	pH 6.5 + sucrose	pH 4.5 w/o sucrose	pH 5.5 w/o sucrose	pH 6.5 w/o sucrose
pH 4.5 + sucrose	0.982	0.979	<0.001	<0.001	<0.001
pH 5.5 + sucrose	-	0.994	<0.001	<0.001	<0.001
pH 6.5 + sucrose	-	-	<0.001	<0.001	<0.001
pH 4.5 w/o sucrose	-	-	-	0.091	0.013
pH 5.5 w/o sucrose	-	-	-	-	0.083
Dextran isolated	**pH 5.5 + sucrose**	**pH 6.5 + sucrose**	**pH 4.5 w/o sucrose**	**pH 5.5 w/o sucrose**	**pH 6.5 w/o sucrose**
pH 4.5 + sucrose	0.046	0.038	<0.001	<0.001	<0.001
pH 5.5 + sucrose	-	0.157	<0.001	<0.001	<0.001
pH 6.5 + sucrose	-	-	0.001	<0.001	0.001
pH 4.5 w/o sucrose	-	-	-	0.137	0.068
pH 5.5 w/o sucrose	-	-	-	-	0.286

Appendix 9 Table of p-values representing statistical significance regarding isolated and predicted amounts of dextran, as well as rms radii (R_w) and molecular weights (M_w) of dextrans obtained after different incubation periods using native extracellular dextransucrase of *L. nagelii* TMW 1.1827. - = no significant difference, light gray = $0.05 > p > 0.01$; gray = $0.01 \geq p > 0.001$; dark gray = $p \leq 0.001$.

Dextran isolated	10 min	60 min	180 min	1440 min	Dextran predicted	10 min	60 min	180 min	1440 min
10 min	-	0.406	0.007	0.003	**10Min**	-	0.352	0.004	0.002
60 min	0.406	-	0.044	0.014	**60Min**	0.352	-	0.024	0.012
180 min	0.007	0.044	-	0.091	**180Min**	0.004	0.024	-	0.213
1440 min	0.003	0.014	0.091	-	**1440Min**	0.002	0.012	0.213	-
R_w	**10 min**	**60 min**	**180 min**	**1440 min**	**M_w**	**10 min**	**60 min**	**180 min**	**1440 min**
10 min	-	0.002	0.002	<0.001	**10 min**	-	0.438	0.016	0.009
60 min	0.002	-	0.019	<0.001	**60 min**	0.438	-	0.070	0.041
180 min	0.002	0.019	-	0.273	**180 min**	0.016	0.070	-	0.600
1440 min	<0.001	<0.001	0.273	-	**1440 min**	0.009	0.041	0.600	-

Appendix 10 GC-contents [%] of all contigs, chromosomes and plasmids of the *L. hordei* and *L. nagelii* strains used during this study.

	TMW 1.1907	TMW 1.1823		TMW 1.1822	TMW 1.2353^T	TMW 1.1827	TMW 1.2352^T
Contig 1	34.6	36.3	**Chromosome**	35.0	35.2	36.7	36.8
Contig 2	34.8	37.2	**Plasmid 1**	39.3	31.4	39.2	39.0
Contig 3	34.9	37.6	**Plasmid 2**	37.4	36.7	40.2	
Contig 4	35.5	36.6	**Plasmid 3**	40.1		38.7	
Contig 5	35.0	36.0					
Contig 6	35.0	36.8					
Contig 7	32.8	35.8					
Contig 8	34.6	37.2					
Contig 9	33.7	34.3					
Contig 10	49.4	35.4					
Contig 11	39.4	37.2					
Contig 12	38.4	35.6					
Contig 13	49.2	36.7					
Contig 14	38.7	34.9					
Contig 15	51.1	37.9					
Contig 16		38.7					
Contig 17		41.1					
Contig 18		33.1					
Contig 19		35.2					
Contig 20		34.3					
Contig 21		49.3					
Contig 22		41.6					
Contig 23		36.0					
Contig 24		40.2					
Contig 25		40.9					
Contig 26		51.0					
Contig 27		39.1					
Contig 28		43.2					
Contig 29		40.2					

Appendix 11 Co-linear genes and portions of the genomes of *L. hordei* TMW 1.1822, TMW 1.1907 and TMW 1.2353^T and *L. nagelii* TMW 1.1823, TMW 1.1827 and TMW 1.2352^T compared with each other. OG = orthogroup.

***L. hordei* TMW 1.1822**	**OG in analysis**	**Collinear OG TMW 1.1907**		**Collinear OG TMW 1.2353^T**		**Collinear OG TMW 1.1823**		**Collinear OG TMW 1.1827**		**Collinear OG TMW 1.2352^T**	
Chromosome	2241	2241	100%	2083	92.95%	1685	75.19%	1685	75.19%	1779	79.38%
Plasmid1	73	9	12.33%	37	50.68%	73	100%	73	100%	8	10.96%
Plasmid2	70	0	0%	6	8.57%	37	52.86%	59	84.29%	5	7.14%
Plasmid3	39	0	0%	6	15.38%	13	33.33%	39	100%	5	12.82%
***L. hordei* TMW 1.1907**	**OG in analysis**	**Collinear OG TMW 1.1822**		**Collinear OG TMW 1.2353^T**		**Collinear OG TMW 1.1823**		**Collinear OG TMW 1.1827**		**Collinear OG TMW 1.2352^T**	
Chromosome	2160	2159	99.95%	2032	94.07%	1747	80.88%	1763	81.62%	1722	79.72%
Contig7	66	8	12.12%	0	0%	9	13.64%	7	10.61%	0	0%
Contig11	2	0	0%	0	0%	0	0%	0	0%	0	0%
Contig14	2	0	0%	0	0%	0	0%	0	0%	0	0%
Contig15	2	0	0%	0	0%	0	0%	0	0%	0	0%
***L. hordei* TMW 1.2353^T**	**OG in analysis**	**Collinear OG TMW 1.1822**		**Collinear OG TMW 1.1907**		**Collinear OG TMW 1.1823**		**Collinear OG TMW 1.1827**		**Collinear OG TMW 1.2352^T**	
Chromosome	2049	2029	99.02%	2023	98.73%	1673	81.65%	1673	81.65%	1711	83.50%
Plasmid1	173	0	0%	0	0%	0	0%	0	0%	17	9.83%
Plasmid2	71	33	46.48%	3	4.23%	31	43.66%	31	43.66%	56	78.87%
***L. nagelii* TMW 1.1823**	**OG in analysis**	**Collinear OG TMW 1.1822**		**Collinear OG TMW 1.1907**		**Collinear OG TMW 1.2353^T**		**Collinear OG TMW 1.1827**		**Collinear OG TMW 1.2352^T**	
Chromosome	2211	1647	74.49%	1687	76.30%	1570	71.01%	2210	99.95%	2210	99.95%
Plasmid1	70	70	100%	9	12.86%	34	48.57%	70	100%	8	11.43%
Plasmid2	38	25	65.79%	0	0%	3	7.89%	38	100%	5	13.16%
Contig20	9	0	0%	0	0%	0	0%	0	0%	0	0%
Contig22	4	0	0%	0	0%	0	0%	0	0%	0	0%
Contig24	3	3	100%	3	100%	3	100%	3	100%	3	100%
Contig25	2	0	0%	0	0%	0	0%	0	0%	0	0%
Contig27	2	0	0%	0	0%	0	0%	0	0%	0	0%
Contig28	1	0	0%	0	0%	0	0%	0	0%	0	0%
Contig29	1	0	0%	0	0%	0	0%	0	0%	0	0%
***L. nagelii* TMW 1.1827**	**OG in analysis**	**Collinear OG TMW 1.1822**		**Collinear OG TMW 1.1907**		**Collinear OG TMW 1.2353^T**		**Collinear OG TMW 1.1823**		**Collinear OG TMW 1.2352^T**	
Chromosome	2209	1654	74.88%	1710	77.41%	1564	70.80%	2209	100%	2209	100%
Plasmid1	72	72	100%	7	9.72%	36	50%	72	100%	8	11.11%
Plasmid2	39	39	100%	0	0%	6	15.38%	13	33.33%	5	12.82%
Plasmid3	39	25	64.10%	0	0%	3	7.69%	39	100%	5	12.82%
***L. nagelii* TMW 1.2352^T**	**OG in analysis**	**Collinear OG TMW 1.1822**		**Collinear OG TMW 1.1907**		**Collinear OG TMW 1.2353^T**		**Collinear OG TMW 1.1823**		**Collinear OG TMW 1.1827**	
Chromosome	2353	1774	75.39%	1741	73.99%	1603	68.13%	2187	92.95%	2187	92.95%
Plasmid1	86	11	12.79%	0	0%	56	65.12%	11	12.79%	11	12.79%

Appendix 12 Genomic regions that exhibit the dextransucrase gene (dark grey colour) in *L. hordei* TMW 1.1822 and TMW 1.1907 compared to the same locus in *L. hordei* TMW 1.2353^{T}. Blast identity percentage is coloured according to the scale on the right.

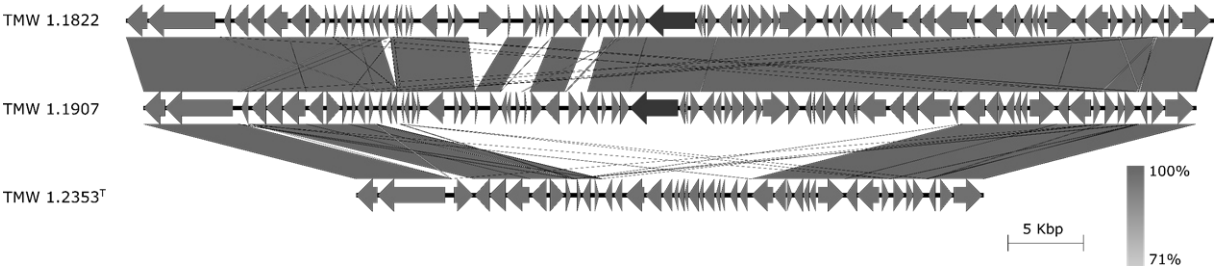

Appendix 13 PCR-detection of dextransucrase genes in strains of the species *L. hordei* (A), *L. nagelii* (B) and *L. hilgardii* (C+D). Panel D shows the PCR-products of genomic (gDNA) and plasmid (pDNA) DNA isolated from *L. hilgardii* TMW 1.2196 and TMW 1.828. Size of PCR-products was estimated according to GeneRuler 1kb DNA ladder (ThermoFisher Scientific). The figures were derived from the Bachelor´s thesis of Henriette Leicher, who was supervised during this work.

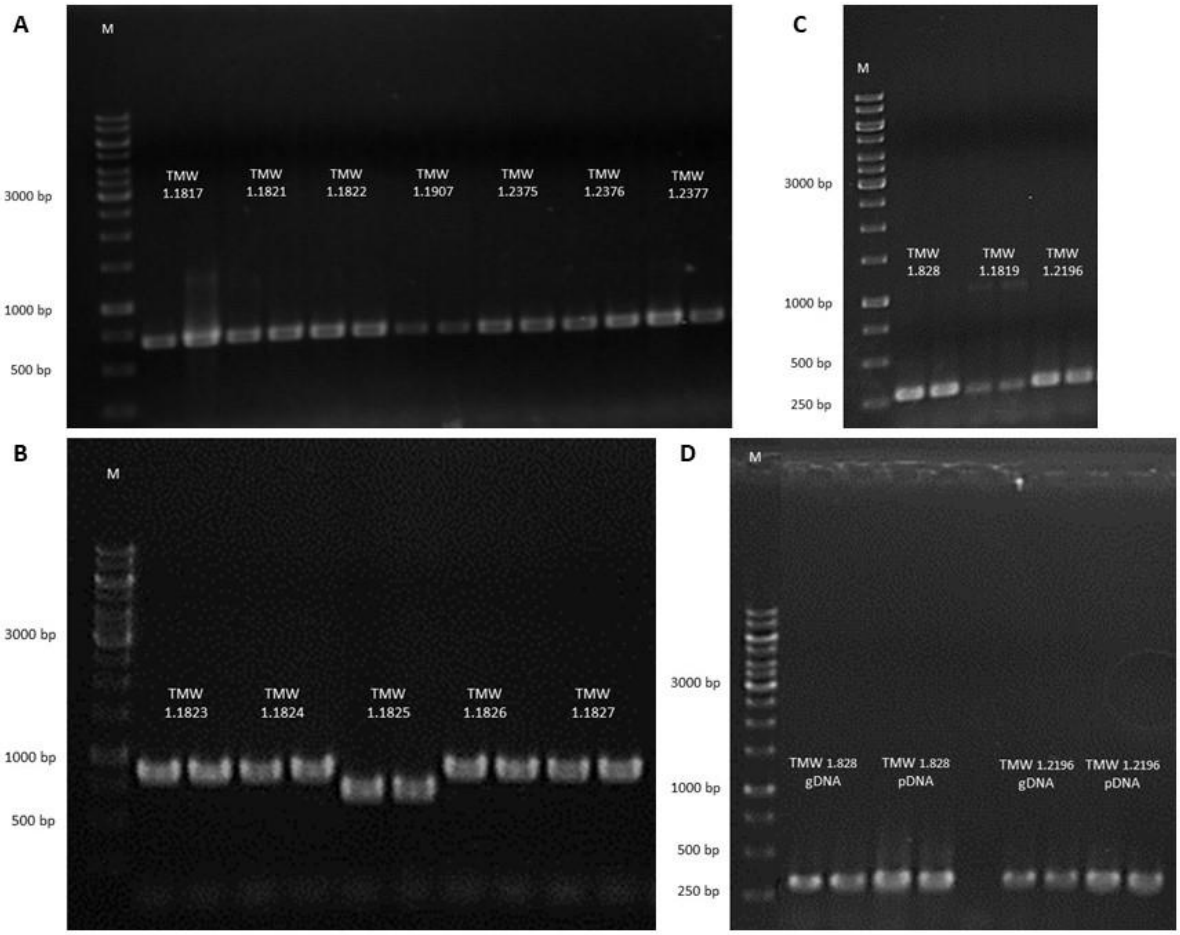

Appendix 14 Distribution of PTS systems encoded within the WGSs of *L. hilgardii, L. hordei* and *L. nagelii* strains. Some orthogroups are found in more than one PTS gene cluster, but with a different composition of subunits.

Family	Subunit	Orthogroup	TMW 1.2196	TMW 1.828	TMW 1.45^T	TMW 1.1822	TMW 1.1907	TMW 1.2353^T	TMW 1.1823	TMW 1.1827	TMW 1.2352^T
Phosphocarrier	HPr	OG0000704	C2L99_13055	CLI91_12835	HMPREF0519_RS09625	BSQ49_08750	CRI84_05315	G6O70_10900	CRI83_10605	BSQ50_08000	G6O73_01140
Phosphocarrier	HPr	OG0002746	C2L99_09440	CLI91_09595	HMPREF0519_RS04010	-	-	-	-	-	-
Phosphotransferase	EI	OG0001094	C2L99_13050	CLI91_12830	HMPREF0519_RS09630	BSQ49_08745	CRI84_05310	G6O70_10895	CRI83_10600	BSQ50_07995	G6O73_01145
PTS^{man}1	IIA	OG0001596	-	-	-	BSQ49_10160	CRI84_06550	G6O70_01365; G6O70_11995	CRI83_07015	BSQ50_10005	G6O73_11605
	IIB	OG0001597	-	-	-	BSQ49_10165	CRI84_06555	G6O70_01370; G6O70_12000	CRI83_07020	BSQ50_10000	G6O73_11610
	IIC	OG0001598	-	-	-	BSQ49_10170	CRI84_06560	G6O70_01375; G6O70_12005	CRI83_07025	BSQ50_09995	G6O73_11615
	IID	OG0001599	-	-	-	BSQ49_10175	CRI84_06565	G6O70_01380; G6O70_12010	CRI83_07030	BSQ50_09990	G6O73_11620
PTS^{man}2	IID	OG0001116	C2L99_12055	CLI91_12130	HMPREF0519_RS10745	BSQ49_11155	CRI84_07400	G6O70_02250	CRI83_07745	BSQ50_11285	G6O73_10325
	IIC	OG0000254	C2L99_12050	CLI91_12125	HMPREF0519_RS10740	BSQ49_11160	CRI84_07405	G6O70_02255	CRI83_07740	BSQ50_11290	G6O73_10320
	IIAB	OG0001542	-	-	-	BSQ49_11165	CRI84_07410	G6O70_02260	CRI83_07735	BSQ50_11295	G6O73_10315
	IIB	OG0000830	C2L99_12045	CLI91_12120	HMPREF0519_RS10735	BSQ49_11170	CRI84_07415	G6O70_02265	CRI83_07730	BSQ50_11300	G6O73_10310
	IIA	OG0000255	C2L99_12040	CLI91_12115	HMPREF0519_RS10730	-	-	-	-	-	-
	IIA	OG0001090	-	-	-	BSQ49_11175	CRI84_07420	G6O70_02270	CRI83_07725	BSQ50_11305	G6O73_10305
PTS^{man}3	IIB	OG0001789	-	-	-	BSQ49_04065	CRI84_03835	G6O70_06730	CRI83_00265	BSQ50_05030	G6O73_05005

	IIC	OG0001790	-	-	-	BSQ49_04070	CRI84_03830	G6O70_06735	CRI83_00270	BSQ50_05035	G6O73_05000
	IID	OG0001791	-	-	-	BSQ49_04075	CRI84_03825	G6O70_06740	CRI83_00275	BSQ50_05040	G6O73_04995
	IIA	OG0001792	-	-	-	BSQ49_04080	CRI84_03820	G6O70_06745	CRI83_00280	BSQ50_05045	G6O73_04990
PTS^{man}4	IIB	OG0001966	-	-	-	BSQ49_00105	CRI84_08110	-	CRI83_00460	BSQ50_05225	G6O73_04720
	IIC	OG0002238	-	-	-	BSQ49_00110	CRI84_08115	-	CRI83_00465	BSQ50_05230	G6O73_04715
	IID	OG0002239	-	-	-	BSQ49_00115	CRI84_08120	-	CRI83_00470	BSQ50_05235	G6O73_04710
	IIA	OG0000255	-	-	-	BSQ49_00120	CRI84_08125	-	CRI83_00475	BSQ50_05240	G6O73_04705
PTS^{man}5	IIB	OG0003302	-	-	-	BSQ49_11565	CRI84_07805	-	-	-	-
	IIA	OG0002261	-	-	-	BSQ49_11570	CRI84_07810	-	-	-	-
	IID	OG0002262	-	-	-	BSQ49_11575	CRI84_07815	-	-	-	-
	IIBC	OG0003303	-	-	-	BSQ49_11580	CRI84_07820	-	-	-	-
PTS^{man}6	IIC	OG0003753	-	-	-	BSQ49_12345	-	-	-	-	-
	IIA	OG0003754	-	-	-	BSQ49_12350	-	-	-	-	-
	IIB	OG0003755	-	-	-	BSQ49_12355	-	-	-	-	-
	IIC	OG0003312	-	-	-	BSQ49_12360	-	-	-	-	-
	IID	OG0003313	-	-	-	BSQ49_12365	-	-	-	-	-
PTS^{man}7	IIA	OG0003762	-	-	-	BSQ49_12455	-	-	-	-	-
	IID	OG0002262	-	-	-	BSQ49_12460	-	-	-	-	-
	IIC	OG0002261	-	-	-	BSQ49_12465	-	-	-	-	-
	IIB	OG0003314	-	-	-	BSQ49_12470	-	-	-	-	-
PTS^{man}8	IID	OG0003380	-	-	-	-	-	-	CRI83_00070	BSQ50_04835	G6O73_05215

	IIC	OG0003381	-	-	-	-	-	-	CRI83_00065	BSQ50_04830	G6O73_05220
	IIB	OG0000830	-	-	-	-	-	-	CRI83_00060	BSQ50_04825	G6O73_05225
	IIA	OG0003382	-	-	-	-	-	-	CRI83_00055	BSQ50_04820	G6O73_05230
PTS^{man}9	IID	OG0003477	-	-	-	-	-	-	CRI83_07070	BSQ50_09950	G6O73_11660
	IIA	OG0001090	-	-	-	-	-	-	CRI83_07050	BSQ50_09970	G6O73_11640
	IIA	OG0000255	-	-	-	-	-	-	CRI83_07055	BSQ50_09965	G6O73_11645
	IIB	OG0003476	-	-	-	-	-	-	CRI83_07060	BSQ50_09960	G6O73_11650
	IIC	OG0000254	-	-	-	-	-	-	CRI83_07065	BSQ50_09955	G6O73_11655
PTS^{fru}1	IIA	OG0001752	-	-	-	BSQ49_11295	CRI84_07550	G6O70_02350	CRI83_00925	BSQ50_05695	G6O73_04285
	IICB	OG0001754	-	-	-	BSQ49_11305	CRI84_07560	G6O70_02360	CRI83_00915	BSQ50_05685	G6O73_04295
PTS^{fru}2	IIAB	OG0001605	-	-	-	BSQ49_02110	CRI84_10160	G6O70_04710	CRI83_00120	BSQ50_04885	G6O73_05150
	IIB	OG0001777	-	-	-	BSQ49_02115	CRI84_10165	G6O70_04715	CRI83_00125	BSQ50_04890	G6O73_05145
	IIC	OG0001778	-	-	-	BSQ49_02120	CRI84_10170	G6O70_04720	CRI83_00130	BSQ50_04895	G6O73_05140
	IIA	OG0001604	-	-	-	BSQ49_02105	CRI84_10155	G6O70_04705	CRI83_00115	BSQ50_04880	G6O73_05155
	IIB	OG0004938	-	-	-	BSQ49_02100	-	-	-	-	-
PTS^{fru}3	IIBCA	OG0002861	-	-	-	-	-	-	-	-	G6O73_00100; G6O73_12310
PTS^{fru}4	IIABC	OG0001995	-	-	-	BSQ49_09170	CRI84_05730	G6O70_11320	CRI83_09880	BSQ50_09885	G6O73_11715
PTS^{scr}	IIBCA	OG0001212	C2L99_06810	CLI91_04265	HMPREF0519_RS04365	BSQ49_00775	CRI84_08885	G6O70_03375	CRI83_04570	BSQ50_03385	G6O73_06685
PTS^{gat}1	IIA	OG0002000	-	-	-	BSQ49_09785	-	-	-	-	-
	IIB	OG0002241	-	-	-	BSQ49_09775	-	-	-	-	-

	IIC	OG0001454	-	-	-	BSQ49_09780	-	-	-	-	-
	IIA	OG0001604	-	-	-	BSQ49_09790	-	-	-	-	-
PTS^{gat}2	IIA	OG0002000	-	-	-	BSQ49_00660	-	-	CRI83_09600	BSQ50_09230	G6O73_00035; G6O73_12245
	IIB	OG0002859	-	-	-	-	-	-	CRI83_09595	BSQ50_09225	G6O73_00040; G6O73_12250
	IIC	OG0001454	-	-	-	BSQ49_00670	-	-	CRI83_09590	BSQ50_09220	G6O73_00045; G6O73_12255
	IIB	OG0002241	-	-	-	BSQ49_00665	-	-	-	-	-
PTS^{gat}3	IIC	OG0001454	-	-	-	-	-	-	CRI83_10115	BSQ50_09655	-
	IIB	OG0002241	-	-	-	-	-	-	CRI83_10110	BSQ50_09660	-
	IIA	OG0003496	-	-	-	-	-	-	CRI83_10105	BSQ50_09665	-
PTS^{gut}	IIA	OG0002883	-	-	-	-	-	-	CRI83_03400	BSQ50_04555	G6O73_05480
	IIB	OG0002884	-	-	-	-	-	-	CRI83_03405	BSQ50_04550	G6O73_05485
	IIC	OG0002885	-	-	-	-	-	-	CRI83_03410	BSQ50_04545	G6O73_05490
PTS^{lac}1	IIB	OG0002908	-	-	-	-	-	-	CRI83_06780	BSQ50_10240	G6O73_11365
	IIC	OG0002909	-	-	-	-	-	-	CRI83_06785	BSQ50_10235	G6O73_11370
	IIA	OG0002910	-	-	-	-	-	-	CRI83_06790	BSQ50_10230	G6O73_11375
	IIA	OG0002911	-	-	-	-	-	-	CRI83_06800	BSQ50_10220	G6O73_11385
PTS^{lac}2	IIB	OG0000165	-	-	-	-	CRI84_05560	G6O70_11155	CRI83_05725; CRI83_08685;	BSQ50_00995; BSQ50_02330;	G6O73_00570; G6O73_07740;

									CRI83_11985	BSQ50_08615	G6O73_09100
	IIA	OG0000193	-	-	-	-	CRI84_05555	G6O70_11150	CRI83_05720; CRI83_08680; CRI83_11990	BSQ50_01000; BSQ50_02335; BSQ50_08610	G6O73_00575; G6O73_07735; G6O73_09095
	IIC	OG0000084	-	-	-	-	CRI84_05565	G6O70_11160	CRI83_05715; CRI83_08690; CRI83_11980	BSQ50_01005; BSQ50_02325; BSQ50_08620	G6O73_00565; G6O73_07745; G6O73_09090
PTS^{lac}3	IIB	OG0000165	-	-	-	BSQ49_09000	-	-	-	-	-
	IIA	OG0004984	-	-	-	BSQ49_08995	-	-	-	-	-
	IIC	OG0000084	-	-	-	BSQ49_09005	-	-	-	-	-
PTS^{glc}1	IIBCA	OG0000055	-	-	-	BSQ49_01110; BSQ49_05795; BSQ49_09270; BSQ49_09740	CRI84_05825; CRI84_06220; CRI84_09225	G6O70_11750	CRI83_00025; CRI83_00095; CRI83_01000	BSQ50_04790; BSQ50_04860; BSQ50_05770	G6O73_04210; G6O73_05180; G6O73_05185; G6O73_05260
PTS^{glc}2	IIBCA	OG0002111	-	-	-	-	-	-	CRI83_06590	BSQ50_10430	G6O73_11195
PTS^{glc}3	IIBCA	OG0003719	-	-	-	BSQ49_09575	CRI84_06100	-	-	-	-
Isolated PTS subunits	ManIIA	OG0000255	-	-	-	BSQ49_12395	-	-	-	-	-
	ManIIC	OG0000308	C2L99_10410	CLI91_10475	HMPREF0519_RS02055	BSQ49_00230	CRI84_08420	G6O70_02860	CRI83_07245	BSQ50_00230	G6O73_09855
	ManIIA	OG0001400	-	-	-	BSQ49_10415	CRI84_06745	G6O70_01570	CRI83_00980	BSQ50_05750	G6O73_08550; G6O73_04230
	ManIIB	OG0001966	-	-	-	-	-	G6O70_02750	-	-	-

	FruIIAC	OG0001514	-	-	-	BSQ49_00330	CRI84_08520	G6O70_02965	CRI83_07170	BSQ50_00305	G6O73_09780
	GutIIA	OG0001376	-	-	-	BSQ49_03310	CRI84_04590	G6O70_06005	CRI83_05145	BSQ50_02810	G6O73_07260
	GlcIIA	OG0001500	C2L99_10385	CLI91_10500	HMPREF0519_RS02030	-	-	-	CRI83_09635	BSQ50_09265	G6O73_12210
	GlcIIA	OG0002112	-	-	-	-	-	-	CRI83_10015	BSQ50_09755	-
	GlcIIC	OG0003397	-	-	-	-	-	-	CRI83_03955	BSQ50_03995	G6O73_06040
	GlcIIC	OG0005079	-	-	-	-	-	-	-	-	G6O73_05265
	GlcIIB	OG0005080	-	-	-	-	-	-	-	-	G6O73_05270
	LacIIC	OG0000084	-	-	-	BSQ49_01210	CRI84_09325	G6O70_03820	-	-	-
	LacIIB	OG0000165	-	-	-	BSQ49_00610	CRI84_08790	G6O70_03230	-	-	-
	LacIIA	OG0000193	-	-	-	BSQ49_01220	CRI84_09335	G6O70_03830	-	-	-
	LacIIC	OG0002106	-	-	-	BSQ49_05510	CRI84_02545	G6O70_07850	-	-	-
	LacIIB	OG0002354	C2L99_15480	CLI91_15415	HMPREF0519_RS10620	-	-	-	-	-	-
	LacIIA	OG0002355	C2L99_15485	CLI91_15420	HMPREF0519_RS10625	-	-	-	-	-	-
	LacIIC	OG0003443	-	-	-	-	-	-	CRI83_07335	BSQ50_00140	G6O73_09950
	IIC	OG0001379	-	-	-	BSQ49_02395	CRI84_10560	G6O70_05005	CRI83_10325	BSQ50_01785	-

Appendix 15 Orthogroups and locus-tags of all transporters and MFS transporters found in the analyzed genomes.

Compound	**Orthogroup**	**TMW 1.2196**	**TMW 1.828**	**TMW 1.45^{T}**	**TMW 1.1822**	**TMW 1.1907**	**TMW 1.2353^{T}**	**TMW 1.1823**	**TMW 1.1827**	**TMW 1.2352^{T}**
Fucose	OG0002977	C2L99_09435	CLI91_09590	HMPREF0519_RS04020	-	-	-	-	-	-
Fucose	OG0001691	C2L99_10370; C2L99_12685	CLI91_10515; CLI91_12575	HMPREF0519_RS02015	-	-	-	-	-	G6O73_04885

Glucose (SCL5)	OG0003326	-	-	-	-	-	-	CRI83_08815	BSQ50_08745	G6O73_00440
Glucose/ Rhamnose (possibly incomplete)	OG0000078	C2L99_01580; C2L99_11915	CLI91_00665; CLI91_06115	HMPREF0519_RS00170; HMPREF0519_RS10260	BSQ49_08470	CRI84_11075	G6O70_10610	CRI83_01025	BSQ50_05795	G6O73_04180
Glucose/ Rhamnose	OG0003377	-	-	-	-	-	-	CRI83_00140	BSQ50_04905	G6O73_05130
Arabinose/ Xylose/ Galactose	OG0000022	C2L99_01135; C2L99_01980; C2L99_03305; C2L99_04610; C2L99_06035	CLI91_01065; CLI91_03240; CLI91_04750; CLI91_09770; CLI91_14970	HMPREF0519_RS01535; HMPREF0519_RS01540; HMPREF0519_RS02780; HMPREF0519_RS07515; HMPREF0519_RS07520; HMPREF0519_RS09885; HMPREF0519_RS12510; HMPREF0519_RS13190	BSQ49_10680	-	G6O70_01770	CRI83_04415; CRI83_09680	BSQ50_03535; BSQ50_09310	G6O73_06515
Arabinose/ Xylose/ Galactose	OG0003175	-	-	-	BSQ49_10345	CRI84_06695	G6O70_01530	-	-	-
Hexuronate/ Glucarate/ Galactarate/ Galactonate	OG0001694	C2L99_06175	CLI91_06350	HMPREF0519_RS02295	-	CRI84_08830	G6O70_03320	-	-	G6O73_04850
Hexuronate/ Glucarate/ Galactarate/ Galactonate	OG0003826	-	-	-	-	-	-	CRI83_00505	BSQ50_05270	-
Melibiose/ Lactose/ Raffinose	OG0001658	C2L99_01265; C2L99_12800	CLI91_09900; CLI91_12460	HMPREF0519_RS13000	-	-	-	-	-	G6O73_12075
Melibiose/ Lactose/ Raffinose	OG0002774	-	-	-	-	-	-	CRI83_09810	BSQ50_09435	G6O73_12150

Melibiose/ Lactose/ Raffinose	OG0000099	C2L99_05900 ; C2L99_08100	CLI91_03545; CLI91_08405	HMPREF0519 _RS02880; HMPREF0519 _RS08580	BSQ49_11070 ; BSQ49_11955	CRI84_07325	G6O70_02150	CRI83_08290; CRI83_11420	BSQ50_11190 ; BSQ50_11780	G6O73_10420 ; G6O73_11830
Sucrose	OG0000199	C2L99_03320 ; C2L99_06565	CLI91_04765; CLI91_06740	HMPREF0519 _RS03490; HMPREF0519 _RS10345	BSQ49_01975	CRI84_10025	G6O70_04520	CRI83_08900	BSQ50_08830	G6O73_00355
Sucrose	OG0001216	C2L99_08980 ; C2L99_12945	CLI91_00520; CLI91_09135	HMPREF0519 _RS00325	BSQ49_09925	-	G6O70_01115	CRI83_11275	BSQ50_08980	G6O73_00190
Oligosaccharides (pot. Sucrose/ Lactose)	OG0001590	C2L99_08135	CLI91_03510	-	BSQ49_12435	-	-	CRI83_00325	BSQ50_05090	G6O73_04940
Melibiose/ Lactose/ Raffinose	OG0001500	C2L99_10385	CLI91_10500	HMPREF0519 _RS02030	-	-	-	CRI83_09635	BSQ50_09265	G6O73_12210

Appendix 16 Distribution and locus-tags of gene clusters encoding subunits of ABC-transporters putatively involved in carbohydrate metabolism.

Transporter	**Orthogroup**	**Subunit**	**TMW 1.2196**	**TMW 1.828**	**TMW 1.45^T**	**TMW 1.1822**	**TMW 1.1907**	**TMW 1.2353^T**	**TMW 1.1823**	**TMW 1.1827**	**TMW 1.2352^T**
Glycerol-3-P/ Maltose	OG0001223	Permease UgpA/MalF	C2L99_04335	CLI91_02965	HMPREF0519_RS01380	BSQ49_10435	CRI84_06765	G6O70_01590	CRI83_04610	BSQ50_03345	G6O73_06725
	OG0001224	Permease UgpE/MalG	C2L99_04340	CLI91_02970	HMPREF0519_RS01385	BSQ49_10440	CRI84_06770	G6O70_01595	CRI83_04605	BSQ50_03350	G6O73_06720
	OG0001225	Substrate-binding protein UgpB/MalE	C2L99_04345	CLI91_02975	HMPREF0519_RS01390	BSQ49_10445	CRI84_06775	G6O70_01600	CRI83_04600	BSQ50_03355	G6O73_06715
	OG0001131	ATP-binding protein UgpC/MalK	C2L99_04330	CLI91_02960	HMPREF0519_RS01375	BSQ49_10430	CRI84_06760	G6O70_01585	CRI83_04615	BSQ50_03340	G6O73_06730
Glycerol-3-P/ Maltose	OG0003171	Substrate-binding protein UgpB/MalE	-	-	-	BSQ49_10570	-	G6O70_00985	-	-	-
	OG0003172	Permease UgpA/MalF	-	-	-	BSQ49_10565	-	G6O70_00990	-	-	-
	OG0003173	Permease UgpE/MalG	-	-	-	BSQ49_10560	-	G6O70_00995	-	-	-

	OG0001244	ATP-binding protein UgpC/MalK	C2L99_02750	CLI91_02275	HMPREF0519_RS03140	BSQ49_01165; BSQ49_10380; BSQ49_10590	CRI84_06710	G6O70_00980	-	-	-
	OG0000017	alpha-glucosidase	C2L99_03315; C2L99_06570; C2L99_08985; C2L99_09475	CLI91_04760; CLI91_06745; CLI91_09140; CLI91_09630	HMPREF0519_RS03495; HMPREF0519_RS08590; HMPREF0519_RS10350	BSQ49_01980; BSQ49_10580; BSQ49_11585	CRI84_07825; CRI84_10030	G6O70_04525	CRI83_06455; CRI83_06580; CRI83_08895	BSQ50_08825; BSQ50_10440; BSQ50_10560	G6O73_00360; G6O73_11050; G6O73_11185
Glycerol-3-P/ Maltose	OG0003268	cellobiose phosphorylase	-	-	-	BSQ49_01135	CRI84_09250	-	-	-	-
	OG0003269	Substrate-binding protein UgpB/MalE	-	-	-	BSQ49_01140	CRI84_09255	-	-	-	-
	OG0003270	Permease UgpA/MalF	-	-	-	BSQ49_01145	CRI84_09260	-	-	-	-
	OG0001586	Permease UgpE/MalG	C2L99_02755	CLI91_02280	-	BSQ49_01150; BSQ49_10385	CRI84_06715; CRI84_09265	-	-	-	-
	OG0001244	ATP-binding protein UgpC/MalK	C2L99_02750	CLI91_02275	HMPREF0519_RS03140	BSQ49_01165; BSQ49_10380; BSQ49_10590	CRI84_06710	G6O70_00980	-	-	-
Glycerol-3-P/ Maltose	OG0001586	Permease UgpE/MalG	C2L99_02755	CLI91_02280	-	BSQ49_01150; BSQ49_10385	CRI84_06715; CRI84_09265	-	-	-	-
	OG0001244	ATP-binding protein UgpC/MalK	C2L99_02750	CLI91_02275	HMPREF0519_RS03140	BSQ49_01165; BSQ49_10380; BSQ49_10590	CRI84_06710	G6O70_00980	-	-	-

	OG0002208	Permease UgpA/MalF	C2L99_02760	CLI91_02285	-	BSQ49_10390	CRI84_06720	-	-	-	-
	OG0002207	Substrate-binding protein UgpB/MalE	C2L99_02765	CLI91_02290	-	BSQ49_10395	CRI84_06725	-	-	-	-
Nucleosides	OG0001888	Permease NupB/NupC	-	-	-	BSQ49_11365	CRI84_07610	G6O70_02410	-	-	-
	OG0001887	Permease NupB/NupC	-	-	-	BSQ49_11370	CRI84_07615	G6O70_02415	-	-	-
	OG0001886	ATP-binding protein NupA	-	-	-	BSQ49_11375	CRI84_07620	G6O70_02420	-	-	-
	OG0001636	Susbtrate-binding protein BmpA	-	-	-	BSQ49_11380	CRI84_07625	G6O70_02425	-	-	-
	OG0001404	Nucleoside hydrolase	C2L99_04560	CLI91_03190	HMPREF0519_RS01485	BSQ49_11385	CRI84_07630	G6O70_02430	-	-	-

Appendix 17 Distribution and locus-tags involved in pathways of the central carbohydrate metabolism.

Pathway	**Enzyme**	**EC-number**	**Orthogroup**	**TMW 1.2196**	**TMW 1.828**	**TMW 1.45^T**	**TMW 1.1822**	**TMW 1.1907**	**TMW 1.2353^T**	**TMW 1.1823**	**TMW 1.1827**	**TMW 1.2352^T**
EMP-Pathway	Hexokinase	2.7.1.1	OG0000223	C2L99_05065	CLI91_05545	HMPREF0519_RS06375	BSQ49_07715	CRI84_00455	G6O70_09810	CRI83_02565	BSQ50_07330	G6O73_02120
	Sugarkinase (pot. Fructo-/Glucokinase)	2.7.1.4/ 2.7.1.1	OG0000102	C2L99_12940	CLI91_00515	HMPREF0519_RS00330	BSQ49_00760; BSQ49_12430	CRI84_08870	G6O70_03360	CRI83_04585	BSQ50_03370	G6O73_06700
	Sugarkinase (pot. Fructo-/Glucokinase)	2.7.1.4/ 2.7.1.1	OG0001606	-	-	-	BSQ49_04160; BSQ49_09505	CRI84_03785	G6O70_06780; G6O70_11620	CRI83_10145	BSQ50_09625	G6O73_11975
	Fructokinase	2.7.1.4	OG0003421	-	-	-	-	-	-	CRI83_11995	BSQ50_02340	G6O73_07730
	Glucose-6-P-Isomerase	5.3.1.9	OG0000203	C2L99_12920	CLI91_00495	HMPREF0519_RS00350	BSQ49_08465	CRI84_11070	G6O70_10605	CRI83_08650	BSQ50_08580	G6O73_00605

	6-P-Fructokinase	2.7.1.11	OG0001385	-	-	-	BSQ49_06450	CRI84_01725	G6O70_08540	CRI83_01560	BSQ50_06330	G6O73_03660
	1-P-fructokinase (Tagatose-6-P-kinase)	2.7.1.56/ 2.7.1.144	OG0001375	-	-	-	BSQ49_00325	CRI84_08515	G6O70_02960	CRI83_07175	BSQ50_00300	G6O73_09785
	1-P-fructokinase (Tagatose-6-P-kinase)	2.7.1.56/ 2.7.1.144	OG0002274	-	-	-	-	-	-	CRI83_09550	BSQ50_09180	G6O73_00095; G6O73_12305
	Fructose-1,6-bP aldolase	4.1.2.13	OG0001382	-	-	-	BSQ49_08535	CRI84_11140	G6O70_10675	CRI83_03025	BSQ50_07790	G6O73_01660
	Fructose-1,6-bP aldolase	4.1.2.13	OG0002278	-	-	-	-	-	-	CRI83_00075	BSQ50_04840	G6O73_05205
	Triosephosphate isomerase	5.3.1.1	OG0000210	C2L99_07210	CLI91_07465	HMPREF0519_RS07060	BSQ49_03170	CRI84_04735	G6O70_05850	CRI83_05305	BSQ50_02645	G6O73_07420
	Glycerinaldehyd-3P-dehydrogenase	1.2.1.12	OG0000051	C2L99_05360; C2L99_07195; C2L99_07520	CLI91_00125; CLI91_07450; CLI91_11275	HMPREF0519_RS00615; HMPREF0519_RS00765; HMPREF0519_RS07070	BSQ49_03160	CRI84_02320; CRI84_04745	G6O70_05840	CRI83_05315	BSQ50_02635	G6O73_07430
	Glycerinaldehyd-3P-dehydrogenase	1.2.1.12	OG0004961	-	-	-	BSQ49_05725	-	-	-	-	-
	Glyceraldehyde-3P-dehydrogenase (NADP-dependent)	1.2.1.9	OG0002635	C2L99_10950	CLI91_11855	HMPREF0519_RS01025	-	-	-	-	-	-
	Phosphoglycerate-kinase	2.7.2.3	OG0000396	C2L99_07200	CLI91_07455	HMPREF0519_RS07065	BSQ49_03165	CRI84_04740	G6O70_05845	CRI83_05310	BSQ50_02640	G6O73_07425
	Phosphoglycerate-mutase	5.4.2.11	OG0000310	C2L99_01700	CLI91_00785	HMPREF0519_RS10150	BSQ49_09945	CRI84_06385	G6O70_11830	CRI83_09525	BSQ50_09155	G6O73_00130
	Enolase	4.2.1.11	OG0000397	C2L99_07215	CLI91_07470	HMPREF0519_RS07055	BSQ49_03175	CRI84_04730	G6O70_05855	CRI83_05300	BSQ50_02650	G6O73_07415

	Enolase	4.2.1.11	OG0003351	-	-	-	-	-	-	CRI83_01115	BSQ50_05885	G6O73_04090
	Pyruvate-kinase	2.7.1.40	OG0000604	C2L99_00855	CLI91_08275	HMPREF0519_RS05450	BSQ49_06445	CRI84_01730	G6O70_08535	CRI83_01555	BSQ50_06325	G6O73_03665
	Pyruvate phosphate dikinase	2.7.9.1	OG0003123	C2L99_03590	CLI91_02680	-	-	-	-	-	-	-
	Pyruvate, water dikinase	2.7.9.2	OG0003422	-	-	-	-	-	-	CRI83_09030	BSQ50_01625	G6O73_08445
Gluconeogenesis	Fructose-1,6-bisphosphatase	3.1.3.11	OG0001521	-	-	-	BSQ49_09960	CRI84_06400	G6O70_11845	CRI83_09540	BSQ50_09170	G6O73_00115
PPP/ PKP/ ED-Pathways	Glucose-6-P-dehydrogenase	1.1.1.49	OG0000281	C2L99_01440	CLI91_11580	HMPREF0519_RS07305	BSQ49_03650	CRI84_04250	G6O70_06345	CRI83_04965	BSQ50_02990	G6O73_07080
	6-P-gluconolactonase	3.1.1.31	OG0000774	C2L99_02260	CLI91_01345	HMPREF0519_RS08355	BSQ49_03305	CRI84_04595	G6O70_06000	CRI83_05150	BSQ50_02805	G6O73_07265
	6-P-gluconate dehydrogenase	1.1.1.44	OG0000280	C2L99_01445	CLI91_11585	HMPREF0519_RS07300	BSQ49_07235	CRI84_00935	G6O70_09330	CRI83_02085	BSQ50_06855	G6O73_02600
	6-P-gluconate dehydrogenase	1.1.1.44	OG0000370	C2L99_13415	CLI91_13050	HMPREF0519_RS11060	BSQ49_02900	CRI84_05005	G6O70_05545	CRI83_11135	BSQ50_02265	G6O73_07800
	6-P-gluconate dehydrogenase	1.1.1.44	OG0001077	C2L99_10350	CLI91_10535	HMPREF0519_RS01995	BSQ49_00400	CRI84_08590	G6O70_03035	CRI83_05160	BSQ50_02795	G6O73_07275
	6-P-gluconate dehydrogenase	1.1.1.44	OG0001522	C2L99_01275	CLI91_09910	HMPREF0519_RS07465	-	-	-	CRI83_06635	BSQ50_10385	G6O73_11235
	Ribose-5-P isomerase A	5.3.1.6	OG0000176	C2L99_12085; C2L99_12670	CLI91_12160; CLI91_12590	HMPREF0519_RS10775	BSQ49_02745	CRI84_05160	G6O70_05390	CRI83_10990	BSQ50_02120	G6O73_07945
	Ribose-5-P isomerase A	5.3.1.6	OG0001825	-	-	-	BSQ49_09175	CRI84_05735	G6O70_11325	CRI83_09875	BSQ50_09890	G6O73_11710
	Ribose-5-P isomerase A	5.3.1.6	OG0001799	-	-	-	BSQ49_05320	CRI84_02735	G6O70_07650	CRI83_08920	BSQ50_08850	G6O73_00335

	Ribose-5-P isomerase A	5.3.1.6	OG0002587	C2L99_13000	CLI91_00575	HMPREF0519_RS00285	-	-	-	-	-	-
	Ribose-5-P isomerase B	5.3.1.6	OG0002878	-	-	-	-	-	-	CRI83_00105	BSQ50_04870	G6O73_05170
	Ribulose-P 3-epimerase	5.1.3.1	OG0000550	C2L99_07905	CLI91_05735	HMPREF0519_RS06200	BSQ49_07630	CRI84_00540	G6O70_09725	CRI83_02480	BSQ50_07245	G6O73_02205
	Ribulose-P 3-epimerase	5.1.3.1	OG0002879	-	-	-	-	-	-	CRI83_00100	BSQ50_04865	G6O73_05175
	Ribulose-P 3-epimerase	5.1.3.1	OG0004988	-	-	-	BSQ49_09765	-	-	-	-	-
	Transketolase	2.2.1.1	OG0001832	-	-	-	BSQ49_05775	CRI84_02255	-	CRI83_04405	BSQ50_03545	G6O73_06505
	Transketolase	2.2.1.1	OG0003705	-	-	-	BSQ49_05770	CRI84_02260	-	-	-	-
	Transaldolase	2.2.1.2	-	-	-	-	-	-	-	-	-	-
	Xylulose-5-P phosphoketolase	4.1.2.9	OG0000124	C2L99_01365; C2L99_06775	CLI91_04230; CLI91_11505	HMPREF0519_RS07380; HMPREF0519_RS13285	BSQ49_05445	CRI84_02610	G6O70_07775	CRI83_09685	BSQ50_09315	G6O73_12190
	Gluconokinase	2.7.1.12	OG0001154	C2L99_14120	CLI91_13910	HMPREF0519_RS09510	-	-	-	CRI83_06640	BSQ50_10380	G6O73_11240
	Phosphogluconate dehydratase	4.2.1.12	-	-	-	-	-	-	-	-	-	-
	KDG-Kinase	2.7.1.45	OG0001505	C2L99_01965	CLI91_01050	HMPREF0519_RS09900	-	-	-	CRI83_12050	BSQ50_09515	G6O73_12050
	KDG-Kinase	2.7.1.45	OG0001556	C2L99_03045; C2L99_03340	CLI91_04490; CLI91_04785	HMPREF0519_RS10320; HMPREF0519_RS10495	-	-	-	-	-	-
	KDG-Kinase	2.7.1.45	OG0002018	-	-	-	-	-	-	CRI83_09815	BSQ50_09440; BSQ50_09485;	G6O73_12085; G6O73_12130

											BSQ50_09525	
	KDG-Kinase	2.7.1.45	OG0003486	-	-	-	-	-	-	CRI83_09855	BSQ50_09480	G6O73_12090
	KDPG-aldolase	4.1.2.14	OG0000832	C2L99_03310	CLI91_04755	HMPREF0519_RS13425	BSQ49_00655	-	-	CRI83_09850; CRI83_10220; CRI83_12045	BSQ50_09475; BSQ50_09510; BSQ50_09550	G6O73_12055; G6O73_12095
	Galactonate dehydratase	4.2.1.6	OG0003267	-	-	-	BSQ49_00675	-	-	CRI83_10235	BSQ50_09535	-
Leloir-Pathway	MFS Transporter Melibiose/ Lactose/ Raffinose	-	OG0001500	C2L99_10385	CLI91_10500	HMPREF0519_RS02030	-	-	-	CRI83_09635	BSQ50_09265	G6O73_12210
	MFS transporter Oligosaccharide (pot. Sucrose/ Lactose	-	OG0001590	C2L99_08135	CLI91_03510	-	BSQ49_12435	-	-	CRI83_00325	BSQ50_05090	G6O73_04940
	beta-galactosidase	3.2.1.23	OG0001593	C2L99_09680; C2L99_11950	CLI91_06080; CLI91_13520	-	-	-	-	CRI83_09640	BSQ50_09270	G6O73_12205
	Aldose 1-epimerase	5.1.3.3	OG0000829	C2L99_01150; C2L99_13885	CLI91_07675; CLI91_09785	HMPREF0519_RS07500	-	-	-	CRI83_09620; CRI83_09660	BSQ50_09250	G6O73_00015; G6O73_12225
	Aldose 1-epimerase	5.1.3.3	OG0001326	-	-	-	-	-	-	CRI83_09565; CRI83_09820	BSQ50_09195; BSQ50_09445	G6O73_00075; G6O73_12080; G6O73_12125; G6O73_12285
	Galactokinase	2.7.1.6	OG0001410	C2L99_13340	CLI91_12975	HMPREF0519_RS10990	-	-	-	CRI83_09630	BSQ50_09260	G6O73_00005; G6O73_12215
	UDP-glucose-hexose-1-P uridylyltransferas	2.7.7.12	OG0001411	C2L99_13350	CLI91_12985	HMPREF0519_RS11000	-	-	-	CRI83_09625	BSQ50_09255	G6O73_00010;

	e/ Galactose-1-P uridylyltransferase											G6O73_12220
	UDP-glucose 4-epimerase	5.1.3.2	OG0000236	C2L99_13345	CLI91_12980	HMPREF0519_RS10995	BSQ49_09970	CRI84_06410	G6O70_11855	CRI83_09615	BSQ50_09245	G6O73_00020; G6O73_12230
Tagatose-6-P-pathway	PTS galacticol IIC	-	OG0001454	-	-	-	BSQ49_00670; BSQ49_09780	-	-	CRI83_09590; CRI83_10115	BSQ50_09220; BSQ50_09655	G6O73_00045; G6O73_12255
	PTS galacticol IIB	-	OG0002859	-	-	-	-	-	-	CRI83_09595	BSQ50_09225	G6O73_00040; G6O73_12250
	PTS galacticol IIA	-	OG0002000	-	-	-	BSQ49_00660; BSQ49_09785	-	-	CRI83_09600	BSQ50_09230	G6O73_00035; G6O73_12245
	Galactose-6-P isomerase subunit A	5.3.1.26	OG0002271	-	-	-	-	-	-	CRI83_09580	BSQ50_09210	G6O73_00060; G6O73_12270
	Galactose-6-P isomerase subunit B	5.3.1.26	OG0002272	-	-	-	-	-	-	CRI83_09575	BSQ50_09205	G6O73_00065; G6O73_12275
	1-P-fructokinase (Tagatose-6-P-kinase)	2.7.1.56/ 2.7.1.144	OG0001375	-	-	-	BSQ49_00325	CRI84_08515	G6O70_02960	CRI83_07175	BSQ50_00300	G6O73_09785
	Tagatose-6-P-kinase	2.7.1.144	OG0002013	-	-	-	-	-	-	CRI83_09555	BSQ50_09185	G6O73_00085; G6O73_12295
	1-P-fructokinase (Tagatose-6-P-kinase)	2.7.1.56/ 2.7.1.144	OG0002274	-	-	-	-	-	-	CRI83_09550	BSQ50_09180	G6O73_00095; G6O73_12305
	Tagatose 1,6-bP aldolase	4.1.2.40	OG0000997	C2L99_00480	CLI91_01945	HMPREF0519_RS09055	-	-	-	CRI83_09570	BSQ50_09200	G6O73_00070; G6O73_00105; G6O73_12

												280; G6O73_12315
Sucrose degradation	Dextransucrase	2.4.1.5	OG0000414	C2L99_15130	CLI91_15455	-	BSQ49_11535	CRI84_07775	-	CRI83_04440	BSQ50_03510	-
	beta-fructosidase	3.2.1.26/ 3.2.1.80	OG0001065	-	-	-	BSQ49_09800	CRI84_06255	G6O70_11780	-	-	-
	Sucrose-6-P hydrolase	3.2.1.26	OG0001456	-	-	-	BSQ49_00770	CRI84_08880	G6O70_03370	CRI83_04575	BSQ50_03380	G6O73_06690
	Sucrose-6-P hydrolase	3.2.1.26	OG0002074	-	-	-	-	-	-	CRI83_00320	BSQ50_05085	G6O73_04945
	Sucrose-6-P hydrolase	3.2.1.26	OG0003384	-	-	-	-	-	-	CRI83_00035	BSQ50_04800	G6O73_05250
	Sucrose phosphorylase	2.4.1.7	OG0002480	C2L99_08095	CLI91_03550	HMPREF0519_RS08585	-	-	-	-	-	-
	Glucohydrolase	3.2.1.20	OG0001706	-	-	-	BSQ49_09930	-	G6O70_01110	CRI83_11280	BSQ50_08985	G6O73_00185; G6O73_09060
	Glucohydrolase	3.2.1.20	OG0003092	C2L99_08090	CLI91_03555	-	-	-	-	-	-	-
	Glucohydrolase	3.2.1.20	OG0000017	C2L99_03315; C2L99_06570; C2L99_08985; C2L99_09475	CLI91_04760; CLI91_06745; CLI91_09140; CLI91_09630	HMPREF0519_RS03495; HMPREF0519_RS08590; HMPREF0519_RS10350	BSQ49_01980; BSQ49_10580; BSQ49_11585	CRI84_07825; CRI84_10030	G6O70_04525	CRI83_06455; CRI83_06580; CRI83_08895	BSQ50_08825; BSQ50_10440; BSQ50_10560	G6O73_00360; G6O73_11050; G6O73_11185
Arabinose degradation	alpha-N-arabinofuranosidase GH43	3.2.1.55	OG0001946	C2L99_03350; C2L99_03165	CLI91_04610; CLI91_04795	-	-	-	-	-	-	G6O73_11845
	alpha-N-arabinofuranosidase GH43	3.2.1.55	OG0002213	C2L99_03360; C2L99_03175	CLI91_04620; CLI91_04805	-	-	-	-	-	-	-
	alpha-N-arabinofuranosidase GH43	3.2.1.55	OG0003086	C2L99_10560	CLI91_10690	-	-	-	-	-	-	-

	alpha-N-arabinofuranosidase GH43	3.2.1.55	OG0003093	C2L99_08140	CLI91_03505	-	-	-	-	-	-	-
	alpha-N-arabinofuranosidase GH43	3.2.1.55	OG0004041	C2L99_09700	CLI91_13540	-	-	-	-	-	-	-
	MFS-Transporter Arabinose/ Xylose/ Galactose	-	OG0000022	C2L99_01135; C2L99_01980; C2L99_03305; C2L99_04610; C2L99_06035	CLI91_01065; CLI91_03240; CLI91_04750; CLI91_09770; CLI91_14970	HMPREF0519_RS01535; HMPREF0519_RS01540; HMPREF0519_RS02780; HMPREF0519_RS07515; HMPREF0519_RS07520; HMPREF0519_RS09885; HMPREF0519_RS12510; HMPREF0519_RS13190	BSQ49_10680	-	G6O70_01770	CRI83_09680; CRI83_04415	BSQ50_03535; BSQ50_09310	G6O73_06515
	L-arabinose isomerase	5.3.1.4	OG0001909	C2L99_01130	CLI91_09765	-	-	-	-	CRI83_09665	BSQ50_09295	-
	Ribulokinase/ Xylulokinase	2.7.1.16	OG0001651	C2L99_02790	CLI91_02315	HMPREF0519_RS03115	-	-	-	CRI83_09675	BSQ50_09305	-
	L-ribulose-5-P 4-epimerase	5.1.3.4	OG0001650	C2L99_02785	CLI91_02310	HMPREF0519_RS03120	-	-	-	CRI83_09670	BSQ50_09300	-
Mannitol-Cycle	Mannitol-1-P 5-dehydrogenase	1.1.1.17	OG0001751	-	-	-	BSQ49_11290	CRI84_07545	G6O70_02345	CRI83_00930	BSQ50_05700	G6O73_04280
	Mannitol-1-P 5-dehydrogenase	1.1.1.17	OG0001953	C2L99_01245	CLI91_09880	-	-	-	-	CRI83_12040	BSQ50_09505	G6O73_12060

	Mannitol-1-phosphatase	3.1.3.22	-	-	-	-	-	-	-	-	-	-
	Mannitol-2-dehydrogenase	1.1.1.67	-	-	-	-	-	-	-	-	-	-

Appendix 18 Distribution and locus-tags of genes coding for enzymes that are involved in pyruvate metabolism.

Enzyme	**E.C. number**	**Orthogroup**	**TMW 1.2196**	**TMW 1.828**	**TMW 1.45^{T}**	**TMW 1.1822**	**TMW 1.1907**	**TMW 1.2353^{T}**	**TMW 1.1823**	**TMW 1.1827**	**TMW 1.2352^{T}**
L-lactate dehydrogenase	1.1.1.27	OG0000063	C2L99_09230; C2L99_10875	CLI91_09385; CLI91_11780	HMPREF0519_RS01100; HMPREF0519_RS09775	BSQ49_00225; BSQ49_01840	CRI84_08415; CRI84_09890	G6O70_02855; G6O70_04385	CRI83_00665; CRI83_08700	BSQ50_05430; BSQ50_08630	G6O73_00555; G6O73_04560
L-lactate dehydrogenase	1.1.1.27	OG0000336	C2L99_14650	CLI91_09090	HMPREF0519_RS11795	BSQ49_02565	CRI84_10390	G6O70_05190	CRI83_10495	BSQ50_01955	G6O73_08110
D-lactate dehydrogenase	1.1.1.28	OG0000047	C2L99_00265; C2L99_06385; C2L99_11260	CLI91_01730; CLI91_06560; CLI91_11965	HMPREF0519_RS01710; HMPREF0519_RS02165; HMPREF0519_RS08835	BSQ49_02390; BSQ49_08200	CRI84_10565; CRI84_11485	G6O70_05000; G6O70_10320	CRI83_10320	BSQ50_01780	G6O73_08290
D-lactate dehydrogenase	1.1.1.28	OG0000013	C2L99_03115; C2L99_03615; C2L99_10535; C2L99_11320	CLI91_02705; CLI91_04560; CLI91_10665; CLI91_12025	HMPREF0519_RS01760; HMPREF0519_RS06005; HMPREF0519_RS10450	BSQ49_00820; BSQ49_08860; BSQ49_09040; BSQ49_11500	CRI84_05420; CRI84_05600; CRI84_07740; CRI84_08935	G6O70_00960; G6O70_11015; G6O70_11190	CRI83_06890; CRI83_07760; CRI83_11380	BSQ50_09085; BSQ50_10130; BSQ50_10655	G6O73_10960; G6O73_11480
D-lactate dehydrogenase	1.1.1.28	OG0003258	-	-	-	BSQ49_09470	CRI84_06015	-	-	-	-
D-lactate dehydrogenase	1.1.1.28	OG0000182	C2L99_11480	CLI91_10980	HMPREF0519_RS05110	BSQ49_06755	CRI84_01420	G6O70_08845	CRI83_01870	BSQ50_06640	G6O73_03360
Pyruvate dehydrogenase (E1)	1.2.4.1	OG0001182	C2L99_03835	CLI91_05135	HMPREF0519_RS12300	BSQ49_00265	CRI84_08455	G6O70_02900	CRI83_07230	BSQ50_00245	G6O73_09840
Pyruvate dehydrogenase (E1)	1.2.4.1	OG0001183	C2L99_03830	CLI91_05140	HMPREF0519_RS12305	BSQ49_00270	CRI84_08460	G6O70_02905	CRI83_07225	BSQ50_00250	G6O73_09835

Pyruvate dehydrogenase (E1)	1.2.4.1	OG0002840	-	-	-	BSQ49_09685	CRI84_06165; CRI84_08365	-	-	-	-
Pyruvate dehydrogenase (E1)	1.2.4.1	OG0002841	-	-	-	BSQ49_09690	CRI84_06170; CRI84_08360	-	-	-	-
Dihydrolipoyl-transacetylase (E2)	2.3.1.12	OG0003293	-	-	-	BSQ49_09680	CRI84_06160	-	-	-	-
Dihydrolipoyl-transacetylase (E2)	2.3.1.12	OG0001184	C2L99_03825	CLI91_05145	HMPREF0519_RS12310	BSQ49_00275	CRI84_08465	G6O70_02910	CRI83_07220	BSQ50_00255	G6O73_09830
Dihydrolipoyl-dehydrogenase (E3)	1.8.1.4	OG0000252	C2L99_03820	CLI91_05150	HMPREF0519_RS12315	BSQ49_00280; BSQ49_09695	CRI84_06175; CRI84_08470	G6O70_02915	CRI83_07215	BSQ50_00260	G6O73_09825
Formate C-acetyltransferase 1	2.3.1.54	OG0001788	-	-	-	BSQ49_04055	CRI84_03845	G6O70_06715	CRI83_03560	BSQ50_04395	G6O73_05635
Formate C-acetyltransferase 1	2.3.1.54	OG0001787	-	-	-	BSQ49_04050	CRI84_03850	G6O70_06710	CRI83_03565	BSQ50_04390	G6O73_05640
Formate C-acetyltransferase 2	2.3.1.54	OG0003494	-	-	-	-	-	-	CRI83_09795	BSQ50_09420	-
Pyruvate:ferredoxin oxidoreductase	1.2.7.1	OG0003858	-	-	-	-	-	-	CRI83_09805	BSQ50_09430	-
Phosphate acetyltransferase	2.3.1.8	OG0000402	C2L99_07260	CLI91_07515	HMPREF0519_RS07010	BSQ49_03225	CRI84_04675	G6O70_05920	CRI83_05255	BSQ50_02695	G6O73_07370
Pyruvate oxidase	1.2.3.3	OG0000025	C2L99_05390; C2L99_06755; C2L99_06805	CLI91_00095; CLI91_04210; CLI91_04260	HMPREF0519_RS00650; HMPREF0519_RS04370; HMPREF0519_RS04425; HMPREF0519_RS05890;	BSQ49_00895; BSQ49_08970	CRI84_05530; CRI84_09010	G6O70_03465; G6O70_11125	CRI83_06030; CRI83_10790	BSQ50_00690; BSQ50_08185	G6O73_00965; G6O73_09415

					HMPREF0519_RS11140						
Acetate kinase	2.7.1.2	OG0001202	C2L99_01225	CLI91_09860	HMPREF0519_RS07475	BSQ49_02260	CRI84_10310	G6O70_04860	CRI83_08970	BSQ50_01685	G6O73_08385
Acetate kinase	2.7.1.2	OG0001815	-	-	-	BSQ49_08260	CRI84_11425	G6O70_10385	CRI83_08420	BSQ50_08365	G6O73_00765
Acetate kinase	2.7.1.2	OG0000079	C2L99_11560	CLI91_10900	HMPREF0519_RS05030	BSQ49_03440; BSQ49_09540	CRI84_04460; CRI84_06065	G6O70_06135; G6O70_11645	CRI83_02940; CRI83_03385	BSQ50_04570; BSQ50_07705	G6O73_01745; G6O73_05465
Acetate kinase	2.7.1.2	OG0003847	-	-	-	-	-	-	CRI83_09730	BSQ50_09355	-
Bifunctional acetaldehyde-CoA/alcohol dehydrogenase	1.2.1.10/ 1.1.1.1	OG0001061	C2L99_01390	CLI91_11530	HMPREF0519_RS07355	BSQ49_09535	CRI84_06060	G6O70_11640	CRI83_03390	BSQ50_04565	G6O73_05470
Acetolactate synthase	2.2.1.6	OG0000795	C2L99_04600	CLI91_03230	HMPREF0519_RS01525	BSQ49_01410	CRI84_09525	G6O70_04020	CRI83_05580	BSQ50_01140	G6O73_08950
Acetolactate synthase	2.2.1.6	OG0001922	C2L99_12480	CLI91_12285	HMPREF0519_RS08075	BSQ49_10210	-	-	-	-	-
Acetolactate decarboxylase	4.1.1.5	OG0000958	C2L99_04605	CLI91_03235	HMPREF0519_RS01530	BSQ49_10250	CRI84_06595	G6O70_01425	CRI83_06650	BSQ50_10370	G6O73_11250
Diacetyl reductase	1.1.1.304	OG0000003	C2L99_02660; C2L99_02865; C2L99_03085; C2L99_04295; C2L99_05275; C2L99_05855; C2L99_06185; C2L99_07685; C2L99_09295; C2L99_09400; C2L99_1042	CLI91_00210; CLI91_02185; CLI91_02390; CLI91_02925; CLI91_04530; CLI91_06045; CLI91_06360; CLI91_07935; CLI91_08360; CLI91_09450; CLI91_0955	HMPREF0519_RS00525; HMPREF0519_RS01335; HMPREF0519_RS02060; HMPREF0519_RS02530; HMPREF0519_RS02920; HMPREF0519_RS03045; HMPREF0519_RS05845;	BSQ49_09635	-	-	CRI83_00435	BSQ50_05200	-

			0; C2L99_11745; C2L99_13180; C2L99_14255; C2L99_15030	5; CLI91_10465; CLI91_12735; CLI91_14155; CLI91_15490	HMPREF0519_RS06010; HMPREF0519_RS10465; HMPREF0519_RS13175; HMPREF0519_RS13180						
Butanediol dehydrogenase	1.1.1.4	OG0000117	C2L99_02205	CLI91_01290	HMPREF0519_RS08300	BSQ49_10255	CRI84_06600	G6O70_01430	CRI83_00570; CRI83_09610; CRI83_12030	BSQ50_05335; BSQ50_09240; BSQ50_09495	G6O73_00025; G6O73_04655; G6O73_12235
Pyruvat carboxylase	6.4.1.1	OG0001809	-	-	-	BSQ49_07335	CRI84_00835	G6O70_09430	CRI83_02175	BSQ50_06945	G6O73_02505

Appendix 19 Differentially abundant proteins within the cellular proteomes of *L. hordei* TMW 1.1822 in the presence of sucrose compared to glucose. Positive log_2 fold-change (FC) values represent proteins with a higher abundancy in sucrose, while negative log_2 FC values represent proteins with a higher abundancy in glucose compared to the respective other sugar.

#	-Log_{10} (p-value)	Log2 FC	Gene loci	Function	SEED Category
1	4.75	0.32	BSQ49_00075	Adenylosuccinate synthase	Nucleosides and Nucleotides
2	4.46	0.30	BSQ49_00265	Pyruvate dehydrogenase E1 subunit alpha	Carbohydrates
3	4.57	0.36	BSQ49_00270	Pyruvate dehydrogenase E1 subunit beta	Carbohydrates
4	2.33	1.64	BSQ49_00320	DeoR family transcriptional regulator	Carbohydrates
5	8.37	1.22	BSQ49_00325	1-phosphofructokinase	Carbohydrates
6	9.08	1.17	BSQ49_00330	PTS^{fru} EIIC	Carbohydrates
7	3.79	-0.35	BSQ49_00410	Crp/Fnr family transcriptional regulator	-
8	4.27	-0.41	BSQ49_00475	Succinate-semialdehyde dehydrogenase	-
9	7.13	0.95	BSQ49_00555	Glycerol kinase	Fatty Acids, Lipids, and Isoprenoids
10	5.78	0.75	BSQ49_00560	Glycerol-3-P dehydrogenase	Fatty Acids, Lipids, and Isoprenoids

11	5.96	1.16	BSQ49_00610	PTS^{lac} EIIB	Carbohydrates
12	7.61	1.21	BSQ49_00615	6-P-beta-glucosidase	Carbohydrates
13	6.01	0.52	BSQ49_00770	Sucrose-6-P hydrolase	-
14	8.10	1.04	BSQ49_00775	PTS^{scr} EIIBCA	Carbohydrates
15	3.81	0.35	BSQ49_01215; BSQ49_06130	6-P-beta-glucosidase	Carbohydrates
16	3.94	0.38	BSQ49_01220	PTS^{lac} EIIA	Carbohydrates
17	2.87	-0.43	BSQ49_01980	Glucohydrolase (putative alpha-glucosidase)	-
18	2.42	-0.87	BSQ49_02890	Hypothetical protein	DNA Metabolism
19	3.18	-0.49	BSQ49_04135	Biotin-independent malonate decarboxylase subunit beta	-
20	3.70	-0.38	BSQ49_04165	6-P-beta-glucosidase	Carbohydrates
21	4.28	-0.37	BSQ49_04665	HAD family hydrolase	-
22	6.96	-0.46	BSQ49_06450	6-phosphofructokinase	Carbohydrates
23	3.01	-0.59	BSQ49_08370	TIGR00268 family protein	-
24	3.23	-0.45	BSQ49_08455	Histidinol-phosphatase	Amino Acids and Derivatives
25	3.74	-0.39	BSQ49_08460	alpha/beta hydrolase	-
26	8.03	-0.75	BSQ49_08465	Glucose-6-P isomerase	Carbohydrates
27	4.61	-0.32	BSQ49_08745	phosphoenolpyruvate--protein phosphotransferase EI	Carbohydrates
28	5.24	-0.39	BSQ49_09735; BSQ49_09265	6-P-beta-glucosidase	Carbohydrates
29	4.17	-0.41	BSQ49_09740	PTS^{glc} EIIABC	Carbohydrates
30	2.41	-0.49	BSQ49_09745	Transcriptional antiterminator	Carbohydrates
31	3.87	-0.40	BSQ49_09920	LacI family transcriptional regulator	-
32	3.98	-1.12	BSQ49_09925	MFS transporter (sucrose-specific)	-
33	6.18	-0.46	BSQ49_09930	Glucohydrolase (putative alpha-glucosidase)	Carbohydrates
34	3.15	1.90	BSQ49_09960	Fructose-1,6-bisphosphatase	Carbohydrates
35	4.08	1.11	BSQ49_09965	Hypothetical protein	-
36	3.37	-0.39	BSQ49_10015	Dihydroneopterin aldolase	-
37	8.94	3.66	BSQ49_10160	PTS^{man} EIIA	-
38	12.55	3.24	BSQ49_10165	PTS^{man} EIIB	-

39	4.93	3.85	BSQ49_10170	PTS^{man} EIIC	-
40	9.13	3.43	BSQ49_10175	PTS^{man} EIID	-
41	3.41	0.35	BSQ49_10255	Butanediol dehydrogenase	Amino Acids and Derivatives
42	9.64	1.42	BSQ49_10570	ABC-transporter substrate-binding protein UgpB/MalE	Carbohydrates
43	7.83	1.12	BSQ49_10590	ABC-transporter ATP-binding protein UgpC/MalK	Carbohydrates
44	5.81	-0.74	BSQ49_11155	PTS^{man} EIID	-
45	3.13	-0.70	BSQ49_11160	PTS^{man} EIIC	-
46	6.01	-0.76	BSQ49_11165	PTS^{man} EIIAB	Cell Wall and Capsule
47	4.83	-0.79	BSQ49_11170	PTS^{man} EIIB	Cell Wall and Capsule
48	4.34	-0.32	BSQ49_11175	Transcription antiterminator BglG	-
49	10.60	1.60	BSQ49_11290	Mannitol-1-phosphate 5-dehydrogenase	Carbohydrates
50	7.24	1.64	BSQ49_11295	PTS^{fru} EIIA	-
51	4.10	1.52	BSQ49_11300	Transcriptional regulator	Carbohydrates
52	12.28	2.73	BSQ49_11305	PTS^{fru} EIICB	Carbohydrates
53	5.61	0.51	BSQ49_11795	GH25 muramidase (putative)	-

Appendix 20 Differentially abundant proteins within the cellular proteomes of *L. nagelii* TMW 1.1827 in the presence of sucrose compared to glucose. Positive log_2 fold-change (FC) values represent proteins with a higher abundancy in sucrose, while negative log_2 FC values represent proteins with a higher abundancy in glucose compared to the respective other sugar.

#	$-Log_{10}$ (p-value)	Log2 FC	Gene loci	Function	SEED Category
1	10.20	1.91	BSQ50_00300	1-phosphofructokinase	Carbohydrates
2	10.91	1.97	BSQ50_00305	PTS^{fru} EIIC	Carbohydrates
3	4.24	1.04	BSQ50_00310	Hypothetical protein	-
4	4.36	0.40	BSQ50_00530	Glycerol kinase	Fatty Acids, Lipids, and Isoprenoids
5	2.76	0.66	BSQ50_01500	Hypothetical protein	-
6	4.20	0.35	BSQ50_01810	Hypothetical protein	-
7	2.61	0.56	BSQ50_01930	holo-ACP synthase	Fatty Acids, Lipids, and Isoprenoids
8	2.68	-0.48	BSQ50_03215	[citrate (pro-3S)-lyase] ligase	Carbohydrates

9	8.80	1.26	BSQ50_03380	Sucrose-6-P hydrolase	-
10	9.51	2.03	BSQ50_03385	PTS^{scr} EIIBCA	Carbohydrates
11	7.93	-3.06	BSQ50_03510	Dextransucrase	Stress Response
12	3.68	-0.39	BSQ50_03745	o-succinylbenzoate--CoA ligase	Cofactors, Vitamins, Prosthetic Groups, Pigments
13	4.76	0.46	BSQ50_04405	Aspartate ammonia-lyase	Amino Acids and Derivatives
14	4.69	-0.43	BSQ50_04660	Hypothetical protein	Cell Wall and Capsule
15	4.54	-0.71	BSQ50_05525	Glucosaminidase (putative)	Stress Response
16	7.54	1.39	BSQ50_05685	PTS^{fru} EIICB	Carbohydrates
17	3.72	0.49	BSQ50_05690	Hypothetical protein	Carbohydrates
18	5.60	1.00	BSQ50_05695	PTS^{fru} EIIA	-
19	6.75	0.73	BSQ50_05700	Mannitol-1-phosphate 5-dehydrogenase	Carbohydrates
20	5.06	-0.63	BSQ50_06045	Glucose-1-P thymidylyltransferase	-
21	2.85	-0.46	BSQ50_06365	Cystathionine gamma-synthase	Amino Acids and Derivatives
22	1.40	-3.19	BSQ50_07320	DUF3042 domain-containing protein	-
23	2.84	0.45	BSQ50_07635	Aspartate aminotransferase	Amino Acids and Derivatives
24	3.28	0.53	BSQ50_07785	Hypothetical protein	-
25	4.58	-0.31	BSQ50_08580	Glucose-6-P isomerase	Carbohydrates
26	1.91	0.87	BSQ50_08855	50S ribosomal protein L33	-
27	7.23	4.10	BSQ50_08870	30S ribosomal protein S14	Protein Metabolism
28	4.47	-0.37	BSQ50_08980	MFS transporter (sucrose-specific)	-
29	3.45	0.37	BSQ50_09170	Fructose-1,6-bisphosphatase	Carbohydrates
30	2.38	2.87	BSQ50_09175	Hypothetical protein	-
31	4.56	-0.42	BSQ50_09530	L-idonate 5-dehydrogenase	Carbohydrates
32	3.86	-0.39	BSQ50_10430	PTS^{glc} EIIBCA	-
33	3.28	-0.53	BSQ50_10455	Prevent-host-death family protein	Regulation and Cell signaling
34	2.09	-1.60	BSQ50_10700	Hypothetical protein	-
35	5.12	-0.52	BSQ50_11235	NlpC/P60 domain-containing protein	-
36	3.90	-0.34	BSQ50_11285	PTS^{man} EIID	-
37	4.89	-0.35	BSQ50_11295	PTS^{man} EIIA	Cell Wall and Capsule

38	3.40	-0.38	BSQ50_11415	Cytochrome ubiquinol oxidase subunit I	Respiration

Appendix 21 Differentially abundant proteins within the exoproteomes of *L. hordei* TMW 1.1822 in the presence of sucrose compared to glucose. Positive $\log_2$ fold-change (FC) values represent proteins with a higher abundancy in sucrose, while negative $\log_2$ FC values represent proteins with a higher abundancy in glucose compared to the respective other sugar.

#	-Log_{10} (p-value)	Log2 FC	Gene loci	Function	SEED Category
1	3.27	2.15	BSQ49_00005	DNA polymerase III subunit beta	DNA Metabolism
2	3.02	1.41	BSQ49_00045; BSQ49_04955	Single-stranded DNA-binding protein	DNA Metabolism
3	1.80	1.56	BSQ49_00075	Adenylosuccinate synthase	Nucleosides and Nucleotides
4	1.64	1.34	BSQ49_00325	1-phosphofructokinase	Carbohydrates
5	1.91	2.37	BSQ49_00330	PTS^{fru} EIIC	Carbohydrates
6	2.87	2.29	BSQ49_00365	UDP-galactopyranose mutase	-
7	2.32	0.79	BSQ49_00415	Fatty acid-binding protein DegV	-
8	3.20	-2.26	BSQ49_00575	Hypothetical protein	Cell Wall and Capsule
9	1.85	0.77	BSQ49_00585	2-Cys peroxiredoxin	Sulfur Metabolism
10	2.59	0.49	BSQ49_00620	Peptidase	-
11	3.77	1.92	BSQ49_00775	PTS^{scr} EIIBCA	Carbohydrates
12	3.51	0.58	BSQ49_01060; BSQ49_11180; BSQ49_02160	Peptide ABC-transporter substrate-binding protein	Membrane Transport
13	2.78	1.19	BSQ49_01075	Peptide ABC-transporter ATP-binding protein	Membrane Transport
14	2.46	2.94	BSQ49_01105	Glutamine-hydrolyzing GMP synthase	Nucleosides and Nucleotides
15	2.01	-0.67	BSQ49_01360	Cold-shock protein	Stress Response
16	2.36	2.54	BSQ49_01410	Acetolactate synthase large subunit	Carbohydrates
17	3.65	2.43	BSQ49_01420	Serine--tRNA ligase	Protein Metabolism
18	1.85	2.33	BSQ49_01505	DNA-directed RNA polymerase subunit beta	Virulence, Disease and Defense
19	1.90	2.72	BSQ49_01510	DNA-directed RNA polymerase subunit beta	Virulence, Disease and Defense
20	3.30	1.31	BSQ49_01520	30S ribosomal protein S12	Virulence, Disease and Defense
21	3.35	0.91	BSQ49_01525	30S ribosomal protein S7	Virulence, Disease and Defense

22	3.47	0.99	BSQ49_01530	Translation elongation factor G	Virulence, Disease and Defense
23	3.12	1.08	BSQ49_01540	30S ribosomal protein S10	Protein Metabolism
24	5.04	1.33	BSQ49_01545	50S ribosomal protein L3	Protein Metabolism
25	2.92	1.14	BSQ49_01550	50S ribosomal protein L4	Protein Metabolism
26	4.00	0.94	BSQ49_01555	50S ribosomal protein L23	Protein Metabolism
27	4.61	1.21	BSQ49_01560	50S ribosomal protein L2	Protein Metabolism
28	3.08	0.91	BSQ49_01570	50S ribosomal protein L22	Protein Metabolism
29	1.92	0.74	BSQ49_01575	30S ribosomal protein S3	Protein Metabolism
30	1.58	1.87	BSQ49_01580	50S ribosomal protein L16	Protein Metabolism
31	1.64	0.72	BSQ49_01605	50S ribosomal protein L5	Protein Metabolism
32	2.62	0.65	BSQ49_01615	30S ribosomal protein S8	Protein Metabolism
33	1.92	0.69	BSQ49_01620	50S ribosomal protein L6	Protein Metabolism
34	2.89	0.84	BSQ49_01625	50S ribosomal protein L18	Protein Metabolism
35	2.61	0.61	BSQ49_01630	30S ribosomal protein S5	Protein Metabolism
36	4.27	1.15	BSQ49_01640	50S ribosomal protein L15	Protein Metabolism
37	2.14	0.88	BSQ49_01645	Preprotein translocase subunit SecY	-
38	2.76	0.81	BSQ49_01650	Adenylate kinase	Nucleosides and Nucleotides
39	2.37	2.28	BSQ49_01665	30S ribosomal protein S13	Protein Metabolism
40	2.68	1.62	BSQ49_01670	30S ribosomal protein S11	Protein Metabolism
41	1.53	0.82	BSQ49_01675	DNA-directed RNA polymerase subunit alpha	RNA Metabolism
42	1.64	0.71	BSQ49_01680	50S ribosomal protein L17	Protein Metabolism
43	3.30	1.33	BSQ49_01705	50S ribosomal protein L13	Protein Metabolism
44	3.24	1.01	BSQ49_01710	30S ribosomal protein S9	Protein Metabolism
45	2.27	2.12	BSQ49_01915	Aspartyl/glutamyl-tRNA amidotransferase subunit A	Protein Metabolism
46	1.74	1.32	BSQ49_01920	Aspartyl/glutamyl-tRNA amidotransferase subunit B	Protein Metabolism
47	2.50	1.78	BSQ49_01945	Amino acid ABC-transporter substrate-binding protein	-
48	4.33	-0.86	BSQ49_02250	Peptidoglycan-binding protein LysM	-
49	2.78	1.47	BSQ49_02280	Tyrosine--tRNA ligase	Protein Metabolism
50	2.67	2.23	BSQ49_02340	Methionine--tRNA ligase	Protein Metabolism

51	1.60	1.77	BSQ49_02410	Ribose-phosphate pyrophosphokinase	Nucleosides and Nucleotides
52	3.85	-2.22	BSQ49_02450	Hypothetical protein	-
53	2.30	1.60	BSQ49_02485	CTP synthase	Nucleosides and Nucleotides
54	3.37	2.86	BSQ49_02535	ATP-dependent RNA helicase	-
55	2.73	0.68	BSQ49_02565	L-lactate dehydrogenase	Carbohydrates
56	1.94	1.53	BSQ49_02610	Cell division protein FtsH	Cofactors, Vitamins, Prosthetic Groups, Pigments
57	2.06	1.62	BSQ49_02620	Lysine--tRNA ligase	Protein Metabolism
58	5.67	-4.44	BSQ49_02715	LytR family transcriptional regulator	Regulation and Cell signaling
59	4.94	-0.62	BSQ49_02730	NlpC/P60 domain containing protein	-
60	3.19	1.01	BSQ49_02740	Aminopeptidase	Protein Metabolism
61	2.60	3.04	BSQ49_02770	Glutamate--tRNA ligase	Cofactors, Vitamins, Prosthetic Groups, Pigments
62	1.90	2.17	BSQ49_02805	Transcription termination/antitermination protein NusG	RNA Metabolism
63	3.02	1.04	BSQ49_02815	50S ribosomal protein L11	Protein Metabolism
64	2.87	0.91	BSQ49_02820	50S ribosomal protein L1	Protein Metabolism
65	3.93	0.95	BSQ49_02825	50S ribosomal protein L10	Protein Metabolism
66	3.87	2.18	BSQ49_02840	Class 1b ribonucleoside-diphosphate reductase subunit beta	Nucleosides and Nucleotides
67	2.29	0.77	BSQ49_02845; BSQ49_11640	Ribonucleotide-diphosphate reductase subunit alpha	Nucleosides and Nucleotides
68	4.23	1.38	BSQ49_02990	Chaperonin GroL	Protein Metabolism
69	1.65	1.68	BSQ49_03020	Ribosomal subunit interface protein	Protein Metabolism
70	3.25	0.93	BSQ49_03095	Phosphoglucomutase	Cell Wall and Capsule
71	1.63	1.58	BSQ49_03120; BSQ49_09640	S-ribosylhomocysteine lyase	Amino Acids and Derivatives
72	4.75	1.54	BSQ49_03140	ATP-dependent Clp endopeptidase	Protein Metabolism
73	2.66	0.76	BSQ49_03160	Type I glyceraldehyde-3-phosphate dehydrogenase	Cofactors, Vitamins, Prosthetic Groups, Pigments
74	2.78	0.78	BSQ49_03165	Phosphoglycerate kinase	Carbohydrates
75	2.63	0.88	BSQ49_03175	Phosphopyruvate hydratase	Carbohydrates
76	7.94	-1.73	BSQ49_03195	Hypothetical protein	-
77	2.95	0.64	BSQ49_03225	Phosphate acetyltransferase	Carbohydrates
78	1.51	1.28	BSQ49_03305	6-phosphogluconolactonase	Carbohydrates

79	6.70	3.56	BSQ49_03370	recombinase RecA	DNA Metabolism
80	2.15	1.72	BSQ49_03570	tRNA preQ1(34) S-adenosylmethionine ribosyltransferase-isomerase QueA	RNA Metabolism
81	2.15	1.54	BSQ49_03585	3-hydroxyacyl-[acyl-carrier-protein] dehydratase FabZ	Fatty Acids, Lipids, and Isoprenoids
82	1.52	0.84	BSQ49_03645	Enoyl-[acyl-carrier-protein] reductase	Fatty Acids, Lipids, and Isoprenoids
83	2.47	2.86	BSQ49_03760	D-alanine--poly(phosphoribitol) ligase subunit 1	Cell Wall and Capsule
84	3.58	-0.75	BSQ49_03890	Hypothetical protein	-
85	1.93	1.77	BSQ49_04015	dTDP-4-dehydrorhamnose 3,5-epimerase	Cell Wall and Capsule
86	1.55	1.04	BSQ49_04025	dTDP-4-dehydrorhamnose reductase	Cell Wall and Capsule
87	2.63	0.43	BSQ49_04095	Manganese-dependent inorganic pyrophosphatase	Phosphorus Metabolism
88	1.63	0.77	BSQ49_04260	Aromatic amino acid aminotransferase	Amino Acids and Derivatives
89	1.68	1.09	BSQ49_04365	Hypothetical protein	-
90	1.74	-0.63	BSQ49_04440	Firmicu-CTERM sorting domain-containing protein	-
91	6.43	-0.79	BSQ49_04470	Hypothetical protein	-
92	2.85	1.10	BSQ49_04620	30S ribosomal protein S4	Protein Metabolism
93	3.83	1.99	BSQ49_04645	Valine--tRNA ligase	Protein Metabolism
94	1.88	2.25	BSQ49_04680	Rod shape-determining protein	Cell Division and Cell Cycle
95	1.98	1.90	BSQ49_04810	Asparagine--tRNA ligase	Protein Metabolism
96	3.05	2.06	BSQ49_04865	Phenylalanine--tRNA ligase subunit beta	Protein Metabolism
97	1.75	1.62	BSQ49_04905	Hypothetical protein	-
98	5.28	3.69	BSQ49_04980	Hypothetical protein	-
99	6.44	3.00	BSQ49_05080	Phage capsid protein	Phages, Prophages, Transposable elements, Plasmids
100	2.66	-0.48	BSQ49_05300	Hypothetical protein	-
101	2.81	1.73	BSQ49_05420	Dipeptidase	-
102	4.10	3.66	BSQ49_05445	Phosphoketolase	Carbohydrates
103	3.18	0.82	BSQ49_06375	30S ribosomal protein S1	Protein Metabolism
104	2.28	0.72	BSQ49_06445	Pyruvate kinase	Carbohydrates
105	2.66	2.13	BSQ49_06450	6-phosphofructokinase	Carbohydrates
106	4.29	1.99	BSQ49_06490	Cystathionine gamma-synthase	Amino Acids and Derivatives
107	1.78	0.84	BSQ49_06510	Glycine--tRNA ligase subunit beta	Protein Metabolism

108	2.45	2.21	BSQ49_06575	Aspartate--tRNA ligase	Protein Metabolism
109	2.12	1.86	BSQ49_06580	Histidine--tRNA ligase	Protein Metabolism
110	4.73	1.07	BSQ49_06655	Molecular chaperone DnaK	Protein Metabolism
111	1.76	1.28	BSQ49_06660	Nucleotide exchange factor GrpE	Protein Metabolism
112	1.66	0.77	BSQ49_06700	Transcription termination/antitermination protein NusA	RNA Metabolism
113	2.60	1.59	BSQ49_06715	Proline--tRNA ligase	Protein Metabolism
114	2.20	2.03	BSQ49_06740	UMP kinase	-
115	3.48	1.04	BSQ49_06745	Translation elongation factor Ts	Protein Metabolism
116	2.71	0.99	BSQ49_06750	30S ribosomal protein S2	Protein Metabolism
117	2.14	1.14	BSQ49_06755	D-lactate dehydrogenase	Carbohydrates
118	1.36	1.20	BSQ49_06845	Elongation factor P	Protein Metabolism
119	1.58	2.58	BSQ49_06855	50S ribosomal protein L27	Protein Metabolism
120	4.69	1.25	BSQ49_06865	50S ribosomal protein L21	Protein Metabolism
121	2.04	2.02	BSQ49_07030	F0F1 ATP synthase subunit beta	-
122	2.98	3.23	BSQ49_07040	F0F1 ATP synthase subunit alpha	-
123	2.11	2.50	BSQ49_07230	DNA-binding response regulator	Virulence, Disease and Defense
124	2.89	2.67	BSQ49_07235	Phosphogluconate dehydrogenase (NADP(+)-dependent, decarboxylating)	Carbohydrates
125	1.98	0.61	BSQ49_07245	Trigger factor	-
126	1.70	0.72	BSQ49_07250	Translation elongation factor Tu	Virulence, Disease and Defense
127	3.34	0.83	BSQ49_07270	Aspartate-semialdehyde dehydrogenase	Amino Acids and Derivatives
128	2.24	2.12	BSQ49_07275	30S ribosomal protein S15	Protein Metabolism
129	1.47	1.38	BSQ49_07350	GTP-binding protein TypA	Protein Metabolism
130	1.82	0.82	BSQ49_07380	Ribonuclease J	RNA Metabolism
131	2.73	2.13	BSQ49_07440	Isoleucine--tRNA ligase	Protein Metabolism
132	2.11	1.94	BSQ49_07445	Cell division protein DivIVA	Cell Division and Cell Cycle
133	1.55	1.53	BSQ49_07465	Cell division protein FtsZ	Cell Division and Cell Cycle
134	2.74	1.18	BSQ49_07550	50S ribosomal protein L19	Protein Metabolism
135	3.56	1.54	BSQ49_07600	Phosphate acyltransferase	Fatty Acids, Lipids, and Isoprenoids
136	2.58	1.52	BSQ49_07610	Hypothetical protein	Fatty Acids, Lipids, and Isoprenoids

137	1.77	1.59	BSQ49_07685	Type I glutamate--ammonia ligase	Cell Wall and Capsule
138	1.78	1.24	BSQ49_07715	Glucokinase	Carbohydrates
139	5.42	-0.72	BSQ49_07785	Acetyltransferase	-
140	2.99	2.80	BSQ49_07880	50S ribosomal protein L20	Virulence, Disease and Defense
141	3.43	0.61	BSQ49_07890	Translation initiation factor IF-3	Virulence, Disease and Defense
142	2.53	3.10	BSQ49_07895	threonine--tRNA ligase	Protein Metabolism
143	2.20	1.98	BSQ49_07940	UDP-N-acetylmuramate--L-alanine ligase	Cell Wall and Capsule
144	2.33	0.63	BSQ49_07995	Peptidylprolyl isomerase	Membrane Transport
145	1.65	1.24	BSQ49_08065	Methionine adenosyltransferase	Amino Acids and Derivatives
146	1.82	2.24	BSQ49_08310	Transcriptional regulator	Cofactors, Vitamins, Prosthetic Groups, Pigments
147	3.07	0.64	BSQ49_08465	Glucose-6-phosphate isomerase	Carbohydrates
148	1.93	2.03	BSQ49_08720	Glycerol phosphate lipoteichoic acid synthase	Cell Wall and Capsule
149	3.34	0.72	BSQ49_08745	Phosphoenolpyruvate--protein phosphotransferase EI	Carbohydrates
150	1.81	-0.69	BSQ49_08750	Phosphocarrier protein HPr	-
151	2.88	1.71	BSQ49_08760	ATP-dependent Clp protease ATP-binding subunit	Protein Metabolism
152	1.57	1.90	BSQ49_08840	UTP--glucose-1-phosphate uridylyltransferase	-
153	1.93	1.69	BSQ49_08970	Pyruvate oxidase	Carbohydrates
154	1.92	1.15	BSQ49_09030	7-cyano-7-deazaguanine reductase	-
155	2.31	2.67	BSQ49_09155	Elongation factor P	Protein Metabolism
156	3.56	2.57	BSQ49_09185	FAD-dependent oxidoreductase	-
157	2.30	1.45	BSQ49_09190	Pyridine nucleotide-disulfide oxidoreductase	-
158	6.16	-1.11	BSQ49_09335	Hypothetical protein	Cell Wall and Capsule
159	5.18	-0.67	BSQ49_09340	Hypothetical protein	Cell Wall and Capsule
160	4.56	-0.73	BSQ49_09415	Hypothetical protein	-
161	2.31	2.16	BSQ49_09755	Succinate-semialdehyde dehydrogenase	-
162	4.81	4.75	BSQ49_09800	β-fructosidase (putative)	-
163	3.04	0.78	BSQ49_09945	Phosphoglyceromutase	Miscellaneous
164	1.93	1.40	BSQ49_09970	UDP-glucose 4-epimerase GalE	Cell Wall and Capsule
165	2.96	1.51	BSQ49_10060	Cyclopropane-fatty-acyl-phospholipid synthase	-

166	2.97	-0.58	BSQ49_10225	Hypothetical protein	-
167	1.84	1.97	BSQ49_10470	IMP dehydrogenase	Nucleosides and Nucleotides
168	1.55	-1.85	BSQ49_10650	Hypothetical protein	Cell Wall and Capsule
169	1.80	1.66	BSQ49_10720	Redox-regulated ATPase YchF	Protein Metabolism
170	3.57	-0.60	BSQ49_10765	Flagellar hook protein FliD	-
171	3.84	-0.69	BSQ49_10770	Flagellin	-
172	3.71	-0.81	BSQ49_10840	Flagellar hook-associated protein FlgL	-
173	2.79	-0.58	BSQ49_10845	Flagellar hook-associated protein FlgK	-
174	3.86	-0.78	BSQ49_10920	Flagellar biosynthesis protein FlgG	-
175	3.40	-0.65	BSQ49_10925	Flagellar hook-basal body protein FlgG	-
176	4.57	-0.61	BSQ49_10975	Flagellar basal body rod protein FlgG	-
177	4.09	-0.63	BSQ49_10985	Flagellar basal body rod modification protein	-
178	4.18	-0.64	BSQ49_10990	Flagellar protein FliK	-
179	3.14	-0.52	BSQ49_11015	Flagellar M-ring protein FliF	-
180	2.09	-0.58	BSQ49_11025	Flagellar basal body rod protein FlgC	-
181	2.28	-0.51	BSQ49_11030	Flagellar basal-body rod protein FlgB	-
182	2.42	-0.47	BSQ49_11125	NlpC/P60 domain containing protein	Cell Wall and Capsule
183	2.94	0.86	BSQ49_11155	PTS^{man} EIID	-
184	1.48	1.13	BSQ49_11160	PTS^{man} EIIC	-
185	2.11	3.15	BSQ49_11245	FAD-dependent oxidoreductase	Respiration
186	4.10	2.14	BSQ49_11285	Glutamine--fructose-6-phosphate aminotransferase	Cell Wall and Capsule
187	3.31	2.34	BSQ49_11290	Mannitol-1-phosphate 5-dehydrogenase	Carbohydrates
188	6.14	3.09	BSQ49_11535	Dextransucrase	-
189	2.13	1.45	BSQ49_11725	Peptidase M13	-
190	4.79	7.49	BSQ49_11795	GH25 muramidase (putative)	-
191	1.73	1.10	BSQ49_12115	Fructoselysine-6-P deglycase	-
192	2.39	2.54	BSQ49_12370	Fructoselysine-6-P deglycase	-
193	1.58	1.72	BSQ49_12550	Cadmium-translocating P-type ATPase	Virulence, Disease and Defense
194	5.20	-0.72	BSQ49_12635	Hypothetical protein	-

Appendix 22 Differentially abundant proteins within the exoproteomes of *L. nagelii* TMW 1.1827 in the presence of sucrose compared to glucose. Positive $\log_2$ fold-change (FC) values represent proteins with a higher abundancy in sucrose, while negative $\log_2$ FC values represent proteins with a higher abundancy in glucose compared to the respective other sugar.

#	-Log_{10} (p-value)	Log2 FC	Gene loci	Function	SEED Category
1	3.96	1.52	BSQ50_01725	Hypothetical protein	-
2	6.64	2.73	BSQ50_05515	GH53 *endo*-1,4-betagalactosidase (putative)	-
3	5.64	1.79	BSQ50_05525	Mannosyl-glycoprotein *endo*-beta-N-acetylglucosaminidase (putative)	Stress Response
4	7.43	-1.99	BSQ50_06045	Glucose-1-P thymidylyltransferase	-

10 List of publications and Student theses

Parts of this thesis have been published with Julia Bechtner as principal investigator and sole first author, joint first author, or as co-author.

Peer-reviewed journals (First authors are underlined)

Di Xu, **Julia Bechtner**, Jürgen Behr, Lara Eisenbach, Andreas Geißler, Rudi F. Vogel (2019). Lifestyle of *Lactobacillus hordei* isolated from water kefir based on genomic, proteomic and physiological characterization. *International Journal of Food Microbiology, 290*, 141-149. doi:10.1016/j.ijfoodmicro.2018.10.004

Julia Bechtner, Daniel Wefers, Jonas Schmid, Rudi F. Vogel, Frank Jakob (2019). Identification and comparison of two closely related dextransucrases released by water kefir borne *Lactobacillus hordei* TMW 1.1822 and *Lactobacillus nagelii* TMW 1.1827. *Microbiology, 165*(9), 956-966. doi:10.1099/mic.0.000825

Jonas Schmid, **Julia Bechtner**, Rudi F. Vogel, Frank Jakob (2019). A systematic approach to study the pH-dependent release, productivity and product specificity of dextransucrases. *Microbial Cell Factories, 18*(1), 153. doi:10.1186/s12934-019-1208-8

Franziska Münkel, **Julia Bechtner**, Viktor Eckel, Anja Fischer, Frauke Herbi, Frank Jakob, Daniel Wefers (2019). Detailed structural characterization of glucans produced by glucansucrases from *Leuconostoc citreum* TMW 2.1194. *Journal of Agricultural and Food Chemistry, 67*(24), 6856-6866. doi:10.1021/acs.jafc.9b01822

Di Xu, Jürgen Behr, Andreas Geißler, **Julia Bechtner**, Christina Ludwig, Rudi F. Vogel (2019). Label-free quantitative proteomic analysis reveals the lifestyle of *Lactobacillus hordei* in the presence of *Saccharomyces cerevisiae*. *International Journal of Food Microbiology, 294*, 18-26. doi:10.1016/j.ijfoodmicro.2019.01.010

Julia Bechtner, Di Xu, Jürgen Behr, Christina Ludwig, Rudi F. Vogel (2019). Proteomic analysis of *Lactobacillus nagelii* in the presence of *Saccharomyces cerevisiae* isolated from water kefir and comparison with *Lactobacillus hordei*. *Frontiers in Microbiology, 10*(325). doi:10.3389/fmicb.2019.00325

Julia Bechtner, Christina Ludwig, Michael Kiening, Frank Jakob, Rudi F. Vogel (2020). Living the sweet life: How *Liquorilactobacillus hordei* TMW 1.1822 changes its behavior in the presence of sucrose in comparison to glucose. *Foods, 9*(9), 1150. doi:10.3390/foods9091150

Julia Bechtner, Verena Hassler, Daniel Wefers, Rudi F. Vogel, Frank Jakob (2021). Insights into extracellular dextran formation by *Liquorilactobacillus nagelii* TMW 1.1827 using secretomes obtained in the presence or absence of sucrose. *Enzyme and Microbial Technology, 143*, 109724. doi.org/10.1016/j.enzmictec.2020.109724

Conference contributions (First authors are underlined)

Viktor Eckel, **Julia Bechtner**, Frank Jakob, Rudi F. Vogel, Molecular diversity of glucan production in *Lactobacillus* strains from water kefir. Poster presentation, *13th International Symposium on Lactic Acid Bacteria*, 2017, Egmond aan Zee, Netherlands

Julia Bechtner, Rudi F. Vogel, Frank Jakob, Identification of a novel type of dextransucrase in water kefir adapted *Lactobacillus hordei* TMW 1.1822, Poster presentation, *8th Congress of European Microbiologists*, 2019, Glasgow, Scotland

Student theses

The following student theses were supervised or co-supervised during this work. The resulting raw data were partially incorporated into this thesis with written permission of the respective students.

Henriette Leicher. PCR-based group-specific detection of different types of dextransucrases in lactic acid bacteria derived from water kefir. Bachelor thesis, 2018.

Swetlana Gerkhardt. Growing of *B. aquikefiri* and *B. tibiigranuli* in water kefir medium depending on different sugars/EPS. Internship, 2019.

Juliana Geromüller. Motilität von *Lactobacillus hordei* und *L. nagelii*. Internship, 2020.

Sabine Winkler. Genetische und physiologische Differenzierung von *Lactobacillus hilgardii* Isolaten aus Wasserkefir und anderen Habitaten. Master thesis, 2019.